Fundamentals of Robotic Mechanical Systems: Theory, Methods, and Algorithms, Second Edition

Jorge Angeles

Springer

Mechanical Engineering Series

Frederick F. Ling
Series Editor

Springer
New York
Berlin
Heidelberg
Hong Kong
London
Milan
Paris
Tokyo

Mechanical Engineering Series

J. Angeles, **Fundamentals of Robotic Mechanical Systems: Theory, Methods, and Algorithms, 2nd ed.**

P. Basu, C. Kefa, and L. Jestin, **Boilers and Burners: Design and Theory**

J.M. Berthelot, **Composite Materials: Mechanical Behavior and Structural Analysis**

I.J. Busch-Vishniac, **Electromechanical Sensors and Actuators**

J. Chakrabarty, **Applied Plasticity**

G. Chryssolouris, **Laser Machining: Theory and Practice**

V.N. Constantinescu, **Laminar Viscous Flow**

G.A. Costello, **Theory of Wire Rope, 2nd ed.**

K. Czolczynski, **Rotordynamics of Gas-Lubricated Journal Bearing Systems**

M.S. Darlow, **Balancing of High-Speed Machinery**

J.F. Doyle, **Nonlinear Analysis of Thin-Walled Structures: Statics, Dynamics, and Stability**

J.F. Doyle, **Wave Propagation in Structures: Spectral Analysis Using Fast Discrete Fourier Transforms, 2nd ed.**

P.A. Engel, **Structural Analysis of Printed Circuit Board Systems**

A.C. Fischer-Cripps, **Introduction to Contact Mechanics**

A.C. Fischer-Cripps, **Nanoindentation**

J. García de Jalón and E. Bayo, **Kinematic and Dynamic Simulation of Multibody Systems: The Real-Time Challenge**

W.K. Gawronski**, Dynamics and Control of Structures: A Modal Approach**

K.C. Gupta, **Mechanics and Control of Robots**

J. Ida and J.P.A. Bastos, **Electromagnetics and Calculations of Fields**

M. Kaviany, **Principles of Convective Heat Transfer, 2nd ed.**

M. Kaviany, **Principles of Heat Transfer in Porous Media, 2nd ed.**

E.N. Kuznetsov, **Underconstrained Structural Systems**

(continued after index)

Mechanical Engineering Series *(continued from page ii)*

P. Ladevèze, **Nonlinear Computational Structural Mechanics: New Approaches and Non-Incremental Methods of Calculation**

A. Lawrence, **Modern Inertial Technology: Navigation, Guidance, and Control, 2nd ed.**

R.A. Layton, **Principles of Analytical System Dynamics**

F.F. Ling, W.M. Lai, D.A. Lucca, **Fundamentals of Surface Mechanics With Applications, 2nd ed.**

C.V. Madhusudana, **Thermal Contact Conductance**

D.P. Miannay, **Fracture Mechanics**

D.P. Miannay, **Time-Dependent Fracture Mechanics**

D.K. Miu, **Mechatronics: Electromechanics and Contromechanics**

D. Post, B. Han, and P. Ifju, **High Sensitivity Moiré: Experimental Analysis for Mechanics and Materials**

F.P. Rimrott, **Introductory Attitude Dynamics**

S.S. Sadhal, P.S. Ayyaswamy, and J.N. Chung, **Transport Phenomena with Drops and Bubbles**

A.A. Shabana, **Theory of Vibration: An Introduction, 2nd ed.**

A.A. Shabana, **Theory of Vibration: Discrete and Continuous Systems, 2nd ed.**

Jorge Angeles

Fundamentals of Robotic Mechanical Systems

Theory, Methods, and Algorithms

Second Edition

Springer

Jorge Angeles
Department of Mechanical Engineering
and Centre for Intelligent Machines
McGill University
817 Sherbrooke Street
Montreal, Quebec H3A 2K6, Canada
angeles@cim.mcgill.ca

Series Editor
Frederick F. Ling
Ernest F. Gloyna Regents Chair in Engineering
Department of Mechanical Engineering
The University of Texas at Austin
Austin, TX 78712-1063, USA
and
William Howard Hart Professor Emeritus
Department of Mechanical Engineering,
Aeronautical Engineering and Mechanics
Rensselaer Polytechnic Institute
Troy, NY 12180-3590, USA

Library of Congress Cataloging-in-Publication Data
Angeles, Jorge, 1943–
Fundamentals of robotic mechanical systems : theory, methods, and algorithms / Jorge Angeles.—2nd ed.
p. cm.—(Mechanical engineering series)
Includes bibliographical references and index.
ISBN 0-387-95368-X (alk. paper)
1. Robotics. I. Title. II. Mechanical engineering series (Berlin, Germany)
TJ211 .A545 2002
629.8'92—dc21 2001054911

ISBN 0-387-95368-X Printed on acid-free paper.

Printed in the United States of America.

9 8 7 6 5 4 3 2 1 SPIN 10853235

Typesetting: Pages created by the author using a Springer TeX macro package.

www.springer-ny.com

Springer-Verlag New York Berlin Heidelberg
A member of BertelsmannSpringer Science+Business Media GmbH

To Anne-Marie, who has given me
not only her love, but also her precious time,
without which this book would not have been possible.

Mechanical Engineering Series

Frederick F. Ling
Series Editor

Advisory Board

Series Preface

Mechanical engineering, an engineering discipline borne of the needs of the industrial revolution, is once again asked to do its substantial share in the call for industrial renewal. The general call is urgent as we face profound issues of productivity and competitiveness that require engineering solutions, among others. The Mechanical Engineering Series features graduate texts and research monographs intended to address the need for information in contemporary areas of mechanical engineering.

The series is conceived as a comprehensive one that covers a broad range of concentrations important to mechanical engineering graduate education and research. We are fortunate to have a distinguished roster of consulting editors on the advisory board, each an expert in one of the areas of concentration. The names of the consulting editors are listed on the facing page of this volume. The areas of concentration are: applied mechanics; biomechanics; computational mechanics; dynamic systems and control; energetics; mechanics of materials; processing; production systems; thermal science; and tribology.

Austin, Texas — Frederick F. Ling

Preface to the Second Edition

The theory, methods and algorithms behind the development of robotic mechanical systems continue developing at a rate faster than they can be recorded. The second edition of *Fundamentals of Robotic Mechanical Systems* does not claim a comprehensive account of developments up-to-date. Nevertheless, an attempt has been made to update the most impacting developments in these activities. Since the appearance of the first edition, many milestones can be cited. Advances in a host of applications areas can be mentioned, e.g., laparoscopy, haptics, and manufacturing, to mention a representative sample.

Perhaps the most impressive achievements to be cited lie in the realm of space exploration. Indeed, in the period of interest we have seen the successful landing of the *Sojourner* on Mars, with the wheeled robot *Pathfinder* roaming on the Martian landscape in 1997. Along the same lines, the infrastructure of the International Space Station was set in orbit in 2000, with the installation of *Canadarm2*, the successor of *Canadarm*, following suit in 2001. Not less impressive are the achievements recorded on the theoretical side of the areas of interest, although these have received much less media attention. To cite just one such accomplishment, one *open question* mentioned in the first edition was definitely closed in 1998 with a paper presented at the *International Workshop on Advances in Robot Kinematics*. This question pertains to the 40th-degree polynomial derived by Husty—as reported in 1996 in a paper in *Mechanism and Machine Theory*—and allowing the computation of all forward-kinematics solutions of a general Stewart-Gough platform. Dietmaier reported an algorithm in that workshop that is capable of generating a set of geometric parameters of the

platform that indeed lead to 40 real solutions. The conclusion then is that Husty's polynomial is indeed minimal.

In producing the Second Edition, we took the opportunity to clear the manuscript of errors and inaccuracies. An in-depth revision was conducted in-between. Special thanks go to Dr. Kourosh Etemadi Zanganeh, Canmet (Nepean, Ontario, Canada), for his invaluable help in the rewriting of Chapter 8. Profs. Carlos López-Cajún, Universidad Autónoma de Querétaro (Mexico), and J. Jesús Cervantes-Sánchez, Universidad de Guanajuato (Mexico) pointed out many inconsistencies in the first edition. Moreover, Dr. Zheng Liu, Canadian Space Agency, St.-Hubert (Quebec, Canada), who is teaching a course based on the first six chapters of the book at McGill University, pointed out mistakes and gave valuable suggestions for improving the readability of the book. All these suggestions were incorporated in the Second Edition as suggested, except for one: While Dr. Liu suggested to expand on the use of Euler angles in Chapter 2, because of their appeal to robotics engineers in industry, we decided to add, instead, a couple of exercises to the list corresponding to this chapter. The reason is that, in the author's personal opinion, Euler angles are a necessary evil. Not being frame-invariant, their manipulation tends to become extremely cumbersome, as illustrated with those examples. Euler angles may be good for visualizing rigid-body rotations, but they are very bad at solving problems associated with these rotations using a computer or simple longhand calculations. Needless to say, the feedback received from students throughout over 15 years of using this material in the classroom, is highly acknowledged.

One word of caution is in order: RVS, the software system used to visualize robot motions and highlighted in the first edition, has not received either maintenance or updating. It still runs on SGI machines, but we have no plans for its porting into Windows.

Since there is always room for improvement, we welcome suggestions from our readership. Please address these to the author, to the e-mail address included below. Updates on the book will be posted at

`www.cim.mcgill.ca/~rmsl`

The Solutions Manual has been expanded, to include more solutions of sampled problems. By the same token, the number of exercises at the end of the book has been expanded. The manual is typeset in LaTeX with Autocad drawings; it is available upon request from the publisher.

Last, but by no means least, thanks are due to Dr. Svetlana Ostrovskaya, a Postdoctoral Fellow at McGill University, for her help with Chapter 10 and the editing of the Second Edition.

Montreal, January 2002

Jorge Angeles
`angeles@cim.mcgill.ca`

Preface to the First Edition

No todos los pensamientos son algorítmicos.

—Mario Bunge[1]

The beginnings of modern robotics can be traced back to the late sixties with the advent of the microprocessor, which made possible the computer control of a multiaxial manipulator. Since those days, robotics has evolved from a technology developed around this class of manipulators for the replaying of a preprogrammed task to a multidiscipline encompassing many branches of science and engineering. Research areas such as computer vision, artificial intelligence, and speech recognition play key roles in the development and implementation of robotics; these are, in turn, multidisciplines supported by computer science, electronics, and control, at their very foundations. Thus we see that robotics covers a rather broad spectrum of knowledge, the scope of this book being only a narrow band of this spectrum, as outlined below.

Contemporary robotics aims at the design, control, and implementation

[1] *Not all thinking processes are algorithmic*—translation of the author—personal communication during the *Symposium on the Brain-Mind Problem. A Tribute to Professor Mario Bunge on His 75th Birthday*, Montreal, September 30, 1994.

of systems capable of performing a task defined at a high level, in a language resembling those used by humans to communicate among themselves. Moreover, robotic systems can take on forms of all kinds, ranging from the most intangible, such as interpreting images collected by a space sound, to the most concrete, such as cutting tissue in a surgical operation. We can, therefore, notice that motion is not essential to a robotic system, for this system is meant to replace humans in many of their activities, moving being but one of them. However, since robots evolved from early programmable manipulators, one tends to identify robots with motion and manipulation. Certainly, robots may rely on a mechanical system to perform their intended tasks. When this is the case, we can speak of *robotic mechanical systems*, which are the subject of this book. These tasks, in turn, can be of a most varied nature, mainly involving motions such as manipulation, but they can also involve locomotion. Moreover, manipulation can be as simple as displacing objects from a belt conveyor to a magazine. On the other hand, manipulation can also be as complex as displacing these objects while observing constraints on both motion and force, e.g., when cutting live tissue of vital organs. We can, thus, distinguish between plain manipulation and dextrous manipulation. Furthermore, manipulation can involve locomotion as well.

The task of a robotic mechanical system is, hence, intimately related to motion control, which warrants a detailed study of mechanical systems as elements of a robotic system. The aim of this book can, therefore, be stated as *establishing the foundations on which the design, control, and implementation of robotic mechanical systems are based.*

The book evolved from sets of lecture notes developed at McGill University over the last twelve years, while I was teaching a two-semester sequence of courses on robotic mechanical systems. For this reason, the book comprises two parts—an introductory and an intermediate part on robotic mechanical systems. Advanced topics, such as redundant manipulators, manipulators with flexible links and joints, and force control, are omitted. The feedback control of robotic mechanical systems is also omitted, although the book refers the reader, when appropriate, to the specialized literature. An aim of the book is to serve as a textbook in a one-year robotics course; another aim is to serve as a reference to the practicing engineer.

The book assumes some familiarity with the mathematics taught in any engineering or science curriculum in the first two years of college. Familiarity with elementary mechanics is helpful, but not essential, for the elements of this science needed to understand the mechanics of robotic systems are covered in the first three chapters, thereby making the book self-contained. These three chapters, moreover, are meant to introduce the reader to the notation and the basics of mathematics and rigid-body mechanics needed in the study of the systems at hand. The material covered in the same chapters can thus serve as reading material for a course on the mathematics of robotics, intended for sophomore students of science and engineering,

prior to a more formal course on robotics.

The first chapter is intended to give the reader an overview of the subject matter and to highlight the major issues in the realm of robotic mechanical systems. Chapter 2 is devoted to notation, nomenclature, and the basics of linear transformations to understand best the essence of rigid-body kinematics, an area that is covered in great detail throughout the book. A unique feature of this chapter is the discussion of the hand-eye calibration problem: Many a paper has been written in an attempt to solve this fundamental problem, always leading to a cumbersome solution that invokes nonlinear-equation solving, a task that invariably calls for an iterative procedure; moreover, within each iteration, a singular-value decomposition, itself iterative as well, is required. In Chapter 2, a novel approach is introduced, which resorts to invariant properties of rotations and leads to a *direct solution*, involving straightforward matrix and vector multiplications. Chapter 3 reviews, in turn, the basic theorems of rigid-body kinetostatics and dynamics. The viewpoint here represents a major departure from most existing books on robotic manipulators: proper orthogonal matrices can be regarded as coordinate transformations indeed, but they can also be regarded as representations, once a coordinate frame has been selected, of rigid-body rotations. I adopt the latter viewpoint, and hence, fundamental concepts are explained in terms of their invariant properties, i.e., properties that are independent of the coordinate frame adopted. Hence, matrices are used first and foremost to represent the physical motions undergone by rigid bodies and systems thereof; they are to be interpreted as such when studying the basics of rigid-body mechanics in this chapter. Chapter 4 is the first chapter entirely devoted to robotic mechanical systems, properly speaking. This chapter covers extensively the kinematics of robotic manipulators of the serial type. However, as far as displacement analysis is concerned, the chapter limits itself to the simplest robotic manipulators, namely, those with a *decoupled architecture*, i.e., those that can be decomposed into a *regional architecture* for the positioning of one point of their end-effector (EE), and a *local architecture* for the orientation of their EE. In this chapter, the notation of Denavit and Hartenberg is introduced and applied consistently throughout the book. Jacobian matrices, workspaces, singularities, and kinetostatic performance indices are concepts studied in this chapter. A novel algorithm is included for the determination of the workspace boundary of positioning manipulators. Furthermore, Chapter 5 is devoted to the topic of trajectory planning, while limiting its scope to problems suitable to a first course on robotics; this chapter thus focuses on pick-and-place operations. Chapter 6, moreover, introduces the dynamics of robotic manipulators of the serial type, while discussing extensively the recursive Newton-Euler algorithm and laying the foundations of multibody dynamics, with an introduction to the Euler-Lagrange formulation. The latter is used to derive the general algebraic structure of the mathematical models of the systems under study, thus completing the introductory part

of the book.

The intermediate part comprises four chapters. Chapter 7 is devoted to the increasingly important problem of determining the angular velocity and the angular acceleration of a rigid body, when the velocity and acceleration of a set of its points are known. Moreover, given the intermediate level of the chapter, only the theoretical aspects of the problem are studied, and hence, perfect measurements of point position, velocity, and acceleration are assumed, thereby laying the foundations for the study of the same problems in the presence of noisy measurements. This problem is finding applications in the control of parallel manipulators, which is the reason why it is included here. If time constraints so dictate, this chapter can be omitted, for it is not needed in the balance of the book.

The formulation of the inverse kinematics of the most general robotic manipulator of the serial type, leading to a univariate polynomial of the 16th degree, not discussed in previous books on robotics, is included in Chapter 8. Likewise, the direct kinematics of the platform manipulator popularly known as the *Stewart platform*, a.k.a. the *Stewart-Gough platform*, leading to a 16th-degree monovariate polynomial, is also given due attention in this chapter. Moreover, an alternative approach to the monovariate-polynomial solution of the two foregoing problems, that is aimed at solving them *semi-graphically*, is introduced in this chapter. With this approach, the underlying multivariate algebraic system of equations is reduced to a system of two nonlinear bivariate equations that are trigonometric rather than polynomial. Each of these two equations, then, leads to a contour in the plane of the two variables, the desired solutions being found as the coordinates of the intersections of the two contours.

Discussed in Chapter 9 is the problem of trajectory planning as pertaining to continuous paths, which calls for some concepts of differential geometry, namely, the Frenet-Serret equations relating the tangent, normal, and binormal vectors of a smooth curve to their rates of change with respect to the arc length. The chapter relies on cubic parametric splines for the synthesis of the generated trajectories in joint space, starting from their descriptions in Cartesian space. Finally, Chapter 10 completes the discussion initiated in Chapter 6, with an outline of the dynamics of parallel manipulators and rolling robots. Here, a multibody dynamics approach is introduced, as in the foregoing chapter, that eases the formulation of the underlying mathematical models.

Two appendices are included: Appendix A summarizes a series of facts from the kinematics of rotations, that are available elsewhere, with the purpose of rendering the book self-contained; Appendix B is devoted to the numerical solution of over- and underdetermined linear algebraic systems, its purpose being to guide the reader to the existing robust techniques for the computation of least-square and minimum-norm solutions. The book concludes with a set of problems, along with a list of references, for all ten chapters.

On Notation

The important issue of notation is given due attention. In figuring out the notation, I have adopted what I call the C^3 *norm*. Under this norm, the notation should be

1. *C*omprehensive,
2. *C*oncise, and
3. *C*onsistent.

Within this norm, I have used boldface fonts to indicate vectors and matrices, with uppercases reserved for matrices and lowercases for vectors. In compliance with the invariant approach adopted at the outset, I do not regard vectors solely as arrays, but as geometric or mechanical objects. Regarding such objects as arrays is necessary only when it is required to perform operations with them for a specific purpose. An essential feature of vectors in a discussion is their dimension, which is indicated with a single number, as opposed to the convention whereby vectors are regarded as matrix arrays of numbers; in this convention, the dimension has to be indicated with two numbers, one for the number of columns, and one for the number of rows; in the case of vectors, the latter is always one, and hence, need not be mentioned. Additionally, calligraphic literals are reserved for sets of points or of other objects. Since variables are defined every time that they are introduced, and the same variable is used in the book to denote different concepts in different contexts, a list of symbols is not included.

How to Use the Book

The book can be used as a reference or as a text for the teaching of the mechanics of robots to an audience that ranges from junior undergraduates to doctoral students. In an introductory course, the instructor may have to make choices regarding what material to skip, given that the duration of a regular semester does not allow to cover all that is included in the first six chapters. Topics that can be skipped, if time so dictates, are the discussions, in Chapter 4, of workspaces and performance indices, and the section on simulation in Chapter 6. Under strict time constraints, the whole Chapter 5 can be skipped, but then, the instructor will have to refrain from assigning problems or projects that include calculating the inverse dynamics of a robot performing pick-and-place operations. None of these has been included in Section 6 of the Exercises.

If sections of Chapters 4 and 5 have been omitted in a first course, it is highly advisable to include them in a second course, prior to discussing the chapters included in the intermediate part of the book.

Acknowledgements

For the technical support received during the writing of this book, I am indebted to many people: First and foremost, Eric Martin and Ferhan Bulca, Ph.D. candidates under my cosupervision, are deeply thanked for their invaluable help and unlimited patience in the editing of the manuscript and the professional work displayed in the production of the drawings. With regard to this task, Dr. Max A. González-Palacios, currently Assistant Professor of Mechanical Engineering at Universidad Iberoamericana at León, Mexico, is due special recognition for the high standards he set while working on his Ph.D. at McGill University. My colleagues Ken J. Waldron, Clément Gosselin, and Jean-Pierre Merlet contributed with constructive criticism. Dr. Andrés Kecskeméthy proofread major parts of the manuscript during his sabbatical leave at McGill University. In doing this, Dr. Kecskeméthy corrected a few derivations that were flawed. Discussions on geometry and analysis held with Dr. Manfred Husty, of Leoben University, in Austria, also a sabbaticant at McGill University, were extremely fruitful in clearing up many issues in Chapters 2 and 3. An early version of the manuscript was deeply scrutinized by Meyer Nahon, now Associate Professor at the University of Victoria, when he was completing his Ph.D. at McGill University. Discussions with Farzam Ranjbaran, a Ph.D. candidate at McGill University, on kinetostatic performance indices, helped clarify many concepts around this issue. Dr. Kourosh Etemadi Zanganeh contributed with ideas for a more effective discussion of the parametric representation of paths in Chapter 9 and with some of the examples in Chapters 4 and 8 during his work at McGill University as a Ph.D. student. The material supplied by Clément Gosselin on trajectory planning helped me start the writing of Chapter 5. All individuals and institutions who contributed with graphical material are given due credit in the book. Here, they are all deeply acknowledged.

A turning point in writing this manuscript was the academic year 1991–1992, during which I could achieve substantial progress while on sabbatical leave at the Technical University of Munich under an Alexander von Humboldt Research Award. Deep gratitude is expressed here to both the AvH Foundation and Prof. Friedrich Pfeiffer, Director of the Institute B for Mechanics and my host in Munich. Likewise, Prof. Manfred Broy, of the Computer Science Institute at the Technical University of Munich, is herewith acknowledged for having given me access to his Unix network when the need arose. The intellectual environment at the Technical University of Munich was a source of encouragement and motivation to pursue the writing of the book.

Moreover, financial support from NSERC[2] and Quebec's FCAR, [3] in the form of research and strategic grants, are duly acknowledged. IRIS,[4] a

[2]Natural Sciences and Engineering Research Council, of Canada.
[3]*Fonds pour la formation de chercheurs et l'aide à la recherche.*
[4]Institute for Robotics and Intelligent Systems.

network of Canadian centers of excellence, supported this work indirectly through project grants in the areas of robot design and robot control. An invaluable tool in developing material for the book proved to be RVS, the McGill Robot Visualization System, developed in the framework of an NSERC Strategic Grant on robot design, and the two IRIS project grants mentioned above. RVS was developed by John Darcovich, a Software Engineer at McGill University for about four years, and now at CAE Electronics Ltd., of Saint-Laurent, Quebec. While RVS is user-friendly and available upon request, no technical support is offered. For further details on RVS, the reader is invited to look at the home page of the McGill University Centre for Intelligent Machines:

`http://www.cim.mcgill.ca/~rvs`

Furthermore, Lenore Reismann, a professional technical editor based in Redwood City, California, proofread parts of the manuscript and edited its language with great care. Lenore's professional help is herewith highly acknowledged. Dr. Rüdiger Gebauer, mathematics editor at Springer-Verlag New York, is gratefully acknowledged for his encouragement in pursuing this project. Springer-Verlag's Dr. Thomas von Foerster is likewise acknowledged for the care with which he undertook the production of the book, while his colleague Steven Pisano, for his invaluable help in the copyediting of the final draft. Steven and his staff not only took care of the fine points of the typesetting, but also picked up a few technical flaws in that draft. Last, but not least, may I acknowledge the excellent facilities and research environment provided by the Centre for Intelligent Machines, the Department of Mechanical Engineering of McGill University, and McGill University as a whole, which were instrumental in completing this rather lengthy project.

Montreal, December 1996 Jorge Angeles

This page intentionally left blank

Contents

This page intentionally left blank

1

An Overview of Robotic Mechanical Systems

1.1 Introduction

In defining the scope of our subject, we have to establish the genealogy of robotic mechanical systems. These are, obviously, a subclass of the much broader class of *mechanical systems*. Mechanical systems, in turn, constitute a subset of the more general concept of *dynamic systems*. Therefore, in the final analysis, we must have an idea of what, in general, a *system* is.

The *Concise Oxford Dictionary* defines system as a "complex whole, set of connected things or parts, organized body of material or immaterial things," whereas the *Random House College Dictionary* defines the same as "an assemblage or combination of things or parts forming a complex or unitary whole." *Le Petit Robert*, in turn, defines system as "Ensemble possédant une structure, constituant un tout organique," which can be loosely translated as "A structured assemblage constituting an organic whole." In the foregoing definitions, we note that the underlying idea is that of a set of elements interacting as a whole.

On the other hand, a *dynamic system* is a subset of the set of systems. For our purposes, we can dispense with a rigorous definition of this concept. Suffice it to say that a dynamic system is a system in which one can distinguish three elements, namely, a *state*, an *input*, and an *output*, in addition to a rule of transition from one current state to a future one. Moreover, the state is a *functional* of the input and a function of a *previous* state. In

this concept, then, the idea of order is important, and can be taken into account by properly associating each state value with time. The state at every instant is a functional, as opposed to a function, of the input, which is characteristic of dynamic systems. This means that the state of a dynamic system at a certain instant is determined not only by the value of the input at that instant, but also by the past history of that input. By virtue of this property, dynamic systems are said to have *memory*.

On the contrary, systems whose state at a given instant is only a *function* of the input at the current time are static and are said to have no memory. Additionally, since the state of a dynamic system is a result of all the past history of the input, the future values of this having no influence on the state, dynamic systems are said to be *nonanticipative* or *causal*. By the same token, systems whose state is the result of future values of the input are said to be *anticipative* or *noncausal*. In fact, we will not need to worry about the latter, and hence, all systems we will study can be assumed to be causal.

Obviously, a mechanical system is a system composed of mechanical elements. If this system complies with the definition of dynamic system, then we end up with a *dynamic mechanical system*. For brevity, we will refer to such systems as *mechanical systems*, the dynamic property being taken for granted throughout the book. Mechanical systems of this type are those that occur whenever the inertia of their elements is accounted for. Static mechanical systems are those in which inertia is neglected. Moreover, the elements constituting a mechanical system are rigid and deformable solids, compressible and incompressible fluids, and inviscid and viscous fluids.

From the foregoing discussion, then, it is apparent that mechanical systems can be constituted either by lumped-parameter or by distributed-parameter elements. The former reduce to particles; rigid bodies; massless, conservative springs; and massless, nonconservative dashpots. The latter appear whenever bodies are modeled as continuous media. In this book, we will focus on lumped-parameter mechanical systems.

Furthermore, a mechanical system can be either natural or man-made, the latter being the subject of our study. Man-made mechanical systems can be either controlled or uncontrolled. Most engineering systems are controlled mechanical systems, and hence, we will focus on these. Moreover, a controlled mechanical system may be *robotic* or nonrobotic. The latter are systems supplied with primitive controllers, mostly analog, such as thermostats, servovalves, etc. Robotic mechanical systems, in turn, can be *programmable*, such as most current industrial robots, or *intelligent*, as discussed below. Programmable mechanical systems obey motion commands either stored in a memory device or generated on-line. In either case, they need primitive sensors, such as joint encoders, accelerometers, and dynamometers.

Intelligent robots or, more broadly speaking, *intelligent machines*, are yet to be demonstrated, but have become the focus of intensive research.

If intelligent machines are ever feasible, they will depend highly on a sophisticated sensory system and the associated hardware and software for the processing of the information supplied by the sensors. The processed information would then be supplied to the actuators in charge of producing the desired motion of the robot. Contrary to programmable robots, whose operation is limited to *structured environments*, intelligent machines should be capable of reacting to unpredictable changes in an *unstructured environment*. Thus, intelligent machines should be supplied with decision-making capabilities aimed at mimicking the natural decision-making process of living organisms. This is the reason why such systems are termed intelligent in the first place. Thus, intelligent machines are expected to *perceive* their environment and draw conclusions based on this perception. What is supposed to make these systems *intelligent* is their capability of perceiving, which involves a certain element of subjectivity. By far, the most complex of perception tasks, both in humans and machines, is visual (Levine, 1985; Horn, 1986).

In summary, then, an intelligent machine is expected to (*i*) *perceive* the environment; (*ii*) *reason* about the perceived information; (*iii*) *make decisions* based on this perception; and (*iv*) *act* according to a plan specified at a very high level. What the latter means is that the motions undergone by the machine are decided upon based on instructions similar to those given to a human being, like *bring me a glass of water without spilling the water*.

Whether intelligent machines with all the above features will be one day possible or not is still a subject of discussion, sometimes at a philosophical level. Penrose (1994) wrote a detailed discussion refuting the claim that intelligent machines are possible.

A genealogy of mechanical systems, including robotic ones, is given in Fig. 1.1. In that figure, we have drawn a dashed line between mechanical systems and other systems, both man-made and natural, in order to emphasize the interaction of mechanical systems with electrical, thermal, and other systems, including the human system, which is present in telemanipulators, to be discussed below.

1.2 The General Structure of Robotic Mechanical Systems

From Section 1.1, then, a robotic mechanical system is composed of a few subsystems, namely, (*i*) a mechanical subsystem composed in turn of both rigid and deformable bodies, although the systems we will study here are composed only of the former; (*ii*) a sensing subsystem; (*iii*) an actuation subsystem; (*iv*) a controller; and (*v*) an information-processing subsystem. Additionally, these subsystems communicate among themselves via *interfaces*, whose function consists basically of decoding the transmitted information from one medium to another. Figure 1.2 shows a block diagram

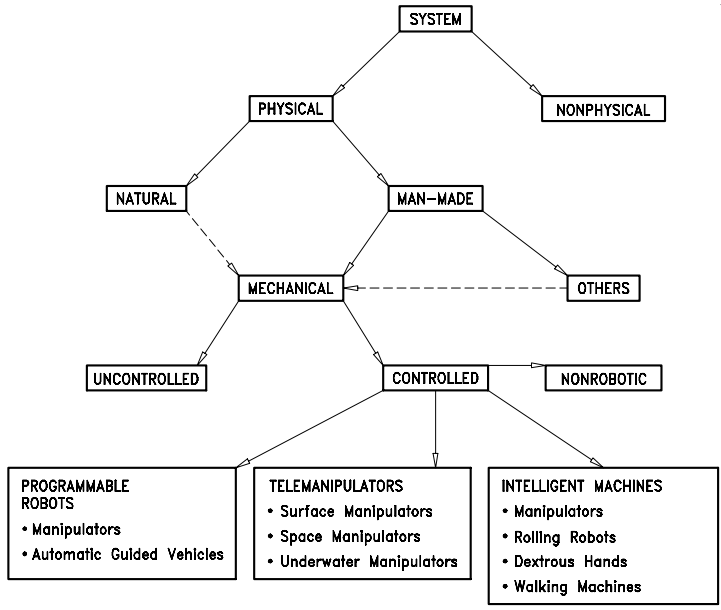

FIGURE 1.1. A genealogy of robotic mechanical systems.

representation of a typical robotic mechanical system. Its input is a *prescribed task*, which is defined either on the spot or off-line. The former case is essential for a machine to be called intelligent, while the latter is present in programmable machines. Thus, tasks would be described to intelligent machines by a software system based on techniques of artificial intelligence (AI). This system would replace the human being in the decision-making process. Programmable robots require human intervention either for the coding of preprogrammed tasks at a very low level or for *telemanipulation*. A very low level of programming means that the motions of the machine are specified as a sequence of either joint motions or Cartesian coordinates associated with landmark points of that specific body performing the task at hand. The output of a robotic mechanical system is the *actual task*, which is monitored by the sensors. The sensors, in turn, transmit task information in the form of feedback signals, to be compared with the prescribed task. The errors between the prescribed and the actual task are then fed back into the controller, which then synthesizes the necessary corrective signals. These are, in turn, fed back into the actuators, which then drive the mechanical system through the required task, thereby closing the loop. The problem of robot control has received extensive attention in the literature, and will not be pursued here. The interested reader is referred to the excellent works on the subject, e.g., those of Samson, Le Borgne, and Espiau (1991) and, at a more introductory level, of Spong and Vidyasagar (1989).

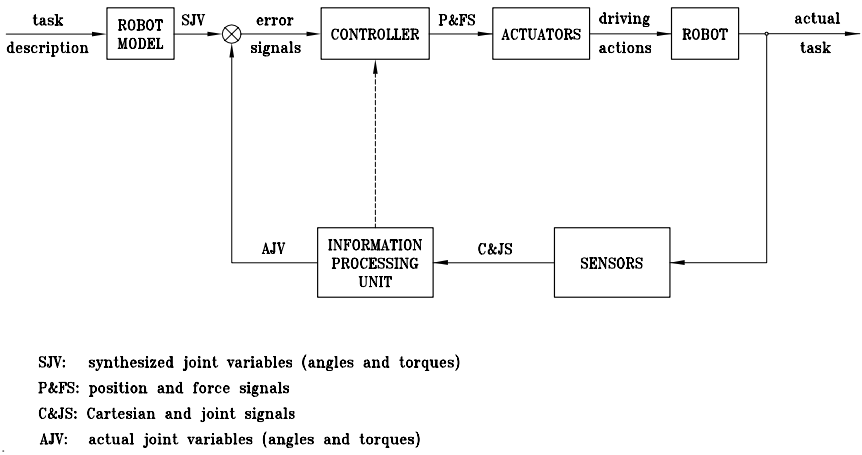

FIGURE 1.2. Block diagram of a general robotic mechanical system.

Of special relevance to robot control is the subject of nonlinear control at large, a pioneer here being Isidori (1989).

Robotic mechanical systems with a human being in their control loop are called *telemanipulators*. Thus, a telemanipulator is a robotic mechanical system in which the task is controlled by a human, possibly aided by sophisticated sensors and display units. The human operator is then a central element in the block diagram loop of Fig. 1.2. Based on the information displayed, the operator makes decisions about corrections in order to accomplish the prescribed task. Shown in Fig. 1.3 is a telemanipulator to be used in space applications, namely, the *Canadarm2*, along with the *Special-Purpose Dextrous Manipulator* (SPDM), both mounted on the *Mobile Servicing System* (MSS). Moreover, a detailed view of the Special-Purpose Dextrous Manipulator is shown in Fig. 1.4. In the manipulators of these two figures, the human operator is an astronaut who commands and monitors the motions of the robot from inside the EVA (extravehicular activity) workstation. The number of controlled axes of each of these manipulators being larger than six, both are termed *redundant*. The challenge here is that the mapping from task coordinates to joint motions is not unique, and hence, among the infinitely many joint trajectories that the operator has at his or her disposal for a given task, an on-board processor must evaluate the best one according to a performance criterion.

While the manipulators of Figs. 1.3 and 1.4 are still at the development stage, examples of robotic mechanical systems in operation are the well-known six-axis industrial manipulators, six-degree-of-freedom flight simulators, walking machines, mechanical hands, and rolling robots. We outline the various features of these systems below.

FIGURE 1.3. Canadarm2 and Special-Purpose Dextrous Manipulator (courtesy of the Canadian Space Agency.)

1.3 Serial Manipulators

Among all robotic mechanical systems mentioned above, robotic manipulators deserve special attention, for various reasons. One is their relevance in industry. Another is that they constitute the simplest of all robotic mechanical systems, and hence, appear as constituents of other, more complex robotic mechanical systems, as will become apparent in later chapters. A manipulator, in general, is a mechanical system aimed at *manipulating* objects. Manipulating, in turn, means to move something with one's hands, as it derives from the Latin *manus*, meaning *hand*. The basic idea behind the foregoing concept is that hands are among the organs that the human brain can control mechanically with the highest accuracy, as the work of an artist like Picasso, of an accomplished guitar player, or of a surgeon can attest.

Hence, a manipulator is any device that helps man perform a manipulating task. Although manipulators have existed ever since man created the first tool, only very recently, namely, by the end of World War II, have manipulators developed to the extent that they are now capable of actually mimicking motions of the human arm. In fact, during WWII, the need arose for manipulating probe tubes containing radioactive substances. This led to the first six-degree-of-freedom (DOF) manipulators.

Shortly thereafter, the need for manufacturing workpieces with high accuracy arose in the aircraft industry, which led to the first numerically-controlled (NC) machine tools. The synthesis of the six-DOF manipulator

FIGURE 1.4. Special-Purpose Dextrous Manipulator (courtesy of the Canadian Space Agency.)

and the NC machine tool produced what became the *robotic manipulator*. Thus, the essential difference between the early manipulator and the evolved *robotic* manipulator is the term *robotic*, which has only recently, as of the late sixties, come into the picture. A robotic manipulator is to be distinguished from the early manipulator by its capability of lending itself to *computer control*. Whereas the early manipulator needed the presence of a manned *master manipulator*, the robotic manipulator can be programmed once and for all to repeat the same task forever. Programmable manipulators have existed for about 30 years, namely, since the advent of microprocessors, which allowed a human master to *teach* the manipulator by actually driving the manipulator itself, or a replica thereof, through a desired task, while recording all motions undergone by the master. Thus, the manipulator would later repeat the identical task by mere playback. However, the capabilities of industrial robots are fully exploited only if the manipulator is programmed with software, rather than actually driving it through its task trajectory, which many a time, e.g., in car-body spot-welding, requires separating the robot from the production line for more than a week. One of the objectives of this book is to develop tools for the programming of robotic manipulators.

However, the capabilities offered by robotic mechanical systems go well beyond the mere playback of preprogrammed tasks. Current research aims at providing robotic systems with software and hardware that will allow them to make decisions on the spot and learn while performing a task. The implementation of such systems calls for task-planning techniques that fall beyond the scope of this book and, hence, will not be treated here. For a glimpse of such techniques, the reader is referred to the work of Latombe (1991) and the references therein.

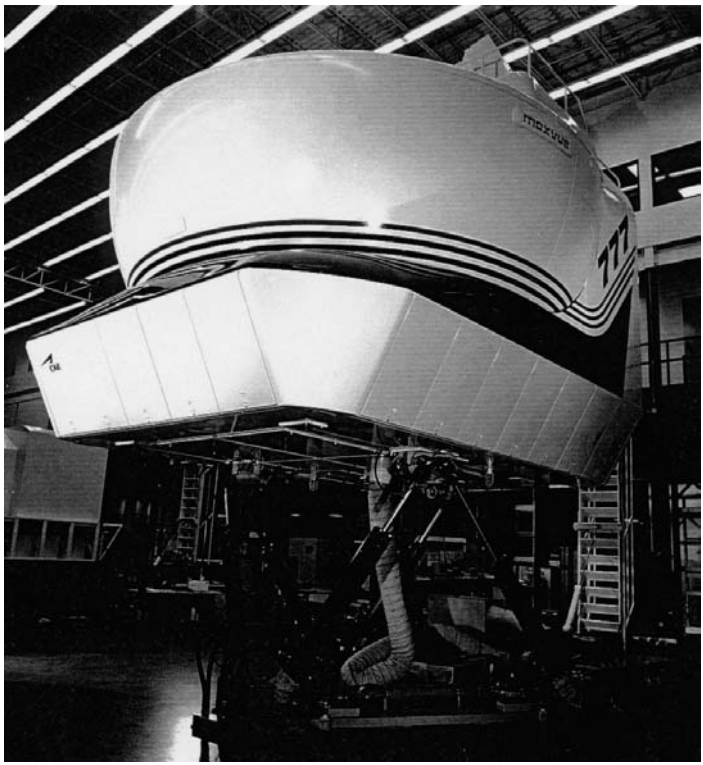

FIGURE 1.5. A six-degree-of-freedom flight simulator (courtesy of CAE Electronics Ltd.)

1.4 Parallel Manipulators

Robotic manipulators first appeared as mechanical systems constituted by a structure consisting of very robust links coupled by either rotational or translating joints, the former being called *revolutes*, the latter *prismatic joints*. Moreover, these structures are a *concatenation* of links, thereby forming an *open kinematic chain*, with each link coupled to a predecessor and a successor, except for the two end links, which are coupled only to either a predecessor or to a successor, but not to both. Because of the *serial* nature of the coupling of links in this type of manipulator, even though they are supplied with structurally robust links, their load-carrying capacity and their stiffness is too low when compared with the same properties in other multiaxis machines, such as NC machine tools. Obviously, a low stiffness implies a low positioning accuracy. In order to remedy these drawbacks, *parallel manipulators* have been proposed to withstand higher payloads with lighter links. In a parallel manipulator, we distinguish one *base platform*, one *moving platform*, and various *legs*. Each leg is, in turn, a kinematic chain of the serial type, whose end links are the two platforms. Contrary to serial manipulators, all of whose joints are actuated, parallel manipulators contain unactuated joints, which brings about a substantial

difference between the two types. The presence of unactuated joints makes the analysis of parallel manipulators, in general, more complex than that of their serial counterparts.

A paradigm of parallel manipulators is the flight simulator, consisting of six legs actuated by hydraulic pistons, as displayed in Fig. 1.5. Recently, an explosion of novel designs of parallel manipulators has occurred aimed at fast assembly operations, namely, the Delta robot (Clavel, 1988), developed at the Lausanne Federal Polytechnic Institute, shown in Fig. 1.6; the Hexa robot (Pierrot et al., 1991), developed at the University of Montpellier; and the Star robot (Hervé and Sparacino, 1992), developed at the *Ecole Centrale* of Paris. One more example of parallel manipulator is the *Truss-arm*, developed at the University of Toronto Institute of Aerospace Studies (UTIAS), shown in Fig. 1.7a (Hughes et al., 1991). Merlet (2000), of the *Institut National de Recherche en Informatique et en Automatique*, Sophia-Antipolis, France, developed a six-axis parallel robot, called in French a *main gauche*, or left hand, shown in Fig. 1.7b, to be used as an aid to another robot, possibly of the serial type, to enhance its dexterity. Hayward, of McGill University, designed and constructed a parallel manipulator to be used as a shoulder module for orientation tasks (Hayward, 1994); the module is meant for three-degree-of-freedom motions, but is provided with four hydraulic actuators, which gives it redundant actuation—Fig. 1.7c.

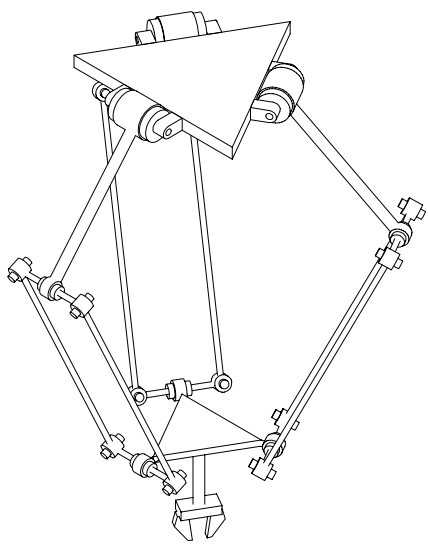

FIGURE 1.6. The Clavel Delta robot.

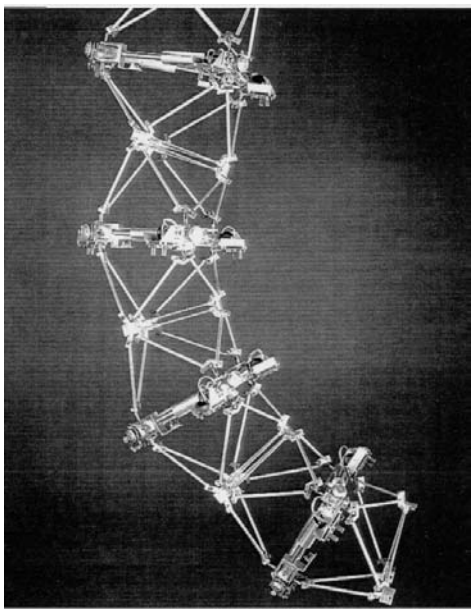

(a)

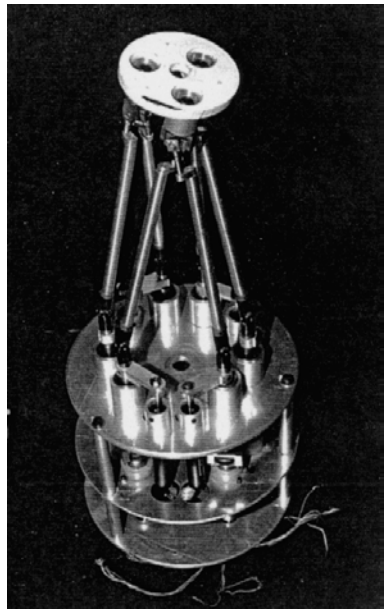

(b)

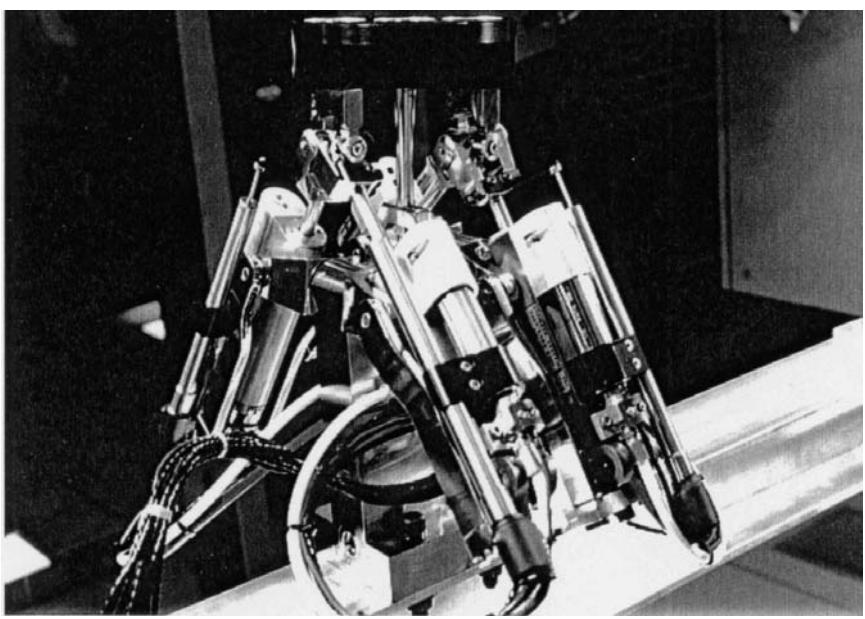

(c)

FIGURE 1.7. A sample of parallel manipulators: (a) The UTIAS Trussarm (courtesy of Prof. P. C. Hughes); (b) the Merlet left hand (courtesy of Dr. J.-P. Merlet); and (c) the Hayward shoulder module (courtesy of Prof. V. Hayward.)

1.5 Robotic Hands

As stated above, the hand can be regarded as the most complex mechanical subsystem of the human manipulation system. Other mechanical subsystems constituting this system are the arm and the forearm. Moreover, the shoulder, coupling the arm with the torso, can be regarded as a *spherical joint*, i.e., the concatenation of three revolute joints with intersecting axes. Furthermore, the arm and the forearm are coupled via the elbow, with the forearm and the hand finally being coupled by the wrist. Frequently, the wrist is modeled as a spherical join as well, while the elbow is modeled as a simple revolute joint. Robotic mechanical systems mimicking the motions of the arm and the forearm constitute the manipulators discussed in the previous section. Here we outline more sophisticated manipulation systems that aim at producing the motions of the human hand, i.e., robotic mechanical hands. These robotic systems are meant to perform *manipulation* tasks, a distinction being made between *simple manipulation* and *dextrous manipulation*. What the former means is the simplest form, in which the fingers play a minor role, namely, by serving as simple static structures that keep an object rigidly attached with respect to the palm of the hand—when the palm is regarded as a rigid body. As opposed to simple manipulation, dextrous manipulation involves a controlled motion of the grasped object with respect to the palm. Simple manipulation can be achieved with the aid of a manipulator and a gripper, and need not be further discussed here. The discussion here is about dextrous manipulation.

In dextrous manipulation, the grasped object is required to move with respect to the palm of the grasping hand. This kind of manipulation appears in performing tasks that require high levels of accuracy, like handwriting or cutting tissue with a scalpel. Usually, grasping hands are multifingered, although some grasping devices exist that are constituted by a simple, open, highly redundant *kinematic chain* (Pettinato and Stephanou, 1989). The kinematics of grasping is discussed in Chapter 4. The basic kinematic structure of a multifingered hand consists of a palm, which plays the role of the base of a simple manipulator, and a set of fingers. Thus, kinematically speaking, a multifingered hand has a *tree topology*, i.e., it entails a common rigid body, the palm, and a set of jointed bodies emanating from the palm. Upon grasping an object with all the fingers, the chain becomes closed with multiple loops. Moreover, the architecture of the fingers is that of a simple manipulator. It consists of a number—two to four—of revolute-coupled links playing the role of phalanges. However, unlike manipulators of the serial type, whose joints are all independently actuated, those of a mechanical finger are not and, in many instances, are driven by one single master actuator, the remaining joints acting as slaves. Many versions of multifingered hands exist: Stanford/JPL; Utah/MIT; TU Munich; Karlsruhe; Bologna; Leuven; Milan; Belgrade; and University of Toronto, among

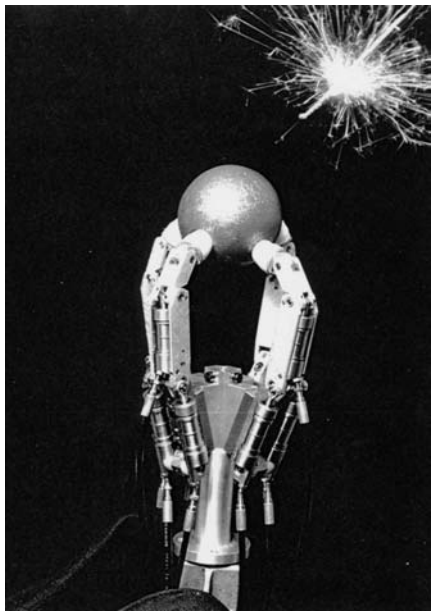

FIGURE 1.8. The four-fingered hydraulically actuated TU Munich Hand (courtesy of Prof. F. Pfeiffer.)

others. Of these, the Utah/MIT Hand (Jacobsen et al., 1984; 1986) is commercially available. It consists of four fingers, one of which is opposed to the other three and hence, plays the role of the human thumb. Each finger consists, in turn, of four phalanges coupled by revolute joints; each of these is driven by two tendons that can deliver force only when in tension, each being actuated independently. The TU Munich Hand, shown in Fig. 1.8, is designed with four identical fingers laid out symmetrically on a hand palm. This hand is hydraulically actuated, and provided with a very high payload-to-weight ratio. Indeed, each finger weighs only 1.470 N, but can exert a force of up to 30 N.

We outline below some problems and research trends in the area of dextrous hands. A key issue here is the programming of the motions of the fingers, which is a much more complicated task than the programming of a six-axis manipulator. In this regard, Liu et al. (1989) introduced a task-analysis approach meant to program robotic hand motions at a higher level. They use a heuristic, knowledge-based approach. From an analysis of the various modes of grasping, they conclude that the requirements for grasping tasks are (*i*) stability, (*ii*) manipulability, (*iii*) torquability, and (*iv*) radial rotatability. Stability is defined as a measure of the tendency of an object to return to its original position after disturbances. Manipulability, as understood in this context, is the ability to impart motion to the object while keeping the fingers in contact with the object. Torquability, or tangential rotatability, is the ability to rotate the long axis of an object—here the authors must assume that the manipulated objects are

convex and can be approximated by three-axis ellipsoids, thereby distinguishing between a longest and a shortest axis—with a minimum force, for a prescribed amount of torque. Finally, radial rotatability is the ability to rotate the grasped object about its long axis with minimum torque about the axis.

Furthermore, Allen et al. (1989) introduced an integrated system of both hardware and software for dextrous manipulation. The system consists of a Sun-3 workstation controlling a Puma 500 arm with VAL-II. The Utah/MIT hand is mounted on the end-effector of the arm. The system integrates force and position sensors with control commands for both the arm and the hand. To demonstrate the effectiveness of their system, the authors implemented a task consisting of removing a light bulb from its socket. Finally, Rus (1992) reports a paradigm allowing the high-level, task-oriented manipulation control of planar hands. Whereas technological aspects of dextrous manipulation are highly advanced, theoretical aspects are still under research in this area. An extensive literature survey, with 405 references on the subject of manipulation, is given by Reynaerts (1995).

1.6 Walking Machines

We focus here on multilegged walking devices, i.e., machines with more than two legs. In walking machines, stability is the main issue. One distinguishes between two types of stability, static and dynamic. Static stability refers to the ability of sustaining a configuration from reaction forces only, unlike dynamic stability, which refers to that ability from both reaction and inertia forces. Intuitively, it is apparent that static stability requires more contact points and, hence, more legs, than dynamic stability. Hopping devices (Raibert, 1986) and bipeds (Vukobratovic and Stepanenko, 1972) are examples of walking machines whose motions aredependent upon dynamic stability. For static balance, a walking machine requires a kinematic structure capable of providing the ground reaction forces needed to balance the weight of the machine. A biped is not capable of static equilibrium because during the swing phase of one leg, the body is supported by a single contact point, which is incapable of producing the necessary balancing forces to keep it in equilibrium. For motion on a horizontal surface, a minimum of three legs is required to produce static stability. Indeed, with three legs, one of these can undergo swing while the remaining two legs are in contact with the ground, and hence, two contact points are present to provide the necessary balancing forces from the ground reactions.

By the same token, the minimum number of legs required to sustain static stability in general is four, although a very common architecture of walking machines is the hexapod, examples of which are the Ohio State University (OSU) Hexapod (Klein et al., 1983) and the OSU Adaptive Suspension Vehicle (ASV) (Song and Waldron, 1989), shown in Fig. 1.10. A six-legged

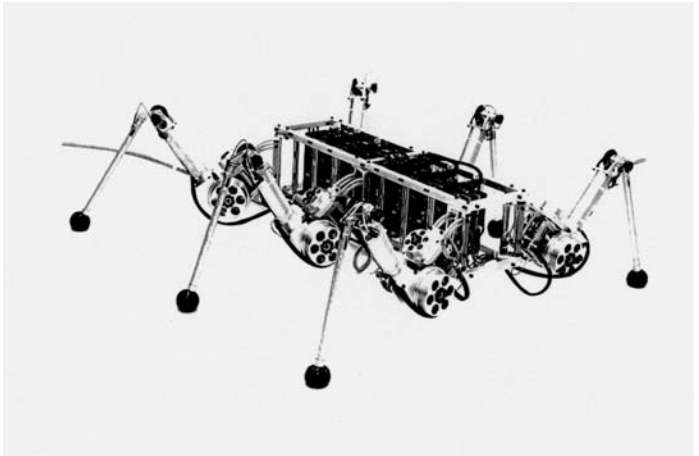

FIGURE 1.9. A prototype of the TU Munich Hexapod (Courtesy of Prof. F. Pfeiffer. Reproduced with permission of TSI Enterprises, Inc.)

walking machine with a design that mimics the locomotion system of the *Carausius morosus* (Graham, 1972), also known as the *walking stick*, has been developed at the Technical University of Munich (Pfeiffer et al., 1995). A prototype of this machine, known as the *TUM Hexapod*, is included in Fig. 1.9. The legs of the TUM Hexapod are operated under neural-network control, which gives them a reflexlike response when encountering obstacles. Upon sensing an obstacle, the leg bounces back and tries again to move forward, but raising the foot to a higher level.

Other machines that are worth mentioning are the Sutherland, Sprout and Associates Hexapod (Sutherland and Ullner, 1984), the Titan series of quadrupeds (Hirose et al., 1985) and the Odetics series of axially symmetric hexapods (Russell, 1983).

A survey of walking machines, of a rather historical interest by now, is given in (Todd, 1985), while a more recent comprehensive account of walking machines is available in a special issue of *The International Journal of Robotics Research* (Volume 9, No. 2).

Walking machines appear as the sole means of providing locomotion in highly unstructured environments. In fact, the unique adaptive suspension provided by these machines allows them to navigate on uneven terrain. However, walking machines cannot navigate on every type of uneven terrain, for they are of limited dimensions. Hence, if terrain irregularities such as a crevasse wider than the maximum horizontal leg reach or a cliff of depth greater than the maximum vertical leg reach are present, then the machine is prevented from making any progress. This limitation, however, can be overcome by providing the machine with the capability of attaching its feet to the terrain in the same way as a mountain climber goes up a cliff. Moreover, machine functionality is limited not only by the topography of the terrain, but also by its constitution. Whereas hard rock poses no serious problem to a walking machine, muddy terrain can hamper its operation to

FIGURE 1.10. The OSU ASV. An example of a six-legged walking machine (courtesy of Prof. K. Waldron. Reproduced with permission of The MIT Press.)

the point that it may jam the machine. Still, under such adverse conditions, walking machines offer a better maneuverability than other vehicles. Some walking machines have been developed and are operational, but their operation is often limited to slow motions. It can be said, however, that like research on multifingered hands, the pace of theoretical research on walking machines has been much slower than that of their technological developments. The above-mentioned OSU ASV and the TU Munich Hexapod are among the most technologically developed walking machines.

1.7 Rolling Robots

While parallel manipulators indeed solve many inherent problems of serial manipulators, their workspaces are more limited than those of the latter. As a matter of fact, even serial manipulators have limited workspaces due to the finite lengths of their links. Manipulators with limited workspaces can be enhanced by mounting them on rolling robots. These are systems evolved from earlier systems called *automatic guided vehicles*, or AGVs for short. AGVs in their most primitive versions are four-wheeled electrically powered vehicles that perform moving tasks with a certain degree of autonomy. However, these vehicles are usually limited to motions along predefined tracks that are either railways or magnetic strips glued to the ground.

The most common rolling robots use conventional wheels, i.e., wheels consisting basically of a pneumatic tire mounted on a hub that rotates

about an axle fixed to the platform of the robot. Thus, the operation of these machines does not differ much from that of conventional terrestrial vehicles. An essential difference between rolling robots and other robotic mechanical systems is the kinematic constraints between wheel and ground in the former. These constraints are of a type known as *nonholonomic*, as discussed in detail in Chapter 6. Nonholonomic constraints are kinematic relations between point velocities and angular velocities that cannot be integrated in the form of algebraic relations between translational and rotational displacement variables. The outcome of this lack of integrability leads to a lack of a one-to-one relationship between Cartesian variables and joint variables. In fact, while angular displacements read by joint encoders of serial manipulators determine uniquely the position and orientation of their end-effector, the angular displacement of the wheels of rolling machines do not determine the position and orientation of the vehicle body. As a matter of fact, the control of rolling robots bears common features with that of the redundancy resolution of manipulators of the serial type at the joint-rate level. In these manipulators, the number of actuated joints is greater than the dimension of the task space. As a consequence, the task velocity does not determine the joint rates. Not surprisingly, the two types of problems are being currently solved using the same tools, namely, differential geometry and Lie algebra (De Luca and Oriolo, 1995).

As a means to supply rolling robots with 3-dof capabilities, omnidirectional wheels (ODW) have been proposed. An example of ODWs are those that bear the name of *Mekanum* wheels, consisting of a hub with rollers on its periphery that roll freely about their axes, the latter being oriented at a constant angle with respect to the hub axle. In Fig. 1.11, a Mekanum wheel is shown, along with a rolling robot supplied with this type of wheels. Rolling robots with ODWs are, thus, 3-dof vehicles, and hence, can translate freely in two horizontal directions and rotate independently about a vertical axis. However, like their 2-dof counterparts, 3-dof rolling robots are also nonholonomic devices, and thus, pose the same problems for their control as the former.

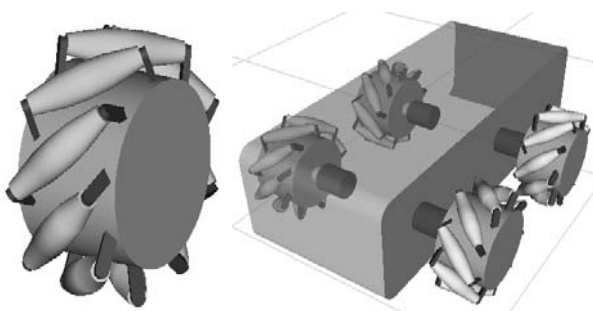

(a) (b)

FIGURE 1.11. (a) A Mekanum wheel; (b) rolling robot supplied with Mekanum wheels.

Recent developments in the technology of rolling robots have been reported that incorporate alternative types of ODWs. For example, Killough and Pin (1992) developed a rolling robot with what they call *orthogonal ball wheels*, consisting basically of spherical wheels that can rotate about two mutually orthogonal axes. West and Asada (1995), in turn, designed a rolling robot with *ball wheels*, i.e., balls that act as omnidirectional wheels; each ball being mounted on a set of rollers, one of which is actuated; hence, three such wheels are necessary to fully control the vehicle. The unactuated rollers serve two purposes, i.e., to provide stability to the wheels and the vehicle, and to measure the rotation of the ball, thereby detecting slip. Furthermore, Borenstein (1993) proposed a mobile robot with four degrees of freedom; these were achieved with two chassis coupled by an extensible link, each chassis being driven by two actuated conventional wheels.

This page intentionally left blank

2

Mathematical Background

2.1 Preamble

First and foremost, the study of motions undergone by robotic mechanical systems or, for that matter, by mechanical systems at large, requires a suitable motion representation. Now, the motion of mechanical systems involves the motion of the particular links comprising those systems, which in this book are supposed to be rigid. The assumption of rigidity, although limited in scope, still covers a wide spectrum of applications, while providing insight into the motion of more complicated systems, such as those involving deformable bodies.

The most general kind of rigid-body motion consists of both translation and rotation. While the study of the former is covered in elementary mechanics courses and is reduced to the mechanics of particles, the latter is more challenging. Indeed, point translation can be studied simply with the aid of 3-dimensional vector calculus, while rigid-body rotations require the introduction of *tensors*, i.e., entities mapping vector spaces into vector spaces.

Emphasis is placed on *invariant* concepts, i.e., items that do not change upon a change of coordinate frame. Examples of invariant concepts are geometric quantities such as distances and angles between lines. Although we may resort to a coordinate frame and vector algebra to compute distances and angles and represent vectors in that frame, the final result will be independent of how we choose that frame. The same applies to quantities whose evaluation calls for the introduction of tensors. Here, we must distinguish

between the physical quantity represented by a vector or a tensor and the representation of that quantity in a coordinate frame using a 1-dimensional array of components in the case of vectors, or a 2-dimensional array in the case of tensors. It is unfortunate that the same word is used in English to denote a vector and its array representation in a given coordinate frame. Regarding tensors, the associated arrays are called *matrices*. By abuse of terminology, we will refer to both tensors and their arrays as matrices, although keeping in mind the essential conceptual differences involved.

2.2 Linear Transformations

The physical 3-dimensional space is a particular case of a *vector space*. A vector space is a set of objects, called *vectors*, that follow certain algebraic rules. Throughout the book, vectors will be denoted by boldface lowercase characters, whereas tensors and their matrix representations will be denoted by boldface uppercase characters. Let $\mathbf{v}$, $\mathbf{v}_1$, $\mathbf{v}_2$, $\mathbf{v}_3$, and $\mathbf{w}$ be elements of a given vector space $\mathcal{V}$, which is *defined over the real field*, and let α and β be two elements of this field, i.e., α and β are two real numbers. Below we summarize the aforementioned rules:

(*i*) The sum of $\mathbf{v}_1$ and $\mathbf{v}_2$, denoted by $\mathbf{v}_1 + \mathbf{v}_2$, is itself an element of $\mathcal{V}$ and is *commutative*, i.e., $\mathbf{v}_1 + \mathbf{v}_2 = \mathbf{v}_2 + \mathbf{v}_1$;

(*ii*) $\mathcal{V}$ contains an element $\mathbf{0}$, called the *zero* vector of $\mathcal{V}$, which, when added to any other element $\mathbf{v}$ of $\mathcal{V}$, leaves it unchanged, i.e., $\mathbf{v}+\mathbf{0} = \mathbf{v}$;

(*iii*) The sum defined in (*i*) is *associative*, i.e., $\mathbf{v}_1+(\mathbf{v}_2+\mathbf{v}_3) = (\mathbf{v}_1+\mathbf{v}_2)+\mathbf{v}_3$;

(*iv*) For every element $\mathbf{v}$ of $\mathcal{V}$, there exists a corresponding element, $\mathbf{w}$, also of $\mathcal{V}$, which, when added to $\mathbf{v}$, produces the zero vector, i.e., $\mathbf{v} + \mathbf{w} = \mathbf{0}$. Moreover, $\mathbf{w}$ is represented as $-\mathbf{v}$;

(*v*) The product $\alpha\mathbf{v}$, or $\mathbf{v}\alpha$, is also an element of $\mathcal{V}$, for every $\mathbf{v}$ of $\mathcal{V}$ and every real α. This product is associative, i.e., $\alpha(\beta\mathbf{v}) = (\alpha\beta)\mathbf{v}$;

(*vi*) If α is the real unity, then $\alpha\mathbf{v}$ is identically $\mathbf{v}$;

(*vii*) The product defined in (*v*) is *distributive* in the sense that (*a*) $(\alpha + \beta)\mathbf{v} = \alpha\mathbf{v} + \beta\mathbf{v}$ and (*b*) $\alpha(\mathbf{v}_1 + \mathbf{v}_2) = \alpha\mathbf{v}_1 + \alpha\mathbf{v}_2$.

Although vector spaces can be defined over other fields, we will deal with vector spaces over the real field unless explicit reference to another field is made. Moreover, vector spaces can be either finite- or infinite-dimensional, but we will not need the latter. In geometry and elementary mechanics, the

dimension of the vector spaces needed is usually three, but when studying multibody systems, an arbitrary finite dimension will be required. The concept of *dimension* of a vector space is discussed in more detail later.

A *linear transformation*, represented as an *operator* $\mathbf{L}$, of a vector space $\mathcal{U}$ into a vector space $\mathcal{V}$, is a rule that assigns to every vector $\mathbf{u}$ of $\mathcal{U}$ at least one vector $\mathbf{v}$ of $\mathcal{V}$, represented as $\mathbf{v} = \mathbf{L}\mathbf{u}$, with $\mathbf{L}$ endowed with two properties:

(*i*) *homogeneity*: $\mathbf{L}(\alpha\mathbf{u}) = \alpha\mathbf{v}$; and

(*ii*) *additivity*: $\mathbf{L}(\mathbf{u}_1 + \mathbf{u}_2) = \mathbf{v}_1 + \mathbf{v}_2$.

Note that, in the foregoing definitions, no mention has been made of components, and hence, vectors and their transformations should not be confused with their *array representations*.

Particular types of linear transformations of the 3-dimensional Euclidean space that will be encountered frequently in this context are *projections*, *reflections*, and *rotations*. One further type of transformation, which is not linear, but nevertheless appears frequently in kinematics, is the one known as *affine transformation*. The foregoing transformations are defined below. It is necessary, however, to introduce additional concepts pertaining to general linear transformations before expanding into these definitions.

The *range* of a linear transformation $\mathbf{L}$ of $\mathcal{U}$ into $\mathcal{V}$ is the set of vectors $\mathbf{v}$ of $\mathcal{V}$ into which some vector $\mathbf{u}$ of $\mathcal{U}$ is mapped, i.e., the range of $\mathbf{L}$ is defined as the set of $\mathbf{v} = \mathbf{L}\mathbf{u}$, for every vector $\mathbf{u}$ of $\mathcal{U}$. The *kernel* of $\mathbf{L}$ is the set of vectors $\mathbf{u}_N$ of $\mathcal{U}$ that are mapped by $\mathbf{L}$ into the zero vector $\mathbf{0} \in \mathcal{V}$. It can be readily proven (see Exercises 2.1–2.3) that the kernel and the range of a linear transformation are both vector subspaces of $\mathcal{U}$ and $\mathcal{V}$, respectively, i.e., they are themselves vector spaces, but of a dimension smaller than or equal to that of their associated vector spaces. Moreover, the kernel of a linear transformation is often called the *nullspace* of the said transformation.

Henceforth, the 3-dimensional Euclidean space is denoted by $\mathcal{E}^3$. Having chosen an origin O for this space, its geometry can be studied in the context of general vector spaces. Hence, points of $\mathcal{E}^3$ will be identified with vectors of the associated 3-dimensional vector space. Moreover, lines and planes passing through the origin are subspaces of dimensions 1 and 2, respectively, of $\mathcal{E}^3$. Clearly, lines and planes not passing through the origin of $\mathcal{E}^3$ are not subspaces but can be handled with the algebra of vector spaces, as will be shown here.

An *orthogonal projection* $\mathbf{P}$ of $\mathcal{E}^3$ onto itself is a linear transformation of the said space onto a plane Π passing through the origin and having a unit normal $\mathbf{n}$, with the properties:

$$\mathbf{P}^2 = \mathbf{P}, \quad \mathbf{P}\mathbf{n} = \mathbf{0} \tag{2.1a}$$

Any matrix with the first property above is termed *idempotent*. For $n \times n$ matrices, it is sometimes necessary to indicate the lowest integer l for which

an analogous relation follows, i.e., for which $\mathbf{P}^l = \mathbf{P}$. In this case, the matrix is said to be idempotent of degree l.

Clearly, the projection of a position vector $\mathbf{p}$, denoted by $\mathbf{p}'$, onto a plane Π of unit normal $\mathbf{n}$, is $\mathbf{p}$ itself minus the component of $\mathbf{p}$ along $\mathbf{n}$, i.e.,

$$\mathbf{p}' = \mathbf{p} - \mathbf{n}(\mathbf{n}^T\mathbf{p}) \tag{2.1b}$$

where the superscript T denotes either vector or matrix transposition and $\mathbf{n}^T\mathbf{p}$ is equivalent to the usual *dot product* $\mathbf{n} \cdot \mathbf{p}$.

Now, the *identity* matrix $\mathbf{1}$ is defined as the mapping of a vector space $\mathcal{V}$ into itself leaving every vector $\mathbf{v}$ of $\mathcal{V}$ unchanged, i.e.,

$$\mathbf{1}\mathbf{v} = \mathbf{v} \tag{2.2}$$

Thus, $\mathbf{p}'$, as given by eq.(2.1b), can be rewritten as

$$\mathbf{p}' = \mathbf{1}\mathbf{p} - \mathbf{n}\mathbf{n}^T\mathbf{p} \equiv (\mathbf{1} - \mathbf{n}\mathbf{n}^T)\mathbf{p} \tag{2.3}$$

and hence, the *orthogonal projection* $\mathbf{P}$ onto Π can be represented as

$$\mathbf{P} = \mathbf{1} - \mathbf{n}\mathbf{n}^T \tag{2.4}$$

where the product $\mathbf{n}\mathbf{n}^T$ amounts to a 3×3 matrix.

Now we turn to reflections. Here we have to take into account that reflections occur frequently accompanied by rotations, as yet to be studied. Since reflections are simpler to represent, we first discuss these, rotations being discussed in full detail in Section 2.3. What we shall discuss in this section is *pure reflections*, i.e., those occurring without any concomitant rotation. Thus, all reflections studied in this section are pure reflections, but for the sake of brevity, they will be referred to simply as *reflections*.

A *reflection* $\mathbf{R}$ of $\mathcal{E}^3$ onto a plane Π passing through the origin and having a unit normal $\mathbf{n}$ is a linear transformation of the said space into itself such that a position vector $\mathbf{p}$ is mapped by $\mathbf{R}$ into a vector $\mathbf{p}'$ given by

$$\mathbf{p}' = \mathbf{p} - 2\mathbf{n}\mathbf{n}^T\mathbf{p} \equiv (\mathbf{1} - 2\mathbf{n}\mathbf{n}^T)\mathbf{p}$$

Thus, the reflection $\mathbf{R}$ can be expressed as

$$\mathbf{R} = \mathbf{1} - 2\mathbf{n}\mathbf{n}^T \tag{2.5}$$

From eq.(2.5) it is then apparent that a pure reflection is represented by a linear transformation that is symmetric and whose square equals the identity matrix, i.e., $\mathbf{R}^2 = \mathbf{1}$. Indeed, symmetry is apparent from the equation above; the second property is readily proven below:

$$\begin{aligned}\mathbf{R}^2 &= (\mathbf{1} - 2\mathbf{n}\mathbf{n}^T)(\mathbf{1} - 2\mathbf{n}\mathbf{n}^T) \\ &= \mathbf{1} - 2\mathbf{n}\mathbf{n}^T - 2\mathbf{n}\mathbf{n}^T + 4(\mathbf{n}\mathbf{n}^T)(\mathbf{n}\mathbf{n}^T) = \mathbf{1} - 4\mathbf{n}\mathbf{n}^T + 4\mathbf{n}(\mathbf{n}^T\mathbf{n})\mathbf{n}^T\end{aligned}$$

which apparently reduces to **1** because **n** is a unit vector. Note that from the second property above, we find that pure reflections observe a further interesting property, namely,

$$\mathbf{R}^{-1} = \mathbf{R}$$

i.e., every pure reflection equals its inverse. This result can be understood intuitively by noticing that, upon doubly reflecting an image using two mirrors, the original image is recovered. Any square matrix which equals its inverse will be termed *self-inverse* henceforth.

Further, we take to deriving the *orthogonal decomposition* of a given vector **v** into two components, one along and one normal to a unit vector **e**. The component of **v** along **e**, termed here the *axial component*, $\mathbf{v}_{\|}$—read *v-par*—is simply given as

$$\mathbf{v}_{\|} \equiv \mathbf{e}\mathbf{e}^T\mathbf{v} \tag{2.6a}$$

while the corresponding *normal component*, $\mathbf{v}_{\perp}$—read *v-perp*—is simply the difference $\mathbf{v} - \mathbf{v}_{\|}$, i.e.,

$$\mathbf{v}_{\perp} \equiv \mathbf{v} - \mathbf{v}_{\|} \equiv (\mathbf{1} - \mathbf{e}\mathbf{e}^T)\mathbf{v} \tag{2.6b}$$

the matrix in parentheses in the foregoing equation being rather frequent in kinematics. This matrix will appear when studying rotations.

Further concepts are now recalled: The *basis* of a vector space $\mathcal{V}$ is a set of *linearly independent* vectors of $\mathcal{V}$, $\{\mathbf{v}_i\}_1^n$, in terms of which any vector **v** of $\mathcal{V}$ can be expressed as

$$\mathbf{v} = \alpha_1\mathbf{v}_1 + \alpha_2\mathbf{v}_2 + \cdots + \alpha_n\mathbf{v}_n, \tag{2.7}$$

where the elements of the set $\{\alpha_i\}_1^n$ are all elements of the field over which $\mathcal{V}$ is defined, i.e., they are real numbers in the case at hand. The number n of elements in the set $\mathcal{B} = \{\mathbf{v}_i\}_1^n$ is called *the dimension* of $\mathcal{V}$. Note that *any* set of n linearly independent vectors of $\mathcal{V}$ can play the role of a basis of this space, but once this basis is defined, the set of real coefficients $\{\alpha_i\}_1^n$ for expressing a given vector **v** is *unique*.

Let $\mathcal{U}$ and $\mathcal{V}$ be two vector spaces of dimensions m and n, respectively, and **L** a linear transformation of $\mathcal{U}$ into $\mathcal{V}$, and define bases $\mathcal{B}_U$ and $\mathcal{B}_V$ for $\mathcal{U}$ and $\mathcal{V}$ as

$$\mathcal{B}_U = \{\mathbf{u}_j\}_1^m, \quad \mathcal{B}_V = \{\mathbf{v}_i\}_1^n \tag{2.8}$$

Since each $\mathbf{L}\mathbf{u}_j$ is an element of $\mathcal{V}$, it can be represented uniquely in terms of the vectors of $\mathcal{B}_V$, namely, as

$$\mathbf{L}\mathbf{u}_j = l_{1j}\mathbf{v}_1 + l_{2j}\mathbf{v}_2 + \cdots + l_{nj}\mathbf{v}_n, \quad j = 1, \ldots, m \tag{2.9}$$

Consequently, in order to represent the *images* of the m vectors of $\mathcal{B}_U$, namely, the set $\{\mathbf{L}\mathbf{u}_j\}_1^m$, $n \times m$ real numbers l_{ij}, for $i = 1, \ldots, n$ and

$j = 1, \ldots, m$, are necessary. These real numbers are now arranged in the $n \times m$ array $[\mathbf{L}]_{\mathcal{B}_U}^{\mathcal{B}_V}$ defined below:

$$[\mathbf{L}]_{\mathcal{B}_U}^{\mathcal{B}_V} \equiv \begin{bmatrix} l_{11} & l_{12} & \cdots & l_{1m} \\ l_{21} & l_{22} & \cdots & l_{2m} \\ \vdots & \vdots & \ddots & \vdots \\ l_{n1} & l_{n2} & \cdots & l_{nm} \end{bmatrix} \tag{2.10}$$

The foregoing array is thus called the *matrix representation of* $\mathbf{L}$ *with respect to* $\mathcal{B}_U$ *and* $\mathcal{B}_V$. We thus have an important definition, namely,

Definition 2.2.1 *The* j*th column of the matrix representation of* $\mathbf{L}$ *with respect to the bases* $\mathcal{B}_U$ *and* $\mathcal{B}_V$ *is composed of the* n *real coefficients* l_{ij} *of the representation of the image of the* j*th vector of* $\mathcal{B}_U$ *in terms of* $\mathcal{B}_V$.

The notation introduced in eq.(2.10) is rather cumbersome, for it involves one subscript and one superscript. Moreover, each of these is subscripted. In practice, the bases involved are self-evident, which makes an explicit mention of these unnecessary. In particular, when the mapping $\mathbf{L}$ is a mapping of $\mathcal{U}$ onto itself, then a single basis suffices to represent $\mathbf{L}$ in matrix form. In this case, its bracket will bear only a subscript, and no superscript, namely, $[\mathbf{L}]_{\mathcal{B}}$. Moreover, we will use, henceforth, the concept of basis and coordinate frame interchangeably, since one implies the other.

Two different bases are unavoidable when the two spaces under study are physically distinct, which is the case in velocity analyses of manipulators. As we will see in Chapter 4, in these analyses we distinguish between the velocity of the manipulator in Cartesian space and that in the joint-rate space. While the Cartesian-space velocity—or Cartesian velocity, for brevity—consists, in general, of a 6-dimensional vector containing the 3-dimensional angular velocity of the end-effector and the translational velocity of one of its points, the latter is an n-dimensional vector. Moreover, if the manipulator is coupled by revolute joints only, the units of the joint-rate vector are all s^{-1}, whereas the Cartesian velocity contains some components with units of s^{-1} and others with units of ms^{-1}.

Further definitions are now recalled. Given a mapping $\mathbf{L}$ of an n-dimensional vector space $\mathcal{U}$ into the n-dimensional vector space $\mathcal{V}$, a nonzero vector $\mathbf{e}$ that is mapped by $\mathbf{L}$ into a multiple of itself, $\lambda\mathbf{e}$, is called an *eigenvector* of $\mathbf{L}$, the scalar λ being called an *eigenvalue* of $\mathbf{L}$. The eigenvalues of $\mathbf{L}$ are determined by the equation

$$\det(\lambda\mathbf{1} - \mathbf{L}) = 0 \tag{2.11}$$

Note that the matrix $\lambda\mathbf{1} - \mathbf{L}$ is *linear* in λ, and since the determinant of an $n \times n$ matrix is a homogeneous nth-order function of its entries, the left-hand side of eq.(2.11) is an nth-degree polynomial in λ. The foregoing polynomial is termed *the characteristic polynomial of* $\mathbf{L}$. Hence, every $n \times n$

matrix $\mathbf{L}$ has n complex eigenvalues, even if $\mathbf{L}$ is defined over the real field. If it is, then its complex eigenvalues appear in conjugate pairs. Clearly, the eigenvalues of $\mathbf{L}$ are the roots of its characteristic polynomial, while eq.(2.11) is called the *characteristic equation* of $\mathbf{L}$.

Example 2.2.1 *What is the representation of the reflection* $\mathbf{R}$ *of* $\mathcal{E}^3$ *into itself, with respect to the x-y plane, in terms of unit vectors parallel to the X, Y, Z axes that form a coordinate frame* $\mathcal{F}$*?*

Solution: Note that in this case, $\mathcal{U} = \mathcal{V} = \mathcal{E}^3$ and, hence, it is not necessary to use two different bases for $\mathcal{U}$ and $\mathcal{V}$. Now, let $\mathbf{i}$, $\mathbf{j}$, $\mathbf{k}$, be unit vectors parallel to the X, Y, and Z axes of a frame $\mathcal{F}$. Clearly,

$$\begin{aligned} \mathbf{R}\mathbf{i} &= \mathbf{i} \\ \mathbf{R}\mathbf{j} &= \mathbf{j} \\ \mathbf{R}\mathbf{k} &= -\mathbf{k} \end{aligned}$$

Thus, the representations of the images of $\mathbf{i}$, $\mathbf{j}$ and $\mathbf{k}$ under $\mathbf{R}$, in $\mathcal{F}$, are

$$[\,\mathbf{R}\mathbf{i}\,]_{\mathcal{F}} = \begin{bmatrix} 1 \\ 0 \\ 0 \end{bmatrix}, \quad [\,\mathbf{R}\mathbf{j}\,]_{\mathcal{F}} = \begin{bmatrix} 0 \\ 1 \\ 0 \end{bmatrix}, \quad [\,\mathbf{R}\mathbf{k}\,]_{\mathcal{F}} = \begin{bmatrix} 0 \\ 0 \\ -1 \end{bmatrix}$$

where subscripted brackets are used to indicate the representation frame. Hence, the matrix representation of $\mathbf{R}$ in $\mathcal{F}$, denoted by $[\,\mathbf{R}\,]_{\mathcal{F}}$, is

$$[\,\mathbf{R}\,]_{\mathcal{F}} = \begin{bmatrix} 1 & 0 & 0 \\ 0 & 1 & 0 \\ 0 & 0 & -1 \end{bmatrix}$$

2.3 Rigid-Body Rotations

A *linear isomorphism*, i.e., a one-to-one linear transformation mapping a space $\mathcal{V}$ onto itself, is called an *isometry* if it preserves distances between any two points of $\mathcal{V}$. If $\mathbf{u}$ and $\mathbf{v}$ are regarded as the position vectors of two such points, then the distance d between these two points is defined as

$$d \equiv \sqrt{(\mathbf{u}-\mathbf{v})^T(\mathbf{u}-\mathbf{v})} \tag{2.12}$$

The volume V of the tetrahedron defined by the origin and three points of the 3-dimensional Euclidean space of position vectors $\mathbf{u}$, $\mathbf{v}$, and $\mathbf{w}$ is obtained as one-sixth of the absolute value of the *double mixed product* of these three vectors,

$$V \equiv \frac{1}{6}\,|\mathbf{u}\times\mathbf{v}\cdot\mathbf{w}| = \frac{1}{6}\,|\det[\,\mathbf{u} \quad \mathbf{v} \quad \mathbf{w}\,]| \tag{2.13}$$

i.e., if a 3×3 array $[\mathbf{A}]$ is defined in terms of the components of $\mathbf{u}$, $\mathbf{v}$, and $\mathbf{w}$, in a given basis, then the first column of $[\mathbf{A}]$ is given by the three components of $\mathbf{u}$, the second and third columns being defined analogously.

Now, let $\mathbf{Q}$ be an isometry mapping the triad $\{\mathbf{u}, \mathbf{v}, \mathbf{w}\}$ into $\{\mathbf{u}', \mathbf{v}', \mathbf{w}'\}$. Moreover, the distance from the origin to the points of position vectors $\mathbf{u}$, $\mathbf{v}$, and $\mathbf{w}$ is given simply as $\|\mathbf{u}\|$, $\|\mathbf{v}\|$, and $\|\mathbf{w}\|$, which are defined as

$$\|\mathbf{u}\| \equiv \sqrt{\mathbf{u}^T\mathbf{u}}, \quad \|\mathbf{v}\| \equiv \sqrt{\mathbf{v}^T\mathbf{v}}, \quad \|\mathbf{w}\| \equiv \sqrt{\mathbf{w}^T\mathbf{w}} \tag{2.14}$$

Clearly,

$$\|\mathbf{u}'\| = \|\mathbf{u}\|, \quad \|\mathbf{v}'\| = \|\mathbf{v}\|, \quad \|\mathbf{w}'\| = \|\mathbf{w}\| \tag{2.15a}$$

and

$$\det[\,\mathbf{u}' \quad \mathbf{v}' \quad \mathbf{w}'\,] = \pm\det[\,\mathbf{u} \quad \mathbf{v} \quad \mathbf{w}\,] \tag{2.15b}$$

If, in the foregoing relations, the sign of the determinant is preserved, the isometry represents a *rotation*; otherwise, it represents a reflection. Now, let $\mathbf{p}$ be the position vector of any point of $\mathcal{E}^3$, its image under a rotation $\mathbf{Q}$ being $\mathbf{p}'$. Hence, distance preservation requires that

$$\mathbf{p}^T\mathbf{p} = \mathbf{p}'^T\mathbf{p}' \tag{2.16}$$

where

$$\mathbf{p}' = \mathbf{Q}\mathbf{p} \tag{2.17}$$

condition (2.16) thus leading to

$$\mathbf{Q}^T\mathbf{Q} = \mathbf{1} \tag{2.18}$$

where $\mathbf{1}$ was defined in Section 2.2 as the *identity* 3×3 *matrix*, and hence, eq.(2.18) states that $\mathbf{Q}$ is an *orthogonal matrix*. Moreover, let $\mathbf{T}$ and $\mathbf{T}'$ denote the two matrices defined below:

$$\mathbf{T} = [\,\mathbf{u} \quad \mathbf{v} \quad \mathbf{w}\,], \quad \mathbf{T}' = [\,\mathbf{u}' \quad \mathbf{v}' \quad \mathbf{w}'\,] \tag{2.19}$$

from which it is clear that

$$\mathbf{T}' = \mathbf{Q}\mathbf{T} \tag{2.20}$$

Now, for a rigid-body rotation, eq.(2.15b) should hold with the positive sign, and hence,

$$\det(\mathbf{T}) = \det(\mathbf{T}') \tag{2.21a}$$

and, by virtue of eq.(2.20), we conclude that

$$\det(\mathbf{Q}) = +1 \tag{2.21b}$$

Therefore, $\mathbf{Q}$ is a *proper orthogonal matrix*, i.e., it is a proper isometry. Now we have

Theorem 2.3.1 *The eigenvalues of a proper orthogonal matrix* $\mathbf{Q}$ *lie on the unit circle centered at the origin of the complex plane.*

Proof: Let λ be one of the eigenvalues of $\mathbf{Q}$ and $\mathbf{e}$ the corresponding eigenvector, so that

$$\mathbf{Q}\mathbf{e} = \lambda\mathbf{e} \tag{2.22}$$

In general, $\mathbf{Q}$ is not expected to be symmetric, and hence, λ is not necessarily real. Thus, λ is considered complex, in general. In this light, when transposing both sides of the foregoing equation, we will need to take the complex conjugates as well. Henceforth, the complex conjugate of a vector or a matrix will be indicated with an asterisk as a superscript. As well, the conjugate of a complex variable will be indicated with a bar over the said variable. Thus, the transpose conjugate of the latter equation takes on the form

$$\mathbf{e}^*\mathbf{Q}^* = \overline{\lambda}\mathbf{e}^* \tag{2.23}$$

Multiplying the corresponding sides of the two previous equations yields

$$\mathbf{e}^*\mathbf{Q}^*\mathbf{Q}\mathbf{e} = \overline{\lambda}\lambda\mathbf{e}^*\mathbf{e} \tag{2.24}$$

However, $\mathbf{Q}$ has been assumed real, and hence, $\mathbf{Q}^*$ reduces to $\mathbf{Q}^T$, the foregoing equation thus reducing to

$$\mathbf{e}^*\mathbf{Q}^T\mathbf{Q}\mathbf{e} = \overline{\lambda}\lambda\mathbf{e}^*\mathbf{e} \tag{2.25}$$

But $\mathbf{Q}$ is orthogonal by assumption, and hence, it obeys eq.(2.18), which means that eq.(2.25) reduces to

$$\mathbf{e}^*\mathbf{e} = |\lambda|^2\mathbf{e}^*\mathbf{e} \tag{2.26}$$

where $|\cdot|$ denotes the *modulus* of the complex variable within it. Thus, the foregoing equation leads to

$$|\lambda|^2 = 1 \tag{2.27}$$

thereby completing the intended proof. As a direct consequence of Theorem 2.3.1, we have

Corollary 2.3.1 *A proper orthogonal* 3×3 *matrix has at least one eigenvalue that is* $+1$*.*

Now, let $\mathbf{e}$ be the eigenvector of $\mathbf{Q}$ associated with the eigenvalue $+1$. Thus,

$$\mathbf{Q}\mathbf{e} = \mathbf{e} \tag{2.28}$$

What eq.(2.28) states is summarized as a theorem below:

Theorem 2.3.2 (Euler, 1776) *A rigid-body motion about a point* O *leaves fixed a set of points lying on a line* $\mathcal{L}$ *that passes through* O *and is parallel to the eigenvector* $\mathbf{e}$ *of* $\mathbf{Q}$ *associated with the eigenvalue* $+1$*.*

A further result, that finds many applications in robotics and, in general, in system theory, is given below:

Theorem 2.3.3 (Cayley-Hamilton) *Let $P(\lambda)$ be the characteristic polynomial of an $n \times n$ matrix $\mathbf{A}$, i.e.,*

$$P(\lambda) = \det(\lambda \mathbf{1} - \mathbf{A}) = \lambda^n + a_{n-1}\lambda^{n-1} + \cdots + a_1\lambda + a_0 \tag{2.29}$$

Then $\mathbf{A}$ satisfies its characteristic equation, i.e.,

$$\mathbf{A}^n + a_{n-1}\mathbf{A}^{n-1} + \cdots + a_1\mathbf{A} + a_0\mathbf{1} = \mathbf{O} \tag{2.30}$$

where $\mathbf{O}$ is the $n \times n$ zero matrix.

Proof: See (Kaye and Wilson, 1998).

What the Cayley-Hamilton Theorem states is that any power $p \geq n$ of the $n \times n$ matrix $\mathbf{A}$ can be expressed as a linear combination of the first n powers of $\mathbf{A}$—the 0th power of $\mathbf{A}$ is, of course, the $n \times n$ identity matrix $\mathbf{1}$. An important consequence of this result is that any *analytic* matrix function of $\mathbf{A}$ can be expressed not as an infinite series, but as a sum, namely, a linear combination of the first n powers of $\mathbf{A}$: $\mathbf{1}$, $\mathbf{A}$, $\ldots$, $\mathbf{A}^{n-1}$. An *analytic* function $f(x)$ of a real variable x is, in turn, a function with a series expansion. Moreover, an analytic matrix function of a matrix argument $\mathbf{A}$ is defined likewise, an example of which is the exponential function. From the previous discussion, then, the exponential of $\mathbf{A}$ can be written as a linear combination of the first n powers of $\mathbf{A}$. It will be shown later that any proper orthogonal matrix $\mathbf{Q}$ can be represented as the exponential of a skew-symmetric matrix derived from the unit vector $\mathbf{e}$ of $\mathbf{Q}$, of eigenvalue $+1$, and the associated angle of rotation, as yet to be defined.

2.3.1 The Cross-Product Matrix

Prior to introducing the matrix representation of a rotation, we will need a few definitions. We will start by defining the partial derivative of a vector with respect to another vector. This is a matrix, as described below: In general, let $\mathbf{u}$ and $\mathbf{v}$ be vectors of spaces $\mathcal{U}$ and $\mathcal{V}$, of dimensions m and n, respectively. Furthermore, let t be a real variable and f be real-valued function of t, $\mathbf{u} = \mathbf{u}(t)$ and $\mathbf{v} = \mathbf{v}(\mathbf{u}(t))$ being m- and n-dimensional vector functions of t as well, with $f = f(\mathbf{u}, \mathbf{v})$. The derivative of $\mathbf{u}$ with respect to t, denoted by $\dot{\mathbf{u}}(t)$, is an m-dimensional vector whose ith component is the derivative of the ith component of $\mathbf{u}$ in a given basis, u_i, with respect to t. A similar definition follows for $\dot{\mathbf{v}}(t)$. The partial derivative of f with respect to $\mathbf{u}$ is an m-dimensional vector whose ith component is the partial derivative of f with respect to u_i, with a corresponding definition for the partial derivative of f with respect to $\mathbf{v}$. The foregoing derivatives, as all

other vectors, will be assumed, henceforth, to be *column* arrays. Thus,

$$\frac{\partial f}{\partial \mathbf{u}} \equiv \begin{bmatrix} \partial f/\partial u_1 \\ \partial f/\partial u_2 \\ \vdots \\ \partial f/\partial u_m \end{bmatrix}, \quad \frac{\partial f}{\partial \mathbf{v}} \equiv \begin{bmatrix} \partial f/\partial v_1 \\ \partial f/\partial v_2 \\ \vdots \\ \partial f/\partial v_n \end{bmatrix} \tag{2.31}$$

Furthermore, the partial derivative of $\mathbf{v}$ with respect to $\mathbf{u}$ is an $n \times m$ array whose (i, j) entry is defined as $\partial v_i/\partial u_j$, i.e.,

$$\frac{\partial \mathbf{v}}{\partial \mathbf{u}} \equiv \begin{bmatrix} \partial v_1/\partial u_1 & \partial v_1/\partial u_2 & \cdots & \partial v_1/\partial u_m \\ \partial v_2/\partial u_1 & \partial v_2/\partial u_2 & \cdots & \partial v_2/\partial u_m \\ \vdots & \vdots & \ddots & \vdots \\ \partial v_n/\partial u_1 & \partial v_n/\partial u_2 & \cdots & \partial v_n/\partial u_m \end{bmatrix} \tag{2.32}$$

Hence, the total derivative of f with respect to $\mathbf{u}$ can be written as

$$\frac{df}{d\mathbf{u}} = \frac{\partial f}{\partial \mathbf{u}} + \left(\frac{\partial \mathbf{v}}{\partial \mathbf{u}}\right)^T \frac{\partial f}{\partial \mathbf{v}} \tag{2.33}$$

If, moreover, f is an explicit function of t, i.e., if $f = f(\mathbf{u}, \mathbf{v}, t)$ and $\mathbf{v} = \mathbf{v}(\mathbf{u}, t)$, then, one can write the total derivative of f with respect to t as

$$\frac{df}{dt} = \frac{\partial f}{\partial t} + \left(\frac{\partial f}{\partial \mathbf{u}}\right)^T \frac{d\mathbf{u}}{dt} + \left(\frac{\partial f}{\partial \mathbf{v}}\right)^T \frac{\partial \mathbf{v}}{\partial t} + \left(\frac{\partial f}{\partial \mathbf{v}}\right)^T \frac{\partial \mathbf{v}}{\partial \mathbf{u}} \frac{d\mathbf{u}}{dt} \tag{2.34}$$

The total derivative of $\mathbf{v}$ with respect to t can be written, likewise, as

$$\frac{d\mathbf{v}}{dt} = \frac{\partial \mathbf{v}}{\partial t} + \frac{\partial \mathbf{v}}{\partial \mathbf{u}} \frac{d\mathbf{u}}{dt} \tag{2.35}$$

Example 2.3.1 *Let the components of* $\mathbf{v}$ *and* $\mathbf{x}$ *in a certain reference frame* $\mathcal{F}$ *be given as*

$$[\,\mathbf{v}\,]_{\mathcal{F}} = \begin{bmatrix} v_1 \\ v_2 \\ v_3 \end{bmatrix}, \quad [\,\mathbf{x}\,]_{\mathcal{F}} = \begin{bmatrix} x_1 \\ x_2 \\ x_3 \end{bmatrix} \tag{2.36a}$$

Then

$$[\,\mathbf{v} \times \mathbf{x}\,]_{\mathcal{F}} = \begin{bmatrix} v_2 x_3 - v_3 x_2 \\ v_3 x_1 - v_1 x_3 \\ v_1 x_2 - v_2 x_1 \end{bmatrix} \tag{2.36b}$$

Hence,

$$\left[\frac{\partial(\mathbf{v} \times \mathbf{x})}{\partial \mathbf{x}}\right]_{\mathcal{F}} = \begin{bmatrix} 0 & -v_3 & v_2 \\ v_3 & 0 & -v_1 \\ -v_2 & v_1 & 0 \end{bmatrix} \tag{2.36c}$$

Henceforth, the partial derivative of the cross product of any 3-dimensional vectors $\mathbf{v}$ and $\mathbf{x}$ will be denoted by the 3×3 matrix $\mathbf{V}$. For obvious reasons, $\mathbf{V}$ is termed the *cross-product matrix* of vector $\mathbf{v}$. Sometimes the cross-product matrix of a vector $\mathbf{v}$ is represented as $\widetilde{\mathbf{v}}$, but we do not follow this notation for the sake of consistency, since we decided at the outset to represent matrices with boldface uppercase letters. Thus, the foregoing cross product admits the alternative representations

$$\mathbf{v} \times \mathbf{x} = \mathbf{V}\mathbf{x} \tag{2.37}$$

Now, the following is apparent:

Theorem 2.3.4 *The cross-product matrix* $\mathbf{A}$ *of any 3-dimensional vector* $\mathbf{a}$ *is skew-symmetric, i.e.,*

$$\mathbf{A}^T = -\mathbf{A}$$

and, as a consequence,

$$\mathbf{a} \times (\mathbf{a} \times \mathbf{b}) = \mathbf{A}^2\mathbf{b} \tag{2.38}$$

where $\mathbf{A}^2$ *can be readily proven to be*

$$\mathbf{A}^2 = -\|\mathbf{a}\|^2\mathbf{1} + \mathbf{a}\mathbf{a}^T \tag{2.39}$$

with $\|\cdot\|$ *denoting the* Euclidean norm *of the vector inside it.*

Note that given *any* 3-dimensional vector $\mathbf{a}$, its cross-product matrix $\mathbf{A}$ is *uniquely* defined. Moreover, this matrix is skew-symmetric. The converse also holds, i.e., given any 3×3 skew-symmetric matrix $\mathbf{A}$, its associated *vector* is uniquely defined as well. This result is made apparent from Example 2.3.1 and will be discussed further when we define the *axial vector* of an arbitrary 3×3 matrix below.

2.3.2 The Rotation Matrix

In deriving the matrix representation of a rotation, we should recall Theorem 2.3.2, which suggests that an explicit representation of $\mathbf{Q}$ in terms of its eigenvector $\mathbf{e}$ is possible. Moreover, this representation must contain information on the amount of the rotation under study, which is nothing but the *angle of rotation*. Furthermore, line $\mathcal{L}$, mentioned in *Euler's Theorem*, is termed the *axis of rotation* of the motion of interest. In order to derive the aforementioned representation, consider the rotation depicted in Fig. 2.1 of angle ϕ about line $\mathcal{L}$.

From Fig. 2.1(a), clearly, one can write

$$\mathbf{p}' = \overrightarrow{OQ} + \overrightarrow{QP'} \tag{2.40}$$

where $\overrightarrow{OQ}$ is the axial component of $\mathbf{p}$ along vector $\mathbf{e}$, which is derived as in eq.(2.6a), namely,

$$\overrightarrow{OQ} = \mathbf{e}\mathbf{e}^T\mathbf{p} \tag{2.41}$$

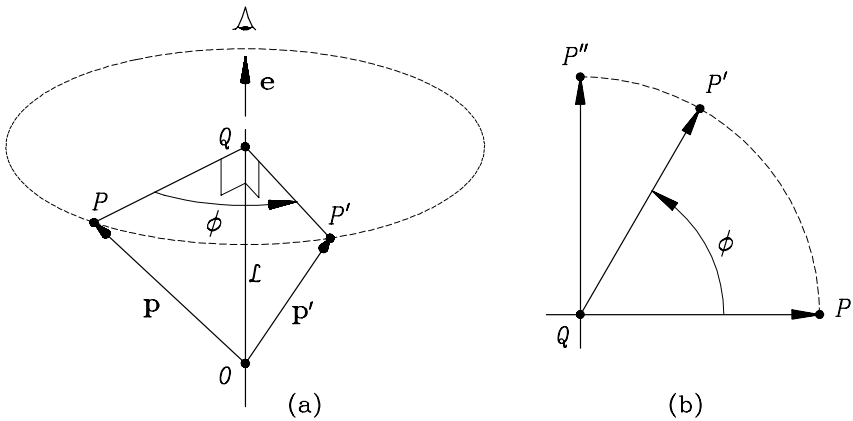

FIGURE 2.1. Rotation of a rigid body about a line.

Furthermore, from Fig. 2.1b,

$$\overrightarrow{QP'} = (\cos\phi)\ \overrightarrow{QP}\ + (\sin\phi)\ \overrightarrow{QP''} \tag{2.42}$$

with $\overrightarrow{QP}$ being nothing but the *normal component* of $\mathbf{p}$ with respect to $\mathbf{e}$, as introduced in eq.(2.6b), i.e.,

$$\overrightarrow{QP} = (\mathbf{1} - \mathbf{e}\mathbf{e}^T)\mathbf{p} \tag{2.43}$$

and $\overrightarrow{QP''}$ given as

$$\overrightarrow{QP''} = \mathbf{e} \times \mathbf{p} \equiv \mathbf{E}\mathbf{p} \tag{2.44}$$

Substitution of eqs.(2.44) and (2.43) into eq.(2.42) leads to

$$\overrightarrow{QP'} = \cos\phi(\mathbf{1} - \mathbf{e}\mathbf{e}^T)\mathbf{p} + \sin\phi\mathbf{E}\mathbf{p} \tag{2.45}$$

If now eqs.(2.41) and (2.45) are substituted into eq.(2.40), one obtains

$$\mathbf{p}' = \mathbf{e}\mathbf{e}^T\mathbf{p} + \cos\phi(\mathbf{1} - \mathbf{e}\mathbf{e}^T)\mathbf{p} + \sin\phi\mathbf{E}\mathbf{p} \tag{2.46}$$

Thus, eq.(2.40) reduces to

$$\mathbf{p}' = [\mathbf{e}\mathbf{e}^T + \cos\phi(\mathbf{1} - \mathbf{e}\mathbf{e}^T) + \sin\phi\mathbf{E}]\mathbf{p} \tag{2.47}$$

From eq.(2.47) it is apparent that $\mathbf{p}'$ is a linear transformation of $\mathbf{p}$, the said transformation being given by the matrix inside the brackets, which is the rotation matrix $\mathbf{Q}$ sought, i.e.,

$$\mathbf{Q} = \mathbf{e}\mathbf{e}^T + \cos\phi(\mathbf{1} - \mathbf{e}\mathbf{e}^T) + \sin\phi\mathbf{E} \tag{2.48}$$

A special case arises when $\phi = \pi$,

$$\mathbf{Q} = -\mathbf{1} + 2\mathbf{e}\mathbf{e}^T, \quad \text{for } \phi = \pi \tag{2.49}$$

whence it is apparent that $\mathbf{Q}$ is symmetric if $\phi = \pi$. Of course, $\mathbf{Q}$ becomes symmetric also when $\phi = 0$, but this is a rather obvious case, leading to $\mathbf{Q} = \mathbf{1}$. Except for these two cases, the rotation matrix is not symmetric. However, under no circumstance does the rotation matrix become skew-symmetric, for a 3×3 skew-symmetric matrix is by necessity singular, which contradicts the property of proper orthogonal matrices of eq.(2.21b).

Now one more representation of $\mathbf{Q}$ in terms of $\mathbf{e}$ and ϕ is given. For a fixed axis of rotation, i.e., for a fixed value of $\mathbf{e}$, the rotation matrix $\mathbf{Q}$ is a function of the angle of rotation ϕ, only. Thus, the series expansion of $\mathbf{Q}$ in terms of ϕ is

$$\mathbf{Q}(\phi) = \mathbf{Q}(0) + \mathbf{Q}'(0)\phi + \frac{1}{2!}\mathbf{Q}''(0)\phi^2 + \cdots + \frac{1}{k!}\mathbf{Q}^{(k)}(0)\phi^k + \cdots \tag{2.50}$$

where the superscript (k) stands for the kth derivative of $\mathbf{Q}$ with respect to ϕ. Now, from the definition of $\mathbf{E}$, one can readily prove the relations below:

$$\mathbf{E}^{(2k+1)} = (-1)^k\mathbf{E}, \quad \mathbf{E}^{2k} = (-1)^k(\mathbf{1} - \mathbf{e}\mathbf{e}^T) \tag{2.51}$$

Furthermore, using eqs.(2.48) and (2.51), one can readily show that

$$\mathbf{Q}^{(k)}(0) = \mathbf{E}^k \tag{2.52}$$

with $\mathbf{E}$ defined already as the cross-product matrix of $\mathbf{e}$. Moreover, from eqs.(2.50) and (2.52), $\mathbf{Q}(\phi)$ can be expressed as

$$\mathbf{Q}(\phi) = \mathbf{1} + \mathbf{E}\phi + \frac{1}{2!}\mathbf{E}^2\phi^2 + \cdots + \frac{1}{k!}\mathbf{E}^k\phi^k + \cdots$$

whose right-hand side is nothing but the exponential of $\mathbf{E}\phi$, i.e.,

$$\mathbf{Q}(\phi) = e^{\mathbf{E}\phi} \tag{2.53}$$

Equation (2.53) is the exponential representation of the rotation matrix in terms of its *natural invariants*, $\mathbf{e}$ and ϕ. The foregoing parameters are termed *invariants* because they are clearly independent of the coordinate axes chosen to represent the rotation under study. The adjective *natural* is necessary to distinguish them from other invariants that will be introduced presently. This adjective seems suitable because the said invariants stem naturally from Euler's Theorem.

Now, in view of eqs.(2.51), the above series can be written as

$$\mathbf{Q}(\phi) = \mathbf{1} + \left[-\frac{1}{2!}\phi^2 + \frac{1}{4!}\phi^4 - \cdots + \frac{1}{(2k)!}(-1)^k\phi^{2k} + \cdots\right](\mathbf{1} - \mathbf{e}\mathbf{e}^T)$$
$$+ \left[\phi - \frac{1}{3!}\phi^3 + \cdots + \frac{1}{(2k+1)!}(-1)^k\phi^{2k+1} + \cdots\right]\mathbf{E}$$

The series inside the first brackets is apparently $\cos\phi - 1$, while that in the second is $\sin\phi$. We have, therefore, an alternative representation of $\mathbf{Q}$, namely,

$$\mathbf{Q} = \mathbf{1} + \sin\phi\mathbf{E} + (1 - \cos\phi)\mathbf{E}^2 \tag{2.54}$$

which is an expected result in view of the Cayley-Hamilton Theorem.

The Canonical Forms of the Rotation Matrix

The rotation matrix takes on an especially simple form if the axis of rotation coincides with one of the coordinate axes. For example, if the X axis is parallel to the axis of rotation, i.e., parallel to vector $\mathbf{e}$, in a frame that we will label $\mathcal{X}$, then, we will have

$$[\,\mathbf{e}\,]_{\mathcal{X}} = \begin{bmatrix} 1 \\ 0 \\ 0 \end{bmatrix}, \quad [\,\mathbf{E}\,]_{\mathcal{X}} = \begin{bmatrix} 0 & 0 & 0 \\ 0 & 0 & -1 \\ 0 & 1 & 0 \end{bmatrix}, \quad [\,\mathbf{E}^2\,]_{\mathcal{X}} = \begin{bmatrix} 0 & 0 & 0 \\ 0 & -1 & 0 \\ 0 & 0 & -1 \end{bmatrix}$$

In the $\mathcal{X}$-frame, then,

$$[\,\mathbf{Q}\,]_{\mathcal{X}} = \begin{bmatrix} 1 & 0 & 0 \\ 0 & \cos\phi & -\sin\phi \\ 0 & \sin\phi & \cos\phi \end{bmatrix} \tag{2.55a}$$

Likewise, if we define the coordinate frames $\mathcal{Y}$ and $\mathcal{Z}$ so that their Y and Z axes, respectively, coincide with the axis of rotation, then

$$[\,\mathbf{Q}\,]_{\mathcal{Y}} = \begin{bmatrix} \cos\phi & 0 & \sin\phi \\ 0 & 1 & 0 \\ -\sin\phi & 0 & \cos\phi \end{bmatrix} \tag{2.55b}$$

and

$$[\,\mathbf{Q}\,]_{\mathcal{Z}} = \begin{bmatrix} \cos\phi & -\sin\phi & 0 \\ \sin\phi & \cos\phi & 0 \\ 0 & 0 & 1 \end{bmatrix} \tag{2.55c}$$

The representations of eqs.(2.55a–c) can be called the X-, Y-, and Z-*canonical forms* of the rotation matrix. In many instances, a rotation matrix cannot be derived directly from information on the original and the final orientations of a rigid body, but the overall motion can be readily decomposed into a sequence of simple rotations taking the above canonical forms. An application of canonical forms lies in the parameterization of rotations by means of *Euler angles*, consisting of three successive rotations, ϕ, θ and ψ, about one axis of a coordinate frame. Euler angles are introduced in Exercise 2.18, and applications thereof in Exercises 2.35, 2.36, 3.9, and 3.10.

2.3.3 The Linear Invariants of a 3×3 Matrix

Now we introduce two *linear invariants* of 3×3 matrices. Given *any* 3×3 matrix $\mathbf{A}$, its *Cartesian decomposition*, the counterpart of the Cartesian representation of complex numbers, consists of the sum of its symmetric part, $\mathbf{A}_S$, and its skew-symmetric part, $\mathbf{A}_{SS}$, defined as

$$\mathbf{A}_S \equiv \frac{1}{2}(\mathbf{A} + \mathbf{A}^T), \quad \mathbf{A}_{SS} \equiv \frac{1}{2}(\mathbf{A} - \mathbf{A}^T) \tag{2.56}$$

The *axial vector* or for brevity, the *vector* of $\mathbf{A}$, is the vector $\mathbf{a}$ with the property

$$\mathbf{a} \times \mathbf{v} \equiv \mathbf{A}_{SS}\mathbf{v} \tag{2.57}$$

for any 3-dimensional vector $\mathbf{v}$. The *trace* of $\mathbf{A}$ is the sum of the eigenvalues of $\mathbf{A}_S$, which are real. Since no coordinate frame is involved in the above definitions, these are invariant. When calculating these invariants, of course, a particular coordinate frame must be used. Let us assume that the entries of matrix $\mathbf{A}$ in a certain coordinate frame are given by the array of real numbers a_{ij}, for $i, j = 1, 2, 3$. Moreover, let $\mathbf{a}$ have components a_i, for $i = 1, 2, 3$, in the same frame. The above-defined invariants are thus calculated as

$$\text{vect}(\mathbf{A}) \equiv \mathbf{a} \equiv \frac{1}{2}\begin{bmatrix} a_{32} - a_{23} \\ a_{13} - a_{31} \\ a_{21} - a_{12} \end{bmatrix}, \quad \text{tr}(\mathbf{A}) \equiv a_{11} + a_{22} + a_{33} \tag{2.58}$$

From the foregoing definitions, the following is now apparent:

Theorem 2.3.5 *The vector of a 3×3 matrix vanishes if and only if it is symmetric, whereas the trace of an $n \times n$ matrix vanishes if the matrix is skew symmetric.*

Other useful relations are given below. For any 3-dimensional vectors $\mathbf{a}$ and $\mathbf{b}$,

$$\text{vect}(\mathbf{a}\mathbf{b}^T) = -\frac{1}{2}\mathbf{a} \times \mathbf{b} \tag{2.59}$$

and

$$\text{tr}(\mathbf{a}\mathbf{b}^T) = \mathbf{a}^T\mathbf{b} \tag{2.60}$$

The second relation is quite straightforward, but the first one is less so; a proof of the first relation is given below: Let $\mathbf{w}$ denote $\text{vect}(\mathbf{a}\mathbf{b}^T)$. From Definition (2.57), for any 3-dimensional vector $\mathbf{v}$,

$$\mathbf{w} \times \mathbf{v} = \mathbf{W}\mathbf{v} \tag{2.61}$$

where $\mathbf{W}$ is the skew-symmetric component of $\mathbf{a}\mathbf{b}^T$, namely,

$$\mathbf{W} \equiv \frac{1}{2}(\mathbf{a}\mathbf{b}^T - \mathbf{b}\mathbf{a}^T) \tag{2.62}$$

and hence,

$$\mathbf{W}\mathbf{v} = \mathbf{w} \times \mathbf{v} = \frac{1}{2}[(\mathbf{b}^T\mathbf{v})\mathbf{a} - (\mathbf{a}^T\mathbf{v})\mathbf{b}] \tag{2.63}$$

Now, let us compare the last expression with the double cross product $(\mathbf{b} \times \mathbf{a}) \times \mathbf{v}$, namely,

$$(\mathbf{b} \times \mathbf{a}) \times \mathbf{v} = (\mathbf{b}^T\mathbf{v})\mathbf{a} - (\mathbf{a}^T\mathbf{v})\mathbf{b} \tag{2.64}$$

from which it becomes apparent that

$$\mathbf{w} = \frac{1}{2}\mathbf{b} \times \mathbf{a} \tag{2.65}$$

and the aforementioned relation readily follows.

Note that Theorem 2.3.5 states a *necessary and sufficient* condition for the vanishing of the vector of a 3×3 matrix, but only a sufficient condition for the vanishing of the trace of an $n \times n$ matrix. What this implies is that the trace of an $n \times n$ matrix can vanish without the matrix being necessarily skew symmetric, but the trace of a skew-symmetric matrix necessarily vanishes. Also note that whereas the vector of a matrix is defined *only* for 3×3 matrices, the trace can be defined more generally for $n \times n$ matrices.

2.3.4 The Linear Invariants of a Rotation

From the invariant representations of the rotation matrix, eqs.(2.48) and (2.54), it is clear that the first two terms of $\mathbf{Q}$, $\mathbf{e}\mathbf{e}^T$ and $\cos\phi(\mathbf{1} - \mathbf{e}\mathbf{e}^T)$, are symmetric, whereas the third one, $\sin\phi\mathbf{E}$, is skew-symmetric. Hence,

$$\text{vect}(\mathbf{Q}) = \text{vect}(\sin\phi\,\mathbf{E}) = \sin\phi\,\mathbf{e} \tag{2.66}$$

whereas

$$\text{tr}(\mathbf{Q}) = \text{tr}[\mathbf{e}\mathbf{e}^T + \cos\phi(\mathbf{1} - \mathbf{e}\mathbf{e}^T)] \equiv \mathbf{e}^T\mathbf{e} + \cos\phi(3 - \mathbf{e}^T\mathbf{e}) = 1 + 2\cos\phi \tag{2.67}$$

from which one can readily solve for $\cos\phi$, namely,

$$\cos\phi = \frac{\text{tr}(\mathbf{Q}) - 1}{2} \tag{2.68}$$

Henceforth, the vector of $\mathbf{Q}$ will be denoted by $\mathbf{q}$ and its components in a given coordinate frame by q_1, q_2, and q_3. Moreover, rather than using $\text{tr}(\mathbf{Q})$ as the other linear invariant, $q_0 \equiv \cos\phi$ will be introduced to refer to the *linear invariants of the rotation matrix*. Hence, the rotation matrix is fully defined by *four scalar parameters*, namely $\{q_i\}_0^3$, which will be conveniently stored in the 4-dimensional array $\boldsymbol{\lambda}$, defined as

$$\boldsymbol{\lambda} \equiv [q_1,\, q_2,\, q_3,\, q_0]^T \tag{2.69}$$

Note, however, that the four components of $\boldsymbol{\lambda}$ are not independent, for they obey the relation

$$\|\mathbf{q}\|^2 + q_0^2 \equiv \sin^2\phi + \cos^2\phi = 1 \tag{2.70}$$

Thus, eq.(2.70) can be written in a more compact form as

$$\|\boldsymbol{\lambda}\|^2 \equiv q_1^2 + q_2^2 + q_3^2 + q_0^2 = 1 \tag{2.71}$$

What eq.(2.70) states has a straightforward geometric interpretation: As a body rotates about a fixed point, its motion can be described in a 4-dimensional space by the motion of a point of position vector $\boldsymbol{\lambda}$ that moves on the surface of the unit sphere centered at the origin of the said space. Alternatively, one can conclude that, as a rigid body rotates about a fixed point, its motion can be described in a 3-dimensional space by the motion of position vector $\mathbf{q}$, which moves within the unit solid sphere centered at the origin of the said space. Given the dependence of the four components of vector $\boldsymbol{\lambda}$, one might be tempted to solve for, say, q_0 from eq.(2.70) in terms of the remaining components, namely, as

$$q_0 = \pm\sqrt{1 - (q_1^2 + q_2^2 + q_3^2)} \tag{2.72}$$

This, however, is not a good idea because the sign ambiguity of eq.(2.72) leaves angle ϕ undefined, for q_0 is nothing but $\cos\phi$. Moreover, the three components of vector $\mathbf{q}$ alone, i.e., $\sin\phi\,\mathbf{e}$, do not suffice to define the rotation represented by $\mathbf{Q}$. Indeed, from the definition of $\mathbf{q}$, one has

$$\sin\phi = \pm\|\mathbf{q}\|, \quad \mathbf{e} = \mathbf{q}/\sin\phi \tag{2.73}$$

from which it is clear that $\mathbf{q}$ alone does not suffice to define the rotation under study, since it leaves angle ϕ undefined. Indeed, the vector of the rotation matrix provides no information about $\cos\phi$. Yet another representation of the rotation matrix is displayed below, in terms of its linear invariants, that is readily derived from representations (2.48) and (2.54), namely,

$$\mathbf{Q} = \frac{\mathbf{q}\mathbf{q}^T}{\|\mathbf{q}\|^2} + q_0\left(\mathbf{1} - \frac{\mathbf{q}\mathbf{q}^T}{\|\mathbf{q}\|^2}\right) + \overline{\mathbf{Q}} \tag{2.74a}$$

in which $\overline{\mathbf{Q}}$ is the cross-product matrix of vector $\mathbf{q}$, i.e.,

$$\overline{\mathbf{Q}} \equiv \frac{\partial(\mathbf{q}\times\mathbf{x})}{\partial\mathbf{x}}$$

for any vector $\mathbf{x}$.

Note that by virtue of eq.(2.70), the representation of $\mathbf{Q}$ given in eq.(2.74a) can be expressed alternatively as

$$\mathbf{Q} = q_0\mathbf{1} + \overline{\mathbf{Q}} + \frac{\mathbf{q}\mathbf{q}^T}{1+q_0} \tag{2.74b}$$

From either eq.(2.74a) or eq.(2.74b) it is apparent that linear invariants are not suitable to represent a rotation when the associated angle is either π or close to it. Note that a rotation through an angle ϕ about an axis given by vector $\mathbf{e}$ is identical to a rotation through an angle $-\phi$ about an axis given by vector $-\mathbf{e}$. Hence, changing the sign of $\mathbf{e}$ does not change the rotation matrix, provided that the sign of ϕ is also changed. Henceforth, we will choose the sign of the components of $\mathbf{e}$ so that $\sin\phi \geq 0$, which is equivalent to assuming that $0 \leq \phi \leq \pi$. Thus, $\sin\phi$ is calculated as $\|\mathbf{q}\|$, while $\cos\phi$ as indicated in eq.(2.68). Obviously, $\mathbf{e}$ is simply $\mathbf{q}$ normalized, i.e., $\mathbf{q}$ divided by its Euclidean norm.

2.3.5 Examples

The examples below are meant to stress the foregoing ideas on rotation invariants.

Example 2.3.2 *If* $[\mathbf{e}]_{\mathcal{F}} = [\sqrt{3}/3, -\sqrt{3}/3, \sqrt{3}/3]^T$ *in a given coordinate frame* $\mathcal{F}$ *and* $\phi = 120°$*, what is* $\mathbf{Q}$ *in* $\mathcal{F}$*?*

Solution: From the data,

$$\cos\phi = -\frac{1}{2}, \quad \sin\phi = \frac{\sqrt{3}}{2}$$

Moreover, in the $\mathcal{F}$ frame,

$$[\,\mathbf{e}\mathbf{e}^T\,]_{\mathcal{F}} = \frac{1}{3}\begin{bmatrix} 1 \\ -1 \\ 1 \end{bmatrix}\begin{bmatrix} 1 & -1 & 1 \end{bmatrix} = \frac{1}{3}\begin{bmatrix} 1 & -1 & 1 \\ -1 & 1 & -1 \\ 1 & -1 & 1 \end{bmatrix}$$

and hence,

$$[\,\mathbf{1} - \mathbf{e}\mathbf{e}^T\,]_{\mathcal{F}} = \frac{1}{3}\begin{bmatrix} 2 & 1 & -1 \\ 1 & 2 & 1 \\ -1 & 1 & 2 \end{bmatrix}, \quad [\,\mathbf{E}\,]_{\mathcal{F}} \equiv \frac{\sqrt{3}}{3}\begin{bmatrix} 0 & -1 & -1 \\ 1 & 0 & -1 \\ 1 & 1 & 0 \end{bmatrix}$$

Thus, from eq.(2.48),

$$[\mathbf{Q}]_{\mathcal{F}} = \frac{1}{3}\begin{bmatrix} 1 & -1 & 1 \\ -1 & 1 & -1 \\ 1 & -1 & 1 \end{bmatrix} - \frac{1}{6}\begin{bmatrix} 2 & 1 & -1 \\ 1 & 2 & 1 \\ -1 & 1 & 2 \end{bmatrix} + \frac{3}{6}\begin{bmatrix} 0 & -1 & -1 \\ 1 & 0 & -1 \\ 1 & 1 & 0 \end{bmatrix}$$

i.e.,

$$[\mathbf{Q}]_{\mathcal{F}} = \begin{bmatrix} 0 & -1 & 0 \\ 0 & 0 & -1 \\ 1 & 0 & 0 \end{bmatrix}$$

Example 2.3.3 *The matrix representation of a linear transformation* $\mathbf{Q}$ *in a certain reference frame* $\mathcal{F}$ *is given below. Find out whether the said transformation is a rigid-body rotation. If it is, find its natural invariants.*

$$[\,\mathbf{Q}\,]_{\mathcal{F}} = \begin{bmatrix} 0 & 1 & 0 \\ 0 & 0 & 1 \\ 1 & 0 & 0 \end{bmatrix}$$

Solution: First the given array is tested for orthogonality:

$$[\,\mathbf{Q}\,]_{\mathcal{F}}[\,\mathbf{Q}^T\,]_{\mathcal{F}} = \begin{bmatrix} 0 & 1 & 0 \\ 0 & 0 & 1 \\ 1 & 0 & 0 \end{bmatrix} \begin{bmatrix} 0 & 0 & 1 \\ 1 & 0 & 0 \\ 0 & 1 & 0 \end{bmatrix} = \begin{bmatrix} 1 & 0 & 0 \\ 0 & 1 & 0 \\ 0 & 0 & 1 \end{bmatrix}$$

thereby showing that the said array is indeed orthogonal. Thus, the linear transformation could represent a reflection or a rotation. In order to decide which one this represents, the determinant of the foregoing array is computed:

$$\det(\,\mathbf{Q}\,) = +1$$

which makes apparent that $\mathbf{Q}$ indeed represents a rigid-body rotation. Now, its natural invariants are computed. The unit vector $\mathbf{e}$ can be computed as the eigenvector of $\mathbf{Q}$ associated with the eigenvalue $+1$. This requires, however, finding a nontrivial solution of a homogeneous linear system of three equations in three unknowns. This is not difficult to do, but it is cumbersome and is not necessary. In order to find $\mathbf{e}$ and ϕ, it is recalled that $\mathrm{vect}(\mathbf{Q}) = \sin\phi\,\mathbf{e}$, which is readily computed with differences only, as indicated in eq.(2.58), namely,

$$[\,\mathbf{q}\,]_{\mathcal{F}} \equiv \sin\phi\,[\mathbf{e}]_{\mathcal{F}} = -\frac{1}{2}\begin{bmatrix} 1 \\ 1 \\ 1 \end{bmatrix}$$

Under the assumption that $\sin\phi \geq 0$, then,

$$\sin\phi \equiv \|\mathbf{q}\| = \frac{\sqrt{3}}{2}$$

and hence,

$$[\mathbf{e}]_{\mathcal{F}} = \frac{[\mathbf{q}]_{\mathcal{F}}}{\|\mathbf{q}\|} = -\frac{\sqrt{3}}{3}\begin{bmatrix} 1 \\ 1 \\ 1 \end{bmatrix}$$

and

$$\phi = 60^\circ \quad \text{or} \quad 120^\circ$$

The foregoing ambiguity is resolved by the trace of $\mathbf{Q}$, which yields

$$1 + 2\cos\phi \equiv \mathrm{tr}(\mathbf{Q}) = 0, \quad \cos\phi = -\frac{1}{2}$$

The negative sign of $\cos\phi$ indicates that ϕ lies in the second quadrant—it cannot lie in the third quadrant because of our assumption about the sign of $\sin\phi$—and hence

$$\phi = 120^\circ$$

Example 2.3.4 *A coordinate frame X_1, Y_1, Z_1 is rotated into a configuration X_2, Y_2, Z_2 in such a way that*

$$X_2 = -Y_1, \quad Y_2 = Z_1, \quad Z_2 = -X_1$$

Find the matrix representation of the rotation in X_1, Y_1, Z_1 coordinates. From this representation, compute the direction of the axis and the angle of rotation.

Solution: Let $\mathbf{i}_1$, $\mathbf{j}_1$, $\mathbf{k}_1$ be unit vectors parallel to X_1, Y_1, Z_1, respectively, $\mathbf{i}_2$, $\mathbf{j}_2$, $\mathbf{k}_2$ being defined correspondingly. One has

$$\mathbf{i}_2 = -\mathbf{j}_1, \quad \mathbf{j}_2 = \mathbf{k}_1, \quad \mathbf{k}_2 = -\mathbf{i}_1$$

and hence, from Definition 2.2.1, the matrix representation $[\,\mathbf{Q}\,]_1$ of the rotation under study in the X_1, Y_1, Z_1 coordinate frame is readily derived:

$$[\,\mathbf{Q}\,]_1 = \begin{bmatrix} 0 & 0 & -1 \\ -1 & 0 & 0 \\ 0 & 1 & 0 \end{bmatrix}$$

from which the linear invariants follow, namely,

$$[\mathbf{q}]_1 \equiv [\,\mathrm{vect}(\mathbf{Q})\,]_1 = \sin\phi\,[\,\mathbf{e}\,]_1 = \frac{1}{2}\begin{bmatrix} 1 \\ -1 \\ -1 \end{bmatrix}, \quad \cos\phi = \frac{1}{2}[\,\mathrm{tr}(\mathbf{Q}) - 1\,] = -\frac{1}{2}$$

Under our assumption that $\sin\phi \geq 0$, we obtain

$$\sin\phi = \|\mathbf{q}\| = \frac{\sqrt{3}}{2}, \quad [\,\mathbf{e}\,]_1 = \frac{[\mathbf{q}]_1}{\sin\phi} = \frac{\sqrt{3}}{3}\begin{bmatrix} 1 \\ -1 \\ -1 \end{bmatrix}$$

From the foregoing values for $\sin\phi$ and $\cos\phi$, angle ϕ is computed uniquely as

$$\phi = 120^\circ$$

Example 2.3.5 *Show that the matrix $\mathbf{P}$ given in eq.(2.4) satisfies properties (2.1a).*

Solution: First, we prove idempotency, i.e.,

$$\begin{aligned} \mathbf{P}^2 &= (\mathbf{1} - \mathbf{n}\mathbf{n}^T)(\mathbf{1} - \mathbf{n}\mathbf{n}^T) \\ &= \mathbf{1} - 2\mathbf{n}\mathbf{n}^T + \mathbf{n}\mathbf{n}^T\mathbf{n}\mathbf{n}^T = \mathbf{1} - \mathbf{n}\mathbf{n}^T = \mathbf{P} \end{aligned}$$

thereby showing that $\mathbf{P}$ is, indeed, idempotent. Now we prove that $\mathbf{n}$ is an eigenvector of $\mathbf{P}$ with eigenvalue, 0 and hence, $\mathbf{n}$ spans the nullspace of $\mathbf{P}$. In fact,

$$\mathbf{Pn} = (\mathbf{1} - \mathbf{nn}^T)\mathbf{n} = \mathbf{n} - \mathbf{nn}^T\mathbf{n} = \mathbf{n} - \mathbf{n} = \mathbf{0}$$

thereby completing the proof.

Example 2.3.6 *The representations of three linear transformations in a given coordinate frame $\mathcal{F}$ are given below:*

$$[\,\mathbf{A}\,]_{\mathcal{F}} = \frac{1}{3}\begin{bmatrix} 2 & 1 & 2 \\ -2 & 2 & 1 \\ -1 & -2 & 2 \end{bmatrix}$$

$$[\,\mathbf{B}\,]_{\mathcal{F}} = \frac{1}{3}\begin{bmatrix} 2 & 1 & 1 \\ 1 & 2 & -1 \\ 1 & -1 & 2 \end{bmatrix}$$

$$[\,\mathbf{C}\,]_{\mathcal{F}} = \frac{1}{3}\begin{bmatrix} 1 & 2 & 2 \\ 2 & 1 & -2 \\ 2 & -2 & 1 \end{bmatrix}$$

One of the foregoing matrices is an orthogonal projection, one is a reflection, and one is a rotation. Identify each of these and give its invariants.

Solution: From representations (2.48) and (2.54), it is clear that a rotation matrix is symmetric if and only if $\sin\phi = 0$. This means that a rotation matrix cannot be symmetric unless its angle of rotation is either 0 or π, i.e., unless its trace is either 3 or -1. Since $[\,\mathbf{B}\,]_{\mathcal{F}}$ and $[\,\mathbf{C}\,]_{\mathcal{F}}$ are symmetric, they cannot be rotations, unless their traces take on the foregoing values. Their traces are thus evaluated below:

$$\mathrm{tr}(\mathbf{B}) = 2, \quad \mathrm{tr}(\mathbf{C}) = 1$$

which thus rules out the foregoing matrices as suitable candidates for rotations. Thus, $\mathbf{A}$ is the only candidate left for proper orthogonality, its suitability being tested below:

$$[\,\mathbf{AA}^T\,]_{\mathcal{F}} = \frac{1}{9}\begin{bmatrix} 9 & 0 & 0 \\ 0 & 9 & 0 \\ 0 & 0 & 9 \end{bmatrix}, \quad \det(\mathbf{A}) = +1$$

and hence, $\mathbf{A}$ indeed represents a rotation. Its natural invariants are next computed:

$$\sin\phi\,[\mathbf{e}]_{\mathcal{F}} = [\mathrm{vect}(\mathbf{A})]_{\mathcal{F}} = \frac{1}{2}\begin{bmatrix} -1 \\ 1 \\ -1 \end{bmatrix}, \quad \cos\phi = \frac{1}{2}[\mathrm{tr}(\mathbf{A}) - 1] = \frac{1}{2}(2-1) = \frac{1}{2}$$

We assume, as usual, that $\sin\phi \geq 0$. Then,

$$\sin\phi = \|\text{vect}(\mathbf{A})\| = \frac{\sqrt{3}}{2}, \quad \text{i.e., } \phi = 60^\circ$$

Moreover,

$$[\mathbf{e}]_{\mathcal{F}} = \frac{[\text{vect}(\mathbf{A})]_{\mathcal{F}}}{\|\text{vect}(\mathbf{A})\|} = \frac{\sqrt{3}}{3}\begin{bmatrix} -1 \\ 1 \\ -1 \end{bmatrix}$$

Now, one matrix of $\mathbf{B}$ and $\mathbf{C}$ is an orthogonal projection and the other is a reflection. To be a reflection, a matrix has to be orthogonal. Hence, each matrix is tested for orthogonality:

$$[\,\mathbf{B}\mathbf{B}^T\,]_{\mathcal{F}} = \frac{1}{9}\begin{bmatrix} 6 & 3 & 3 \\ 3 & 6 & -3 \\ 3 & -3 & 6 \end{bmatrix} = [\,\mathbf{B}^2\,]_{\mathcal{F}} = [\,\mathbf{B}\,]_{\mathcal{F}}, \; [\,\mathbf{C}\mathbf{C}^T\,]_{\mathcal{F}} = \frac{1}{9}\begin{bmatrix} 9 & 0 & 0 \\ 0 & 9 & 0 \\ 0 & 0 & 9 \end{bmatrix}$$

thereby showing that $\mathbf{C}$ is orthogonal and $\mathbf{B}$ is not. Furthermore, $\det(\mathbf{C}) = -1$, which confirms that $\mathbf{C}$ is a reflection. Now, if $\mathbf{B}$ is a projection, it is bound to be singular and idempotent. From the orthogonality test it is clear that it is idempotent. Moreover, one can readily verify that $\det(\mathbf{B}) = 0$, and hence $\mathbf{B}$ is singular. The unit vector $[\,\mathbf{n}\,]_{\mathcal{F}} = [\,n_1,\, n_2,\, n_3\,]^T$ spanning its nullspace is determined from the general form of projections, eq.(2.1a), whence it is apparent that

$$\mathbf{n}\mathbf{n}^T = \mathbf{1} - \mathbf{B}$$

Therefore, if a solution $\mathbf{n}$ has been found, then $-\mathbf{n}$ is also a solution, i.e., *the problem admits two solutions*, one being the negative of the other. These two solutions are found below, by first rewriting the above system of equations in component form:

$$\begin{bmatrix} n_1^2 & n_1n_2 & n_1n_3 \\ n_1n_2 & n_2^2 & n_2n_3 \\ n_1n_3 & n_2n_3 & n_3^2 \end{bmatrix} = \frac{1}{3}\begin{bmatrix} 1 & -1 & -1 \\ -1 & 1 & 1 \\ -1 & 1 & 1 \end{bmatrix}$$

Now, from the diagonal entries of the above matrices, it is apparent that the three components of $\mathbf{n}$ have identical absolute values, i.e., $\sqrt{3}/3$. Moreover, from the off-diagonal entries of the same matrices, the second and third components of $\mathbf{n}$ bear equal signs, but we cannot tell whether positive or negative, because of the quadratic nature of the problem at hand. The two solutions are thus obtained as

$$\mathbf{n} = \pm\frac{\sqrt{3}}{3}\begin{bmatrix} 1 \\ -1 \\ -1 \end{bmatrix}$$

which is the only invariant of $\mathbf{B}$.

We now look at $\mathbf{C}$, which is a reflection, and hence, bears the form

$$\mathbf{C} = \mathbf{1} - 2\mathbf{n}\mathbf{n}^T$$

In order to determine $\mathbf{n}$, note that

$$\mathbf{n}\mathbf{n}^T = \frac{1}{2}(\mathbf{1} - \mathbf{C})$$

or in component form,

$$\begin{bmatrix} n_1^2 & n_1 n_2 & n_1 n_3 \\ n_1 n_2 & n_2^2 & n_2 n_3 \\ n_1 n_3 & n_2 n_3 & n_3^2 \end{bmatrix} = \frac{1}{3}\begin{bmatrix} 1 & -1 & -1 \\ -1 & 1 & 1 \\ -1 & 1 & 1 \end{bmatrix}$$

which is identical to the matrix equation derived in the case of matrix $\mathbf{B}$. Hence, the solution is the same, i.e.,

$$\mathbf{n} = \pm\frac{\sqrt{3}}{3}\begin{bmatrix} 1 \\ -1 \\ -1 \end{bmatrix}$$

thereby finding the invariant sought.

Example 2.3.7 *The vector and the trace of a rotation matrix* $\mathbf{Q}$*, in a certain reference frame* $\mathcal{F}$*, are given as*

$$[\text{vect}(\mathbf{Q})]_{\mathcal{F}} = \frac{1}{2}\begin{bmatrix} -1 \\ 1 \\ -1 \end{bmatrix}, \quad \text{tr}(\mathbf{Q}) = 2$$

Find the matrix representation of $\mathbf{Q}$ *in the given coordinate frame and in a frame having its* Z*-axis parallel to* $\text{vect}(\mathbf{Q})$*.*

Solution: We shall resort to eq.(2.74a) to determine the rotation matrix $\mathbf{Q}$. The quantities involved in the aforementioned representation of $\mathbf{Q}$ are readily computed, as shown below:

$$[\,\mathbf{q}\mathbf{q}^T\,]_{\mathcal{F}} = \frac{1}{4}\begin{bmatrix} 1 & -1 & 1 \\ -1 & 1 & -1 \\ 1 & -1 & 1 \end{bmatrix}, \quad \|\mathbf{q}\|^2 = \frac{3}{4}, \quad [\,\overline{\mathbf{Q}}\,]_{\mathcal{F}} = \frac{1}{2}\begin{bmatrix} 0 & 1 & 1 \\ -1 & 0 & 1 \\ -1 & -1 & 0 \end{bmatrix}$$

from which $\mathbf{Q}$ follows:

$$[\,\mathbf{Q}\,]_{\mathcal{F}} = \frac{1}{3}\begin{bmatrix} 2 & 1 & 2 \\ -2 & 2 & 1 \\ -1 & -2 & 2 \end{bmatrix}$$

in the given coordinate frame. Now, let $\mathcal{Z}$ denote a coordinate frame whose Z-axis is parallel to $\mathbf{q}$. Hence,

$$[\,\mathbf{q}\,]_{\mathcal{Z}} = \frac{\sqrt{3}}{2}\begin{bmatrix} 0 \\ 0 \\ 1 \end{bmatrix}, \quad [\,\mathbf{q}\mathbf{q}^T\,]_{\mathcal{Z}} = \frac{3}{4}\begin{bmatrix} 0 & 0 & 0 \\ 0 & 0 & 0 \\ 0 & 0 & 1 \end{bmatrix}, \quad [\,\overline{\mathbf{Q}}\,]_{\mathcal{Z}} = \frac{\sqrt{3}}{2}\begin{bmatrix} 0 & -1 & 0 \\ 1 & 0 & 0 \\ 0 & 0 & 0 \end{bmatrix}$$

which readily leads to

$$[\,\mathbf{Q}\,]_{\mathcal{Z}} = \begin{bmatrix} 1/2 & -\sqrt{3}/2 & 0 \\ \sqrt{3}/2 & 1/2 & 0 \\ 0 & 0 & 1 \end{bmatrix}$$

and is in the Z-canonical form.

Example 2.3.8 *A procedure for trajectory planning produced a matrix representing a rotation for a certain* pick-and-place operation*, as shown below:*

$$[\,\mathbf{Q}\,] = \begin{bmatrix} 0.433 & -0.500 & z \\ x & 0.866 & -0.433 \\ 0.866 & y & 0.500 \end{bmatrix}$$

where x, y, and z are entries that are unrecognizable due to failures in the printing hardware. Knowing that $\mathbf{Q}$ is in fact a rotation matrix, find the missing entries.

Solution: Since $\mathbf{Q}$ is a rotation matrix, the product $\mathbf{P} \equiv \mathbf{Q}^T\mathbf{Q}$ should equal the 3×3 identity matrix, and $\det(\mathbf{Q})$ should be $+1$. The foregoing product is computed first:

$$[\,\mathbf{P}\,]_{\mathcal{F}} = \begin{bmatrix} 0.437 + z^2 & 0.433(x - z - 1) & 0.5(-y + z) + 0.375 \\ * & 0.937 + x^2 & 0.866(x + y) - 0.216 \\ * & * & 1 + y^2 \end{bmatrix}$$

where the entries below the diagonal have not been printed because the matrix is symmetric. Upon equating the diagonal entries of the foregoing array to unity, we obtain

$$x = \pm 0.250, \quad y = 0, \quad z = \pm 0.750$$

while the vanishing of the off-diagonal entries leads to

$$x = 0.250, \quad y = 0, \quad z = -0.750$$

which can be readily verified to produce $\det(\mathbf{Q}) = +1$.

2.3.6 The Euler-Rodrigues Parameters

The invariants defined so far, namely, the natural and the linear invariants of a rotation matrix, are not the only ones that are used in kinematics. Additionally, one has the *Euler parameters*, or *Euler-Rodrigues parameters*, as Cheng and Gupta (1989) propose that they should be called, represented here as $\mathbf{r}$ and r_0. The Euler-Rodrigues parameters are defined as

$$\mathbf{r} \equiv \sin\left(\frac{\phi}{2}\right)\,\mathbf{e}, \quad r_0 = \cos\left(\frac{\phi}{2}\right) \tag{2.75}$$

One can readily show that $\mathbf{Q}$ takes on a quite simple form in terms of the Euler-Rodrigues parameters, namely,

$$\mathbf{Q} = ({r_0}^2 - \mathbf{r} \cdot \mathbf{r})\mathbf{1} + 2\mathbf{r}\mathbf{r}^T + 2r_0\mathbf{R} \tag{2.76}$$

in which $\mathbf{R}$ is the cross-product matrix of $\mathbf{r}$, i.e.,

$$\mathbf{R} \equiv \frac{\partial(\mathbf{r} \times \mathbf{x})}{\partial \mathbf{x}}$$

for arbitrary $\mathbf{x}$.

Note that the Euler-Rodrigues parameters appear quadratically in the rotation matrix. Hence, these parameters cannot be computed with simple sums and differences. A closer inspection of eq.(2.74b) reveals that the linear invariants appear *almost linearly* in the rotation matrix. This means that the rotation matrix, as given by eq.(2.74b), is composed of two types of terms, namely, linear and rational. Moreover, the rational term is composed of a quadratic expression in the numerator and a linear expression in the denominator, the ratio thus being linear, which explains why the linear invariants can be obtained by sums and differences from the rotation matrix.

The relationship between the linear invariants and the Euler-Rodrigues parameters can be readily derived, namely,

$$r_0 = \pm\sqrt{\frac{1 + q_0}{2}}, \quad \mathbf{r} = \frac{\mathbf{q}}{2r_0}, \quad \phi \neq \pi \tag{2.77}$$

Furthermore, note that, if $\phi = \pi$, then $r_0 = 0$, and formulae (2.77) fail to produce $\mathbf{r}$. However, from eq.(2.75),

$$\text{For } \phi = \pi\text{:} \quad \mathbf{r} = \mathbf{e}, \quad r_0 = 0 \tag{2.78}$$

We now derive invariant relations between the rotation matrix and the Euler-Rodrigues parameters. To do this, we resort to the concept of *matrix square root*. As a matter of fact, the square root of a square matrix is nothing but a particular case of an *analytic function* of a square matrix, discussed in connection with Theorem 2.3.3 and the exponential representation of the rotation matrix. Indeed, the square root of a square matrix is an analytic function of that matrix, and hence, admits a series expansion in powers of the matrix. Moreover, by virtue of the Cayley-Hamilton Theorem (Theorem 2.3.3) the said square root should be, for a 3×3 matrix, a linear combination of the identity matrix $\mathbf{1}$, the matrix itself, and its square, the coefficients being found using the eigenvalues of the matrix.

Furthermore, from the geometric meaning of a rotation through the angle ϕ about an axis parallel to the unit vector $\mathbf{e}$, it is apparent that the square of the matrix representing the foregoing rotation is itself a rotation about the same axis, but through the angle 2ϕ. By the same token, the square

root of the same matrix is again a rotation matrix about the same axis, but through an angle $\phi/2$. Now, while the square of a matrix is unique, its square root is not. This fact is apparent for diagonalizable matrices, whose diagonal entries are their eigenvalues. Each eigenvalue, whether positive or negative, admits two square roots, and hence, a diagonalizable $n \times n$ matrix admits as many square roots as there are combinations of the two possible roots of individual eigenvalues, disregarding rearrangements of the latter. Such a number is 2^n, and hence, a 3×3 matrix admits eight square roots. For example, the eight square roots of the identity 3×3 matrix are displayed below:

$$\begin{bmatrix} 1 & 0 & 0 \\ 0 & 1 & 0 \\ 0 & 0 & 1 \end{bmatrix}, \quad \begin{bmatrix} 1 & 0 & 0 \\ 0 & 1 & 0 \\ 0 & 0 & -1 \end{bmatrix}, \quad \begin{bmatrix} 1 & 0 & 0 \\ 0 & -1 & 0 \\ 0 & 0 & 1 \end{bmatrix}, \quad \begin{bmatrix} -1 & 0 & 0 \\ 0 & 1 & 0 \\ 0 & 0 & 1 \end{bmatrix},$$

$$\begin{bmatrix} 1 & 0 & 0 \\ 0 & -1 & 0 \\ 0 & 0 & -1 \end{bmatrix}, \quad \begin{bmatrix} -1 & 0 & 0 \\ 0 & 1 & 0 \\ 0 & 0 & -1 \end{bmatrix}, \quad \begin{bmatrix} -1 & 0 & 0 \\ 0 & -1 & 0 \\ 0 & 0 & 1 \end{bmatrix}, \quad \begin{bmatrix} -1 & 0 & 0 \\ 0 & -1 & 0 \\ 0 & 0 & -1 \end{bmatrix}$$

In fact, the foregoing result can be extended to orthogonal matrices as well and, for that matter, to any square matrix with n linearly independent eigenvectors. That is, an $n \times n$ orthogonal matrix admits 2^n square roots. However, not all eight square roots of a 3×3 orthogonal matrix are orthogonal. In fact, not all eight square roots of a 3×3 proper orthogonal matrix are proper orthogonal either. Of these square roots, nevertheless, there is one that is proper orthogonal, the one representing a rotation of $\phi/2$. We will denote this particular square root of $\mathbf{Q}$ by $\sqrt{\mathbf{Q}}$. The Euler-Rodrigues parameters of $\mathbf{Q}$ can thus be expressed as the linear invariants of $\sqrt{\mathbf{Q}}$, namely,

$$\mathbf{r} = \text{vect}(\sqrt{\mathbf{Q}}), \quad r_0 = \frac{\text{tr}(\sqrt{\mathbf{Q}}) - 1}{2} \tag{2.79}$$

It is important to recognize the basic differences between the linear invariants and the Euler-Rodrigues parameters. Whereas the former can be readily derived from the matrix representation of the rotation involved by simple additions and subtractions, the latter require square roots and entail sign ambiguities. However, the former fail to produce information on the axis of rotation whenever the angle of rotation is π, whereas the latter produce that information *for any value of the angle of rotation.*

The Euler-Rodrigues parameters are nothing but the *quaternions* invented by Sir William Rowan Hamilton (1844) in an extraordinary moment of creativity on Monday, October 16, 1843, as "Hamilton, accompanied by Lady Hamilton, was walking along the Royal Canal in Dublin towards the Royal Irish Academy, where Hamilton was to preside a meeting." (Altmann, 1989).

Moreover, the Euler-Rodrigues parameters should not be confused with the *Euler angles*, which are not invariant and hence, admit multiple definitions. The foregoing means that no single set of Euler angles exists for a given rotation matrix, the said angles depending on how the rotation is decomposed into three simpler rotations. For this reason, Euler angles will not be stressed here. The reader is referred to Exercise 18 for a short discussion of Euler angles; Synge (1960) includes a classical treatment, while Kane, Likins and Levinson provide an extensive discussion of the same.

Example 2.3.9 *Find the Euler-Rodrigues parameters of the proper orthogonal matrix* $\mathbf{Q}$ *given as*

$$\mathbf{Q} = \frac{1}{3}\begin{bmatrix} -1 & 2 & 2 \\ 2 & -1 & 2 \\ 2 & 2 & -1 \end{bmatrix}$$

Solution: Since the given matrix is symmetric, its angle of rotation is π and its vector linear invariant vanishes, which prevents us from finding the direction of the axis of rotation from the linear invariants; moreover, expressions (2.77) do not apply. However, we can use eq.(2.49) to find the unit vector $\mathbf{e}$ parallel to the axis of rotation, i.e.,

$$\mathbf{e}\mathbf{e}^T = \frac{1}{2}(\mathbf{1} + \mathbf{Q})$$

or in component form,

$$\begin{bmatrix} e_1^2 & e_1e_2 & e_1e_3 \\ e_1e_2 & e_2^2 & e_2e_3 \\ e_1e_3 & e_2e_3 & e_3^2 \end{bmatrix} = \frac{1}{3}\begin{bmatrix} 1 & 1 & 1 \\ 1 & 1 & 1 \\ 1 & 1 & 1 \end{bmatrix}$$

A simple inspection of the components of the two sides of the above equation reveals that all three components of $\mathbf{e}$ are identical and moreover, of the same sign, but we cannot tell which sign this is. Therefore,

$$\mathbf{e} = \pm\frac{\sqrt{3}}{3}\begin{bmatrix} 1 \\ 1 \\ 1 \end{bmatrix}$$

Moreover, from the symmetry of $\mathbf{Q}$, we know that $\phi = \pi$, and hence,

$$\mathbf{r} = \mathbf{e}\sin\left(\frac{\phi}{2}\right) = \pm\frac{\sqrt{3}}{3}\begin{bmatrix} 1 \\ 1 \\ 1 \end{bmatrix}, \quad r_0 = \cos\left(\frac{\phi}{2}\right) = 0$$

2.4 Composition of Reflections and Rotations

As pointed out in Section 2.2, reflections occur often accompanied by rotations. The effect of this combination is that the rotation destroys the two properties of pure reflections, symmetry and self-inversion, as defined in Section 2.2. Indeed, let $\mathbf{R}$ be a pure reflection, taking on the form appearing in eq.(2.5), and $\mathbf{Q}$ an arbitrary rotation, taking on the form of eq.(2.48). The product of these two transformations, $\mathbf{QR}$, denoted by $\mathbf{T}$, is apparently neither symmetric nor self-inverse, as the reader can readily verify. Likewise, the product of these two transformations in the reverse order is neither symmetric nor self-inverse.

As a consequence of the foregoing discussion, an improper orthogonal transformation that is not symmetric can always be decomposed into the product of a rotation and a pure reflection, the latter being symmetric and self-inverse. Moreover, this decomposition can take on the form of any of the two possible orderings of the rotation and the reflection. Note, however, that once the order has been selected, the decomposition is not unique. Indeed, if we want to decompose $\mathbf{T}$ in the above paragraph into the product $\mathbf{QR}$, then we can freely choose the unit normal $\mathbf{n}$ of the plane of reflection and write

$$\mathbf{R} \equiv \mathbf{1} - 2\mathbf{n}\mathbf{n}^T$$

vector $\mathbf{n}$ then being found from

$$\mathbf{n}\mathbf{n}^T = \frac{1}{2}(\mathbf{1} - \mathbf{R})$$

Hence, the factor $\mathbf{Q}$ of that decomposition is obtained as

$$\mathbf{Q} = \mathbf{T}\mathbf{R}^{-1} \equiv \mathbf{T}\mathbf{R} = \mathbf{T} - 2(\mathbf{T}\mathbf{n})\mathbf{n}^T$$

where use has been made of the self-inverse property of $\mathbf{R}$. Any other selection of vector $\mathbf{n}$ will lead to a different decomposition of $\mathbf{T}$.

Example 2.4.1 *Join the palms of your two hands in the position adopted by swimmers when preparing for plunging, while holding a sheet of paper between them. The sheet defines a plane in each hand that we will call the* hand plane*, its unit normal, pointing outside of the hand, being called the* hand normal *and represented as vectors* $\mathbf{n}_R$ *and* $\mathbf{n}_L$ *for the right and left hand, respectively. Moreover, let* $\mathbf{o}_R$ *and* $\mathbf{o}_L$ *denote unit vectors pointing in the direction of the finger axes of each of the two hands. Thus, in the swimmer position described above,* $\mathbf{n}_L = -\mathbf{n}_R$ *and* $\mathbf{o}_L = \mathbf{o}_R$*. Now, without moving your right hand, let the left hand attain a position whereby the left-hand normal lies at right angles with the right-hand normal, the palm pointing downwards and the finger axes of the two hands remaining parallel. Find the representation of the transformation carrying the right hand to the final configuration of the left hand, in terms of the unit vectors* $\mathbf{n}_R$ *and* $\mathbf{o}_R$*.*

Solution: Let us regard the desired transformation $\mathbf{T}$ as the product of a rotation $\mathbf{Q}$ by a pure reflection $\mathbf{R}$, in the form $\mathbf{T} = \mathbf{QR}$. Thus, the transformation occurs so that the reflection takes place first, then the rotation. The reflection is simply that mapping the right hand into the left hand, and hence, the reflection plane is simply the hand plane, i.e.,

$$\mathbf{R} = \mathbf{1} - 2\mathbf{n}_R\mathbf{n}_R^T$$

Moreover, the left hand rotates from the swimmer position about an axis parallel to the finger axes through an angle of 90° clockwise from your viewpoint, i.e., in the positive direction of vector $\mathbf{o}_R$. Hence, the form of the rotation involved can be derived readily from eq.(2.48) and the above information, namely,

$$\mathbf{Q} = \mathbf{o}_R\mathbf{o}_R^T + \mathbf{O}_R$$

where $\mathbf{O}_R$ is the cross-product matrix of $\mathbf{o}_R$. Hence, upon performing the product $\mathbf{QR}$, we have

$$\mathbf{T} = \mathbf{o}_R\mathbf{o}_R^T + 2\mathbf{O}_R - 2(\mathbf{o}_R \times \mathbf{n}_R)\mathbf{n}_R^T$$

which is the transformation sought.

2.5 Coordinate Transformations and Homogeneous Coordinates

Crucial to robotics is the unambiguous description of the geometrical relations among the various bodies in the environment surrounding a robot. These relations are established by means of *coordinate frames*, or *frames*, for brevity, attached to each rigid body in the scene, including the robot links. The origins of these frames, moreover, are set at landmark points and orientations defined by key geometric entities like lines and planes. For example, in Chapter 4 we attach two frames to every moving link of a serial robot, with origin at a point on each of the axis of the two joints coupling this link with its two neighbors. Moreover, the Z-axis of each frame is defined, according to the Denavit-Hartenberg notation, introduced in that chapter, along each joint axis, while the X-axis of the frame closer to the base—termed the fore frame—is defined along the common perpendicular to the two joint axes. The origin of the same frame is thus defined as the intersection of the fore axis with the common perpendicular to the two axes. This section is devoted to the study of the coordinate transformations of vectors when these are represented in various frames.

2.5.1 Coordinate Transformations Between Frames with a Common Origin

We will refer to two coordinate frames in this section, namely, $\mathcal{A} = \{X, Y, Z\}$ and $\mathcal{B} = \{\mathcal{X}, \mathcal{Y}, \mathcal{Z}\}$. Moreover, let $\mathbf{Q}$ be the rotation carrying $\mathcal{A}$ into $\mathcal{B}$, i.e.,

$$\mathbf{Q}: \quad \mathcal{A} \quad \rightarrow \quad \mathcal{B} \tag{2.80}$$

The purpose of this subsection is to establish the relation between the representations of the position vector of a point P in $\mathcal{A}$ and $\mathcal{B}$, denoted by $[\,\mathbf{p}\,]_{\mathcal{A}}$ and $[\,\mathbf{p}\,]_{\mathcal{B}}$, respectively. Let

$$[\,\mathbf{p}\,]_{\mathcal{A}} = \begin{bmatrix} x \\ y \\ z \end{bmatrix} \tag{2.81}$$

We want to find $[\,\mathbf{p}\,]_{\mathcal{B}}$ in terms of $[\,\mathbf{p}\,]_{\mathcal{A}}$ and $\mathbf{Q}$, when the latter is represented in either frame. The coordinate transformation can best be understood if we regard point P as attached to frame $\mathcal{A}$, as if it were a point of a box with sides of lengths x, y, and z, as indicated in Fig. 2.2a. Now, frame $\mathcal{A}$ undergoes a rotation $\mathbf{Q}$ about its origin that carries it into a new attitude, that of frame $\mathcal{B}$, as illustrated in Fig. 2.2b. Point P in its rotated position is labeled Π, of position vector $\boldsymbol{\pi}$, i.e.,

$$\boldsymbol{\pi} = \mathbf{Q}\mathbf{p} \tag{2.82}$$

It is apparent that the relative position of point P with respect to its box does not change under the foregoing rotation, and hence,

$$[\,\boldsymbol{\pi}\,]_{\mathcal{B}} = \begin{bmatrix} x \\ y \\ z \end{bmatrix} \tag{2.83}$$

Moreover, let

$$[\,\boldsymbol{\pi}\,]_{\mathcal{A}} = \begin{bmatrix} \xi \\ \eta \\ \zeta \end{bmatrix} \tag{2.84}$$

The relation between the two representations of the position vector of any point of the 3-dimensional Euclidean space is given by

Theorem 2.5.1 *The representations of the position vector $\boldsymbol{\pi}$ of any point in two frames $\mathcal{A}$ and $\mathcal{B}$, denoted by $[\,\boldsymbol{\pi}\,]_{\mathcal{A}}$ and $[\,\boldsymbol{\pi}\,]_{\mathcal{B}}$, respectively, are related by*

$$[\,\boldsymbol{\pi}\,]_{\mathcal{A}} = [\,\mathbf{Q}\,]_{\mathcal{A}}[\,\boldsymbol{\pi}\,]_{\mathcal{B}} \tag{2.85}$$

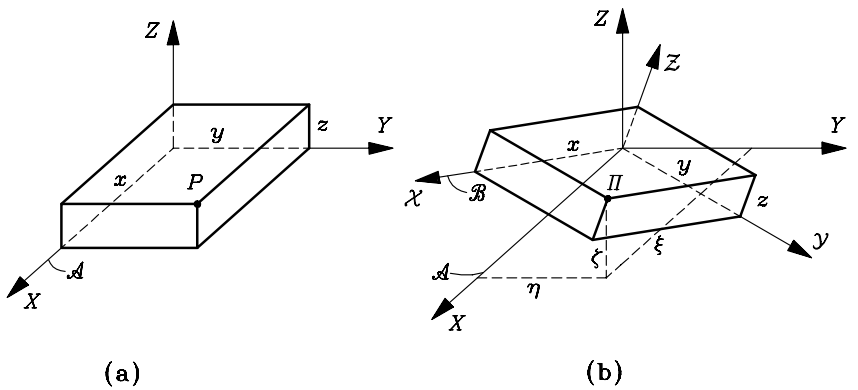

FIGURE 2.2. Coordinate transformation: (a) coordinates of point P in the $\mathcal{A}$-frame; and (b) relative orientation of frame $\mathcal{B}$ with respect to $\mathcal{A}$.

Proof: Let us write eq.(2.82) in $\mathcal{A}$:

$$[\,\boldsymbol{\pi}\,]_{\mathcal{A}} = [\,\mathbf{Q}\,]_{\mathcal{A}}[\,\mathbf{p}\,]_{\mathcal{A}} \tag{2.86}$$

Now, from Fig. 2.2b and eqs.(2.81) and (2.83) it is apparent that

$$[\,\boldsymbol{\pi}\,]_{\mathcal{B}} = [\,\mathbf{p}\,]_{\mathcal{A}} \tag{2.87}$$

Upon substituting eq.(2.87) into eq.(2.86), we obtain

$$[\,\boldsymbol{\pi}\,]_{\mathcal{A}} = [\,\mathbf{Q}\,]_{\mathcal{A}}[\,\boldsymbol{\pi}\,]_{\mathcal{B}} \tag{2.88}$$

q.e.d. Moreover, we have

Theorem 2.5.2 *The representations of* $\mathbf{Q}$ *carrying* $\mathcal{A}$ *into* $\mathcal{B}$ *in these two frames are identical, i.e.,*

$$[\,\mathbf{Q}\,]_{\mathcal{A}} = [\,\mathbf{Q}\,]_{\mathcal{B}} \tag{2.89}$$

Proof: Upon substitution of eq.(2.82) into eq.(2.85), we obtain

$$[\,\mathbf{Q}\mathbf{p}\,]_{\mathcal{A}} = [\,\mathbf{Q}\,]_{\mathcal{A}}[\,\mathbf{Q}\mathbf{p}\,]_{\mathcal{B}}$$

or

$$[\,\mathbf{Q}\,]_{\mathcal{A}}[\,\mathbf{p}\,]_{\mathcal{A}} = [\,\mathbf{Q}\,]_{\mathcal{A}}[\,\mathbf{Q}\mathbf{p}\,]_{\mathcal{B}}$$

Now, since $\mathbf{Q}$ is orthogonal, it is nonsingular, and hence, $[\,\mathbf{Q}\,]_{\mathcal{A}}$ can be deleted from the foregoing equation, thus leading to

$$[\,\mathbf{p}\,]_{\mathcal{A}} = [\,\mathbf{Q}\,]_{\mathcal{B}}[\,\mathbf{p}\,]_{\mathcal{B}} \tag{2.90}$$

However, by virtue of Theorem 2.5.1, the two representations of $\mathbf{p}$ observe the relation

$$[\,\mathbf{p}\,]_{\mathcal{A}} = [\,\mathbf{Q}\,]_{\mathcal{A}}[\,\mathbf{p}\,]_{\mathcal{B}} \tag{2.91}$$

the theorem being proved upon equating the right-hand sides of eqs.(2.90) and (2.91).

Note that the foregoing theorem states a relation valid only for the conditions stated therein. The reader should not conclude from this result that rotation matrices have the same representations in every frame. This point is stressed in Example 2.5.1. Furthermore, we have

Theorem 2.5.3 *The inverse relation of Theorem 2.5.1 is given by*

$$[\,\boldsymbol{\pi}\,]_{\mathcal{B}} = [\,\mathbf{Q}^T\,]_{\mathcal{B}}[\,\boldsymbol{\pi}\,]_{\mathcal{A}} \tag{2.92}$$

Proof: This is straightforward in light of the two foregoing theorems, and is left to the reader as an exercise.

Example 2.5.1 *Coordinate frames $\mathcal{A}$ and $\mathcal{B}$ are shown in Fig. 2.3. Find the representations of $\mathbf{Q}$ rotating $\mathcal{A}$ into $\mathcal{B}$ in these two frames and show that they are identical. Moreover, if $[\,\mathbf{p}\,]_{\mathcal{A}} = [\,1,\,1,\,1\,]^T$, find $[\,\mathbf{p}\,]_{\mathcal{B}}$.*

Solution: Let $\mathbf{i}$, $\mathbf{j}$, and $\mathbf{k}$ be unit vectors in the directions of the X-, Y-, and Z-axes, respectively; unit vectors $\boldsymbol{\iota}$, $\boldsymbol{\gamma}$, and $\boldsymbol{\kappa}$ are defined likewise as parallel to the $\mathcal{X}$-, $\mathcal{Y}$-, and $\mathcal{Z}$-axes of Fig. 2.3. Therefore,

$$\mathbf{Q}\,\mathbf{i} \equiv \boldsymbol{\iota} = -\mathbf{k}, \quad \mathbf{Q}\,\mathbf{j} \equiv \boldsymbol{\gamma} = -\mathbf{i}, \quad \mathbf{Q}\,\mathbf{k} \equiv \boldsymbol{\kappa} = \mathbf{j}$$

Therefore, using Definition 2.2.1, the matrix representation of $\mathbf{Q}$ carrying $\mathcal{A}$ into $\mathcal{B}$, in $\mathcal{A}$, is given by

$$[\,\mathbf{Q}\,]_{\mathcal{A}} = \begin{bmatrix} 0 & -1 & 0 \\ 0 & 0 & 1 \\ -1 & 0 & 0 \end{bmatrix}$$

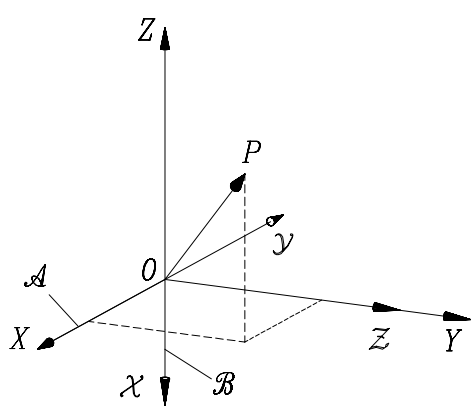

FIGURE 2.3. Coordinate frames $\mathcal{A}$ and $\mathcal{B}$ with a common origin.

Now, in order to find $[\,\mathbf{Q}\,]_{\mathcal{B}}$, we apply $\mathbf{Q}$ to the three unit vectors of $\mathcal{B}$, $\boldsymbol{\iota}$, $\boldsymbol{\gamma}$, and $\boldsymbol{\kappa}$. Thus, for $\boldsymbol{\iota}$, we have

$$\mathbf{Q}\boldsymbol{\iota} = \begin{bmatrix} 0 & -1 & 0 \\ 0 & 0 & 1 \\ -1 & 0 & 0 \end{bmatrix} \begin{bmatrix} 0 \\ 0 \\ -1 \end{bmatrix} = \begin{bmatrix} 0 \\ -1 \\ 0 \end{bmatrix} = -\mathbf{j} = -\boldsymbol{\kappa}$$

Likewise,

$$\mathbf{Q}\boldsymbol{\gamma} = -\boldsymbol{\iota}, \quad \mathbf{Q}\boldsymbol{\kappa} = \boldsymbol{\gamma}$$

again, from Definition 2.2.1, we have

$$[\,\mathbf{Q}\,]_{\mathcal{B}} = \begin{bmatrix} 0 & -1 & 0 \\ 0 & 0 & 1 \\ -1 & 0 & 0 \end{bmatrix} = [\,\mathbf{Q}\,]_{\mathcal{A}}$$

thereby confirming Theorem 2.5.2. Note that the representation of this matrix in any other coordinate frame would be different. For example, if we represent this matrix in a frame whose X-axis is directed along the axis of rotation of $\mathbf{Q}$, then we end up with the X-canonical representation of $\mathbf{Q}$, namely,

$$[\,\mathbf{Q}\,]_{\mathcal{X}} = \begin{bmatrix} 1 & 0 & 0 \\ 0 & \cos\phi & -\sin\phi \\ 0 & \sin\phi & \cos\phi \end{bmatrix}$$

with the angle of rotation ϕ being readily computed as $\phi = 120^\circ$, which thus yields

$$[\,\mathbf{Q}\,]_{\mathcal{X}} = \begin{bmatrix} 1 & 0 & 0 \\ 0 & -1/2 & -\sqrt{3}/2 \\ 0 & \sqrt{3}/2 & -1/2 \end{bmatrix}$$

which apparently has different entries from those of $[\,\mathbf{Q}\,]_{\mathcal{A}}$ and $[\,\mathbf{Q}\,]_{\mathcal{B}}$ found above.

Now, from eq.(2.92),

$$[\,\mathbf{p}\,]_{\mathcal{B}} = \begin{bmatrix} 0 & 0 & -1 \\ -1 & 0 & 0 \\ 0 & 1 & 0 \end{bmatrix} \begin{bmatrix} 1 \\ 1 \\ 1 \end{bmatrix} = \begin{bmatrix} -1 \\ -1 \\ 1 \end{bmatrix}$$

a result that can be readily verified by inspection.

2.5.2 Coordinate Transformation with Origin Shift

Now, if the coordinate origins do not coincide, let $\mathbf{b}$ be the position vector of $\mathcal{O}$, the origin of $\mathcal{B}$, from O, the origin of $\mathcal{A}$, as shown in Fig. 2.4. The corresponding coordinate transformation from $\mathcal{A}$ to $\mathcal{B}$, the counterpart of Theorem 2.5.1, is given below.

Theorem 2.5.4 *The representations of the position vector* $\mathbf{p}$ *of a point* P *of the Euclidean 3-dimensional space in two frames* $\mathcal{A}$ *and* $\mathcal{B}$ *are related by*

$$[\,\mathbf{p}\,]_{\mathcal{A}} = [\,\mathbf{b}\,]_{\mathcal{A}} + [\,\mathbf{Q}\,]_{\mathcal{A}}[\,\boldsymbol{\pi}\,]_{\mathcal{B}} \tag{2.93a}$$

$$[\,\boldsymbol{\pi}\,]_{\mathcal{B}} = [\,\mathbf{Q}^T\,]_{\mathcal{B}}([\,-\mathbf{b}\,]_{\mathcal{A}} + [\,\mathbf{p}\,]_{\mathcal{A}}) \tag{2.93b}$$

with $\mathbf{b}$ *defined as the vector directed from the origin of* $\mathcal{A}$ *to that of* $\mathcal{B}$*, and* $\boldsymbol{\pi}$ *the vector directed from the origin of* $\mathcal{B}$ *to* P*, as depicted in Fig. 2.4.*

Proof: We have, from Fig. 2.4,

$$\mathbf{p} = \mathbf{b} + \boldsymbol{\pi} \tag{2.94}$$

If we express the above equation in the $\mathcal{A}$-frame, we obtain

$$[\,\mathbf{p}\,]_{\mathcal{A}} = [\,\mathbf{b}\,]_{\mathcal{A}} + [\,\boldsymbol{\pi}\,]_{\mathcal{A}}$$

where $\boldsymbol{\pi}$ is assumed to be readily available in $\mathcal{B}$, and so the foregoing equation must be expressed as

$$[\,\mathbf{p}\,]_{\mathcal{A}} = [\,\mathbf{b}\,]_{\mathcal{A}} + [\,\mathbf{Q}\,]_{\mathcal{A}}[\,\boldsymbol{\pi}\,]_{\mathcal{B}}$$

which thus proves eq.(2.93a). To prove eq.(2.93b), we simply solve eq.(2.94) for $\boldsymbol{\pi}$ and apply eq.(2.92) to the equation thus resulting, which readily leads to the desired relation.

Example 2.5.2 *If* $[\,\mathbf{b}\,]_{\mathcal{A}} = [\,-1, -1, -1\,]^T$ *and* $\mathcal{A}$ *and* $\mathcal{B}$ *have the relative orientations given in Example 2.5.1, find the position vector, in* $\mathcal{B}$*, of a point* P *of position vector* $[\,\mathbf{p}\,]_{\mathcal{A}}$ *given as in the same example.*

Solution: What we obviously need is $[\,\boldsymbol{\pi}\,]_{\mathcal{B}}$, which is given in eq.(2.93b). We thus compute first the sum inside the parentheses of that equation, i.e.,

$$[\,-\mathbf{b}\,]_{\mathcal{A}} + [\,\mathbf{p}\,]_{\mathcal{A}} = \begin{bmatrix} 2 \\ 2 \\ 2 \end{bmatrix}$$

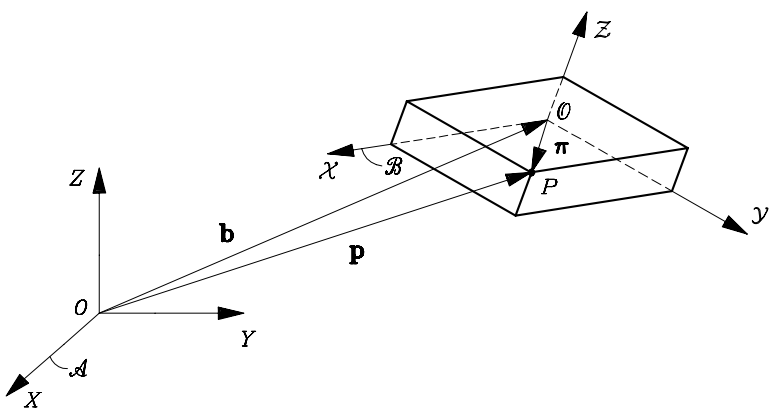

FIGURE 2.4. Coordinate frames with different origins.

We need further $[\,\mathbf{Q}^T\,]_{\mathcal{B}}$, which can be readily derived from $[\,\mathbf{Q}\,]_{\mathcal{B}}$. We do not have as yet this matrix, but we have $[\,\mathbf{Q}^T\,]_{\mathcal{A}}$, which is identical to $[\,\mathbf{Q}^T\,]_{\mathcal{B}}$ by virtue of Theorem 2.5.2. Therefore,

$$[\,\boldsymbol{\pi}\,]_{\mathcal{B}} = \begin{bmatrix} 0 & 0 & -1 \\ -1 & 0 & 0 \\ 0 & 1 & 0 \end{bmatrix} \begin{bmatrix} 2 \\ 2 \\ 2 \end{bmatrix} = \begin{bmatrix} -2 \\ -2 \\ 2 \end{bmatrix}$$

a result that the reader is invited to verify by inspection.

2.5.3 Homogeneous Coordinates

The general coordinate transformation, involving a shift of the origin, is not linear, in general, as can be readily realized by virtue of the *nonhomogeneous* term involved, i.e., the first term of the right-hand side of eq.(2.93a), which is independent of $\mathbf{p}$. Such a transformation, nevertheless, can be represented in homogeneous form if *homogeneous coordinates* are introduced. These are defined below: Let $[\,\mathbf{p}\,]_{\mathcal{M}}$ be the coordinate array of a *finite* point P in reference frame $\mathcal{M}$. What we mean by a finite point is one whose coordinates are all finite. We are thus assuming that the point P at hand is not *at infinity*, points at infinity being dealt with later. The homogeneous coordinates of P are those in the 4-dimensional array $\{\mathbf{p}\}_{\mathcal{M}}$, defined as

$$\{\mathbf{p}\}_{\mathcal{M}} \equiv \begin{bmatrix} [\,\mathbf{p}\,]_{\mathcal{M}} \\ 1 \end{bmatrix} \tag{2.95}$$

The *affine transformation* of eq.(2.93a) can now be rewritten in homogeneous-coordinate form as

$$\{\mathbf{p}\}_{\mathcal{A}} = \{\mathbf{T}\}_{\mathcal{A}}\{\boldsymbol{\pi}\}_{\mathcal{B}} \tag{2.96}$$

where $\{\mathbf{T}\}_{\mathcal{A}}$ is defined as a 4×4 array, i.e.,

$$\{\mathbf{T}\}_{\mathcal{A}} \equiv \begin{bmatrix} [\,\mathbf{Q}\,]_{\mathcal{A}} & [\,\mathbf{b}\,]_{\mathcal{A}} \\ [\,\mathbf{0}^T\,]_{\mathcal{A}} & 1 \end{bmatrix} \tag{2.97}$$

The inverse transformation of that defined in eq.(2.97) is derived from eq.(2.93a & b), i.e.,

$$\{\,\mathbf{T}^{-1}\,\}_{\mathcal{B}} = \begin{bmatrix} [\,\mathbf{Q}^T\,]_{\mathcal{B}} & [\,-\mathbf{b}\,]_{\mathcal{B}} \\ [\,\mathbf{0}^T\,]_{\mathcal{B}} & 1 \end{bmatrix} \tag{2.98}$$

Furthermore, homogeneous transformations can be concatenated. Indeed, let $\mathcal{F}_k$, for $k = i-1,\ i,\ i+1$, denote three coordinate frames, with origins at O_k. Moreover, let $\mathbf{Q}_{i-1}$ be the rotation carrying $\mathcal{F}_{i-1}$ into an orientation coinciding with that of $\mathcal{F}_i$. If a similar definition for $\mathbf{Q}_i$ is adopted, then $\mathbf{Q}_i$ denotes the rotation carrying $\mathcal{F}_i$ into an orientation coinciding with

that of $\mathcal{F}_{i+1}$. First, the case in which all three origins coincide is considered. Clearly,

$$[\,\mathbf{p}\,]_i = [\,\mathbf{Q}_{i-1}^T\,]_{i-1}[\,\mathbf{p}\,]_{i-1} \tag{2.99}$$

$$[\,\mathbf{p}\,]_{i+1} = [\,\mathbf{Q}_i^T\,]_i[\,\mathbf{p}\,]_i = [\,\mathbf{Q}_i^T\,]_i[\,\mathbf{Q}_{i-1}^T\,]_{i-1}[\,\mathbf{p}\,]_{i-1} \tag{2.100}$$

the inverse relation of that appearing in eq.(2.100) being

$$[\,\mathbf{p}\,]_{i-1} = [\,\mathbf{Q}_{i-1}\,]_{i-1}[\,\mathbf{Q}_i\,]_i[\,\mathbf{p}\,]_{i+1} \tag{2.101}$$

If now the origins do not coincide, let $\mathbf{a}_{i-1}$ and $\mathbf{a}_i$ denote the vectors $\overrightarrow{O_{i-1}O_i}$ and $\overrightarrow{O_iO_{i+1}}$, respectively. The homogeneous-coordinate transformations $\{\mathbf{T}_{i-1}\}_{i-1}$ and $\{\mathbf{T}_i\}_i$ thus arising are obviously

$$\{\mathbf{T}_{i-1}\}_{i-1} = \begin{bmatrix} [\,\mathbf{Q}_{i-1}\,]_{i-1} & [\,\mathbf{a}_{i-1}\,]_{i-1} \\ [\,\mathbf{0}^T\,]_{i-1} & 1 \end{bmatrix}, \quad \{\mathbf{T}_i\}_i = \begin{bmatrix} [\,\mathbf{Q}_i\,]_i & [\,\mathbf{a}_i\,]_i \\ [\,\mathbf{0}^T\,]_i & 1 \end{bmatrix} \tag{2.102}$$

whereas their inverse transformations are

$$\{\mathbf{T}_{i-1}^{-1}\}_i = \begin{bmatrix} [\,\mathbf{Q}_{i-1}^T\,]_i & [\,\mathbf{Q}_{i-1}^T\,]_i[\,-\mathbf{a}_{i-1}\,]_{i-1} \\ [\,\mathbf{0}^T\,]_i & 1 \end{bmatrix} \tag{2.103}$$

$$\{\mathbf{T}_i^{-1}\}_{i+1} = \begin{bmatrix} [\,\mathbf{Q}_i^T\,]_{i+1} & [\mathbf{Q}_i^T\,]_{i+1}[\,-\mathbf{a}_i\,]_i \\ [\,\mathbf{0}^T\,]_{i+1} & 1 \end{bmatrix} \tag{2.104}$$

Hence, the coordinate transformations involved are

$$\{\mathbf{p}\}_{i-1} = \{\mathbf{T}_{i-1}\}_{i-1}\{\mathbf{p}\}_i \tag{2.105}$$

$$\{\mathbf{p}\}_{i-1} = \{\mathbf{T}_{i-1}\}_{i-1}\{\mathbf{T}_i\}_i\{\mathbf{p}\}_{i+1} \tag{2.106}$$

the corresponding inverse transformations being

$$\{\,\mathbf{p}\,\}_i = \{\mathbf{T}_{i-1}^{-1}\}_i\{\,\mathbf{p}\,\}_{i-1} \tag{2.107}$$

$$\{\,\mathbf{p}\,\}_{i+1} = \{\mathbf{T}_i^{-1}\}_{i+1}\{\,\mathbf{p}\,\}_i = \{\mathbf{T}_i^{-1}\}_{i+1}\{\mathbf{T}_{i-1}^{-1}\}_i\{\,\mathbf{p}\,\}_{i-1} \tag{2.108}$$

Now, if P lies at infinity, we can express its homogeneous coordinates in a simpler form. To this end, we rewrite expression (2.95) in the form

$$\{\mathbf{p}\}_{\mathcal{M}} \equiv \|\mathbf{p}\| \begin{bmatrix} [\,\mathbf{e}\,]_{\mathcal{M}} \\ 1/\|\mathbf{p}\| \end{bmatrix}$$

and hence,

$$\lim_{\|\mathbf{p}\|\to\infty}\{\mathbf{p}\}_{\mathcal{M}} = \left(\lim_{\|\mathbf{p}\|\to\infty}\|\mathbf{p}\|\right)\left(\lim_{\|\mathbf{p}\|\to\infty}\begin{bmatrix} [\,\mathbf{e}\,]_{\mathcal{M}} \\ 1/\|\mathbf{p}\| \end{bmatrix}\right)$$

or

$$\lim_{\|\mathbf{p}\|\to\infty}\{\mathbf{p}\}_{\mathcal{M}} = \left(\lim_{\|\mathbf{p}\|\to\infty}\|\mathbf{p}\|\right)\begin{bmatrix} [\,\mathbf{e}\,]_{\mathcal{M}} \\ 0 \end{bmatrix}$$

We now define the *homogeneous coordinates of a point P lying at infinity* as the 4-dimensional array appearing in the foregoing expression, i.e.,

$$\{\,\mathbf{p}_\infty\,\}_{\mathcal{M}} \equiv \begin{bmatrix} [\,\mathbf{e}\,]_{\mathcal{M}} \\ 0 \end{bmatrix} \tag{2.109}$$

which means that a point at infinity, in homogeneous coordinates, has only a direction, given by the unit vector $\mathbf{e}$, but an undefined location. When working with objects within the atmosphere of the earth, for example, stars can be regarded as lying at infinity, and hence, their location is completely specified simply by their longitude and latitude, which suffice to define the direction cosines of a unit vector in spherical coordinates.

On the other hand, a rotation matrix can be regarded as composed of three columns, each representing a unit vector, e.g.,

$$\mathbf{Q} = [\,\mathbf{e}_1 \quad \mathbf{e}_2 \quad \mathbf{e}_3\,]$$

where the triad $\{\,\mathbf{e}_k\,\}_1^3$ is orthonormal. We can thus represent $\{\,\mathbf{T}\,\}_{\mathcal{A}}$ of eq.(2.97) in the form

$$\{\,\mathbf{T}\,\}_{\mathcal{A}} = \begin{bmatrix} \mathbf{e}_1 & \mathbf{e}_2 & \mathbf{e}_3 & \mathbf{b} \\ 0 & 0 & 0 & 1 \end{bmatrix} \tag{2.110}$$

thereby concluding that the columns of the 4×4 matrix $\mathbf{T}$ represent the homogeneous coordinates of a set of corresponding points, the first three of which are at infinity.

Example 2.5.3 *An ellipsoid is centered at a point $O_{\mathcal{B}}$ of position vector $\mathbf{b}$, its three axes $\mathcal{X}$, $\mathcal{Y}$, and $\mathcal{Z}$ defining a coordinate frame $\mathcal{B}$. Moreover, its semiaxes have lengths $a = 1$, $b = 2$, and $c = 3$, the coordinates of $O_{\mathcal{B}}$ in a coordinate frame $\mathcal{A}$ being $[\,\mathbf{b}\,]_{\mathcal{A}} = [\,1,\, 2,\, 3\,]^T$. Additionally, the direction cosines of $\mathcal{X}$ are $(0.933,\, 0.067,\, -0.354)$, whereas $\mathcal{Y}$ is perpendicular to $\mathbf{b}$ and to the unit vector $\mathbf{u}$ that is parallel to the $\mathcal{X}$-axis. Find the equation of the ellipsoid in $\mathcal{A}$. (This example has relevance in collision-avoidance algorithms, some of which approximate manipulator links as ellipsoids, thereby easing tremendously the computational requirements.)*

Solution: Let $\mathbf{u}$, $\mathbf{v}$, and $\mathbf{w}$ be unit vectors parallel to the $\mathcal{X}$-, $\mathcal{Y}$-, and $\mathcal{Z}$-axes, respectively. Then,

$$[\,\mathbf{u}\,]_{\mathcal{A}} = \begin{bmatrix} 0.933 \\ 0.067 \\ -0.354 \end{bmatrix}, \quad \mathbf{v} = \frac{\mathbf{u} \times \mathbf{b}}{\|\mathbf{u} \times \mathbf{b}\|}, \quad \mathbf{w} = \mathbf{u} \times \mathbf{v}$$

and hence,

$$[\,\mathbf{v}\,]_{\mathcal{A}} = \begin{bmatrix} 0.243 \\ -0.843 \\ 0.481 \end{bmatrix}, \quad [\,\mathbf{w}\,]_{\mathcal{A}} = \begin{bmatrix} -0.266 \\ -0.535 \\ -0.803 \end{bmatrix}$$

from which the rotation matrix $\mathbf{Q}$, rotating the axes of $\mathcal{A}$ into orientations coinciding with those of $\mathcal{B}$, can be readily represented in $\mathcal{A}$, or in $\mathcal{B}$ for that matter, as

$$[\,\mathbf{Q}\,]_{\mathcal{A}} = [\,\mathbf{u},\,\mathbf{v},\,\mathbf{w}\,]_{\mathcal{A}} = \begin{bmatrix} 0.933 & 0.243 & -0.266 \\ 0.067 & -0.843 & -0.535 \\ -0.354 & 0.481 & -0.803 \end{bmatrix}$$

On the other hand, if the coordinates of a point P in $\mathcal{A}$ and $\mathcal{B}$ are $[\,\mathbf{p}\,]_{\mathcal{A}} = [\,p_1,\,p_2,\,p_3\,]^T$ and $[\,\boldsymbol{\pi}\,]_{\mathcal{B}} = [\,\pi_1,\,\pi_2,\,\pi_3\,]^T$, respectively, then the equation of the ellipsoid in $\mathcal{B}$ is clearly

$$\mathcal{B}\text{:}\quad \frac{\pi_1^2}{1^2} + \frac{\pi_2^2}{2^2} + \frac{\pi_3^2}{3^2} = 1$$

Now, what is needed in order to derive the equation of the ellipsoid in $\mathcal{A}$ is simply a relation between the coordinates of P in $\mathcal{B}$ and those in $\mathcal{A}$. These coordinates are related by eq.(2.93b), which requires $[\,\mathbf{Q}^T\,]_{\mathcal{B}}$, while we have $[\,\mathbf{Q}\,]_{\mathcal{A}}$. Nevertheless, by virtue of Theorem 2.5.2

$$[\,\mathbf{Q}^T\,]_{\mathcal{B}} = [\,\mathbf{Q}^T\,]_{\mathcal{A}} = \begin{bmatrix} 0.933 & 0.067 & -0.354 \\ 0.243 & -0.843 & 0.481 \\ -0.266 & -0.535 & -0.803 \end{bmatrix}$$

Hence,

$$[\,\boldsymbol{\pi}\,]_{\mathcal{B}} = \begin{bmatrix} 0.933 & 0.067 & -0.354 \\ 0.243 & -0.843 & 0.481 \\ -0.266 & -0.535 & -0.803 \end{bmatrix} \left(\begin{bmatrix} -1 \\ -2 \\ -3 \end{bmatrix} + \begin{bmatrix} p_1 \\ p_2 \\ p_3 \end{bmatrix} \right)$$

Therefore,

$$\begin{aligned} \pi_1 &= 0.933p_1 + 0.067p_2 - 0.354p_3 - 0.005 \\ \pi_2 &= 0.243p_1 - 0.843p_2 + 0.481p_3 \\ \pi_3 &= -0.266p_1 - 0.535p_2 - 0.803p_3 + 3.745 \end{aligned}$$

Substitution of the foregoing relations into the ellipsoid equation in $\mathcal{B}$ leads to

$$\begin{aligned} \mathcal{A}\text{:}\quad & 32.1521{p_1}^2 + 7.70235{p_2}^2 + 9.17286{p_3}^2 - 8.30524p_1 - 16.0527p_2 \\ & -23.9304p_3 + 9.32655p_1p_2 + 9.02784p_2p_3 - 19.9676p_1p_3 + 20.101 = 0 \end{aligned}$$

which is the equation sought, as obtained using computer algebra.

2.6 Similarity Transformations

Transformations of the position vector of points under a change of coordinate frame involving both a translation of the origin and a rotation of the coordinate axes was the main subject of Section 2.5. In this section, we study the transformations of components of vectors other than the position vector, while extending the concept to the transformation of matrix entries. How these transformations take place is the subject of this section.

What is involved in the present discussion is a *change of basis* of the associated vector spaces, and hence, this is not limited to 3-dimensional vector spaces. That is, n-dimensional vector spaces will be studied in this section. Moreover, only isomorphisms, i.e., transformations $\mathbf{L}$ of the n-dimensional vector space $\mathcal{V}$ onto itself will be considered. Let $\mathcal{A} = \{\mathbf{a}_i\}_1^n$ and $\mathcal{B} = \{\mathbf{b}_i\}_1^n$ be two *different* bases of the same space $\mathcal{V}$. Hence, any vector $\mathbf{v}$ of $\mathcal{V}$ can be expressed in either of two ways, namely,

$$\mathbf{v} = \alpha_1\mathbf{a}_1 + \alpha_2\mathbf{a}_2 + \cdots + \alpha_n\mathbf{a}_n \tag{2.111}$$

$$\mathbf{v} = \beta_1\mathbf{b}_1 + \beta_2\mathbf{b}_2 + \cdots + \beta_n\mathbf{b}_n \tag{2.112}$$

from which two representations of $\mathbf{v}$ are readily derived, namely,

$$[\,\mathbf{v}\,]_{\mathcal{A}} = \begin{bmatrix} \alpha_1 \\ \alpha_2 \\ \vdots \\ \alpha_n \end{bmatrix}, \quad [\,\mathbf{v}\,]_{\mathcal{B}} = \begin{bmatrix} \beta_1 \\ \beta_2 \\ \vdots \\ \beta_n \end{bmatrix} \tag{2.113}$$

Furthermore, let the two foregoing bases be related by

$$\mathbf{b}_j = a_{1j}\mathbf{a}_1 + a_{2j}\mathbf{a}_2 + \cdots + a_{nj}\mathbf{a}_n, \quad j = 1, \ldots, n \tag{2.114}$$

Now, in order to find the relationship between the two representations of eq.(2.113), eq.(2.114) is substituted into eq.(2.112), which yields

$$\begin{aligned} \mathbf{v} = {} & \beta_1(a_{11}\mathbf{a}_1 + a_{21}\mathbf{a}_2 + \cdots + a_{n1}\mathbf{a}_n) \\ & + \beta_2(a_{12}\mathbf{a}_1 + a_{22}\mathbf{a}_2 + \cdots + a_{n2}\mathbf{a}_n) \\ & \qquad \vdots \\ & + \beta_n(a_{1n}\mathbf{a}_1 + a_{2n}\mathbf{a}_2 + \cdots + a_{nn}\mathbf{a}_n) \end{aligned} \tag{2.115}$$

This can be rearranged to yield

$$\begin{aligned} \mathbf{v} = {} & (a_{11}\beta_1 + a_{12}\beta_2 + \cdots + a_{1n}\beta_n)\mathbf{a}_1 \\ & + (a_{21}\beta_1 + a_{22}\beta_2 + \cdots + a_{2n}\beta_n)\mathbf{a}_2 \\ & \qquad \vdots \\ & + (a_{n1}\beta_1 + a_{n2}\beta_2 + \cdots + a_{nn}\beta_n)\mathbf{a}_n \end{aligned} \tag{2.116}$$

Comparing eq.(2.116) with eq.(2.111), one readily derives

$$[\,\mathbf{v}\,]_{\mathcal{A}} = [\,\mathbf{A}\,]_{\mathcal{A}}[\,\mathbf{v}\,]_{\mathcal{B}} \tag{2.117}$$

where

$$[\,\mathbf{A}\,]_{\mathcal{A}} \equiv \begin{bmatrix} a_{11} & a_{12} & \cdots & a_{1n} \\ a_{21} & a_{22} & \cdots & a_{2n} \\ \vdots & \vdots & \ddots & \vdots \\ a_{n1} & a_{n2} & \cdots & a_{nn} \end{bmatrix} \tag{2.118}$$

which are the relations sought. Clearly, the inverse relationship of eq.(2.117) is

$$[\,\mathbf{v}\,]_{\mathcal{B}} = [\,\mathbf{A}^{-1}\,]_{\mathcal{A}}[\,\mathbf{v}\,]_{\mathcal{A}} \tag{2.119}$$

Next, let $\mathbf{L}$ have the representation in $\mathcal{A}$ given below:

$$[\,\mathbf{L}\,]_{\mathcal{A}} = \begin{bmatrix} l_{11} & l_{12} & \cdots & l_{1n} \\ l_{21} & l_{22} & \cdots & l_{2n} \\ \vdots & \vdots & \ddots & \vdots \\ l_{n1} & l_{n2} & \cdots & l_{nn} \end{bmatrix} \tag{2.120}$$

Now we aim at finding the relationship between $[\,\mathbf{L}\,]_{\mathcal{A}}$ and $[\,\mathbf{L}\,]_{\mathcal{B}}$. To this end, let $\mathbf{w}$ be the image of $\mathbf{v}$ under $\mathbf{L}$, i.e.,

$$\mathbf{L}\mathbf{v} = \mathbf{w} \tag{2.121}$$

which can be expressed in terms of either $\mathcal{A}$ or $\mathcal{B}$ as

$$[\,\mathbf{L}\,]_{\mathcal{A}}[\,\mathbf{v}\,]_{\mathcal{A}} = [\,\mathbf{w}\,]_{\mathcal{A}} \tag{2.122}$$

$$[\,\mathbf{L}\,]_{\mathcal{B}}[\,\mathbf{v}\,]_{\mathcal{B}} = [\,\mathbf{w}\,]_{\mathcal{B}} \tag{2.123}$$

Now we assume that the image vector $\mathbf{w}$ of the transformation of eq.(2.121) is *identical* to that of vector $\mathbf{v}$ in the range of $\mathbf{L}$, which is not always the case. Our assumption is, then, that similar to eq.(2.117),

$$[\,\mathbf{w}\,]_{\mathcal{A}} = [\,\mathbf{A}\,]_{\mathcal{A}}[\,\mathbf{w}\,]_{\mathcal{B}} \tag{2.124}$$

Now, substitution of eq.(2.124) into eq.(2.122) yields

$$[\,\mathbf{A}\,]_{\mathcal{A}}[\,\mathbf{w}\,]_{\mathcal{B}} = [\,\mathbf{L}\,]_{\mathcal{A}}[\,\mathbf{A}\,]_{\mathcal{A}}[\,\mathbf{v}\,]_{\mathcal{B}} \tag{2.125}$$

which can be readily rearranged in the form

$$[\,\mathbf{w}\,]_{\mathcal{B}} = [\,\mathbf{A}^{-1}\,]_{\mathcal{A}}[\,\mathbf{L}\,]_{\mathcal{A}}[\,\mathbf{A}\,]_{\mathcal{A}}[\,\mathbf{v}\,]_{\mathcal{B}} \tag{2.126}$$

Comparing eq.(2.123) with eq.(2.126) readily leads to

$$[\,\mathbf{L}\,]_{\mathcal{B}} = [\,\mathbf{A}^{-1}\,]_{\mathcal{A}}[\,\mathbf{L}\,]_{\mathcal{A}}[\,\mathbf{A}\,]_{\mathcal{A}} \tag{2.127}$$

which upon rearrangement, becomes

$$[\,\mathbf{L}\,]_{\mathcal{A}} = [\,\mathbf{A}]_{\mathcal{A}}[\,\mathbf{L}\,]_{\mathcal{B}}[\,\mathbf{A}^{-1}\,]_{\mathcal{A}} \tag{2.128}$$

Relations (2.117), (2.119), (2.127), and (2.128) constitute what are called *similarity transformations*. These are important because they preserve *invariant* quantities such as the eigenvalues and eigenvectors of matrices, the magnitudes of vectors, the angles between vectors, and so on. Indeed, one has the following:

Theorem 2.6.1 *The characteristic polynomial of a given $n \times n$ matrix remains unchanged under a similarity transformation. Moreover, the eigenvalues of two matrix representations of the same $n \times n$ linear transformation are identical, and if $[\,\mathbf{e}\,]_{\mathcal{B}}$ is an eigenvector of $[\,\mathbf{L}\,]_{\mathcal{B}}$, then under the similarity transformation (2.128), the corresponding eigenvector of $[\,\mathbf{L}\,]_{\mathcal{A}}$ is $[\,\mathbf{e}\,]_{\mathcal{A}} = [\,\mathbf{A}\,]_{\mathcal{A}}[\,\mathbf{e}\,]_{\mathcal{B}}$.*

Proof: From eq.(2.11), the characteristic polynomial of $[\,\mathbf{L}\,]_{\mathcal{B}}$ is

$$P(\lambda) = \det(\lambda[\,\mathbf{1}\,]_{\mathcal{B}} - [\,\mathbf{L}\,]_{\mathcal{B}}) \tag{2.129}$$

which can be rewritten as

$$\begin{aligned} P(\lambda) &\equiv \det(\lambda[\,\mathbf{A}^{-1}\,]_{\mathcal{A}}[\,\mathbf{1}\,]_{\mathcal{A}}[\,\mathbf{A}\,]_{\mathcal{A}} - [\,\mathbf{A}^{-1}\,]_{\mathcal{A}}[\,\mathbf{L}\,]_{\mathcal{A}}[\,\mathbf{A}\,]_{\mathcal{A}}) \\ &= \det([\,\mathbf{A}^{-1}\,]_{\mathcal{A}}(\lambda[\,\mathbf{1}\,]_{\mathcal{A}} - [\,\mathbf{L}\,]_{\mathcal{A}})[\,\mathbf{A}\,]_{\mathcal{A}}) \\ &= \det([\,\mathbf{A}^{-1}\,]_{\mathcal{A}})\det(\lambda[\,\mathbf{1}\,]_{\mathcal{A}} - [\,\mathbf{L}\,]_{\mathcal{A}})\det([\,\mathbf{A}\,]_{\mathcal{A}}) \end{aligned}$$

But

$$\det([\,\mathbf{A}^{-1}\,]_{\mathcal{A}})\det([\,\mathbf{A}\,]_{\mathcal{A}}) = 1$$

and hence, the characteristic polynomial of $[\,\mathbf{L}\,]_{\mathcal{A}}$ is identical to that of $[\,\mathbf{L}\,]_{\mathcal{B}}$. Since both representations have the same characteristic polynomial, they have the same eigenvalues. Now, if $[\,\mathbf{e}\,]_{\mathcal{B}}$ is an eigenvector of $[\,\mathbf{L}\,]_{\mathcal{B}}$ associated with the eigenvalue λ, then

$$[\,\mathbf{L}\,]_{\mathcal{B}}[\,\mathbf{e}\,]_{\mathcal{B}} = \lambda[\,\mathbf{e}\,]_{\mathcal{B}}$$

Next, eq.(2.127) is substituted into the foregoing equation, which thus leads to

$$[\,\mathbf{A}^{-1}\,]_{\mathcal{A}}[\,\mathbf{L}\,]_{\mathcal{A}}[\,\mathbf{A}\,]_{\mathcal{A}}[\,\mathbf{e}\,]_{\mathcal{B}} = \lambda[\,\mathbf{e}\,]_{\mathcal{B}}$$

Upon rearrangement, this equation becomes

$$[\,\mathbf{L}\,]_{\mathcal{A}}[\,\mathbf{A}\,]_{\mathcal{A}}[\,\mathbf{e}\,]_{\mathcal{B}} = \lambda[\,\mathbf{A}\,]_{\mathcal{A}}[\,\mathbf{e}\,]_{\mathcal{B}} \tag{2.130}$$

whence it is apparent that $[\,\mathbf{A}\,]_{\mathcal{A}}[\,\mathbf{e}\,]_{\mathcal{B}}$ is an eigenvector of $[\,\mathbf{L}\,]_{\mathcal{A}}$ associated with the eigenvalue λ, q.e.d.

Theorem 2.6.2 *If* $[\,\mathbf{L}\,]_{\mathcal{A}}$ *and* $[\,\mathbf{L}\,]_{\mathcal{B}}$ *are related by the similarity transformation (2.127), then*

$$[\,\mathbf{L}^k\,]_{\mathcal{B}} = [\,\mathbf{A}^{-1}\,]_{\mathcal{A}}[\,\mathbf{L}^k\,]_{\mathcal{A}}[\,\mathbf{A}\,]_{\mathcal{A}} \tag{2.131}$$

for any integer k.

Proof: This is done by induction. For $k = 2$, one has

$$\begin{aligned}[\,\mathbf{L}^2\,]_{\mathcal{B}} &\equiv [\,\mathbf{A}^{-1}\,]_{\mathcal{A}}[\,\mathbf{L}\,]_{\mathcal{A}}[\,\mathbf{A}\,]_{\mathcal{A}}[\,\mathbf{A}^{-1}\,]_{\mathcal{A}}[\,\mathbf{L}\,]_{\mathcal{A}}[\,\mathbf{A}\,]_{\mathcal{A}} \\ &= [\,\mathbf{A}^{-1}\,]_{\mathcal{A}}[\,\mathbf{L}^2\,]_{\mathcal{A}}[\,\mathbf{A}\,]_{\mathcal{A}}\end{aligned}$$

Now, assume that the proposed relation holds for $k = n$. Then,

$$\begin{aligned}[\,\mathbf{L}^{n+1}\,]_{\mathcal{B}} &\equiv [\,\mathbf{A}^{-1}\,]_{\mathcal{A}}[\,\mathbf{L}^n\,]_{\mathcal{A}}[\,\mathbf{A}\,]_{\mathcal{A}}[\,\mathbf{A}^{-1}\,]_{\mathcal{A}}[\,\mathbf{L}\,]_{\mathcal{A}}[\,\mathbf{A}\,]_{\mathcal{A}} \\ &= [\,\mathbf{A}^{-1}\,]_{\mathcal{A}}[\,\mathbf{L}^{n+1}\,]_{\mathcal{A}}[\,\mathbf{A}\,]_{\mathcal{A}}\end{aligned}$$

i.e., the relation also holds for $k = n + 1$, thereby completing the proof.

Theorem 2.6.3 *The trace of an* $n \times n$ *matrix does not change under a similarity transformation.*

Proof: A preliminary relation will be needed: Let $[\,\mathbf{A}\,]$, $[\,\mathbf{B}\,]$ and $[\,\mathbf{C}\,]$ be three different $n \times n$ matrix arrays, in a given reference frame, that need not be indicated with any subscript. Moreover, let a_{ij}, b_{ij}, and c_{ij} be the components of the said arrays, with indices ranging from 1 to n. Hence, using standard index notation,

$$\mathrm{tr}([\,\mathbf{A}\,]\,[\,\mathbf{B}\,]\,[\,\mathbf{C}\,]) \equiv a_{ij}b_{jk}c_{ki} = b_{jk}c_{ki}a_{ij} \equiv \mathrm{tr}([\,\mathbf{B}\,]\,[\,\mathbf{C}\,]\,[\,\mathbf{A}\,]) \tag{2.132}$$

Taking the trace of both sides of eq.(2.127) and applying the foregoing result produces

$$\mathrm{tr}([\,\mathbf{L}\,]_{\mathcal{B}}) = \mathrm{tr}([\,\mathbf{A}^{-1}\,]_{\mathcal{A}}[\,\mathbf{L}\,]_{\mathcal{A}}[\,\mathbf{A}\,]_{\mathcal{A}}) = \mathrm{tr}([\,\mathbf{A}\,]_{\mathcal{A}}[\,\mathbf{A}^{-1}\,]_{\mathcal{A}}[\,\mathbf{L}\,]_{\mathcal{A}}) = \mathrm{tr}([\,\mathbf{L}\,]_{\mathcal{A}}) \tag{2.133}$$

thereby proving that the trace remains unchanged under a similarity transformation.

Example 2.6.1 *We consider the equilateral triangle sketched in Fig. 2.5, of side length equal to 2, with vertices* P_1, P_2, *and* P_3, *and coordinate frames* $\mathcal{A}$ *and* $\mathcal{B}$ *of axes* X, Y *and* X', Y', *respectively, both with origin at the centroid of the triangle. Let* $\mathbf{P}$ *be a* 2×2 *matrix defined by*

$$\mathbf{P} = [\,\mathbf{p}_1 \quad \mathbf{p}_2\,]$$

with $\mathbf{p}_i$ *denoting the position vector of* P_i *in a given coordinate frame. Show that matrix* $\mathbf{P}$ *does not obey a similarity transformation upon a change of frame, and compute its trace in frames* $\mathcal{A}$ *and* $\mathcal{B}$ *to make it apparent that this matrix does not comply with the conditions of Theorem 2.6.3.*

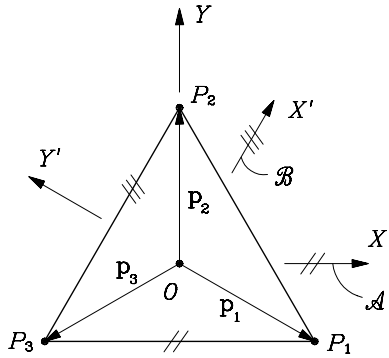

FIGURE 2.5. Two coordinate frames used to represent the position vectors of the corners of an equilateral triangle.

Solution: From the figure it is apparent that

$$[\,\mathbf{P}\,]_{\mathcal{A}} = \begin{bmatrix} 1 & 0 \\ -\sqrt{3}/3 & 2\sqrt{3}/3 \end{bmatrix}, \quad [\,\mathbf{P}\,]_{\mathcal{B}} = \begin{bmatrix} 0 & 1 \\ -2\sqrt{3}/3 & \sqrt{3}/3 \end{bmatrix}$$

Apparently,

$$\mathrm{tr}([\,\mathbf{P}\,]_{\mathcal{A}}) = 1 + \frac{2\sqrt{3}}{3} \neq \mathrm{tr}([\,\mathbf{P}\,]_{\mathcal{B}}) = \frac{\sqrt{3}}{3}$$

The reason why the trace of this matrix did not remain unchanged under a coordinate transformation is that the matrix does not obey a similarity transformation under a change of coordinates. Indeed, vectors $\mathbf{p}_i$ change as

$$[\,\mathbf{p}_i\,]_{\mathcal{A}} = [\,\mathbf{Q}\,]_{\mathcal{A}}[\,\mathbf{p}_i\,]_{\mathcal{B}}$$

under a change of coordinates from $\mathcal{B}$ to $\mathcal{A}$, with $\mathbf{Q}$ denoting the rotation carrying $\mathcal{A}$ into $\mathcal{B}$. Hence,

$$[\,\mathbf{P}\,]_{\mathcal{A}} = [\,\mathbf{Q}\,]_{\mathcal{A}}[\,\mathbf{P}\,]_{\mathcal{B}}$$

which is different from the similarity transformation of eq.(2.128). However, if we now define

$$\mathbf{R} \equiv \mathbf{P}\mathbf{P}^T$$

then

$$[\,\mathbf{R}\,]_{\mathcal{A}} = \begin{bmatrix} 1 & -\sqrt{3}/3 \\ -\sqrt{3}/3 & 5/3 \end{bmatrix}, \quad [\,\mathbf{R}\,]_{\mathcal{B}} = \begin{bmatrix} 1 & \sqrt{3}/3 \\ \sqrt{3}/3 & 5/3 \end{bmatrix}$$

and hence,

$$\mathrm{tr}([\,\mathbf{R}\,]_{\mathcal{B}}) = \frac{8}{3}$$

thereby showing that $\mathbf{R}$ does comply with the conditions of Theorem 2.6.3. Indeed, under a change of frame, matrix $\mathbf{R}$ changes as

$$[\,\mathbf{R}\,]_{\mathcal{A}} = [\,\mathbf{P}\mathbf{P}^T\,]_{\mathcal{A}} = [\,\mathbf{Q}\,]_{\mathcal{A}}[\,\mathbf{P}\,]_{\mathcal{B}}([\,\mathbf{Q}\,]_{\mathcal{A}}[\,\mathbf{P}\,]_{\mathcal{B}})^T = [\,\mathbf{Q}\,]_{\mathcal{A}}[\,\mathbf{P}\mathbf{P}\,]_{\mathcal{B}}^T[\,\mathbf{Q}^T\,]_{\mathcal{A}}$$

which is indeed a similarity transformation.

2.7 Invariance Concepts

From Example 2.6.1 it is apparent that certain properties, like the trace of certain square matrices do not change under a coordinate transformation. For this reason, a matrix like $\mathbf{R}$ of that example is said to be *frame-invariant*, or simply *invariant*, whereas matrix $\mathbf{P}$ of the same example is not. In this section, we formally define the concept of *invariance* and highlight its applications and its role in robotics. Let a scalar, a vector, and a matrix function of the position vector $\mathbf{p}$ be denoted by $f(\mathbf{p})$, $\mathbf{f}(\mathbf{p})$ and $\mathbf{F}(\mathbf{p})$, respectively. The representations of $\mathbf{f}(\mathbf{p})$ in two different coordinate frames, labelled $\mathcal{A}$ and $\mathcal{B}$, will be indicated as $[\mathbf{f}(\mathbf{p})]_{\mathcal{A}}$ and $[\mathbf{f}(\mathbf{p})]_{\mathcal{B}}$, respectively, with a similar notation for the representations of $\mathbf{F}(\mathbf{p})$. Moreover, let the two frames differ both in the location of their origins and in their orientations. Additionally, let the *proper orthogonal* matrix $[\mathbf{Q}]_{\mathcal{A}}$ denote the rotation of coordinate frame $\mathcal{A}$ into $\mathcal{B}$. Then, the scalar function $f(\mathbf{p})$ is said to be frame invariant, or invariant for brevity, if

$$f([\mathbf{p}]_{\mathcal{B}}) = f([\mathbf{p}]_{\mathcal{A}}) \tag{2.134}$$

Moreover, the vector quantity $\mathbf{f}$ is said to be invariant if

$$[\mathbf{f}]_{\mathcal{A}} = [\mathbf{Q}]_{\mathcal{A}}[\mathbf{f}]_{\mathcal{B}} \tag{2.135}$$

and finally, the matrix quantity $\mathbf{F}$ is said to be invariant if

$$[\mathbf{F}]_{\mathcal{A}} = [\mathbf{Q}]_{\mathcal{A}}[\mathbf{F}]_{\mathcal{B}}[\mathbf{Q}^T]_{\mathcal{A}} \tag{2.136}$$

Thus, the difference in origin location becomes irrelevant in this context, and hence, will no longer be considered. From the foregoing discussion, it is clear that the same vector quantity has different components in different coordinate frames; moreover, the same matrix quantity has different entries in different coordinate frames. However, certain scalar quantities associated with vectors, e.g., the inner product, and matrices, e.g., the matrix *moments*, to be defined presently, remain unchanged under a change of frame. Additionally, such vector operations as the cross product of two vectors are invariant. In fact, the scalar product of two vectors $\mathbf{a}$ and $\mathbf{b}$ remains unchanged under a change of frame, i.e.,

$$[\,\mathbf{a}\,]_{\mathcal{A}}^T\,[\,\mathbf{b}\,]_{\mathcal{A}} = [\,\mathbf{a}\,]_{\mathcal{B}}^T\,[\,\mathbf{b}\,]_{\mathcal{B}} \tag{2.137}$$

Additionally,

$$[\,\mathbf{a}\times\mathbf{b}\,]_{\mathcal{A}} = [\,\mathbf{Q}\,]_{\mathcal{A}}\,[\,\mathbf{a}\times\mathbf{b}\,]_{\mathcal{B}} \tag{2.138}$$

The kth *moment* of an $n \times n$ matrix $\mathbf{T}$, denoted by $\mathcal{I}_k$, is defined as (Leigh, 1968)

$$\mathcal{I}_k \equiv \mathrm{tr}(\mathbf{T}^k), \quad k = 0, 1, \ldots \tag{2.139}$$

where $\mathcal{I}_0 = \mathrm{tr}(\mathbf{1}) = n$. Now we have

Theorem 2.7.1 *If the trace of an $n \times n$ matrix $\mathbf{T}$ is invariant, then so are its moments.*

Proof: This is straightforward. Indeed, from Theorem 2.6.2, we have

$$[\,\mathbf{T}^k\,]_{\mathcal{B}} = [\,\mathbf{A}^{-1}\,]_{\mathcal{A}}[\,\mathbf{T}^k\,]_{\mathcal{A}}[\,\mathbf{A}\,]_{\mathcal{A}} \tag{2.140}$$

Now, let $[\,\mathcal{I}_{\mathbf{k}}\,]_{\mathcal{A}}$ and $[\,\mathcal{I}_{\mathbf{k}}\,]_{\mathcal{B}}$ denote the kth moment of $[\,\mathbf{T}\,]_{\mathcal{A}}$ and $[\,\mathbf{T}\,]_{\mathcal{B}}$, respectively. Thus,

$$\begin{aligned}[\,\mathcal{I}_{\mathbf{k}}\,]_{\mathcal{B}} &= \mathrm{tr}(\big[\,\mathbf{A}^{-\mathbf{1}}\,\big]_{\mathcal{A}}\,\big[\,\mathbf{T}^{\mathbf{k}}\,\big]_{\mathcal{A}}\,[\,\mathbf{A}\,]_{\mathcal{A}}) \equiv \mathrm{tr}([\,\mathbf{A}\,]_{\mathcal{A}}\,\big[\,\mathbf{A}^{-\mathbf{1}}\,\big]_{\mathcal{A}}\,\big[\,\mathbf{T}^{\mathbf{k}}\,\big]_{\mathcal{A}}) \\ &= \mathrm{tr}(\big[\,\mathbf{T}^{\mathbf{k}}\,\big]_{\mathcal{A}}) \equiv [\,\mathcal{I}_{\mathbf{k}}\,]_{\mathcal{A}}\end{aligned}$$

thereby completing the proof.

Furthermore,

Theorem 2.7.2 *An $n \times n$ matrix has only n linearly independent moments.*

Proof: Let the characteristic polynomial of $\mathbf{T}$ be

$$P(\lambda) = a_0 + a_1\lambda + \cdots + a_{n-1}\lambda^{n-1} + \lambda^n = 0 \tag{2.141}$$

Upon application of the Cayley-Hamilton Theorem, eq.(2.141) leads to

$$a_0\mathbf{1} + a_1\mathbf{T} + \cdots + a_{n-1}\mathbf{T}^{n-1} + \mathbf{T}^n = \mathbf{0} \tag{2.142}$$

where $\mathbf{1}$ denotes the $n \times n$ identity matrix.

Now, if we take the trace of both sides of eq.(2.142), and Definition (2.139) is recalled, one has

$$a_0\mathcal{I}_0 + a_1\mathcal{I}_1 + \cdots + a_{n-1}\mathcal{I}_{n-1} + \mathcal{I}_n = 0$$

from which it is apparent that $\mathcal{I}_n$ can be expressed as a linear combination of the first n moments of $\mathbf{T}$, $\{\,\mathcal{I}_k\,\}_0^{n-1}$. By simple induction, one can likewise prove that the mth moment is dependent upon the first n moments if $m \geq n$, thereby completing the proof.

The vector invariants of an $n \times n$ matrix are its eigenvectors, which have a direct physical significance in the case of symmetric matrices. The eigenvalues of these matrices are all real, its eigenvectors being also real and mutually orthogonal. Skew-symmetric matrices, in general, need not have either real eigenvalues or real eigenvectors. However, if we limit ourselves to 3×3 skew-symmetric matrices, exactly one of their eigenvalues, and its associated eigenvector, are both real. The eigenvalue of interest is 0, and the associated vector is the axial vector of the matrix under study.

It is now apparent that two $n \times n$ matrices related by a similarity transformation have the same set of moments. Now, by virtue of Theorem 2.7.2, one may be tempted to think that if two $n \times n$ symmetric matrices share

their first n moments $\{\mathcal{I}_k\}_0^{n-1}$, then the two matrices are related by a similarity transformation. A simple example will show that this is not true. Consider the two matrices $\mathbf{A}$ and $\mathbf{B}$ given below:

$$\mathbf{A} = \begin{bmatrix} 1 & 0 \\ 0 & 1 \end{bmatrix}, \quad \mathbf{B} = \begin{bmatrix} 1 & 2 \\ 2 & 1 \end{bmatrix}$$

The two foregoing matrices cannot possibly be related by a similarity transformation, for the first one is the identity matrix, while the second is not. However, the two matrices share the two moments $\mathcal{I}_0 = 2$ and $\mathcal{I}_1 = 2$. Let us now compute the second moments of these matrices:

$$\text{tr}(\mathbf{A}^2) = 2, \quad \text{tr}(\mathbf{B}^2) = \text{tr} \begin{bmatrix} 5 & 4 \\ 4 & 5 \end{bmatrix} = 10$$

which are indeed different. Therefore, to test whether two different matrices represent the same linear transformation, and hence, are related by a similarity transformation, we must verify that they share the same set of $n + 1$ moments $\{\mathcal{I}_k\}_0^n$. In fact, since all $n \times n$ matrices share the same zeroth moment $\mathcal{I}_0 = n$, only the n moments $\{\mathcal{I}_k\}_1^n$ need be tested for a similarity verification. That is, if two $n \times n$ matrices share the same n moments $\{\mathcal{I}_k\}_1^n$, then they represent the same linear transformation, albeit in different coordinate frames.

The foregoing discussion does not apply, in general, to nonsymmetric matrices, for these matrices are not fully characterized by their eigenvalues. For example, consider the matrix

$$\mathbf{A} = \begin{bmatrix} 1 & 1 \\ 0 & 1 \end{bmatrix}$$

Its two first moments are $\mathcal{I}_0 = 2$, $\mathcal{I}_1 = \text{tr}(\mathbf{A}) = 2$, which happen to be the first two moments of the 2×2 identity matrix as well. However, while the identity matrix leaves all 2-dimensional vectors unchanged, matrix $\mathbf{A}$ does not.

Now, if two symmetric matrices, say $\mathbf{A}$ and $\mathbf{B}$, represent the same transformation, they are related by a similarity transformation, i.e., a nonsingular matrix $\mathbf{T}$ exists such that

$$\mathbf{B} = \mathbf{T}^{-1}\mathbf{A}\mathbf{T}$$

Given $\mathbf{A}$ and $\mathbf{T}$, then, finding $\mathbf{B}$ is trivial, a similar statement holding if $\mathbf{B}$ and $\mathbf{T}$ are given; however, if $\mathbf{A}$ and $\mathbf{B}$ are given, finding $\mathbf{T}$ is more difficult. The latter problem occurs sometimes in robotics in the context of *calibration*, to be discussed in Subsection 2.7.1.

Example 2.7.1 *Two symmetric matrices are displayed below. Find out whether they are related by a similarity transformation.*

$$\mathbf{A} = \begin{bmatrix} 1 & 0 & 1 \\ 0 & 1 & 0 \\ 1 & 0 & 2 \end{bmatrix}, \quad \mathbf{B} = \begin{bmatrix} 1 & 0 & 0 \\ 0 & 2 & -1 \\ 0 & -1 & 1 \end{bmatrix}$$

Solution: The traces of the two matrices are apparently identical, namely, 4. Now we have to verify whether their second and third moments are also identical. To do this, we need the square and the cube of the two matrices, from which we then compute their traces. Thus, from

$$\mathbf{A}^2 = \begin{bmatrix} 2 & 0 & 3 \\ 0 & 1 & 0 \\ 3 & 0 & 5 \end{bmatrix}, \quad \mathbf{B}^2 = \begin{bmatrix} 1 & 0 & 0 \\ 0 & 5 & -3 \\ 0 & -3 & 2 \end{bmatrix}$$

we readily obtain

$$\mathrm{tr}(\mathbf{A}^2) = \mathrm{tr}(\mathbf{B}^2) = 8$$

Moreover,

$$\mathbf{A}^3 = \begin{bmatrix} 5 & 0 & 8 \\ 0 & 1 & 0 \\ 8 & 0 & 13 \end{bmatrix}, \quad \mathbf{B}^3 = \begin{bmatrix} 1 & 0 & 0 \\ 0 & 13 & -8 \\ 0 & -8 & 5 \end{bmatrix}$$

whence

$$\mathrm{tr}(\mathbf{A}^3) = \mathrm{tr}(\mathbf{B}^3) = 19$$

Therefore, the two matrices are related by a similarity transformation. Hence, they represent the same linear transformation.

Example 2.7.2 *Same as Example 2.7.1, for the two matrices displayed below:*

$$\mathbf{A} = \begin{bmatrix} 1 & 0 & 2 \\ 0 & 1 & 0 \\ 2 & 0 & 0 \end{bmatrix}, \quad \mathbf{B} = \begin{bmatrix} 1 & 1 & 1 \\ 1 & 1 & 0 \\ 1 & 0 & 0 \end{bmatrix}$$

Solution: As in the previous example, the traces of these matrices are identical, i.e., 2. However, $\mathrm{tr}(\mathbf{A}^2) = 10$, while $\mathrm{tr}(\mathbf{B}^2) = 6$. We thus conclude that the two matrices cannot be related by a similarity transformation.

2.7.1 Applications to Redundant Sensing

A sensor, such as a camera or a range finder, is often mounted on a robotic end-effector to determine the *pose*—i.e., the position and orientation, as defined in Subsection 3.2.3—of an object. If redundant sensors are introduced, and we attach frames $\mathcal{A}$ and $\mathcal{B}$ to each of these, then each sensor can be used to determine the orientation of the end-effector with respect to a reference configuration. This is a simple task, for all that is needed is to measure the rotation $\mathbf{R}$ that each of the foregoing frames underwent from the reference configuration, in which these frames are denoted by $\mathcal{A}_0$ and $\mathcal{B}_0$, respectively. Let us assume that these measurements produce the orthogonal matrices $\mathbf{A}$ and $\mathbf{B}$, representing $\mathbf{R}$ in $\mathcal{A}$ and $\mathcal{B}$, respectively. With

this information we would like to determine the relative orientation $\mathbf{Q}$ of frame $\mathcal{B}$ with respect to frame $\mathcal{A}$, a problem that is called here *instrument calibration*.

We thus have $\mathbf{A} \equiv [\,\mathbf{R}\,]_{\mathcal{A}}$ and $\mathbf{B} \equiv [\,\mathbf{R}\,]_{\mathcal{B}}$, and hence, the algebraic problem at hand consists in determining $[\,\mathbf{Q}\,]_{\mathcal{A}}$ or equivalently, $[\,\mathbf{Q}\,]_{\mathcal{B}}$. The former can be obtained from the similarity transformation of eq.(2.136), which leads to

$$\mathbf{A} = [\,\mathbf{Q}\,]_{\mathcal{A}}\,\mathbf{B}[\,\mathbf{Q}^T\,]_{\mathcal{A}}$$

or

$$\mathbf{A}\,[\,\mathbf{Q}\,]_{\mathcal{A}} = [\,\mathbf{Q}\,]_{\mathcal{A}}\,\mathbf{B}$$

This problem could be solved if we had three invariant vectors associated with each of the two matrices $\mathbf{A}$ and $\mathbf{B}$. Then, each corresponding pair of vectors of these triads would be related by eq.(2.135), thereby obtaining three such vector equations that should be sufficient to compute the nine components of the matrix $\mathbf{Q}$ rotating frame $\mathcal{A}$ into $\mathcal{B}$. However, since $\mathbf{A}$ and $\mathbf{B}$ are orthogonal matrices, they admit only one real invariant vector, namely, their axial vector, and we are short of two vector equations. We thus need two more invariant vectors, represented in both $\mathcal{A}$ and $\mathcal{B}$, to determine $\mathbf{Q}$. The obvious way of obtaining one additional vector in each frame is to take not one, but two measurements of the orientation of $\mathcal{A}_0$ and $\mathcal{B}_0$ with respect to $\mathcal{A}$ and $\mathcal{B}$, respectively. Let the matrices representing these orientations be given, in each of the two coordinate frames, by $\mathbf{A}_i$ and $\mathbf{B}_i$, for $i = 1, 2$. Moreover, let $\mathbf{a}_i$ and $\mathbf{b}_i$, for $i = 1, 2$, be the axial vectors of matrices $\mathbf{A}_i$ and $\mathbf{B}_i$, respectively.

Now we have two possibilities: (i) neither of $\mathbf{a}_1$ and $\mathbf{a}_2$ and, consequently, neither of $\mathbf{b}_1$ and $\mathbf{b}_2$, is zero; and (ii) at least one of $\mathbf{a}_1$ and $\mathbf{a}_2$, and consequently, the corresponding vector of the $\{\,\mathbf{b}_1,\,\mathbf{b}_2\,\}$ pair, vanishes. In the first case, nothing prevents us from computing a third vector of each set, namely,

$$\mathbf{a}_3 = \mathbf{a}_1 \times \mathbf{a}_2, \quad \mathbf{b}_3 = \mathbf{b}_1 \times \mathbf{b}_2 \tag{2.143}$$

In the second case, however, we have two more possibilities, i.e., the angle of rotation of that orthogonal matrix, $\mathbf{A}_1$ or $\mathbf{A}_2$, whose axial vector vanishes is either 0 or π. If the foregoing angle vanishes, then $\mathcal{A}$ underwent a pure translation from $\mathcal{A}_0$, the same holding, of course, for $\mathcal{B}$ and $\mathcal{B}_0$. This means that the corresponding measurement becomes useless for our purposes, and a new measurement is needed, involving a rotation. If, on the other hand, the same angle is π, then the associated rotation is symmetric and the unit vector $\mathbf{e}$ parallel to its axis can be determined from eq.(2.49) in both $\mathcal{A}$ and $\mathcal{B}$. This unit vector, then, would play the role of the vanishing axial vector, and we would thus end up, in any event, with two pairs of nonzero vectors, $\{\mathbf{a}_i\,\}_1^2$ and $\{\mathbf{b}_i\,\}_1^2$. As a consequence, we can always find two triads of nonzero vectors, $\{\,\mathbf{a}_i\,\}_1^3$ and $\{\,\mathbf{b}_i\,\}_1^3$, that are related by

$$\mathbf{a}_i = [\,\mathbf{Q}\,]_{\mathcal{A}}\,\mathbf{b}_i, \quad \text{for } i = 1, 2, 3 \tag{2.144}$$

The problem at hand now reduces to computing $[\,\mathbf{Q}\,]_{\mathcal{A}}$ from eq.(2.144). In order to perform this computation, we write the three foregoing equations in matrix form, namely,

$$\mathbf{E} = [\,\mathbf{Q}\,]_{\mathcal{A}}\,\mathbf{F} \tag{2.145}$$

with $\mathbf{E}$ and $\mathbf{F}$ defined as

$$\mathbf{E} \equiv [\,\mathbf{a}_1 \quad \mathbf{a}_2 \quad \mathbf{a}_3\,], \quad \mathbf{F} \equiv [\,\mathbf{b}_1 \quad \mathbf{b}_2 \quad \mathbf{b}_3\,] \tag{2.146}$$

Now, by virtue of the form in which the two vector triads were defined, none of the two above matrices is singular, and hence, we have

$$[\,\mathbf{Q}\,]_{\mathcal{A}} = \mathbf{E}\mathbf{F}^{-1} \tag{2.147}$$

Moreover, note that the inverse of $\mathbf{F}$ can be expressed in terms of its columns explicitly, without introducing components, if the concept of *reciprocal bases* is recalled (Brand, 1965). Thus,

$$\mathbf{F}^{-1} = \frac{1}{\Delta}\begin{bmatrix}(\mathbf{b}_2 \times \mathbf{b}_3)^T \\ (\mathbf{b}_3 \times \mathbf{b}_1)^T \\ (\mathbf{b}_1 \times \mathbf{b}_2)^T\end{bmatrix}, \quad \Delta \equiv \mathbf{b}_1 \times \mathbf{b}_2 \cdot \mathbf{b}_3 \tag{2.148}$$

Therefore,

$$[\,\mathbf{Q}\,]_{\mathcal{A}} = \frac{1}{\Delta}[\mathbf{a}_1(\mathbf{b}_2 \times \mathbf{b}_3)^T + \mathbf{a}_2(\mathbf{b}_3 \times \mathbf{b}_1)^T + \mathbf{a}_3(\mathbf{b}_1 \times \mathbf{b}_2)^T] \tag{2.149}$$

thereby completing the computation of $[\,\mathbf{Q}\,]_{\mathcal{A}}$ *directly and with simple vector operations.*

Example 2.7.3 (Hand-Eye Calibration) *Determine the relative orientation of a frame $\mathcal{B}$ attached to a camera mounted on a robot end-effector, with respect to a frame $\mathcal{A}$ fixed to the latter, as shown in Fig. 2.6. It is assumed that two measurements of the orientation of the two frames with respect to frames $\mathcal{A}_0$ and $\mathcal{B}_0$ in the reference configuration of the end-effector are available. These measurements produce the orientation matrices $\mathbf{A}_i$ of the frame fixed to the camera and $\mathbf{B}_i$ of the frame fixed to the end-effector, for $i = 1, 2$. The numerical data of this example are given below:*

$$\mathbf{A}_1 = \begin{bmatrix}-0.92592593 & -0.37037037 & -0.07407407 \\ 0.28148148 & -0.80740741 & 0.51851852 \\ -0.25185185 & 0.45925926 & 0.85185185\end{bmatrix}$$

$$\mathbf{A}_2 = \begin{bmatrix}-0.83134406 & 0.02335236 & -0.55526725 \\ -0.52153607 & 0.31240270 & 0.79398028 \\ 0.19200830 & 0.94969269 & -0.24753503\end{bmatrix}$$

$$\mathbf{B}_1 = \begin{bmatrix}-0.90268482 & 0.10343126 & -0.41768659 \\ 0.38511568 & 0.62720266 & -0.67698060 \\ 0.19195318 & -0.77195777 & -0.60599932\end{bmatrix}$$

$$\mathbf{B}_2 = \begin{bmatrix}-0.73851280 & -0.54317226 & 0.39945305 \\ -0.45524951 & 0.83872293 & 0.29881721 \\ -0.49733966 & 0.03882952 & -0.86668653\end{bmatrix}$$

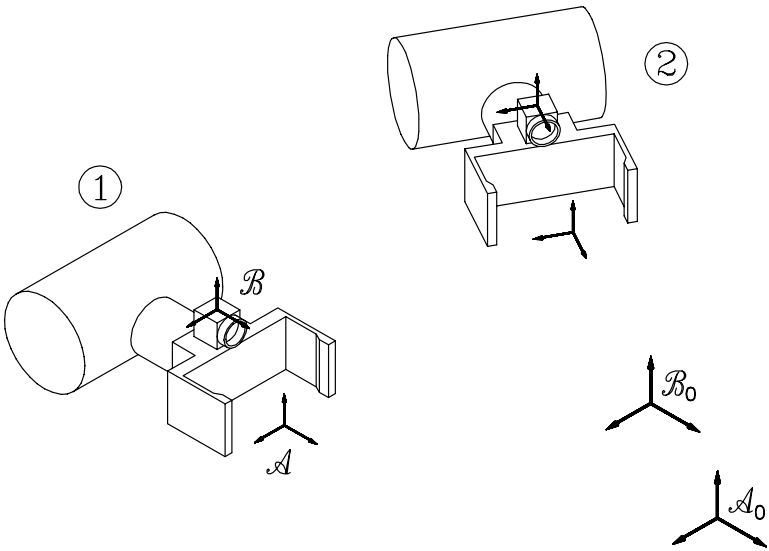

FIGURE 2.6. Measuring the orientation of a camera-fixed coordinate frame with respect to a frame fixed to a robotic end-effector.

Solution: Shiu and Ahmad (1987) formulated this problem in the form of a matrix linear homogeneous equation, while Chou and Kamel (1988) solved the same problem using quaternions and very cumbersome numerical methods that involve singular-value computations. The latter require an iterative procedure within a Newton-Raphson method, itself iterative, for nonlinear-equation solving. Other attempts to solve the same problem have been reported in the literature, but these also resorted to extremely complicated numerical procedures for nonlinear-equation solving (Chou and Kamel, 1991). More recently, Horaud and Dornaika (1995) proposed a more concise method based on quaternions, a.k.a. Euler-Rodrigues parameters, that nevertheless is computationally costlier than the method we use here. The approach outlined in this subsection is essentially the same as that proposed earlier (Angeles, 1989), although here we have adopted a simpler procedure than that of the foregoing reference.

First, the vector of matrix $\mathbf{A}_i$, represented by $\mathbf{a}_i$, and the vector of matrix $\mathbf{B}_i$, represented by $\mathbf{b}_i$, for $i = 1, 2$, are computed from simple differences of the off-diagonal entries of the foregoing matrices, followed by a division by 2 of all the entries thus resulting, which yields

$$\mathbf{a}_1 = \begin{bmatrix} -0.02962963 \\ 0.08888889 \\ 0.32592593 \end{bmatrix}, \quad \mathbf{a}_2 = \begin{bmatrix} 0.07784121 \\ -0.37363778 \\ -0.27244422 \end{bmatrix}$$

$$\mathbf{b}_1 = \begin{bmatrix} -0.04748859 \\ -0.30481989 \\ 0.14084221 \end{bmatrix}, \quad \mathbf{b}_2 = \begin{bmatrix} -0.12999385 \\ 0.44869636 \\ 0.04396138 \end{bmatrix}$$

In the calculations below, 16 digits were used, but only eight are displayed. Furthermore, with the foregoing vectors, we compute $\mathbf{a}_3$ and $\mathbf{b}_3$ from cross products, thus obtaining

$$\mathbf{a}_3 = \begin{bmatrix} 0.09756097 \\ 0.01730293 \\ 0.00415020 \end{bmatrix}$$

$$\mathbf{b}_3 = \begin{bmatrix} -0.07655343 \\ -0.01622096 \\ -0.06091842 \end{bmatrix}$$

Furthermore, Δ is obtained as

$$\Delta = 0.00983460$$

while the individual *rank-one matrices* inside the brackets of eq.(2.149) are calculated as

$$\mathbf{a}_1(\mathbf{b}_2 \times \mathbf{b}_3)^T = \begin{bmatrix} 0.00078822 & 0.00033435 & -0.00107955 \\ -0.00236467 & -0.00100306 & 0.00323866 \\ -0.00867044 & -0.00367788 & 0.01187508 \end{bmatrix}$$

$$\mathbf{a}_2(\mathbf{b}_3 \times \mathbf{b}_1)^T = \begin{bmatrix} -0.00162359 & 0.00106467 & 0.00175680 \\ 0.00779175 & -0.00510945 & -0.00843102 \\ 0.00568148 & -0.00372564 & -0.00614762 \end{bmatrix}$$

$$\mathbf{a}_3(\mathbf{b}_1 \times \mathbf{b}_2)^T = \begin{bmatrix} -0.00746863 & -0.00158253 & -0.00594326 \\ -0.00132460 & -0.00028067 & -0.00105407 \\ -0.00031771 & -0.00006732 & -0.00025282 \end{bmatrix}$$

whence $\mathbf{Q}$ in the $\mathcal{A}$ frame is readily obtained as

$$[\,\mathbf{Q}\,]_{\mathcal{A}} = \begin{bmatrix} -0.84436553 & -0.01865909 & -0.53545750 \\ 0.41714750 & -0.65007032 & -0.63514856 \\ -0.33622873 & -0.75964911 & 0.55667078 \end{bmatrix}$$

thereby completing the desired computation.

3

Fundamentals of Rigid-Body Mechanics

3.1 Introduction

The purpose of this chapter is to lay down the foundations of the kinetostatics and dynamics of rigid bodies, as needed in the study of multibody mechanical systems. With this background, we study the kinetostatics and dynamics of robotic manipulators of the serial type in Chapters 4 and 6, respectively, while devoting Chapter 5 to the study of trajectory planning. The latter requires, additionally, the background of Chapter 4. A special feature of this chapter is the study of the relations between the angular velocity of a rigid body and the time-rates of change of the various sets of rotation invariants introduced in Chapter 2. Similar relations between the angular acceleration and the second time-derivatives of the rotation invariants are also recalled, the corresponding derivations being outlined in Appendix A.

Furthermore, an introduction to the very useful analysis tool known as *screw theory* (Roth, 1984) is included. In this context, the concepts of twist and wrench are introduced, which prove in subsequent chapters to be extremely useful in deriving the kinematic and static, i.e., the *kinetostatic*, relations among the various bodies of multibody mechanical systems.

3.2 General Rigid-Body Motion and Its Associated Screw

In this section, we analyze the general motion of a rigid body. Thus, let A and P be two points of the same rigid body $\mathcal{B}$, the former being a particular reference point, whereas the latter is an arbitrary point of $\mathcal{B}$. Moreover, the position vector of point A in the original configuration is $\mathbf{a}$, and the position vector of the same point in the displaced configuration, denoted by A', is $\mathbf{a}'$. Similarly, the position vector of point P in the original configuration is $\mathbf{p}$, while in the displaced configuration, denoted by P', its position vector is $\mathbf{p}'$. Furthermore, $\mathbf{p}'$ is to be determined, while $\mathbf{a}$, $\mathbf{a}'$, and $\mathbf{p}$ are given, along with the rotation matrix $\mathbf{Q}$. Vector $\mathbf{p}-\mathbf{a}$ can be considered to undergo a rotation $\mathbf{Q}$ about point A throughout the motion taking the body from the original to the final configuration. Since vector $\mathbf{p}-\mathbf{a}$ is mapped into $\mathbf{p}'-\mathbf{a}'$ under the above rotation, one can write

$$\mathbf{p}'-\mathbf{a}'=\mathbf{Q}(\mathbf{p}-\mathbf{a}) \tag{3.1}$$

and hence

$$\mathbf{p}'=\mathbf{a}'+\mathbf{Q}(\mathbf{p}-\mathbf{a}) \tag{3.2}$$

which is the relationship sought. Moreover, let $\mathbf{d}_A$ and $\mathbf{d}_P$ denote the displacements of A and P, respectively, i.e.,

$$\mathbf{d}_A\equiv\mathbf{a}'-\mathbf{a},\quad \mathbf{d}_P\equiv\mathbf{p}'-\mathbf{p} \tag{3.3}$$

From eqs.(3.2) and (3.3) one can readily obtain an expression for $\mathbf{d}_P$, namely,

$$\begin{aligned}\mathbf{d}_P&=\mathbf{a}'-\mathbf{p}+\mathbf{Q}(\mathbf{p}-\mathbf{a})\\&=\mathbf{a}'-\mathbf{a}-\mathbf{p}+\mathbf{Q}(\mathbf{p}-\mathbf{a})+\mathbf{a} &(3.4)\\&=\mathbf{d}_A+(\mathbf{Q}-\mathbf{1})(\mathbf{p}-\mathbf{a}) &(3.5)\end{aligned}$$

What eq.(3.5) states is that the displacement of an arbitrary point P of a rigid body whose position vector in an original configuration is $\mathbf{p}$ is determined by the displacement of one certain point A and the concomitant rotation $\mathbf{Q}$. Clearly, once the displacement of P is known, its position vector $\mathbf{p}'$ can be readily determined. An interesting result in connection with the foregoing discussion is summarized below:

Theorem 3.2.1 *The component of the displacements of all the points of a rigid body undergoing a general motion along the axis of the underlying rotation is a constant.*

Proof: Multiply both sides of eq.(3.5) by $\mathbf{e}^T$, the unit vector parallel to the axis of the rotation represented by $\mathbf{Q}$, thereby obtaining

$$\mathbf{e}^T\mathbf{d}_P=\mathbf{e}^T\mathbf{d}_A+\mathbf{e}^T(\mathbf{Q}-\mathbf{1})(\mathbf{p}-\mathbf{a})$$

Now, the second term of the right-hand side of the above equation vanishes because $\mathbf{Qe} = \mathbf{e}$, and hence, $\mathbf{Q}^T\mathbf{e} = \mathbf{e}$, by hypothesis, the said equation thus leading to

$$\mathbf{e}^T\mathbf{d}_P = \mathbf{e}^T\mathbf{d}_A \equiv d_0 \tag{3.6}$$

thereby showing that the displacements of all points of the body have the same projection d_0 onto the axis of rotation, q.e.d.

As a consequence of the foregoing result, we have the classical *Mozzi-Chasles Theorem* (Mozzi, 1763; Chasles, 1830; Ceccarelli, 1995), namely,

Theorem 3.2.2 (Mozzi, 1763; Chasles, 1830) *Given a rigid body undergoing a general motion, a set of its points located on a line $\mathcal{L}$ undergo identical displacements of minimum magnitude. Moreover, line $\mathcal{L}$ and the minimum-magnitude displacement are parallel to the axis of the rotation involved.*

Proof: The proof is straightforward in light of Theorem 3.2.1, which allows us to express the displacement of an arbitrary point P as the sum of two orthogonal components, namely, one parallel to the axis of rotation, independent of P and denoted by $\mathbf{d}_\parallel$, and one perpendicular to this axis, denoted by $\mathbf{d}_\perp$, i.e.,

$$\mathbf{d}_P = \mathbf{d}_\parallel + \mathbf{d}_\perp \tag{3.7a}$$

where

$$\mathbf{d}_\parallel = \mathbf{e}\mathbf{e}^T\mathbf{d}_P = d_0\mathbf{e}, \quad \mathbf{d}_\perp = (\mathbf{1} - \mathbf{e}\mathbf{e}^T)\mathbf{d}_P \tag{3.7b}$$

and clearly, d_0 is a constant that is defined as in eq.(3.6), while $\mathbf{d}_\parallel$ and $\mathbf{d}_\perp$ are mutually orthogonal. Indeed,

$$\mathbf{d}_\parallel \cdot \mathbf{d}_\perp = d_0\mathbf{e}^T(\mathbf{1} - \mathbf{e}\mathbf{e}^T)\mathbf{d}_P = d_0(\mathbf{e}^T - \mathbf{e}^T)\mathbf{d}_P = 0$$

Now, by virtue of the orthogonality of the two components of $\mathbf{d}_P$, it is apparent that

$$\|\mathbf{d}_P\|^2 = \|\mathbf{d}_\parallel\|^2 + \|\mathbf{d}_\perp\|^2 = d_0^2 + \|\mathbf{d}_\perp\|^2$$

for the displacement $\mathbf{d}_P$ of any point of the body. Now, in order to minimize $\|\mathbf{d}_P\|$ we have to make $\|\mathbf{d}_\perp\|$, and hence, $\mathbf{d}_\perp$ itself, equal to zero, i.e., we must have $\mathbf{d}_P$ parallel to $\mathbf{e}$:

$$\mathbf{d}_P = \alpha\mathbf{e}$$

for a certain scalar α. That is, the displacements of minimum magnitude of the body under study are parallel to the axis of $\mathbf{Q}$, thereby proving the first part of the Mozzi-Chasles Theorem. The second part is also readily proven by noticing that if P^* is a point of minimum magnitude of position vector $\mathbf{p}^*$, its component perpendicular to the axis of rotation must vanish, and hence,

$$\begin{aligned}\mathbf{d}_\perp^* &\equiv (\mathbf{1} - \mathbf{e}\mathbf{e}^T)\mathbf{d}_{P^*} \\ &= (\mathbf{1} - \mathbf{e}\mathbf{e}^T)\mathbf{d}_A + (\mathbf{1} - \mathbf{e}\mathbf{e}^T)(\mathbf{Q} - \mathbf{1})(\mathbf{p}^* - \mathbf{a}) = \mathbf{0}\end{aligned}$$

Upon expansion of the above expression for $\mathbf{d}_{\perp}^{*}$, the foregoing equation leads to

$$(\mathbf{1} - \mathbf{e}\mathbf{e}^T)\mathbf{d}_A + (\mathbf{Q} - \mathbf{1})(\mathbf{p}^* - \mathbf{a}) = \mathbf{0}$$

Now it is apparent that if we define a line $\mathcal{L}$ passing through P^* and parallel to $\mathbf{e}$, then the position vector $\mathbf{p}^* + \lambda\mathbf{e}$ of any of its points P satisfies the foregoing equation. As a consequence, all points of minimum magnitude lie in a line parallel to the axis of rotation of $\mathbf{Q}$, q.e.d.

An important implication of the foregoing theorem is that a rigid body can attain an arbitrary configuration from a given original one, following a screw-like motion of axis $\mathcal{L}$ and pitch p, the latter being defined presently. Thus, it seems appropriate to call $\mathcal{L}$ the *screw axis* of the rigid-body motion.

Note that d_0, as defined in eq.(3.6), is an invariant of the motion at hand. Thus, associated with a rigid-body motion, one can then define a *screw* of axis $\mathcal{L}$ and pitch p. Of course, the pitch is defined as

$$p \equiv \frac{d_0}{\phi} = \frac{\mathbf{d}_P^T\mathbf{e}}{\phi} \qquad \text{or} \qquad p \equiv \frac{2\pi d_0}{\phi} \tag{3.8}$$

which has units of m/rad or, correspondingly, of m/turn. Moreover, the angle ϕ of the rotation involved can be regarded as one more feature of this motion. This angle is, in fact, the *amplitude* associated with the said motion. We will come across screws in discussing velocities and forces acting on rigid bodies, along with their pitches and amplitudes. Thus, it is convenient to introduce this concept at this stage.

3.2.1 The Screw of a Rigid-Body Motion

The screw axis $\mathcal{L}$ is totally specified by a given point P_0 of $\mathcal{L}$ that can be defined, for example, as that lying closest to the origin, and a unit vector $\mathbf{e}$ defining its direction. Expressions for the position vector of P_0, $\mathbf{p}_0$, in terms of $\mathbf{a}$, $\mathbf{a}'$ and $\mathbf{Q}$, are derived below:

If P_0 is defined as above, i.e., as the point of $\mathcal{L}$ lying closest to the origin, then, obviously, $\mathbf{p}_0$ is perpendicular to $\mathbf{e}$, i.e.,

$$\mathbf{e}^T\mathbf{p}_0 = 0 \tag{3.9}$$

Moreover, the displacement $\mathbf{d}_0$ of P_0 is parallel to the vector of $\mathbf{Q}$, and hence, is identical to $\mathbf{d}_{\|}$ defined in eq.(3.7b), i.e., it satisfies

$$(\mathbf{Q} - \mathbf{1})\mathbf{d}_0 = \mathbf{0}$$

where $\mathbf{d}_0$ is given as in eq.(3.5), namely, as

$$\mathbf{d}_0 = \mathbf{d}_A + (\mathbf{Q} - \mathbf{1})(\mathbf{p}_0 - \mathbf{a}) \tag{3.10a}$$

Now, since $\mathbf{d}_0$ is identical to $\mathbf{d}_{\|}$, we have, from eq.(3.7b),

$$\mathbf{d}_A + (\mathbf{Q} - \mathbf{1})(\mathbf{p}_0 - \mathbf{a}) = \mathbf{d}_{\|} \equiv \mathbf{e}\mathbf{e}^T\mathbf{d}_0$$

But from Theorem 3.2.1,

$$\mathbf{e}^T\mathbf{d}_0 = \mathbf{e}^T\mathbf{d}_A$$

and so

$$\mathbf{d}_A + (\mathbf{Q}-\mathbf{1})(\mathbf{p}_0 - \mathbf{a}) = \mathbf{e}\mathbf{e}^T\mathbf{d}_A$$

or after rearranging terms,

$$(\mathbf{Q}-\mathbf{1})\mathbf{p}_0 = (\mathbf{Q}-\mathbf{1})\mathbf{a} - (\mathbf{1}-\mathbf{e}\mathbf{e}^T)\mathbf{d}_A \tag{3.10b}$$

Furthermore, in order to find an expression for $\mathbf{p}_0$, eq.(3.9) is adjoined to eq.(3.10b), thereby obtaining

$$\mathbf{A}\mathbf{p}_0 = \mathbf{b} \tag{3.11}$$

where $\mathbf{A}$ is a 4×3 matrix and $\mathbf{b}$ is a 4-dimensional vector, being given by

$$\mathbf{A} \equiv \begin{bmatrix} \mathbf{Q}-\mathbf{1} \\ \mathbf{e}^T \end{bmatrix}, \quad \mathbf{b} \equiv \begin{bmatrix} (\mathbf{Q}-\mathbf{1})\mathbf{a} - (\mathbf{1}-\mathbf{e}\mathbf{e}^T)\mathbf{d}_A \\ 0 \end{bmatrix} \tag{3.12}$$

Equation (3.11) cannot be solved for $\mathbf{p}_0$ directly, because $\mathbf{A}$ is not a square matrix. In fact, that equation represents an *overdetermined* system of four equations and three unknowns. Thus, in general, that system does not admit a solution. However, the four equations are compatible, and hence in this particular case, a solution of that equation, which turns out to be *unique*, can be determined. In fact, if both sides of eq.(3.11) are multiplied from the left by $\mathbf{A}^T$, we have

$$\mathbf{A}^T\mathbf{A}\mathbf{p}_0 = \mathbf{A}^T\mathbf{b} \tag{3.13}$$

Moreover, if the product $\mathbf{A}^T\mathbf{A}$, which is a 3×3 matrix, is invertible, then $\mathbf{p}_0$ can be computed from eq.(3.13). In fact, the said product is not only invertible, but also admits an inverse that is rather simple to derive, as shown below. Now the rotation matrix $\mathbf{Q}$ is recalled in terms of its *natural invariants*, namely, the unit vector $\mathbf{e}$ parallel to its axis of rotation and the angle of rotation ϕ about this axis, as given in eq.(2.48), reproduced below for quick reference:

$$\mathbf{Q} = \mathbf{e}\mathbf{e}^T + \cos\phi(\mathbf{1} - \mathbf{e}\mathbf{e}^T) + \sin\phi\mathbf{E}$$

where $\mathbf{1}$ represents the 3×3 identity matrix and $\mathbf{E}$ the *cross-product matrix* of $\mathbf{e}$, as introduced in eq.(2.37). Further, eq.(2.48) is substituted into eq.(3.12), which yields

$$\mathbf{A}^T\mathbf{A} = 2(1-\cos\phi)\mathbf{1} - (1-2\cos\phi)\mathbf{e}\mathbf{e}^T \tag{3.14}$$

It is now apparent that the foregoing product is a linear combination of $\mathbf{1}$ and $\mathbf{e}\mathbf{e}^T$. This suggests that its inverse is very likely to be a linear combination of these two matrices as well. If this is in fact true, then one can write

$$(\mathbf{A}^T\mathbf{A})^{-1} = \alpha\mathbf{1} + \beta\mathbf{e}\mathbf{e}^T \tag{3.15}$$

coefficients α and β being determined from the condition that the product of $\mathbf{A}^T\mathbf{A}$ by its inverse should be $\mathbf{1}$, which yields

$$\alpha = \frac{1}{2(1-\cos\phi)}, \quad \beta = \frac{1-2\cos\phi}{2(1-\cos\phi)} \tag{3.16}$$

and hence,

$$(\mathbf{A}^T\mathbf{A})^{-1} = \frac{1}{2(1-\cos\phi)}\mathbf{1} + \frac{1-2\cos\phi}{2(1-\cos\phi)}\mathbf{e}\mathbf{e}^T \tag{3.17}$$

On the other hand,

$$\mathbf{A}^T\mathbf{b} = (\mathbf{Q}-\mathbf{1})^T[(\mathbf{Q}-\mathbf{1})\mathbf{a} - \mathbf{d}_A] \tag{3.18}$$

Upon solving eq.(3.13) for $\mathbf{p}_0$ and substituting relations (3.17) and (3.18) into the expression thus resulting, one finally obtains

$$\mathbf{p}_0 = \frac{(\mathbf{Q}-\mathbf{1})^T(\mathbf{Q}\mathbf{a}-\mathbf{a}')}{2(1-\cos\phi)}, \quad \text{for } \phi \neq 0 \tag{3.19}$$

We have thus defined a line $\mathcal{L}$ of the rigid body under study that is completely defined by its point P_0 of position vector $\mathbf{p}_0$ and a unit vector $\mathbf{e}$ determining its direction. Moreover, we have already defined the pitch of the associated motion, eq.(3.8). The line thus defined, along with the pitch, determines the screw of the motion under study.

3.2.2 The Plücker Coordinates of a Line

Alternatively, the screw axis, and any line for that matter, can be defined more conveniently by its *Plücker coordinates*. In motivating this concept, we recall the equation of a line $\mathcal{L}$ passing through two points P_1 and P_2 of position vectors $\mathbf{p}_1$ and $\mathbf{p}_2$, as shown in Fig. 3.1.

If point P lies in $\mathcal{L}$, then, it must be collinear with P_1 and P_2, a property that is expressed as

$$(\mathbf{p}_2 - \mathbf{p}_1) \times (\mathbf{p} - \mathbf{p}_1) = \mathbf{0}$$

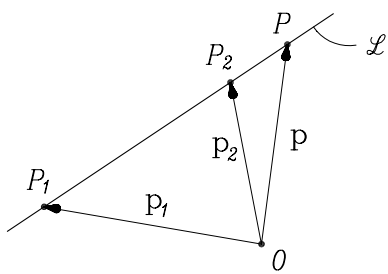

FIGURE 3.1. A line $\mathcal{L}$ passing through two points.

or upon expansion,

$$(\mathbf{p}_2 - \mathbf{p}_1) \times \mathbf{p} + \mathbf{p}_1 \times (\mathbf{p}_2 - \mathbf{p}_1) = \mathbf{0} \tag{3.20}$$

If we now introduce the cross-product matrices $\mathbf{P}_1$ and $\mathbf{P}_2$ of vectors $\mathbf{p}_1$ and $\mathbf{p}_2$ in the above equation, we have an alternative expression for the equation of the line, namely,

$$(\mathbf{P}_2 - \mathbf{P}_1)\mathbf{p} + \mathbf{p}_1 \times (\mathbf{p}_2 - \mathbf{p}_1) = \mathbf{0}$$

The above equation can be regarded as a linear equation in the homogeneous coordinates of point P, namely,

$$[\,\mathbf{P}_2 - \mathbf{P}_1 \quad \mathbf{p}_1 \times (\mathbf{p}_2 - \mathbf{p}_1)\,] \begin{bmatrix} \mathbf{p} \\ 1 \end{bmatrix} = \mathbf{0} \tag{3.21}$$

It is now apparent that the line is defined completely by two vectors, the difference $\mathbf{p}_2 - \mathbf{p}_1$, or its cross-product matrix for that matter, and the cross product $\mathbf{p}_1 \times (\mathbf{p}_2 - \mathbf{p}_1)$. We will thus define a 6-dimensional array $\boldsymbol{\gamma}_{\mathcal{L}}$ containing these two vectors, namely,

$$\boldsymbol{\gamma}_{\mathcal{L}} \equiv \begin{bmatrix} \mathbf{p}_2 - \mathbf{p}_1 \\ \mathbf{p}_1 \times (\mathbf{p}_2 - \mathbf{p}_1) \end{bmatrix} \tag{3.22}$$

whose six scalar entries are the Plücker coordinates of $\mathcal{L}$. Moreover, if we let

$$\mathbf{e} \equiv \frac{\mathbf{p}_2 - \mathbf{p}_1}{\|\mathbf{p}_2 - \mathbf{p}_1\|}, \quad \mathbf{n} \equiv \mathbf{p}_1 \times \mathbf{e} \tag{3.23}$$

then we can write

$$\boldsymbol{\gamma}_{\mathcal{L}} = \|\mathbf{p}_2 - \mathbf{p}_1\| \begin{bmatrix} \mathbf{e} \\ \mathbf{n} \end{bmatrix}$$

The six scalar entries of the above array are the *normalized Plücker coordinates* of $\mathcal{L}$. Vector $\mathbf{e}$ determines the direction of $\mathcal{L}$, while $\mathbf{n}$ determines its location; $\mathbf{n}$ can be interpreted as the moment of a unit force parallel to $\mathbf{e}$ and of line of action $\mathcal{L}$. Hence, $\mathbf{n}$ is called the *moment* of $\mathcal{L}$. Henceforth, only the normalized Plücker coordinates of lines will be used. For brevity, we will refer to these simply as the Plücker coordinates of the line under study. The Plücker coordinates thus defined will be thus stored in a *Plücker array* $\boldsymbol{\kappa}_{\mathcal{L}}$ in the form

$$\boldsymbol{\kappa} = \begin{bmatrix} \mathbf{e} \\ \mathbf{n} \end{bmatrix} \tag{3.24}$$

where for conciseness, we have dropped the subscript $\mathcal{L}$, while assuming that the line under discussion is self-evident.

Note, however, that the six components of the Plücker array, i.e., the *Plücker coordinates* of line $\mathcal{L}$, are not independent, for they obey

$$\mathbf{e} \cdot \mathbf{e} = 1, \quad \mathbf{n} \cdot \mathbf{e} = 0 \tag{3.25}$$

and hence, any line $\mathcal{L}$ has only four independent Plücker coordinates. In the foregoing paragraphs, we have talked about the Plücker array of a line, and not about the Plücker vector; the reason for this distinction is given below. The set of Plücker arrays is a clear example of an array of real numbers not constituting a vector space. What disables Plücker arrays from being vectors are the two constraints that their components must satisfy, namely, (i) the sum of the squares of the first three components of a Plücker array is unity, and (ii) the unit vector of a line is normal to the moment of the line. Nevertheless, we can perform with Plücker arrays certain operations that pertain to vectors, as long as we keep in mind the essential differences. For example, we can multiply Plücker arrays by matrices of the suitable dimension, with entries having appropriate units, as we will show presently.

It must be pointed out that a Plücker array is dependent upon the location of the point with respect to which the moment of the line is measured. Indeed, let $\boldsymbol{\kappa}_A$ and $\boldsymbol{\kappa}_B$ denote the Plücker arrays of the same line $\mathcal{L}$ when its moment is measured at points A and B, respectively. Moreover, this line passes through a point P of position vector $\mathbf{p}$ for a particular origin O. Now, let the moment of $\mathcal{L}$ with respect to A and B be denoted by $\mathbf{n}_A$ and $\mathbf{n}_B$, respectively, i.e.,

$$\mathbf{n}_A \equiv (\mathbf{p} - \mathbf{a}) \times \mathbf{e}, \quad \mathbf{n}_B \equiv (\mathbf{p} - \mathbf{b}) \times \mathbf{e} \tag{3.26}$$

and hence,

$$\boldsymbol{\kappa}_A \equiv \begin{bmatrix} \mathbf{e} \\ \mathbf{n}_A \end{bmatrix}, \quad \boldsymbol{\kappa}_B \equiv \begin{bmatrix} \mathbf{e} \\ \mathbf{n}_B \end{bmatrix} \tag{3.27}$$

Obviously,

$$\mathbf{n}_B - \mathbf{n}_A = (\mathbf{a} - \mathbf{b}) \times \mathbf{e} \tag{3.28}$$

i.e.,

$$\boldsymbol{\kappa}_B = \begin{bmatrix} \mathbf{e} \\ \mathbf{n}_A + (\mathbf{a} - \mathbf{b}) \times \mathbf{e} \end{bmatrix} \tag{3.29}$$

which can be rewritten as

$$\boldsymbol{\kappa}_B = \mathbf{U}\boldsymbol{\kappa}_A \tag{3.30}$$

with the 6×6 matrix $\mathbf{U}$ defined as

$$\mathbf{U} \equiv \begin{bmatrix} \mathbf{1} & \mathbf{O} \\ \mathbf{A} - \mathbf{B} & \mathbf{1} \end{bmatrix} \tag{3.31}$$

while $\mathbf{A}$ and $\mathbf{B}$ are, respectively, the cross-product matrices of vectors $\mathbf{a}$ and $\mathbf{b}$, and $\mathbf{O}$ denotes the 3×3 zero matrix. Given the lower-triangular structure of matrix $\mathbf{U}$, its determinant is simply the product of its diagonal entries, which are all unity. Hence,

$$\det(\mathbf{U}) = 1 \tag{3.32}$$

$\mathbf{U}$ thus belonging to the *unimodular group* of 6×6 matrices. These matrices are rather simple to invert. In fact, as one can readily prove,

$$\mathbf{U}^{-1} = \begin{bmatrix} \mathbf{1} & \mathbf{O} \\ \mathbf{B}-\mathbf{A} & \mathbf{1} \end{bmatrix} \tag{3.33}$$

Relation (3.30) can then be called the *Plücker-coordinate transfer formula*.

Note that upon multiplication of both sides of eq.(3.28) by $(\mathbf{a}-\mathbf{b})$,

$$(\mathbf{a}-\mathbf{b})^T\mathbf{n}_B = (\mathbf{a}-\mathbf{b})^T\mathbf{n}_A \tag{3.34}$$

and hence, the moments of the same line $\mathcal{L}$ with respect to two points are not independent, for they have the same component along the line joining the two points.

A special case of a line, of interest in kinematics, is a *line at infinity*. This is a line with undefined orientation, but with a defined direction of its moment; this moment is, moreover, *independent* of the point with respect to which it is measured. Very informally, the Plücker coordinates of a line at infinity can be derived from the general expression, eq.(3.24), if we rewrite it in the form

$$\boldsymbol{\kappa} = \|\mathbf{n}\| \begin{bmatrix} \mathbf{e}/\|\mathbf{n}\| \\ \mathbf{n}/\|\mathbf{n}\| \end{bmatrix}$$

where clearly $\mathbf{n}/\|\mathbf{n}\|$ is a unit vector; henceforth, this vector will be denoted by $\mathbf{f}$. Now let us take the limit of the above expression as P goes to infinity, i.e., when $\|\mathbf{p}\| \to \infty$, and consequently, as $\|\mathbf{n}\| \to \infty$. Thus,

$$\lim_{\|\mathbf{n}\|\to\infty} \boldsymbol{\kappa} = \left(\lim_{\|\mathbf{n}\|\to\infty} \|\mathbf{n}\|\right)\left(\lim_{\|\mathbf{n}\|\to\infty} \begin{bmatrix} \mathbf{e}/\|\mathbf{n}\| \\ \mathbf{f} \end{bmatrix}\right)$$

whence

$$\lim_{\|\mathbf{n}\|\to\infty} \boldsymbol{\kappa} = \left(\lim_{\|\mathbf{n}\|\to\infty} \|\mathbf{n}\|\right) \begin{bmatrix} \mathbf{0} \\ \mathbf{f} \end{bmatrix}$$

The 6-dimensional array appearing in the above equation is defined as the Plücker array of a line at infinity, $\boldsymbol{\kappa}_\infty$, namely,

$$\boldsymbol{\kappa}_\infty = \begin{bmatrix} \mathbf{0} \\ \mathbf{f} \end{bmatrix} \tag{3.35}$$

Note that a line at infinity of *unit moment* $\mathbf{f}$ can be thought of as being a line lying in a plane perpendicular to the unit vector $\mathbf{f}$, but otherwise with an indefinite location in the plane, except that it is an infinitely large distance from the origin. Thus, lines at infinity vary only in the orientation of the plane in which they lie.

3.2.3 The Pose of a Rigid Body

A possible form of describing a general rigid-body motion, then, is through a set of eight real numbers, namely, the six Plücker coordinates of its screw axis, its pitch, and its amplitude, i.e., its angle. Hence, *a rigid-body motion is fully described by six independent parameters.* Moreover, the pitch can attain values from $-\infty$ to $+\infty$. Alternatively, a rigid-body motion can be described by seven dependent parameters as follows: four invariants of the concomitant rotation—the linear invariants, the natural invariants, or the Euler–Rodrigues parameters, introduced in Section 2.3—and the three components of the displacement of an arbitrary point. Since those invariants are not independent, but subject to one constraint, this description consistently involves six independent parameters. Thus, let a rigid body undergo a general motion of rotation $\mathbf{Q}$ and displacement $\mathbf{d}$ from a reference configuration $\mathcal{C}_0$. If in the new configuration $\mathcal{C}$ a landmark point A of the body has a position vector $\mathbf{a}$, then the *pose array*, or simply the *pose*, $\mathbf{s}$ of the body, is defined as a 7-dimensional array, namely,

$$\mathbf{s} \equiv \begin{bmatrix} \mathbf{q} \\ q_0 \\ \mathbf{d}_A \end{bmatrix} \tag{3.36}$$

where the 3-dimensional vector $\mathbf{q}$ and the scalar q_0 are *any* four invariants of $\mathbf{Q}$. For example, if these are the Euler-Rodrigues parameters, then

$$\mathbf{q} \equiv \sin(\frac{\phi}{2})\mathbf{e}, \quad q_0 \equiv \cos(\frac{\phi}{2})$$

If alternatively, we work with the linear invariants, then

$$\mathbf{q} \equiv (\sin\phi)\mathbf{e}, \quad q_0 \equiv \cos\phi$$

and, of course, if we work instead with the natural invariants, then

$$\mathbf{q} \equiv \mathbf{e}, \quad q_0 \equiv \phi$$

In the first two cases, the constraint mentioned above is

$$\|\mathbf{q}\|^2 + q_0^2 = 1 \tag{3.37}$$

In the last case, the constraint is simply

$$\|\mathbf{e}\|^2 = 1 \tag{3.38}$$

An important problem in kinematics is the computation of the screw parameters, i.e., the components of $\mathbf{s}$, as given in eq.(3.36), from coordinate measurements over a certain finite set of points. From the foregoing discussion, it is clear that the computation of the attitude of a rigid body, given

by matrix **Q** or its invariants, is crucial in solving this problem. Moreover, besides its theoretical importance, this problem, known as *pose estimation*, has also practical relevance. Shown in Fig. 3.2 is the *helmet-mounted display system* used in flight simulators. The helmet is supplied with a set of LEDs (light-emitting diodes) that emit infrared light signals at different frequencies each. These signals are then picked up by two cameras, from whose images the Cartesian coordinates of the LEDs centers are inferred. With these coordinates and knowledge of the LED pattern, the attitude of the pilot's head is determined from the rotation matrix **Q**. Moreover, with this information and that provided via sensors mounted on the lenses, the position of the center of the pupil of the pilot's eyes is then estimated. This position, then, indicates on which part of his or her visual field the pilot's eyes are focusing. In this way, a high-resolution graphics monitor synthesizes the image that the pilot would be viewing with a high level of detail. The rest of the visual field is rendered as a rather blurred image, in order to allocate computer resources where it really matters.

A straightforward method of computing the screw parameters consists of regarding the motion as follows: Choose a certain point A of the body,

FIGURE 3.2. Helmet-mounted display system (courtesy of CAE Electronics Ltd., St.-Laurent, Quebec, Canada.)

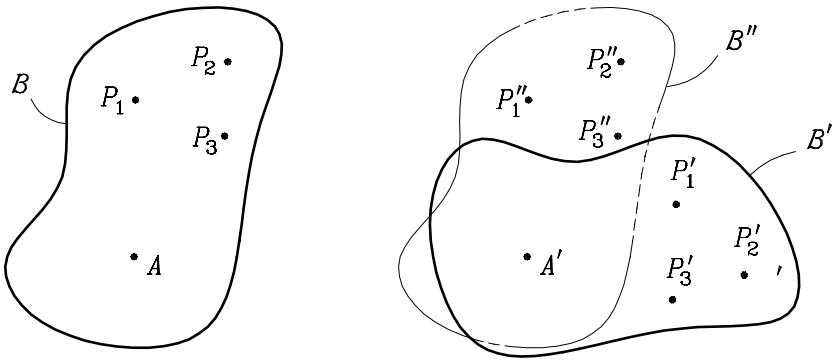

FIGURE 3.3. Decomposition of the displacement of a rigid body.

of position vector $\mathbf{a}$, and track it as the body moves to a displaced configuration, at which point A moves to A', of position vector $\mathbf{a}'$. Assume that the body reaches the displaced configuration $\mathcal{B}'$, passing through an intermediate one $\mathcal{B}''$, which is attained by pure translation. Next, configuration $\mathcal{B}'$ is reached by rotating the body about point A', as indicated in Fig. 3.3.

Matrix $\mathbf{Q}$ can now be readily determined. To do this, define three points of the body, P_1, P_2, and P_3, in such a way that the three vectors defined below are orthonormal and form a right-hand system:

$$\mathbf{e}_1 \equiv \overrightarrow{AP_1}, \quad \mathbf{e}_2 \equiv \overrightarrow{AP_2}, \quad \mathbf{e}_3 \equiv \overrightarrow{AP_3} \tag{3.39}$$

$$\mathbf{e}_i \cdot \mathbf{e}_j = \delta_{ij}, \quad i,j = 1,2,3, \quad \mathbf{e}_3 = \mathbf{e}_1 \times \mathbf{e}_2 \tag{3.40}$$

where δ_{ij} is the *Kronecker delta*, defined as 1 if $i = j$ and 0 otherwise. Now, let the set $\{\mathbf{e}_i\}_1^3$ be labelled $\{\mathbf{e}_i'\}_1^3$ and $\{\mathbf{e}_i''\}_1^3$ in configurations $\mathcal{B}'$ and $\mathcal{B}''$, respectively. Moreover, let q_{ij} denote the entries of the matrix representation of the rotation $\mathbf{Q}$ in a frame X, Y, Z with origin at A and such that the foregoing axes are parallel to vectors $\mathbf{e}_1$, $\mathbf{e}_2$, and $\mathbf{e}_3$, respectively. It is clear, from Definition 2.2.1, that

$$q_{ij} = \mathbf{e}_i \cdot \mathbf{e}_j' \tag{3.41}$$

i.e.,

$$[\,\mathbf{Q}\,] = \begin{bmatrix} \mathbf{e}_1 \cdot \mathbf{e}_1' & \mathbf{e}_1 \cdot \mathbf{e}_2' & \mathbf{e}_1 \cdot \mathbf{e}_3' \\ \mathbf{e}_2 \cdot \mathbf{e}_1' & \mathbf{e}_2 \cdot \mathbf{e}_2' & \mathbf{e}_2 \cdot \mathbf{e}_3' \\ \mathbf{e}_3 \cdot \mathbf{e}_1' & \mathbf{e}_3 \cdot \mathbf{e}_2' & \mathbf{e}_3 \cdot \mathbf{e}_3' \end{bmatrix} \tag{3.42}$$

Note that all $\mathbf{e}_i$ and $\mathbf{e}_i'$ appearing in eq.(3.42) must be represented in the same coordinate frame. Once $\mathbf{Q}$ is determined, computing the remaining screw parameters is straightforward. One can use, for example, eq.(3.19) to determine the point of the screw axis that lies closest to the origin, which would thus allow one to compute the Plücker coordinates of the screw axis.

3.3 Rotation of a Rigid Body About a Fixed Point

In this section, the motion of a rigid body having a point fixed is analyzed. This motion is fully described by a rotation matrix $\mathbf{Q}$ that is proper orthogonal. Now, $\mathbf{Q}$ will be assumed to be a smooth function of time, and hence, the position vector of a point P in an original configuration, denoted here by $\mathbf{p}_0$, is mapped smoothly into a new vector $\mathbf{p}(t)$, namely,

$$\mathbf{p}(t) = \mathbf{Q}(t)\mathbf{p}_0 \tag{3.43}$$

The velocity of P is computed by differentiating both sides of eq.(3.43) with respect to time, thus obtaining

$$\dot{\mathbf{p}}(t) = \dot{\mathbf{Q}}(t)\mathbf{p}_0 \tag{3.44}$$

which is not a very useful expression, because it requires knowledge of the original position of P. A more useful expression can be derived if eq.(3.43) is solved for $\mathbf{p}_0$ and the expression thus resulting is substituted into eq.(3.44), which yields

$$\dot{\mathbf{p}} = \dot{\mathbf{Q}}\mathbf{Q}^T\mathbf{p} \tag{3.45}$$

where the argument t has been dropped because all quantities are now time-varying, and hence, this argument is self-evident. The product $\dot{\mathbf{Q}}\mathbf{Q}^T$ is known as the *angular-velocity matrix* of the rigid-body motion and is denoted by $\mathbf{\Omega}$, i.e.,

$$\mathbf{\Omega} \equiv \dot{\mathbf{Q}}\mathbf{Q}^T \tag{3.46}$$

As a consequence of the orthogonality of $\mathbf{Q}$, one has a basic result, namely,

Theorem 3.3.1 *The angular-velocity matrix is skew symmetric.*

In order to derive the *angular-velocity vector* of a rigid-body motion, we recall the concept of *axial vector*, or simply *vector*, of a 3×3 matrix, introduced in Subsection 2.3.3. Thus, the angular-velocity vector $\boldsymbol{\omega}$ of the rigid-body motion under study is defined as the vector of $\mathbf{\Omega}$, i.e.,

$$\boldsymbol{\omega} \equiv \text{vect}(\mathbf{\Omega}) \tag{3.47}$$

and hence, eq.(3.45) can be written as

$$\dot{\mathbf{p}} = \mathbf{\Omega}\mathbf{p} = \boldsymbol{\omega} \times \mathbf{p} \tag{3.48}$$

from which it is apparent that *the velocity of any point P of a body moving with a point O fixed is perpendicular to line OP.*

3.4 General Instantaneous Motion of a Rigid Body

If a rigid body now undergoes the most general motion, none of its points remains fixed, and the position vector of any of these, P, in a displaced configuration is given by eq.(3.2). Let $\mathbf{a}_0$ and $\mathbf{p}_0$ denote the position vectors of points A and P of Section 3.2, respectively, in the reference configuration $\mathcal{C}_0$, $\mathbf{a}(t)$ and $\mathbf{p}(t)$ being the position vectors of the same points in the displaced configuration $\mathcal{C}$. Moreover, if $\mathbf{Q}(t)$ denotes the rotation matrix, then

$$\mathbf{p}(t) = \mathbf{a}(t) + \mathbf{Q}(t)(\mathbf{p}_0 - \mathbf{a}_0) \tag{3.49}$$

Now, the velocity of P is computed by differentiating both sides of eq.(3.49) with respect to time, thus obtaining

$$\dot{\mathbf{p}}(t) = \dot{\mathbf{a}}(t) + \dot{\mathbf{Q}}(t)(\mathbf{p}_0 - \mathbf{a}_0) \tag{3.50}$$

which again, as expression (3.50), is not very useful, for it requires the values of the position vectors of A and P in the original configuration. However, if eq.(3.49) is solved for $\mathbf{p}_0 - \mathbf{a}_0$ and the expression thus resulting is substituted into eq.(3.50), we obtain

$$\dot{\mathbf{p}} = \dot{\mathbf{a}} + \boldsymbol{\Omega}(\mathbf{p} - \mathbf{a}) \tag{3.51}$$

or in terms of the angular-velocity vector,

$$\dot{\mathbf{p}} = \dot{\mathbf{a}} + \boldsymbol{\omega} \times (\mathbf{p} - \mathbf{a}) \tag{3.52}$$

where the argument t has been dropped for brevity but is implicit, since all variables of the foregoing equation are now functions of time. Furthermore, from eq.(3.52), it is apparent that the result below holds:

$$(\dot{\mathbf{p}} - \dot{\mathbf{a}}) \cdot (\mathbf{p} - \mathbf{a}) = 0 \tag{3.53}$$

which can be summarized as

Theorem 3.4.1 *The relative velocity of two points of the same rigid body is perpendicular to the line joining them.*

Moreover, similar to the outcome of Theorem 3.2.1, one now has an additional result that is derived upon dot-multiplying both sides of eq.(3.52) by $\boldsymbol{\omega}$, namely,

$$\boldsymbol{\omega} \cdot \dot{\mathbf{p}} = \boldsymbol{\omega} \cdot \dot{\mathbf{a}} = \text{constant}$$

and hence,

Corollary 3.4.1 *The projections of the velocities of all the points of a rigid body onto the angular-velocity vector are identical.*

Furthermore, similar to the Mozzi-Chasles Theorem, we have now

Theorem 3.4.2 *Given a rigid body under general motion, a set of its points located on a line $\mathcal{L}'$ undergoes the identical minimum-magnitude velocity $\mathbf{v}_0$ parallel to the angular velocity.*

Definition 3.4.1 *The line containing the points of a rigid body undergoing minimum-magnitude velocities is called the* instant screw axis *(ISA) of the body under the given motion.*

3.4.1 The Instant Screw of a Rigid-Body Motion

From Theorem 3.4.2, the instantaneous motion of a body is equivalent to that of the bolt of a screw of axis $\mathcal{L}'$, the ISA. Clearly, as the body moves, the ISA changes, and the motion of the body is called an *instantaneous screw*. Moreover, since $\mathbf{v}_0$ is parallel to $\boldsymbol{\omega}$, it can be written in the form

$$\mathbf{v}_0 = v_0 \frac{\boldsymbol{\omega}}{\|\boldsymbol{\omega}\|} \tag{3.54}$$

where v_0 is a scalar quantity denoting the signed magnitude of $\mathbf{v}_0$ and bears the sign of $\mathbf{v}_0 \cdot \boldsymbol{\omega}$. Furthermore, the pitch of the instantaneous screw, p', is defined as

$$p' \equiv \frac{v_0}{\|\boldsymbol{\omega}\|} \equiv \frac{\dot{\mathbf{p}} \cdot \boldsymbol{\omega}}{\|\boldsymbol{\omega}\|^2} \quad \text{or} \quad p' \equiv \frac{2\pi v_0}{\|\boldsymbol{\omega}\|} \tag{3.55}$$

which thus bears units of m/rad or correspondingly, of m/turn.

Again, the ISA $\mathcal{L}'$ can be specified uniquely through its Plücker coordinates, stored in the $\mathbf{p}_{\mathcal{L}'}$ array defined as

$$\mathbf{p}_{\mathcal{L}'} \equiv \begin{bmatrix} \mathbf{e}' \\ \mathbf{n}' \end{bmatrix} \tag{3.56}$$

where $\mathbf{e}'$ and $\mathbf{n}'$ are, respectively, the unit vector defining the direction of $\mathcal{L}'$ and its moment about the origin, i.e.,

$$\mathbf{e}' \equiv \frac{\boldsymbol{\omega}}{\|\boldsymbol{\omega}\|}, \quad \mathbf{n}' \equiv \mathbf{p} \times \mathbf{e}' \tag{3.57}$$

$\mathbf{p}$ being the position vector of any point of the ISA. Clearly, $\mathbf{e}'$ is defined uniquely but becomes trivial when the rigid body instantaneously undergoes a pure translation, i.e., a motion during which, instantaneously, $\boldsymbol{\omega} = \mathbf{0}$. In this case, $\mathbf{e}'$ is defined as the unit vector parallel to the associated displacement field. Thus, an instantaneous rigid-body motion is defined by a line $\mathcal{L}'$, a pitch p', and an amplitude $\|\boldsymbol{\omega}\|$. Such a motion is, then, fully determined by six independent parameters, namely, the four independent Plücker coordinates of $\mathcal{L}'$, its pitch, and its amplitude. A line supplied with a pitch is, in general, called a *screw*; a screw supplied with an amplitude representing the magnitude of an angular velocity provides the representation of an instantaneous rigid-body motion that is sometimes called the *twist*, an item that will be discussed more in detail below.

Hence, the instantaneous screw is fully defined by six independent real numbers. Moreover, such as in the case of the screw motion, the pitch of the instantaneous screw can attain values from $-\infty$ to $+\infty$.

The ISA can be alternatively described in terms of the position vector $\mathbf{p}_0'$ of its point lying closest to the origin. Expressions for $\mathbf{p}_0'$ in terms of the position and the velocity of an arbitrary body-point and the angular velocity are derived below. To this end, we decompose $\dot{\mathbf{p}}$ into two orthogonal components, $\dot{\mathbf{p}}_{\parallel}$ and $\dot{\mathbf{p}}_{\perp}$, along and transverse to the angular-velocity vector, respectively. To this end, $\dot{\mathbf{a}}$ is first decomposed into two such orthogonal components, $\dot{\mathbf{a}}_{\parallel}$ and $\dot{\mathbf{a}}_{\perp}$, the former being parallel, the latter normal to the ISA, i.e.,

$$\dot{\mathbf{a}} \equiv \dot{\mathbf{a}}_{\parallel} + \dot{\mathbf{a}}_{\perp} \tag{3.58}$$

These orthogonal components are given as

$$\dot{\mathbf{a}}_{\parallel} \equiv \dot{\mathbf{a}} \cdot \boldsymbol{\omega} \frac{\boldsymbol{\omega}}{\|\boldsymbol{\omega}\|^2} \equiv \frac{\boldsymbol{\omega}\boldsymbol{\omega}^T}{\|\boldsymbol{\omega}\|^2}\dot{\mathbf{a}}, \quad \dot{\mathbf{a}}_{\perp} \equiv \left(\mathbf{1} - \frac{\boldsymbol{\omega}\boldsymbol{\omega}^T}{\|\boldsymbol{\omega}\|^2}\right)\dot{\mathbf{a}} \equiv -\frac{1}{\|\boldsymbol{\omega}\|^2}\boldsymbol{\Omega}^2\dot{\mathbf{a}} \tag{3.59}$$

In the derivation of eq.(3.59) we have used the identity introduced in eq.(2.39), namely,

$$\boldsymbol{\Omega}^2 \equiv \boldsymbol{\omega}\boldsymbol{\omega}^T - \|\boldsymbol{\omega}\|^2\mathbf{1} \tag{3.60}$$

Upon substitution of eq.(3.59) into eq.(3.52), we obtain

$$\dot{\mathbf{p}} = \underbrace{\frac{\boldsymbol{\omega}\boldsymbol{\omega}^T}{\|\boldsymbol{\omega}\|^2}\dot{\mathbf{a}}}_{\dot{\mathbf{p}}_{\parallel}} \underbrace{-\frac{1}{\|\boldsymbol{\omega}\|^2}\boldsymbol{\Omega}^2\dot{\mathbf{a}} + \boldsymbol{\Omega}(\mathbf{p}-\mathbf{a})}_{\dot{\mathbf{p}}_{\perp}} \tag{3.61}$$

Of the three components of $\dot{\mathbf{p}}$, the first, henceforth referred to as its *axial component*, is parallel, the last two being normal to $\boldsymbol{\omega}$. The sum of the last two components is referred to as the *normal component* of $\dot{\mathbf{p}}$. From eq.(3.61) it is apparent that the axial component is independent of $\mathbf{p}$, while the normal component is a linear function of $\mathbf{p}$. An obvious question now arises: *For an arbitrary motion, is it possible to find a certain point of position vector* $\mathbf{p}$ *whose velocity normal component vanishes?* The vanishing of the normal component obviously implies the minimization of the magnitude of $\dot{\mathbf{p}}$. The condition under which this happens can now be written as

$$\dot{\mathbf{p}}_{\perp} = \mathbf{0}$$

or

$$\boldsymbol{\Omega}(\mathbf{p}-\mathbf{a}) - \frac{1}{\|\boldsymbol{\omega}\|^2}\boldsymbol{\Omega}^2\,\dot{\mathbf{a}} = \mathbf{0} \tag{3.62}$$

which can be further expressed as a vector equation linear in $\mathbf{p}$, namely,

$$\boldsymbol{\Omega}\mathbf{p} = \boldsymbol{\Omega}\left(\mathbf{a} + \frac{1}{\|\boldsymbol{\omega}\|^2}\boldsymbol{\Omega}\dot{\mathbf{a}}\right) \tag{3.63}$$

or

$$\boldsymbol{\Omega}(\mathbf{p}-\mathbf{r})=\mathbf{0} \tag{3.64a}$$

with $\mathbf{r}$ defined as

$$\mathbf{r}\equiv\mathbf{a}+\frac{1}{\|\boldsymbol{\omega}\|^2}\boldsymbol{\Omega}\dot{\mathbf{a}} \tag{3.64b}$$

and hence, a possible solution of the foregoing problem is

$$\mathbf{p}=\mathbf{r}=\mathbf{a}+\frac{1}{\|\boldsymbol{\omega}\|^2}\boldsymbol{\Omega}\dot{\mathbf{a}} \tag{3.65}$$

However, this solution is not unique, for eq.(3.64a) does not require that $\mathbf{p}-\mathbf{r}$ be zero, only that this difference lie in the nullspace of $\boldsymbol{\Omega}$, i.e., that $\mathbf{p}-\mathbf{r}$ be linearly dependent with $\boldsymbol{\omega}$. In other words, if a vector $\alpha\boldsymbol{\omega}$ is added to $\mathbf{p}$, then the sum also satisfies eq.(3.63). It is then apparent that eq.(3.63) does not determine a single point whose normal velocity component vanishes but a set of points lying on the ISA, and thus, other solutions are possible. For example, we can find the point of the ISA lying closest to the origin. To this end, let $\mathbf{p}_0'$ be the position vector of that point. This vector is obviously perpendicular to $\boldsymbol{\omega}$, i.e.,

$$\boldsymbol{\omega}^T\mathbf{p}_0'=0 \tag{3.66}$$

Next, eq.(3.63) is rewritten for $\mathbf{p}_0'$, and eq.(3.66) is adjoined to it, thereby deriving an expanded linear system of equations, namely,

$$\mathbf{A}\mathbf{p}_0'=\mathbf{b} \tag{3.67}$$

where $\mathbf{A}$ is a 4×3 matrix and $\mathbf{b}$ is a 4-dimensional vector, both of which are given below:

$$\mathbf{A}\equiv\begin{bmatrix}\boldsymbol{\Omega}\\ \boldsymbol{\omega}^T\end{bmatrix},\quad \mathbf{b}\equiv\begin{bmatrix}\boldsymbol{\Omega}\mathbf{a}+(1/\|\boldsymbol{\omega}\|^2)\boldsymbol{\Omega}^2\dot{\mathbf{a}}\\ 0\end{bmatrix} \tag{3.68}$$

This system is of the same nature as that appearing in eq.(3.11), and hence, it can be solved for $\mathbf{p}_0'$ following the same procedure. Thus, both sides of eq.(3.67) are multiplied from the left by $\mathbf{A}^T$, thereby obtaining

$$\mathbf{A}^T\mathbf{A}\mathbf{p}_0'=\mathbf{A}^T\mathbf{b} \tag{3.69}$$

where

$$\mathbf{A}^T\mathbf{A}=\boldsymbol{\Omega}^T\boldsymbol{\Omega}+\boldsymbol{\omega}\boldsymbol{\omega}^T=-\boldsymbol{\Omega}^2+\boldsymbol{\omega}\boldsymbol{\omega}^T \tag{3.70}$$

Moreover, from eq.(3.60), the rightmost side of the foregoing relation becomes $\|\boldsymbol{\omega}\|^2\mathbf{1}$, and hence, the matrix coefficient of the left-hand side of eq.(3.69) and the right-hand side of the same equation reduce, respectively, to

$$\mathbf{A}^T\mathbf{A}=\|\boldsymbol{\omega}\|^2\mathbf{1},\quad \mathbf{A}^T\mathbf{b}=\boldsymbol{\Omega}(\dot{\mathbf{a}}-\boldsymbol{\Omega}\mathbf{a}) \tag{3.71}$$

Upon substitution of eq.(3.71) into eq.(3.69) and further solving for $\mathbf{p}_0'$, the desired expression is derived:

$$\mathbf{p}_0' = \frac{\boldsymbol{\Omega}(\dot{\mathbf{a}} - \boldsymbol{\Omega}\mathbf{a})}{\|\boldsymbol{\omega}\|^2} \equiv \frac{\boldsymbol{\omega} \times (\dot{\mathbf{a}} - \boldsymbol{\omega} \times \mathbf{a})}{\|\boldsymbol{\omega}\|^2} \tag{3.72}$$

Thus, the instantaneous screw is fully defined by an alternative set of six independent scalars, namely, the three components of its angular velocity $\boldsymbol{\omega}$ and the three components of the velocity of an arbitrary body point A, denoted by $\dot{\mathbf{a}}$. As in the case of the screw motion, we can also represent the instantaneous screw by a line and two additional parameters, as we explain below.

3.4.2 The Twist of a Rigid Body

A line, as we saw earlier, is fully defined by its 6-dimensional Plücker array, which contains only four independent components. Now, if a pitch p is added as a fifth feature to the line or correspondingly, to its Plücker array, we obtain a screw $\mathbf{s}$, namely,

$$\mathbf{s} \equiv \begin{bmatrix} \mathbf{e} \\ \mathbf{p} \times \mathbf{e} + p\mathbf{e} \end{bmatrix} \tag{3.73}$$

An *amplitude* is any scalar A multiplying the foregoing screw. The amplitude produces a twist or a *wrench*, to be discussed presently, depending on its units. The twist or the wrench thus defined can be regarded as an eight-parameter array. These eight parameters, of which only six are independent, are the amplitude, the pitch, and the six Plücker coordinates of the associated line. Clearly, a twist or a wrench is defined completely by six independent real numbers. More generally, a twist can be regarded as a 6-dimensional array defining completely the velocity field of a rigid body, and it comprises the three components of the angular velocity and the three components of the velocity of any of the points of the body.

Below we elaborate on the foregoing concepts. Upon multiplication of the screw appearing in eq.(3.73) by the amplitude A representing the magnitude of an angular velocity, we obtain a twist $\mathbf{t}$, namely,

$$\mathbf{t} \equiv \begin{bmatrix} A\mathbf{e} \\ \mathbf{p} \times (A\mathbf{e}) + p(A\mathbf{e}) \end{bmatrix}$$

where the product $A\mathbf{e}$ can be readily identified as the angular velocity $\boldsymbol{\omega}$ parallel to vector $\mathbf{e}$, of magnitude A. Moreover, the lower part of $\mathbf{t}$ can be readily identified with the velocity of a point of a rigid body. Indeed, if we regard the line $\mathcal{L}$ and point O as sets of points of a rigid body $\mathcal{B}$ moving with an angular velocity $\boldsymbol{\omega}$ and such that point P moves with a velocity $p\boldsymbol{\omega}$ parallel to the angular velocity, then the lower vector of $\mathbf{t}$, denoted by

$\mathbf{v}$, represents the velocity of point O, i.e.,

$$\mathbf{v} = -\boldsymbol{\omega} \times \mathbf{p} + p\boldsymbol{\omega}$$

We can thus express the twist $\mathbf{t}$ as

$$\mathbf{t} \equiv \begin{bmatrix} \boldsymbol{\omega} \\ \mathbf{v} \end{bmatrix} \tag{3.74}$$

A special case of great interest in kinematics is the screw of infinitely large pitch. The form of this screw is derived, very informally, by taking the limit of expression (3.73) as $p \to \infty$, namely,

$$\lim_{p\to\infty} \begin{bmatrix} \mathbf{e} \\ \mathbf{p} \times \mathbf{e} + p\mathbf{e} \end{bmatrix} \equiv \lim_{p\to\infty} \left(p \begin{bmatrix} \mathbf{e}/p \\ (\mathbf{p} \times \mathbf{e})/p + \mathbf{e} \end{bmatrix} \right)$$

which readily leads to

$$\lim_{p\to\infty} \begin{bmatrix} \mathbf{e} \\ \mathbf{p} \times \mathbf{e} + p\mathbf{e} \end{bmatrix} = \left(\lim_{p\to\infty} p \right) \begin{bmatrix} \mathbf{0} \\ \mathbf{e} \end{bmatrix}$$

The *screw of infinite pitch* $\mathbf{s}_\infty$ is defined as the 6-dimensional array appearing in the above equation, namely,

$$\mathbf{s}_\infty \equiv \begin{bmatrix} \mathbf{0} \\ \mathbf{e} \end{bmatrix} \tag{3.75}$$

Note that this screw array is identical to the Plücker array of the line at infinity lying in a plane of unit normal $\mathbf{e}$.

The twist array, as defined in eq.(3.74), with $\boldsymbol{\omega}$ on top, represents the *ray coordinates* of the twist. An exchange of the order of the two Cartesian vectors of this array, in turn, gives rise to the *axis coordinates* of the twist.

The foregoing twist was also termed *motor* by Everett (1875). As Phillips (1990) points out, the word motor is an abbreviation of *mo*ment and vec*tor*. An extensive introduction into motor algebra was published by von Mises (1924), a work that is now available in English (von Mises, 1996). Roth (1984), in turn, provided a summary of these concepts, as applicable to robotics. The foregoing array goes also by other names, such as the German *Kinemate*.

The relationships between the angular-velocity vector and the time derivatives of the invariants of the associated rotation are linear. Indeed, let the three sets of four invariants of rotation, namely, the natural invariants, the linear invariants, and the Euler-Rodrigues parameters be grouped in the 4-dimensional arrays $\boldsymbol{\nu}$, $\boldsymbol{\lambda}$, and $\boldsymbol{\eta}$, respectively, i.e.,

$$\boldsymbol{\nu} \equiv \begin{bmatrix} \mathbf{e} \\ \phi \end{bmatrix}, \quad \boldsymbol{\lambda} \equiv \begin{bmatrix} (\sin\phi)\mathbf{e} \\ \cos\phi \end{bmatrix}, \quad \boldsymbol{\eta} \equiv \begin{bmatrix} [\sin(\phi/2)]\mathbf{e} \\ \cos(\phi/2) \end{bmatrix} \tag{3.76}$$

We then have the linear relations derived in full detail elsewhere (Angeles, 1988), and outlined in Appendix A for quick reference, namely,

$$\dot{\boldsymbol{\nu}} = \mathbf{N}\boldsymbol{\omega}, \quad \dot{\boldsymbol{\lambda}} = \mathbf{L}\boldsymbol{\omega}, \quad \dot{\boldsymbol{\eta}} = \mathbf{H}\boldsymbol{\omega} \tag{3.77a}$$

with $\mathbf{N}$, $\mathbf{L}$, and $\mathbf{H}$ defined as

$$\mathbf{N} \equiv \begin{bmatrix} [\sin\phi/(2(1-\cos\phi))](\mathbf{1} - \mathbf{e}\mathbf{e}^T) - (1/2)\mathbf{E} \\ \mathbf{e}^T \end{bmatrix}, \tag{3.77b}$$

$$\mathbf{L} \equiv \begin{bmatrix} (1/2)[\mathrm{tr}(\mathbf{Q})\mathbf{1} - \mathbf{Q}] \\ -(\sin\phi)\mathbf{e}^T \end{bmatrix}, \tag{3.77c}$$

$$\mathbf{H} \equiv \frac{1}{2}\begin{bmatrix} \cos(\phi/2)\mathbf{1} - \sin(\phi/2)\mathbf{E} \\ -\sin(\phi/2)\mathbf{e}^T \end{bmatrix} \tag{3.77d}$$

where, it is recalled, $\mathrm{tr}(\cdot)$ denotes the trace of its square matrix argument $(\cdot)$, i.e., the sum of the diagonal entries of that matrix.

The inverse relations of those shown in eqs.(3.77a) are to be derived by resorting to the approach introduced when solving eq.(3.67) for $\mathbf{p}_0'$, thereby obtaining

$$\boldsymbol{\omega} = \widetilde{\mathbf{N}}\dot{\boldsymbol{\nu}} = \widetilde{\mathbf{L}}\dot{\boldsymbol{\lambda}} = \widetilde{\mathbf{H}}\dot{\boldsymbol{\eta}} \tag{3.78a}$$

the 3×4 matrices $\widetilde{\mathbf{N}}$, $\widetilde{\mathbf{L}}$, and $\widetilde{\mathbf{H}}$ being defined below:

$$\widetilde{\mathbf{N}} \equiv [\,(\sin\phi)\mathbf{1} + (1-\cos\phi)\mathbf{E} \quad \mathbf{e}\,], \tag{3.78b}$$

$$\widetilde{\mathbf{L}} \equiv [\,\mathbf{1} + [(\sin\phi)/(1+\cos\phi)]\mathbf{E} \quad -[(\sin\phi)/(1+\cos\phi)]\mathbf{e}\,], \tag{3.78c}$$

$$\widetilde{\mathbf{H}} \equiv 2\,[\,[\cos(\phi/2)]\mathbf{1} + [\sin(\phi/2)]\mathbf{E} \quad -[\sin(\phi/2)]\mathbf{e}\,] \tag{3.78d}$$

As a consequence, we have the following:

Caveat *The angular velocity vector is* **not** *a time-derivative, i.e., no Cartesian vector exists whose time-derivative is the angular-velocity vector.*

However, matrices $\mathbf{N}$, $\mathbf{L}$, and $\mathbf{H}$ of eqs.(3.77b–d) can be regarded as *integration factors* that yield time-derivatives.

Now we can write the relationship between the twist and the time-rate of change of the 7-dimensional pose array $\mathbf{s}$, namely,

$$\dot{\mathbf{s}} = \mathbf{T}\mathbf{t} \tag{3.79}$$

where

$$\mathbf{T} \equiv \begin{bmatrix} \mathbf{F} & \mathbf{O}_{43} \\ \mathbf{O} & \mathbf{1} \end{bmatrix} \tag{3.80}$$

in which $\mathbf{O}$ and $\mathbf{O}_{43}$ are the 3×3 and the 4×3 zero matrices, while $\mathbf{1}$ is the 3×3 identity matrix and $\mathbf{F}$ is, correspondingly, $\mathbf{N}$, $\mathbf{L}$, or $\mathbf{H}$, depending upon the invariant representation chosen for the rotation. The inverse relationship of eq.(3.79) takes the form

$$\mathbf{t} = \mathbf{S}\dot{\mathbf{s}} \tag{3.81a}$$

where

$$\mathbf{S} \equiv \begin{bmatrix} \widetilde{\mathbf{F}} & \mathbf{O} \\ \mathbf{O}_{34} & \mathbf{1} \end{bmatrix} \tag{3.81b}$$

in which $\mathbf{O}_{34}$ is the 3×4 zero matrix. Moreover, $\widetilde{\mathbf{F}}$ is one of $\widetilde{\mathbf{N}}$, $\widetilde{\mathbf{L}}$, or $\widetilde{\mathbf{H}}$, depending on the rotation representation adopted, namely, the natural invariants, the linear invariants, or the Euler-Rodrigues parameters, respectively.

A formula that relates the twist of the same rigid body at two different points is now derived. Let A and P be two arbitrary points of a rigid body. The twist at each of these points is defined as

$$\mathbf{t}_A = \begin{bmatrix} \boldsymbol{\omega} \\ \mathbf{v}_A \end{bmatrix}, \quad \mathbf{t}_P = \begin{bmatrix} \boldsymbol{\omega} \\ \mathbf{v}_P \end{bmatrix} \tag{3.82}$$

Moreover, eq.(3.52) can be rewritten as

$$\mathbf{v}_P = \mathbf{v}_A + (\mathbf{a} - \mathbf{p}) \times \boldsymbol{\omega} \tag{3.83}$$

Combining eq.(3.82) with eq.(3.83) yields

$$\mathbf{t}_P = \mathbf{U}\mathbf{t}_A \tag{3.84}$$

where

$$\mathbf{U} \equiv \begin{bmatrix} \mathbf{1} & \mathbf{O} \\ \mathbf{A} - \mathbf{P} & \mathbf{1} \end{bmatrix} \tag{3.85}$$

with the 6×6 matrix $\mathbf{U}$ defined as in eq.(3.31), while $\mathbf{A}$ and $\mathbf{P}$ denote the cross-product matrices of vectors $\mathbf{a}$ and $\mathbf{p}$, respectively. Thus, eq.(3.84) can be fairly called the *twist-transfer formula.*

3.5 Acceleration Analysis of Rigid-Body Motions

Upon differentiation of both sides of eq.(3.51) with respect to time, one obtains

$$\ddot{\mathbf{p}} = \ddot{\mathbf{a}} + \dot{\boldsymbol{\Omega}}(\mathbf{p} - \mathbf{a}) + \boldsymbol{\Omega}(\dot{\mathbf{p}} - \dot{\mathbf{a}}) \tag{3.86}$$

Now, eq.(3.51) is solved for $\dot{\mathbf{p}} - \dot{\mathbf{a}}$, and the expression thus resulting is substituted into eq.(3.86), thereby obtaining

$$\ddot{\mathbf{p}} = \ddot{\mathbf{a}} + (\dot{\boldsymbol{\Omega}} + \boldsymbol{\Omega}^2)(\mathbf{p} - \mathbf{a}) \tag{3.87}$$

where the matrix sum in parentheses is termed the *angular-acceleration matrix* of the rigid-body motion and is represented by $\mathbf{W}$, i.e.,

$$\mathbf{W} \equiv \dot{\boldsymbol{\Omega}} + \boldsymbol{\Omega}^2 \tag{3.88}$$

Clearly, the first term of the right-hand side of eq.(3.88) is skew-symmetric, whereas the second one is symmetric. Thus,

$$\text{vect}(\mathbf{W}) = \text{vect}(\dot{\mathbf{\Omega}}) = \dot{\boldsymbol{\omega}} \tag{3.89}$$

$\dot{\boldsymbol{\omega}}$ being termed the *angular-acceleration vector* of the rigid-body motion. We have now an interesting result, namely,

$$\begin{aligned} \text{tr}(\mathbf{W}) &= \text{tr}(\mathbf{\Omega}^2) = \text{tr}(-\|\boldsymbol{\omega}\|^2\mathbf{1} + \boldsymbol{\omega}\boldsymbol{\omega}^T) \\ &= -\|\boldsymbol{\omega}\|^2\text{tr}(\mathbf{1}) + \boldsymbol{\omega}\cdot\boldsymbol{\omega} = -2\|\boldsymbol{\omega}\|^2 \end{aligned} \tag{3.90}$$

Moreover, eq.(3.87) can be written as

$$\ddot{\mathbf{p}} = \ddot{\mathbf{a}} + \dot{\boldsymbol{\omega}}\times(\mathbf{p}-\mathbf{a}) + \boldsymbol{\omega}\times[\boldsymbol{\omega}\times(\mathbf{p}-\mathbf{a})] \tag{3.91}$$

On the other hand, the time derivative of $\mathbf{t}$, henceforth referred to as the *twist rate*, is displayed below:

$$\dot{\mathbf{t}} \equiv \begin{bmatrix} \dot{\boldsymbol{\omega}} \\ \dot{\mathbf{v}} \end{bmatrix} \tag{3.92}$$

in which $\dot{\mathbf{v}}$ is the acceleration of a point of the body. The relationship between the twist rate and the second time derivative of the screw is derived by differentiation of both sides of eq.(3.79), which yields

$$\ddot{\mathbf{s}} = \mathbf{T}\dot{\mathbf{t}} + \dot{\mathbf{T}}\mathbf{t} \tag{3.93}$$

where

$$\dot{\mathbf{T}} \equiv \begin{bmatrix} \dot{\mathbf{F}} & \mathbf{O}_{43} \\ \mathbf{O} & \mathbf{O} \end{bmatrix} \tag{3.94}$$

and $\mathbf{F}$ is one of $\mathbf{N}$, $\mathbf{L}$, or $\mathbf{H}$, accordingly. The inverse relationship of eq.(3.93) is derived by differentiating both sides of eq.(3.81a) with respect to time, which yields

$$\dot{\mathbf{t}} = \mathbf{S}\ddot{\mathbf{s}} + \dot{\mathbf{S}}\dot{\mathbf{s}} \tag{3.95}$$

where

$$\dot{\mathbf{S}} = \begin{bmatrix} \dot{\tilde{\mathbf{F}}} & \mathbf{O} \\ \mathbf{O}_{34} & \mathbf{O} \end{bmatrix} \tag{3.96}$$

with $\mathbf{O}$ and $\mathbf{O}_{34}$ already defined in eq.(3.81b) as the 3×3 and the 3×4 zero matrices, respectively, while $\dot{\tilde{\mathbf{F}}}$ is one of $\dot{\tilde{\mathbf{N}}}$, $\dot{\tilde{\mathbf{L}}}$, or $\dot{\tilde{\mathbf{H}}}$, according with the type of rotation representation at hand.

Before we take to differentiating the foregoing matrices, we introduce a few definitions: Let

$$\boldsymbol{\lambda} \equiv \begin{bmatrix} \mathbf{u} \\ u_0 \end{bmatrix}, \quad \boldsymbol{\eta} \equiv \begin{bmatrix} \mathbf{r} \\ r_0 \end{bmatrix} \tag{3.97a}$$

i.e.,

$$\mathbf{u} \equiv \sin\phi\mathbf{e}, \quad u_0 \equiv \cos\phi, \quad \mathbf{r} \equiv \sin\left(\frac{\phi}{2}\right)\mathbf{e}, \quad r_0 \equiv \cos\left(\frac{\phi}{2}\right) \tag{3.97b}$$

Thus, the time derivatives sought take on the forms

$$\dot{\mathbf{N}} = \frac{1}{4(1-\cos\phi)}\begin{bmatrix}\mathbf{B}\\ \dot{\mathbf{e}}\end{bmatrix} \tag{3.98a}$$

$$\begin{aligned}\dot{\mathbf{L}} &= \begin{bmatrix}(1/2)[\mathbf{1}\mathrm{tr}(\dot{\mathbf{Q}}) - \dot{\mathbf{Q}}]\\ -(1/2)\boldsymbol{\omega}^T[\mathbf{1}\mathrm{tr}(\mathbf{Q}) - \mathbf{Q}^T]\end{bmatrix}\\ &= \begin{bmatrix}-(\boldsymbol{\omega}\cdot\mathbf{u})\mathbf{1} - (1/2)\boldsymbol{\Omega}\mathbf{Q}\\ -(1/2)\boldsymbol{\omega}^T[\mathbf{1}\mathrm{tr}(\mathbf{Q}) - \mathbf{Q}^T]\end{bmatrix}\end{aligned} \tag{3.98b}$$

$$\dot{\mathbf{H}} = \frac{1}{2}\begin{bmatrix}\dot{r}_0\mathbf{1} - \dot{\mathbf{R}}\\ -\dot{\mathbf{r}}^T\end{bmatrix} \tag{3.98c}$$

where we have used the identities below, which are derived in Appendix A.

$$\mathrm{tr}(\dot{\mathbf{Q}}) \equiv \mathrm{tr}(\boldsymbol{\Omega}\mathbf{Q}) \equiv -2\boldsymbol{\omega}^T\mathbf{u} \tag{3.98d}$$

Furthermore, $\mathbf{R}$ denotes the cross-product matrix of $\mathbf{r}$, and $\mathbf{B}$ is defined as

$$\begin{aligned}\mathbf{B} \equiv\ & -2(\mathbf{e}\cdot\boldsymbol{\omega})\mathbf{1} + 2(3-\cos\phi)(\mathbf{e}\cdot\boldsymbol{\omega})\mathbf{e}\mathbf{e}^T - 2(1+\sin\phi)\boldsymbol{\omega}\mathbf{e}^T\\ & -(2\cos\phi + \sin\phi)\mathbf{e}\boldsymbol{\omega}^T - (\sin\phi)[\boldsymbol{\Omega} - (\mathbf{e}\cdot\boldsymbol{\omega})\mathbf{E}]\end{aligned} \tag{3.98e}$$

Moreover,

$$\dot{\tilde{\mathbf{N}}} = [\,\dot{\phi}(\cos\phi)\mathbf{1} + \dot{\phi}(\sin\theta)\mathbf{E} \quad \dot{\mathbf{e}}\,] \tag{3.99a}$$

$$\dot{\tilde{\mathbf{L}}} = [\,\mathbf{V}/D \quad \dot{\mathbf{u}}\,] \tag{3.99b}$$

$$\dot{\tilde{\mathbf{H}}} = [\,\dot{r}_0\mathbf{1} + \dot{\mathbf{R}} \quad -\dot{\mathbf{r}}\,] \tag{3.99c}$$

where $\mathbf{V}$ and D are defined below:

$$\mathbf{V} \equiv \dot{\mathbf{U}} - (\dot{\mathbf{u}}\mathbf{u}^T + \mathbf{u}\dot{\mathbf{u}}^T) - \frac{\dot{u}_0}{D}(\mathbf{U} - \mathbf{u}\mathbf{u}^T) \tag{3.99d}$$

$$D \equiv 1 + u_0 \tag{3.99e}$$

with $\mathbf{U}$ denoting the cross-product matrix of $\mathbf{u}$.

3.6 Rigid-Body Motion Referred to Moving Coordinate Axes

Although in kinematics no "preferred" coordinate system exists, in dynamics the governing equations of rigid-body motions are valid only in *inertial*

frames. An inertial frame can be defined as a coordinate system that translates with uniform velocity and constant orientation with respect to the stars. Thus, it is important to refer vectors and matrices to inertial frames, but sometimes it is not possible to do so directly. For instance, a spacecraft can be supplied with instruments to measure the velocity and the acceleration of a satellite drifting in space, but the measurements taken from the spacecraft will be referred to a coordinate frame fixed to it, which is not inertial. If the motion of the spacecraft with respect to an inertial coordinate frame is recorded, e.g., from an Earth-based station, then the acceleration of the satellite with respect to an inertial frame can be computed using the foregoing information. How to do this is the subject of this section.

In the realm of kinematics, it is not necessary to distinguish between inertial and noninertial coordinate frames, and hence, it will suffice to call the coordinate systems involved *fixed* and *moving.* Thus, consider the fixed coordinate frame X, Y, Z, which will be labeled $\mathcal{F}$, and the moving coordinate frame $\mathcal{X}$, $\mathcal{Y}$, and $\mathcal{Z}$, which will be labeled $\mathcal{M}$, both being depicted in Fig. 3.4. Moreover, let $\mathbf{Q}$ be the rotation matrix taking frame $\mathcal{F}$ into the orientation of $\mathcal{M}$, and $\mathbf{o}$ the position vector of the origin of $\mathcal{M}$ from the origin of $\mathcal{F}$. Further, let $\mathbf{p}$ be the position vector of point P from the origin of $\mathcal{F}$ and $\boldsymbol{\rho}$ the position vector of the same point from the origin of $\mathcal{M}$. From Fig. 3.4 one has

$$[\,\mathbf{p}\,]_{\mathcal{F}} = [\,\mathbf{o}\,]_{\mathcal{F}} + [\,\boldsymbol{\rho}\,]_{\mathcal{F}} \tag{3.100}$$

where it will be assumed that $\boldsymbol{\rho}$ is not available in frame $\mathcal{F}$, but in $\mathcal{M}$. Hence,

$$[\,\boldsymbol{\rho}\,]_{\mathcal{F}} = [\,\mathbf{Q}\,]_{\mathcal{F}}[\,\boldsymbol{\rho}\,]_{\mathcal{M}} \tag{3.101}$$

Substitution of eq.(3.101) into eq.(3.100) yields

$$[\,\mathbf{p}\,]_{\mathcal{F}} = [\,\mathbf{o}\,]_{\mathcal{F}} + [\,\mathbf{Q}\,]_{\mathcal{F}}[\,\boldsymbol{\rho}\,]_{\mathcal{M}} \tag{3.102}$$

Now, in order to compute the velocity of P, both sides of eq.(3.102) are differentiated with respect to time, which leads to

$$[\,\dot{\mathbf{p}}\,]_{\mathcal{F}} = [\,\dot{\mathbf{o}}\,]_{\mathcal{F}} + [\,\dot{\mathbf{Q}}\,]_{\mathcal{F}}[\,\boldsymbol{\rho}\,]_{\mathcal{M}} + [\,\mathbf{Q}\,]_{\mathcal{F}}[\,\dot{\boldsymbol{\rho}}\,]_{\mathcal{M}} \tag{3.103}$$

Furthermore, from the definition of $\boldsymbol{\Omega}$, eq.(3.46), we have

$$[\,\dot{\mathbf{Q}}\,]_{\mathcal{F}} = [\,\boldsymbol{\Omega}\,]_{\mathcal{F}}[\,\mathbf{Q}\,]_{\mathcal{F}} \tag{3.104}$$

Upon substitution of the foregoing relation into eq.(3.103), we obtain

$$[\,\dot{\mathbf{p}}\,]_{\mathcal{F}} = [\,\dot{\mathbf{o}}\,]_{\mathcal{F}} + [\,\boldsymbol{\Omega}\,]_{\mathcal{F}}[\,\mathbf{Q}\,]_{\mathcal{F}}[\,\boldsymbol{\rho}\,]_{\mathcal{M}} + [\,\mathbf{Q}\,]_{\mathcal{F}}[\,\dot{\boldsymbol{\rho}}\,]_{\mathcal{M}} \tag{3.105}$$

which is an expression for the velocity of P in $\mathcal{F}$ in terms of the velocity of P in $\mathcal{M}$ and the twist of $\mathcal{M}$ with respect to $\mathcal{F}$. Next, the acceleration of P in $\mathcal{F}$ is derived by differentiation of both sides of eq.(3.105) with respect to time, which yields

$$\begin{aligned}[\,\ddot{\mathbf{p}}\,]_{\mathcal{F}} = {} & [\,\ddot{\mathbf{o}}\,]_{\mathcal{F}} + [\,\dot{\boldsymbol{\Omega}}\,]_{\mathcal{F}}[\,\mathbf{Q}\,]_{\mathcal{F}}[\,\boldsymbol{\rho}\,]_{\mathcal{M}} + [\,\boldsymbol{\Omega}\,]_{\mathcal{F}}[\,\dot{\mathbf{Q}}\,]_{\mathcal{F}}[\,\boldsymbol{\rho}\,]_{\mathcal{M}} \\ & + [\,\boldsymbol{\Omega}\,]_{\mathcal{F}}[\,\mathbf{Q}\,]_{\mathcal{F}}[\,\dot{\boldsymbol{\rho}}\,]_{\mathcal{M}} + [\,\dot{\mathbf{Q}}\,]_{\mathcal{F}}[\,\dot{\boldsymbol{\rho}}\,]_{\mathcal{M}} + [\,\mathbf{Q}\,]_{\mathcal{F}}[\,\ddot{\boldsymbol{\rho}}\,]_{\mathcal{M}}\end{aligned} \tag{3.106}$$

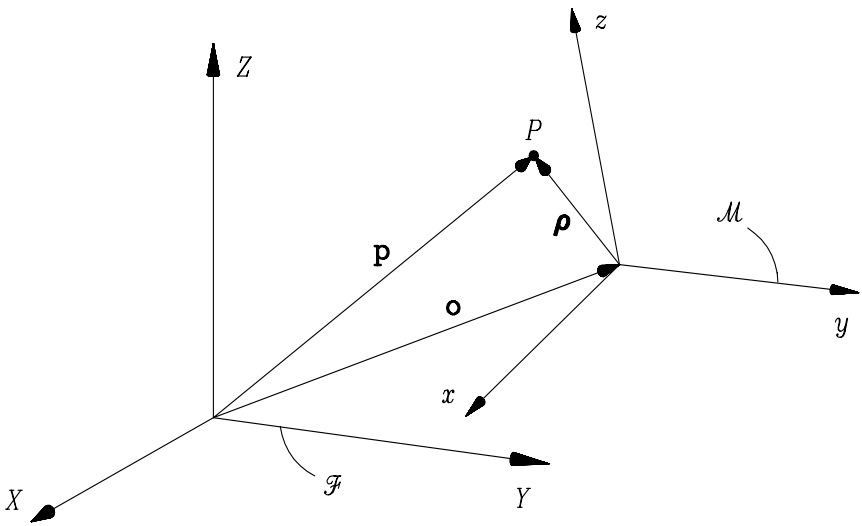

FIGURE 3.4. Fixed and moving coordinate frames.

Further, upon substitution of identity (3.104) into eq.(3.106), we obtain

$$[\ddot{\mathbf{p}}]_{\mathcal{F}} = [\ddot{\mathbf{o}}]_{\mathcal{F}} + ([\dot{\mathbf{\Omega}}]_{\mathcal{F}} + [\mathbf{\Omega}^2]_{\mathcal{F}})[\mathbf{Q}]_{\mathcal{F}}[\boldsymbol{\rho}]_{\mathcal{M}} + 2[\mathbf{\Omega}]_{\mathcal{F}}[\mathbf{Q}]_{\mathcal{F}}[\dot{\boldsymbol{\rho}}]_{\mathcal{M}} + [\mathbf{Q}]_{\mathcal{F}}[\ddot{\boldsymbol{\rho}}]_{\mathcal{M}} \tag{3.107}$$

Moreover, from the results of Section 3.5, it is clear that the first two terms of the right-hand side of eq.(3.107) represent the acceleration of P as a point of $\mathcal{M}$, whereas the fourth term is the acceleration of P measured from $\mathcal{M}$. The third term is what is called the *Coriolis acceleration*, as it was first pointed out by the French mathematician Gustave Gaspard Coriolis (1835).

3.7 Static Analysis of Rigid Bodies

Germane to the velocity analysis of rigid bodies is their force-and-moment analysis. In fact, striking similarities exist between the velocity relations associated with rigid bodies and the forces and moments acting on them. From elementary statics it is known that the resultant of all external actions, i.e., forces and moments, exerted on a rigid body can be reduced to a force $\mathbf{f}$ acting at a point, say A, and a moment $\mathbf{n}_A$. Alternatively, the aforementioned force $\mathbf{f}$ can be defined as acting at an arbitrary point P of the body, as depicted in Fig. 3.5, but then the resultant moment, $\mathbf{n}_P$, changes correspondingly.

In order to establish a relationship between $\mathbf{n}_A$ and $\mathbf{n}_P$, the moment of the first system of force and moment with respect to point P is equated to

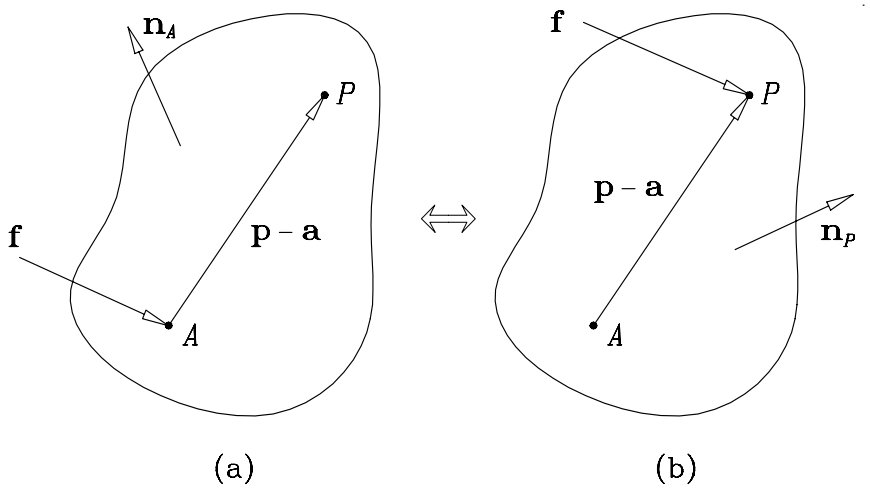

FIGURE 3.5. Equivalent systems of force and moment acting on a rigid body.

the moment about the same point of the second system, thus obtaining

$$\mathbf{n}_P = \mathbf{n}_A + (\mathbf{a} - \mathbf{p}) \times \mathbf{f} \tag{3.108}$$

which can be rewritten as

$$\mathbf{n}_P = \mathbf{n}_A + \mathbf{f} \times (\mathbf{p} - \mathbf{a}) \tag{3.109}$$

whence the analogy with eq.(3.52) is apparent. Indeed, $\mathbf{n}_P$ and $\mathbf{n}_A$ of eq.(3.109) play the role of the velocities of P and A, $\dot{\mathbf{p}}$ and $\dot{\mathbf{a}}$, respectively, whereas $\mathbf{f}$ of eq.(3.109) plays the role of $\boldsymbol{\omega}$ of eq.(3.52). Thus, similar to Theorem 3.4.2, one has

Theorem 3.7.1 *For a given system of forces and moments acting on a rigid body, if the resultant force is applied at any point of a particular line $\mathcal{L}''$, then the resultant moment is of minimum magnitude. Moreover, that minimum-magnitude moment is parallel to the resultant force.*

Hence, the resultant of the system of forces and moments is equivalent to a force $\mathbf{f}$ acting at a point of $\mathcal{L}''$ and a moment $\mathbf{n}$, with both $\mathbf{f}$ and $\mathbf{n}$ parallel to $\mathcal{L}''$. Paraphrasing the definition of the ISA, one defines line $\mathcal{L}''$ as the *axis of the wrench* acting on the body. Let $\mathbf{n}_0$ be the minimum-magnitude moment. Clearly, $\mathbf{n}_0$ can be expressed as $\mathbf{v}_0$ was in eq.(3.54), namely, as

$$\mathbf{n}_0 = n_0 \frac{\mathbf{f}}{\|\mathbf{f}\|}, \quad n_0 \equiv \frac{\mathbf{n}_P \cdot \mathbf{f}}{\|\mathbf{f}\|} \tag{3.110}$$

Moreover, the *pitch of the wrench*, p'', is defined as

$$p'' \equiv \frac{n_0}{\|\mathbf{f}\|} = \frac{\mathbf{n}_P \cdot \mathbf{f}}{\|\mathbf{f}\|^2} \quad \text{or} \quad p'' = \frac{2\pi \mathbf{n}_P \cdot \mathbf{f}}{\|\mathbf{f}\|^2} \tag{3.111}$$

which again has units of m/rad or correspondingly, of m/turn. Of course, the wrench axis can be defined by its Plücker array, $\mathbf{p}_{\mathcal{L}''}$, i.e.,

$$\mathbf{p}_{\mathcal{L}''} \equiv \begin{bmatrix} \mathbf{e}'' \\ \mathbf{n}'' \end{bmatrix}, \quad \mathbf{e}'' = \frac{\mathbf{f}}{\|\mathbf{f}\|}, \quad \mathbf{n}'' = \mathbf{p} \times \mathbf{e}'' \tag{3.112}$$

where $\mathbf{e}''$ is the unit vector parallel to $\mathcal{L}''$, $\mathbf{n}''$ is the moment of $\mathcal{L}''$ about the origin, and $\mathbf{p}$ is the position vector of any point on $\mathcal{L}''$.

The wrench axis is fully specified, then, by the direction of $\mathbf{f}$ and point P_0'' lying closest to the origin of position vector $\mathbf{p}_0''$, which can be derived by analogy with eq.(3.72), namely, as

$$\mathbf{p}_0'' = \frac{1}{\|\mathbf{f}\|^2}\mathbf{f} \times (\mathbf{n}_A - \mathbf{f} \times \mathbf{a}) \tag{3.113}$$

Similar to Theorem 3.4.1, one has

Theorem 3.7.2 *The projection of the resultant moment of a system of moments and forces acting on a rigid body that arises when the resultant force is applied at an arbitrary point of the body onto the wrench axis is constant.*

From the foregoing discussion, then, the wrench applied to a rigid body can be fully specified by the resultant force $\mathbf{f}$ acting at an arbitrary point P and the associated moment, $\mathbf{n}_P$. We shall derive presently the counterpart of the 6-dimensional array of the twist, namely, the wrench array. Upon multiplication of the screw of eq.(3.73) by an amplitude A with units of force, what we will obtain would be a wrench $\mathbf{w}$, i.e., a 6-dimensional array with its first three components having units of force and its last components units of moment. We would like to be able to obtain the power developed by the wrench on the body moving with the twist $\mathbf{t}$ by a simple inner product of the two arrays. However, because of the form the wrench $\mathbf{w}$ has taken, the inner product of these two arrays would be meaningless, for it would involve the sum of two scalar quantities with different units, and moreover, each of the two quantities is without an immediate physical meaning. In fact, the first scalar would have units of force by frequency (angular velocity by force), while the second would have units of moment of moment multiplied by frequency (velocity by moment), thereby leading to a physically meaningless result. This inconsistency can be resolved if we redefine the wrench not simply as the product of a screw by an amplitude, but as a linear transformation of that screw involving the 6×6 array $\mathbf{\Gamma}$ defined as

$$\mathbf{\Gamma} \equiv \begin{bmatrix} \mathbf{O} & \mathbf{1} \\ \mathbf{1} & \mathbf{O} \end{bmatrix} \tag{3.114}$$

where $\mathbf{O}$ and $\mathbf{1}$ denote, respectively, the 3×3 zero and identity matrices. Now we define the wrench as a linear transformation of the screw $\mathbf{s}$ defined

in eq.(3.73). This transformation is obtained upon multiplying $\mathbf{s}$ by the product $A\boldsymbol{\Gamma}$, the amplitude A having units of force, i.e.,

$$\mathbf{w} \equiv A\boldsymbol{\Gamma}\mathbf{s} \equiv \begin{bmatrix} \mathbf{p} \times (A\mathbf{e}) + p(A\mathbf{e}) \\ A\mathbf{e} \end{bmatrix}$$

The foregoing wrench is said to be given in *axis coordinates*, as opposed to the twist, which was given in ray coordinates.

Now, the first three components of the foregoing array can be readily identified as the moment of a force of magnitude A acting along a line of action given by the Plücker array of eq.(3.112), with respect to a point P, to which a moment parallel to that line and of magnitude pA is added. Moreover, the last three components of that array pertain apparently to a force of magnitude A and parallel to the same line. We denote here the above-mentioned moment by $\mathbf{n}$ and the force by $\mathbf{f}$, i.e.,

$$\mathbf{f} \equiv A\mathbf{e}, \quad \mathbf{n} \equiv \mathbf{p} \times \mathbf{f} + p\mathbf{f}$$

The wrench $\mathbf{w}$ is then defined as

$$\mathbf{w} \equiv \begin{bmatrix} \mathbf{n} \\ \mathbf{f} \end{bmatrix} \tag{3.115}$$

which can thus be interpreted as a representation of a system of forces and moments acting on a rigid body, with the force acting at point P of the body $\mathcal{B}$ defined above and a moment $\mathbf{n}$. Under these circumstances, we say that $\mathbf{w}$ *acts* at point P of $\mathcal{B}$.

With the foregoing definitions it is now apparent that the wrench has been defined so that the *inner product* $\mathbf{t}^T\mathbf{w}$ will produce the power Π developed by $\mathbf{w}$ acting at P when $\mathcal{B}$ moves with a twist $\mathbf{t}$ defined at the same point, i.e.,

$$\Pi = \mathbf{t}^T\mathbf{w} \tag{3.116}$$

When a wrench $\mathbf{w}$ that acts on a rigid body moving with the twist $\mathbf{t}$ develops zero power onto the body, we say that the wrench and the twist are *reciprocal* to each other. By the same token, the screws associated with that wrench-twist pair are said to be *reciprocal*. More specifically, let the wrench and the twist be given in terms of their respective screws, $\mathbf{s}_w$ and $\mathbf{s}_t$, as

$$\mathbf{w} = W\boldsymbol{\Gamma}\mathbf{s}_w, \quad \mathbf{t} = T\mathbf{s}_t, \tag{3.117}$$

where W and T are the amplitudes of the wrench and the twist, respectively, while $\boldsymbol{\Gamma}$ is as defined in eq.(3.114). Thus, the two screws $\mathbf{s}_w$ and $\mathbf{s}_t$ are reciprocal if

$$(\boldsymbol{\Gamma}\mathbf{s}_w)^T\mathbf{s}_t \equiv \mathbf{s}_w^T\boldsymbol{\Gamma}^T\mathbf{s}_t = 0 \tag{3.118}$$

and by virtue of the symmetry of $\boldsymbol{\Gamma}$, the foregoing relation can be further expressed as

$$\mathbf{s}_w^T\boldsymbol{\Gamma}\mathbf{s}_t = 0 \quad \text{or} \quad \mathbf{s}_t^T\boldsymbol{\Gamma}\mathbf{s}_w = 0 \tag{3.119}$$

Now, if A and P are arbitrary points of a rigid body, we define the wrench at these points as

$$\mathbf{w}_A \equiv \begin{bmatrix} \mathbf{n}_A \\ \mathbf{f} \end{bmatrix}, \quad \mathbf{w}_P \equiv \begin{bmatrix} \mathbf{n}_P \\ \mathbf{f} \end{bmatrix} \tag{3.120}$$

Therefore, eq.(3.108) leads to

$$\mathbf{w}_P = \mathbf{V}\mathbf{w}_A \tag{3.121}$$

where

$$\mathbf{V} \equiv \begin{bmatrix} \mathbf{1} & \mathbf{A} - \mathbf{P} \\ \mathbf{0} & \mathbf{1} \end{bmatrix} \tag{3.122}$$

and $\mathbf{A}$ and $\mathbf{P}$ were defined in eq.(3.85) as the cross-product matrices of vectors $\mathbf{a}$ and $\mathbf{p}$, respectively. Thus, $\mathbf{w}_P$ is a linear transformation of $\mathbf{w}_A$. By analogy with the twist-transfer formula of eq.(3.84), eq.(3.121) is termed here the *wrench-transfer formula*.

Multiplying the transpose of eq.(3.84) by eq.(3.121) yields

$$\mathbf{t}_P^T \mathbf{w}_P = \mathbf{t}_A^T \mathbf{U}^T \mathbf{V} \mathbf{w}_A \tag{3.123}$$

where

$$\mathbf{U}^T\mathbf{V} = \begin{bmatrix} \mathbf{1} & -\mathbf{A} + \mathbf{P} \\ \mathbf{0} & \mathbf{1} \end{bmatrix} \begin{bmatrix} \mathbf{1} & \mathbf{A} - \mathbf{P} \\ \mathbf{0} & \mathbf{1} \end{bmatrix} = \mathbf{1}_{6\times 6} \tag{3.124}$$

with $\mathbf{1}_{6\times 6}$ denoting the 6×6 identity matrix. Thus, $\mathbf{t}_P^T \mathbf{w}_P = \mathbf{t}_A^T \mathbf{w}_A$, as expected, since the wrench develops the same amount of power, regardless of where the force is assumed to be applied. Also note that an interesting relation between $\mathbf{U}$ and $\mathbf{V}$ follows from eq.(3.124), namely,

$$\mathbf{V}^{-1} = \mathbf{U}^T \tag{3.125}$$

3.8 Dynamics of Rigid Bodies

The equations governing the motion of rigid bodies are recalled in this section and cast into a form suitable to multibody dynamics. To this end, a few definitions are introduced. If a rigid body has a mass density ρ, which need not be constant, then its mass m is defined as

$$m = \int_{\mathcal{B}} \rho d\mathcal{B} \tag{3.126}$$

where $\mathcal{B}$ denotes the region of the 3-dimensional space occupied by the body. Now, if $\mathbf{p}$ denotes the position vector of an arbitrary point of the body, from a previously defined origin O, the *mass first moment* of the body with respect to O, $\mathbf{q}_O$, is defined as

$$\mathbf{q}_O \equiv \int_{\mathcal{B}} \rho \mathbf{p} d\mathcal{B} \tag{3.127}$$

Furthermore, the *mass second moment* of the body with respect to O is defined as

$$\mathbf{I}_O \equiv \int_{\mathcal{B}} \rho[\,(\mathbf{p}\cdot\mathbf{p})\mathbf{1} - \mathbf{p}\mathbf{p}^T\,]d\mathcal{B} \tag{3.128}$$

which is clearly a symmetric matrix. This matrix is also called the moment-of-inertia matrix of the body under study with respect to O. One can readily prove the following result:

Theorem 3.8.1 *The moment of inertia of a rigid body with respect to a point O is positive definite.*

Proof: All we need to prove is that for any vector $\boldsymbol{\omega}$, the quadratic form $\boldsymbol{\omega}^T\mathbf{I}_O\boldsymbol{\omega}$ is positive. But this is so, because

$$\boldsymbol{\omega}^T\mathbf{I}_O\boldsymbol{\omega} = \int_{\mathcal{B}} \rho[\,\|\mathbf{p}\|^2\|\boldsymbol{\omega}\|^2 - (\mathbf{p}\cdot\boldsymbol{\omega})^2\,]d\mathcal{B} \tag{3.129}$$

Now, we recall that

$$\mathbf{p}\cdot\boldsymbol{\omega} = \|\mathbf{p}\|\|\boldsymbol{\omega}\|\cos(\mathbf{p},\boldsymbol{\omega}) \tag{3.130}$$

in which $(\mathbf{p},\boldsymbol{\omega})$ stands for the angle between the two vectors within the parentheses. Substitution of eq.(3.130) into eq.(3.129) leads to

$$\begin{aligned}\boldsymbol{\omega}^T\mathbf{I}_O\boldsymbol{\omega} &= \int_{\mathcal{B}} \rho\|\mathbf{p}\|^2\|\boldsymbol{\omega}\|^2[\,1-\cos^2(\mathbf{p},\boldsymbol{\omega})\,]d\mathcal{B}\\ &= \int_{\mathcal{B}} \rho\|\mathbf{p}\|^2\|\boldsymbol{\omega}\|^2\sin^2(\mathbf{p},\boldsymbol{\omega})d\mathcal{B}\end{aligned}$$

which is a positive quantity that vanishes only in the ideal case of a slender body having all its mass concentrated along a line passing through O and parallel to $\boldsymbol{\omega}$, which would thus render $\sin(\mathbf{p},\boldsymbol{\omega}) = 0$ within the body, thereby completing the proof.

Alternatively, one can prove the positive definiteness of the mass moment of inertia based on physical arguments. Indeed, if vector $\boldsymbol{\omega}$ of the previous discussion is the angular velocity of the rigid body, then the quadratic form of eq.(3.129) turns out to be twice the kinetic energy of the body. Indeed, the said kinetic energy, denoted by T, is defined as

$$T \equiv \int_{\mathcal{B}} \frac{1}{2}\rho\|\dot{\mathbf{p}}\|^2 d\mathcal{B}$$

where $\dot{\mathbf{p}}$ is the velocity of any point P of the body. For the purposes of this discussion, it will be assumed that point O, about which the second moment is defined, is a point of the body that is instantaneously at rest. Thus, if this point is defined as the origin of the Euclidean space, the velocity of any point of the body, moving with an angular velocity $\boldsymbol{\omega}$, is given by

$$\dot{\mathbf{p}} = \boldsymbol{\omega}\times\mathbf{p}$$

which can be rewritten as

$$\dot{\mathbf{p}} = -\mathbf{P}\boldsymbol{\omega}$$

with $\mathbf{P}$ defined as the cross-product matrix of $\mathbf{p}$. Hence,

$$\|\dot{\mathbf{p}}\|^2 = (\mathbf{P}\boldsymbol{\omega})^T\mathbf{P}\boldsymbol{\omega} = \boldsymbol{\omega}^T\mathbf{P}^T\mathbf{P}\boldsymbol{\omega} = -\boldsymbol{\omega}^T\mathbf{P}^2\boldsymbol{\omega}$$

Moreover, by virtue of eq.(2.39), the foregoing expression is readily reducible to

$$\|\dot{\mathbf{p}}\|^2 = \boldsymbol{\omega}^T(\|\mathbf{p}\|^2\mathbf{1} - \mathbf{p}\mathbf{p}^T)\boldsymbol{\omega} \tag{3.131}$$

Therefore, the kinetic energy reduces to

$$T = \frac{1}{2}\int_{\mathcal{B}} \rho\boldsymbol{\omega}^T(\|\mathbf{p}\|^2\mathbf{1} - \mathbf{p}\mathbf{p}^T)\boldsymbol{\omega}d\mathcal{B} \tag{3.132}$$

and since the angular velocity is constant throughout the body, it can be taken out of the integral sign, i.e.,

$$T = \frac{1}{2}\boldsymbol{\omega}^T\left[\int_{\mathcal{B}} \rho(\|\mathbf{p}\|^2\mathbf{1} - \mathbf{p}\mathbf{p}^T)d\mathcal{B}\right]\boldsymbol{\omega} \tag{3.133}$$

The term inside the brackets of the latter equation is readily identified as $\mathbf{I}_O$, and hence, the kinetic energy can be written as

$$T = \frac{1}{2}\boldsymbol{\omega}^T\mathbf{I}_O\boldsymbol{\omega} \tag{3.134}$$

Now, since the kinetic energy is a positive-definite quantity, the quadratic form of eq.(3.134) is consequently positive-definite as well, thereby proving the positive-definiteness of the second moment.

The *mass center* of a rigid body, measured from O, is defined as a point C, not necessarily within the body—think of a homogeneous torus—of position vector $\mathbf{c}$ given by

$$\mathbf{c} \equiv \frac{\mathbf{q}_O}{m} \tag{3.135}$$

Naturally, the mass moment of inertia of the body with respect to its centroid is defined as

$$\mathbf{I}_C \equiv \int_{\mathcal{B}} \rho[\,\|\mathbf{r}\|^2\mathbf{1} - \mathbf{r}\mathbf{r}^T\,]d\mathcal{B} \tag{3.136}$$

where $\mathbf{r}$ is defined, in turn, as

$$\mathbf{r} \equiv \mathbf{p} - \mathbf{c} \tag{3.137}$$

Obviously, the mass moment of inertia of a rigid body about its mass center, also termed its *centroidal mass moment of inertia*, is positive-definite as well. In fact, the mass—or the volume, for that matter—moment of inertia of a rigid body *with respect to any point* is positive-definite. As a

consequence, its three eigenvalues are positive and are referred to as the *principal moments of inertia* of the body. The eigenvectors of the inertia matrix are furthermore mutually orthogonal and define the *principal axes of inertia* of the body. These axes are parallel to the eigenvectors of that matrix and pass through the point about which the moment of inertia is taken. Note, however, that the principal moments and the principal axes of inertia of a rigid body depend on the point with respect to which the moment of inertia is defined. Moreover, let $\mathbf{I}_O$ and $\mathbf{I}_C$ be defined as in eqs.(3.128) and (3.136), with $\mathbf{r}$ defined as in eq.(3.137). It is possible to show that

$$\mathbf{I}_O = \mathbf{I}_C + m(\|\mathbf{c}\|^2\mathbf{1} - \mathbf{c}\mathbf{c}^T) \tag{3.138}$$

Furthermore, the smallest principal moment of inertia of a rigid body attains its minimum value at the mass center of the body. The relationship appearing in eq.(3.138) constitutes the *Theorem of Parallel Axes*.

Henceforth, we assume that $\mathbf{c}$ is the position vector of the mass center in an inertial frame. Now, we recall the Newton-Euler equations governing the motion of a rigid body. Let the body at hand be acted upon by a wrench of force $\mathbf{f}$ applied at its mass center, and a moment $\mathbf{n}_C$. The Newton equation then takes the form

$$\mathbf{f} = m\ddot{\mathbf{c}} \tag{3.139a}$$

whereas the Euler equation is

$$\mathbf{n}_C = \mathbf{I}_C\dot{\boldsymbol{\omega}} + \boldsymbol{\omega} \times \mathbf{I}_C\boldsymbol{\omega} \tag{3.139b}$$

The *momentum* $\mathbf{m}$ and the *angular momentum* $\mathbf{h}_C$ of a rigid body moving with an angular velocity $\boldsymbol{\omega}$ are defined below, the angular momentum being defined with respect to the mass center. These are

$$\mathbf{m} \equiv m\dot{\mathbf{c}}, \quad \mathbf{h}_C \equiv \mathbf{I}_C\boldsymbol{\omega} \tag{3.140}$$

Moreover, the time-derivatives of the foregoing quantities are readily computed as

$$\dot{\mathbf{m}} = m\ddot{\mathbf{c}}, \quad \dot{\mathbf{h}}_C = \mathbf{I}_C\dot{\boldsymbol{\omega}} + \boldsymbol{\omega} \times \mathbf{I}_C\boldsymbol{\omega} \tag{3.141}$$

and hence, eqs.(3.139a & b) take on the forms

$$\mathbf{f} = \dot{\mathbf{m}}, \quad \mathbf{n}_C = \dot{\mathbf{h}}_C \tag{3.142}$$

The set of equations (3.139a) and (3.139b) are known as the *Newton-Euler equations*. These can be written in a more compact form as we describe below. First, we introduce a 6×6 matrix $\mathbf{M}$ that following von Mises (1924), we term the *inertia dyad*, namely,

$$\mathbf{M} \equiv \begin{bmatrix} \mathbf{I}_C & \mathbf{O} \\ \mathbf{O} & m\mathbf{1} \end{bmatrix} \tag{3.143}$$

where $\mathbf{O}$ and $\mathbf{1}$ denote the 3×3 zero and identity matrices. A similar 6×6 matrix was defined by von Mises under the above name. However, von Mises's inertia dyad is full, while the matrix defined above is block-diagonal. Both matrices, nevertheless, denote the same physical property of a rigid body, i.e., its mass and moment of inertia. Now the Newton-Euler equations can be written as

$$\mathbf{M}\dot{\mathbf{t}} + \mathbf{W}\mathbf{M}\mathbf{t} = \mathbf{w} \tag{3.144}$$

in which matrix $\mathbf{W}$, which we shall term, by similarity with the inertia dyad, the *angular-velocity dyad*, is defined, in turn, as

$$\mathbf{W} \equiv \begin{bmatrix} \mathbf{\Omega} & \mathbf{O} \\ \mathbf{O} & \mathbf{O} \end{bmatrix} \tag{3.145}$$

with $\mathbf{\Omega}$ already defined as the angular-velocity matrix; it is, of course, the cross-product matrix of the angular-velocity vector $\boldsymbol{\omega}$. Note that the twist of a rigid body lies in the nullspace of its angular-velocity dyad, i.e.,

$$\mathbf{W}\mathbf{t} = \mathbf{0} \tag{3.146}$$

Further definitions are introduced below: The *momentum screw* of the rigid body about the mass center is the 6-dimensional vector $\boldsymbol{\mu}$ defined as

$$\boldsymbol{\mu} \equiv \begin{bmatrix} \mathbf{I}_C\boldsymbol{\omega} \\ m\dot{\mathbf{c}} \end{bmatrix} = \mathbf{M}\mathbf{t} \tag{3.147}$$

Furthermore, from eqs.(3.141) and definition (3.147), the time-derivative of $\boldsymbol{\mu}$ can be readily derived as

$$\dot{\boldsymbol{\mu}} = \mathbf{M}\dot{\mathbf{t}} + \mathbf{W}\boldsymbol{\mu} = \mathbf{M}\dot{\mathbf{t}} + \mathbf{W}\mathbf{M}\mathbf{t} \tag{3.148}$$

The kinetic energy of a rigid body undergoing a motion in which its mass center moves with velocity $\dot{\mathbf{c}}$ and rotates with an angular velocity $\boldsymbol{\omega}$ is given by

$$T = \frac{1}{2}m\|\dot{\mathbf{c}}\|^2 + \frac{1}{2}\boldsymbol{\omega}^T\mathbf{I}_C\boldsymbol{\omega} \tag{3.149}$$

From the foregoing definitions, then, the kinetic energy can be written in compact form as

$$T = \frac{1}{2}\mathbf{t}^T\mathbf{M}\mathbf{t} \tag{3.150}$$

Finally, the Newton-Euler equations can be written in an even more compact form as

$$\dot{\boldsymbol{\mu}} = \mathbf{w} \tag{3.151}$$

which is a 6-dimensional vector equation.

This page intentionally left blank

4

Kinetostatics of Simple Robotic Manipulators

4.1 Introduction

This chapter is devoted to the *kinetostatics* of robotic manipulators of the serial type, i.e., to the kinematics and statics of these systems. The study is general, but with regard to what is called the *inverse kinematics problem*, we limit the chapter to *decoupled manipulators*, to be defined below. The inverse displacement analysis of general six-axis manipulators is addressed in Chapter 8.

More specifically, we will define a serial, n-axis manipulator. In connection with this manipulator, additionally, we will (i) introduce the *Denavit-Hartenberg notation* for the definition of *link frames* that uniquely determine the *architecture* and the *configuration*, or *posture*, of the manipulator at hand; (ii) define the *Cartesian* and *joint coordinates* of this manipulator; and (iii) introduce its *Jacobian matrix*.

Moreover, with regard to six-axis manipulators, we will (i) define *decoupled* manipulators and provide a procedure for the solution of their displacement inverse kinematics; (ii) formulate and solve the *velocity-resolution* problem, give simplified solutions for decoupled manipulators, and identify their *singularities*; (iii) define the *workspace* of a three-axis positioning manipulator and provide means to display it; (iv) formulate and solve the *acceleration-resolution* problem and give simplified solutions for decoupled manipulators; and (v) analyze manipulators statically, while giving simplified analyses for decoupled manipulators. While doing this, we will devote special attention to *planar manipulators*.

4.2 The Denavit-Hartenberg Notation

One of the first tasks of a robotics engineer is the kinematic modeling of a robotic manipulator. This task consists of devising a model that can be *unambiguously* (*i*) described to a control unit through a database and (*ii*) interpreted by other robotics engineers. The purpose of this task is to give manipulating instructions to a robot, regardless of the dynamics of the manipulated load and the robot itself. The simplest way of kinematically modeling a robotic manipulator is by means of the concept of *kinematic chain*. A kinematic chain is a set of *rigid bodies*, also called *links*, coupled by *kinematic pairs*. A kinematic pair is, then, the coupling of two rigid bodies so as to constrain their relative motion. We distinguish two basic types of kinematic pairs, namely, *upper* and *lower* kinematic pairs. An upper kinematic pair arises between rigid bodies when contact takes place along a line or at a point. This type of coupling occurs in cam-and-follower mechanisms, gear trains, and roller bearings, for example. A lower kinematic pair occurs when contact takes place along a surface common to the two bodies. Six different types of lower kinematic pairs can be distinguished (Hartenberg and Denavit, 1964; Angeles, 1982), but all these can be produced from two basic types, namely, the *rotating pair*, denoted by R and also called *revolute*, and the *sliding pair*, represented by P and also called *prismatic*.

The common surface along which contact takes place in a revolute pair is a circular cylinder, a typical example of this pair being the coupling through journal bearings. Thus, two rigid bodies coupled by a revolute can rotate relative to each other about the axis of the common cylinder, which is thus referred to as the *axis of the revolute*, but are prevented from undergoing relative translations as well as rotations about axes other than the cylinder axis. On the other hand, the common surface of contact between two rigid bodies coupled by a prismatic pair is a prism of arbitrary cross section, and hence, the two bodies coupled in this way are prevented from undergoing any relative rotation and can move only in a pure-translation motion along a direction parallel to the axis of the prism. As an example of this kinematic pair, one can cite the dovetail coupling. Note that whereas the revolute axis is a totally defined line in three-dimensional space, the prismatic pair has no defined axis; this pair has only a direction. That is, the prismatic pair does not have a particular location in space. Bodies coupled by a revolute and a prismatic pair are shown in Fig. 4.1.

Serial manipulators will be considered in this chapter, their associated kinematic chains thus being of the *simple* type, i.e., each and every link is coupled to at most two other links. A *simple kinematic chain* can be either closed or open. It is closed if each and every link is coupled to two other links, the chain then being called a *linkage*; it is open if it contains exactly two links, the end ones, that are coupled to only one other link. Thus, simple kinematic chains studied in this chapter are open, and in the particular robotics terminology, their first link is called the *manipulator base*, whereas their last link is termed the *end-effector (EE)*.

Thus, the kinematic chains associated with manipulators of the serial

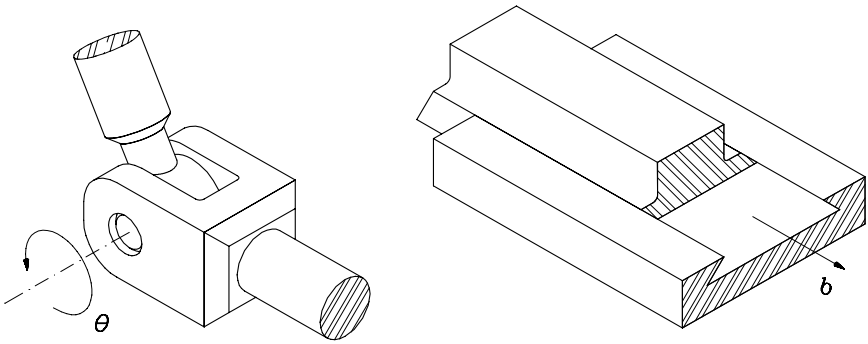

FIGURE 4.1. Revolute and prismatic pair.

type are composed of *binary links*, the intermediate ones, and exactly two *simple links*, those at the ends. Hence, except for the end links, all links carry two kinematic pairs, and as a consequence, two pair axes—however, notice that a prismatic pair has a direction but no axis. In order to uniquely describe the *architecture* of a kinematic chain, i.e., the relative location and orientation of its neighboring pair axes, the Denavit-Hartenberg nomenclature (Denavit and Hartenberg, 1955) is introduced. To this end, links are numbered 0, 1, ..., n, the ith pair being defined as that coupling the $(i-1)$st link with the ith link. Hence, the manipulator is assumed to be composed of $n+1$ links and n pairs; each of the latter can be either R or P, where link 0 is the fixed base, while link n is the end-effector. Next, a coordinate frame $\mathcal{F}_i$ is defined with origin O_i and axes X_i, Y_i, Z_i. This frame is attached to the $(i-1)$st link—**not** to the ith link!—for $i = 1, \ldots, n+1$. For the first n frames, this is done following the rules given below:

1. Z_i is the axis of the ith pair. Notice that there are two possibilities of defining the positive direction of this axis, since each pair axis is only a line, not a directed segment. Moreover, the Z_i axis of a prismatic

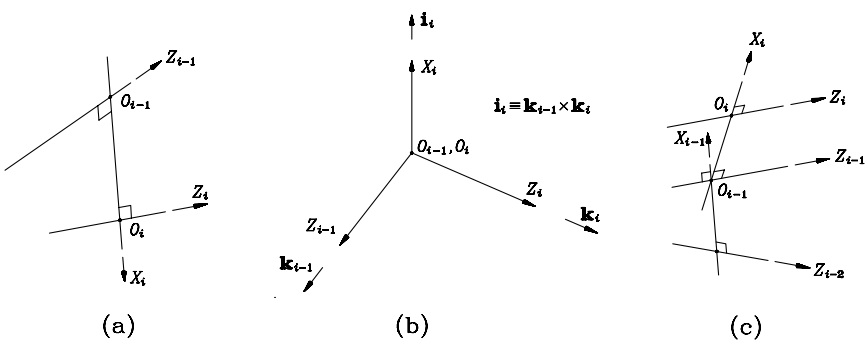

FIGURE 4.2. Definition of X_i when Z_{i-1} and Z_i: (a) are skew; (b) intersect; and (c) are parallel.

pair can be located arbitrarily, since only its direction is defined by the axis of this pair.

2. X_i is defined as the common perpendicular to Z_{i-1} and Z_i, directed from the former to the latter, as shown in Fig. 4.2a. Notice that if these two axes intersect, the positive direction of X_i is undefined and hence, can be freely assigned. Henceforth, we will follow the *right-hand* rule in this case. This means that if unit vectors $\mathbf{i}_i$, $\mathbf{k}_{i-1}$, and $\mathbf{k}_i$ are attached to axes X_i, Z_{i-1}, and Z_i, respectively, as indicated in Fig. 4.2b, then $\mathbf{i}_i$ is defined as $\mathbf{k}_{i-1} \times \mathbf{k}_i$. Moreover, if Z_{i-1} and Z_i are parallel, the location of X_i is undefined. In order to define it uniquely, we will specify X_i as passing through the origin of the $(i-1)$st frame, as shown in Fig. 4.2c.

3. The *distance* between Z_i and Z_{i+1} is defined as a_i, which is thus *nonnegative*.

4. The Z_i-coordinate of the intersection O_i' of Z_i with X_{i+1} is denoted by b_i. Since this quantity is a coordinate, it can be either positive or negative. Its absolute value is the distance between X_i and X_{i+1}, also called the *offset* between successive common perpendiculars.

5. The angle between Z_i and Z_{i+1} is defined as α_i and is measured about the positive direction of X_{i+1}. This item is known as the *twist angle* between successive pair axes.

6. The angle between X_i and X_{i+1} is defined as θ_i and is measured about the positive direction of Z_i.

The $(n+1)$st coordinate frame is attached to the far end of the nth link. Since the manipulator has no $(n+1)$st link, the foregoing rules do not apply to the definition of the last frame. The analyst, thus, has the freedom to define this frame as it best suits the task at hand. Notice that $n+1$ frames, $\mathcal{F}_1$, $\mathcal{F}_2$, ..., $\mathcal{F}_{n+1}$, have been defined, whereas links are numbered from 0 to n. In summary, an n-axis manipulator is composed of $n+1$ links and $n+1$ coordinate frames. These rules are illustrated with an example below.

Consider the architecture depicted in Fig. 4.3, usually referred to as a *Puma robot*, which shows seven links, numbered from 0 to 6, and seven coordinate frames, numbered from 1 to 7. Note that the last frame is arbitrarily defined, but its origin is placed at a specific point of the EE, namely, at the *operation point*, P, which is used to define the task at hand. Furthermore, three axes intersect at a point C, and hence, all points of the last three links move on concentric spheres with respect to C, for which reason the subchain comprising these three links is known as a *spherical wrist*, point C being its *center*. By the same token, the subchain composed of the first four links is called the *arm*. Thus, the wrist is *decoupled* from the arm, and is used for orientation purposes, the arm being used for the

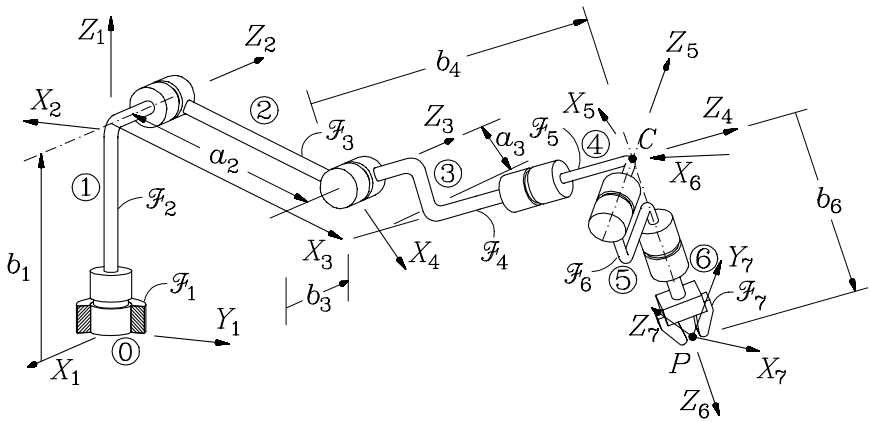

FIGURE 4.3. Coordinate frames of a Puma robot.

positioning of point C. The arm is sometimes called the *regional structure* and the wrist the *local structure*, the overall manipulator thus being of the *decoupled* type.

In the foregoing discussion, if the ith pair is R, then all quantities involved in those definitions are constant, except for θ_i, which is variable and is thus termed the *joint variable* of the ith pair. The other quantities, i.e., a_i, b_i, and α_i, are the *joint parameters* of the said pair. If, alternatively, the ith pair is P, then b_i is variable, and the other quantities are constant. In this case, the joint variable is b_i, and the joint parameters are a_i, α_i, and θ_i. Notice that associated with each joint there are exactly one joint variable and three constant parameters. Hence, an n-axis manipulator has n joint variables—which are henceforth grouped in the n-dimensional vector $\boldsymbol{\theta}$, regardless of whether the joint variables are angular or translational—and $3n$ constant parameters. The latter define the *architecture* of the manipulator, while the former determine its *configuration*, or *posture*.

Whereas the manipulator architecture is fully defined by its $3n$ *Denavit-Hartenberg (DH) parameters*, its posture is fully defined by its n joint variables, also called its *joint coordinates*, once the DH parameters are known. The relative position and orientation between links is fully specified, then, from the discussions of Chapter 2, by (i) the rotation matrix taking the X_i, Y_i, Z_i axes into a configuration in which they are parallel pairwise to the X_{i+1}, Y_{i+1}, Z_{i+1} axes, and (ii) the position vector of the origin of the latter in the former. The representations of the foregoing items in coordinate frame $\mathcal{F}_i$ will be discussed presently. First, we obtain the matrix representation of the rotation $\mathbf{Q}_i$ carrying $\mathcal{F}_i$ into an orientation coincident with that of $\mathcal{F}_{i+1}$, assuming, without loss of generality because we are interested only in changes of orientation, that the two origins are coincident, as depicted in Fig. 4.4. This matrix is most easily derived if the rotation of interest is decomposed into two rotations, as indicated in Fig. 4.5. In that figure, X_i', Y_i', Z_i' is an intermediate coordinate frame $\mathcal{F}_i'$, obtained by

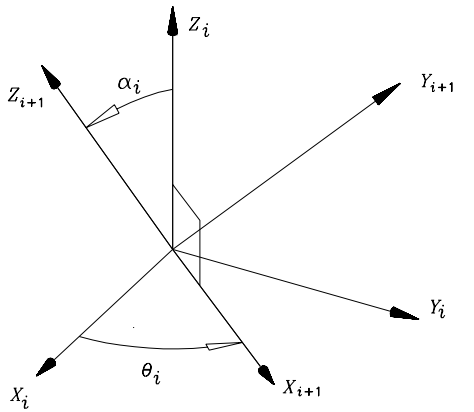

FIGURE 4.4. Relative orientation of the ith and $(i+1)$st coordinate frames.

rotating $\mathcal{F}_i$ about the Z_i axis through an angle θ_i. Then, the intermediate frame is rotated about $X_{i'}$ through an angle α_i, which takes it into a configuration coincident with $\mathcal{F}_{i+1}$. Let the foregoing rotations be denoted by $[\,\mathbf{C}_i\,]_i$ and $[\,\mathbf{\Lambda}_i\,]_{i'}$, respectively, which are readily derived for they are in the canonical forms (2.55c) and (2.55a), respectively.

Moreover, let

$$\lambda_i \equiv \cos\alpha_i, \quad \mu_i \equiv \sin\alpha_i \tag{4.1a}$$

One thus has, using subscripted brackets as introduced in Section 2.2,

$$[\,\mathbf{C}_i\,]_i = \begin{bmatrix} \cos\theta_i & -\sin\theta_i & 0 \\ \sin\theta_i & \cos\theta_i & 0 \\ 0 & 0 & 1 \end{bmatrix}, \quad [\,\mathbf{\Lambda}_i\,]_{i'} = \begin{bmatrix} 1 & 0 & 0 \\ 0 & \lambda_i & -\mu_i \\ 0 & \mu_i & \lambda_i \end{bmatrix} \tag{4.1b}$$

and clearly, the matrix sought is computed simply as

$$[\,\mathbf{Q}_i\,]_i = [\,\mathbf{C}_i\,]_i\,[\,\mathbf{\Lambda}_i\,]_{i'} \tag{4.1c}$$

Henceforth, we will use the abbreviations introduced below:

$$\mathbf{Q}_i \equiv [\,\mathbf{Q}_i\,]_i, \quad \mathbf{C}_i \equiv [\,\mathbf{C}_i\,]_i, \quad \mathbf{\Lambda}_i \equiv [\,\mathbf{\Lambda}_i\,]_{i'} \tag{4.1d}$$

thereby doing away with brackets, when these are self-evident. Thus,

$$\mathbf{Q}_i \equiv [\,\mathbf{Q}_i\,]_i \equiv \begin{bmatrix} \cos\theta_i & -\lambda_i\sin\theta_i & \mu_i\sin\theta_i \\ \sin\theta_i & \lambda_i\cos\theta_i & -\mu_i\cos\theta_i \\ 0 & \mu_i & \lambda_i \end{bmatrix} \tag{4.1e}$$

One more factoring of matrix $\mathbf{Q}_i$, which finds applications in manipulator kinematics, is given below:

$$\mathbf{Q}_i = \mathbf{Z}_i\mathbf{X}_i \tag{4.2a}$$

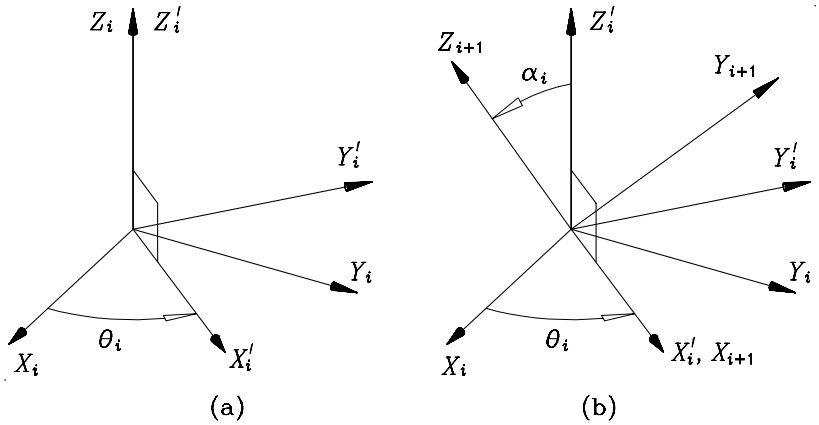

FIGURE 4.5. (a) Rotation about axis Z_i through an angle θ_i; and (b) relative orientation of the i'th and the $(i+1)$st coordinate frames.

with $\mathbf{X}_i$ and $\mathbf{Z}_i$ defined as two *pure reflections*, the former about the Y_iZ_i plane, the latter about the X_iY_i plane, namely,

$$\mathbf{X}_i \equiv \begin{bmatrix} 1 & 0 & 0 \\ 0 & -\lambda_i & \mu_i \\ 0 & \mu_i & \lambda_i \end{bmatrix}, \quad \mathbf{Z}_i \equiv \begin{bmatrix} \cos\theta_i & \sin\theta_i & 0 \\ \sin\theta_i & -\cos\theta_i & 0 \\ 0 & 0 & 1 \end{bmatrix} \tag{4.2b}$$

Note that both $\mathbf{X}_i$ and $\mathbf{Z}_i$ are symmetric and self-inverse—see Section 2.2. In order to derive an expression for the position vector $\mathbf{a}_i$ connecting the origin O_i of $\mathcal{F}_i$ with that of $\mathcal{F}_{i+1}$, O_{i+1}, reference is made to Fig. 4.6, showing the relative positions of the different origins and axes involved. From this figure, clearly,

$$\mathbf{a}_i \equiv \overrightarrow{O_iO}_{i+1} = \overrightarrow{O_iO}_{i'} + \overrightarrow{O_{i'}O}_{i+1} \tag{4.3a}$$

where obviously,

$$[\,\overrightarrow{O_iO}_{i'}\,]_i = \begin{bmatrix} 0 \\ 0 \\ b_i \end{bmatrix}, \quad [\,\overrightarrow{O_{i'}O}_{i+1}\,]_{i+1} = \begin{bmatrix} a_i \\ 0 \\ 0 \end{bmatrix}$$

Now, in order to compute the sum appearing in eq.(4.3a), the two foregoing vectors should be expressed in the same coordinate frame, namely, $\mathcal{F}_i$. Thus,

$$[\,\overrightarrow{O_{i'}O}_{i+1}\,]_i = [\,\mathbf{Q}_i\,]_i\,[\,\overrightarrow{O_{i'}O}_{i+1}\,]_{i+1} = \begin{bmatrix} a_i\cos\theta_i \\ a_i\sin\theta_i \\ 0 \end{bmatrix}$$

and hence,

$$[\,\mathbf{a}_i\,]_i = \begin{bmatrix} a_i \cos\theta_i \\ a_i \sin\theta_i \\ b_i \end{bmatrix} \tag{4.3b}$$

For brevity, we introduce the following definition:

$$\mathbf{a}_i \equiv [\,\mathbf{a}_i\,]_i \tag{4.3c}$$

Similar to the foregoing factoring of $\mathbf{Q}_i$, vector $\mathbf{a}_i$ admits the factoring

$$\mathbf{a}_i = \mathbf{Q}_i \mathbf{b}_i \tag{4.3d}$$

where $\mathbf{b}_i$ is given by

$$\mathbf{b}_i \equiv \begin{bmatrix} a_i \\ b_i \mu_i \\ b_i \lambda_i \end{bmatrix} \tag{4.3e}$$

with the definitions introduced in eq.(4.1a). Hence, vector $\mathbf{b}_i$ is constant for revolute pairs. From the geometry of Fig. 4.6, it should be apparent that $\mathbf{b}_i$ is nothing but $\mathbf{a}_i$ in $\mathcal{F}_{i+1}$, i.e.,

$$\mathbf{b}_i = [\mathbf{a}_i]_{i+1} \ .$$

Matrices $\mathbf{Q}_i$ can also be regarded as coordinate transformations. Indeed, let $\mathbf{i}_i$, $\mathbf{j}_i$, and $\mathbf{k}_i$ be the unit vectors parallel to the X_i, Y_i, and Z_i axes, respectively, directed in the positive direction of these axes. From Fig. 4.6, it is apparent that

$$[\,\mathbf{i}_{i+1}\,]_i = \begin{bmatrix} \cos\theta_i \\ \sin\theta_i \\ 0 \end{bmatrix}, \quad [\,\mathbf{k}_{i+1}\,]_i = \begin{bmatrix} \mu_i \sin\theta_i \\ -\mu \cos\theta_i \\ \lambda_i \end{bmatrix}$$

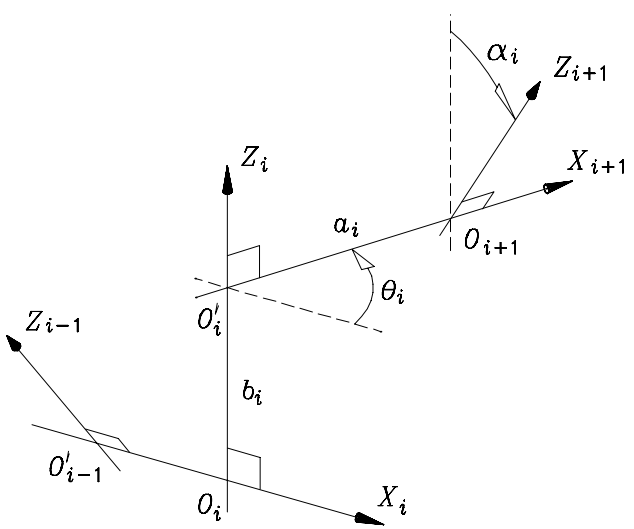

FIGURE 4.6. Layout of three successive coordinate frames.

whence

$$[\,\mathbf{j}_{i+1}\,]_i = [\,\mathbf{k}_{i+1} \times \mathbf{i}_{i+1}\,]_i = \begin{bmatrix} -\lambda_i \sin\theta_i \\ \lambda_i \cos\theta_i \\ \mu_i \end{bmatrix}$$

Therefore, the components of $\mathbf{i}_{i+1}$, $\mathbf{j}_{i+1}$, and $\mathbf{k}_{i+1}$ in $\mathcal{F}_i$ are nothing but the first, second, and third columns of $\mathbf{Q}_i$. In general, then, any vector $\mathbf{v}$ in $\mathcal{F}_{i+1}$ is transformed into $\mathcal{F}_i$ in the form

$$[\,\mathbf{v}\,]_i = [\,\mathbf{Q}_i\,]_i [\,\mathbf{v}\,]_{i+1}$$

which is a similarity transformation, as defined in eq.(2.117). Likewise, any matrix $\mathbf{M}$ in $\mathcal{F}_{i+1}$ is transformed into $\mathcal{F}_i$ by the corresponding similarity transformation, as given by eq.(2.128):

$$[\,\mathbf{M}\,]_i = [\,\mathbf{Q}_i\,]_i [\,\mathbf{M}\,]_{i+1} [\,\mathbf{Q}_i^T\,]_i$$

The inverse relations follow immediately in the form

$$[\,\mathbf{v}\,]_{i+1} = [\,\mathbf{Q}_i^T\,]_i [\,\mathbf{v}\,]_i, \quad [\,\mathbf{M}\,]_{i+1} = [\,\mathbf{Q}_i^T\,]_i [\,\mathbf{M}\,]_i [\,\mathbf{Q}_i\,]_i$$

or upon recalling the first of definitions (4.1d),

$$[\,\mathbf{v}\,]_i = \mathbf{Q}_i [\,\mathbf{v}\,]_{i+1}, \quad [\,\mathbf{M}\,]_i = \mathbf{Q}_i [\,\mathbf{M}\,]_{i+1} \mathbf{Q}_i^T \tag{4.4a}$$

$$[\,\mathbf{v}\,]_{i+1} = \mathbf{Q}_i^T [\,\mathbf{v}\,]_i, \quad [\,\mathbf{M}\,]_{i+1} = \mathbf{Q}_i^T [\,\mathbf{M}\,]_i \mathbf{Q}_i \tag{4.4b}$$

Moreover, if we have a chain of i frames, $\mathcal{F}_1$, $\mathcal{F}_2$, ..., $\mathcal{F}_i$, then the *inward* coordinate transformation from $\mathcal{F}_i$ to $\mathcal{F}_1$ is given by

$$[\,\mathbf{v}\,]_1 = \mathbf{Q}_1 \mathbf{Q}_2 \cdots \mathbf{Q}_{i-1} [\,\mathbf{v}\,]_i \tag{4.5a}$$

$$[\,\mathbf{M}\,]_1 = \mathbf{Q}_1 \mathbf{Q}_2 \cdots \mathbf{Q}_{i-1} [\,\mathbf{M}\,]_i (\mathbf{Q}_1 \mathbf{Q}_2 \cdots \mathbf{Q}_{i-1})^T \tag{4.5b}$$

Likewise, the outward coordinate transformation takes the form

$$[\,\mathbf{v}\,]_i = (\mathbf{Q}_1 \mathbf{Q}_2 \cdots \mathbf{Q}_{i-1})^T [\,\mathbf{v}\,]_1 \tag{4.6a}$$

$$[\,\mathbf{M}\,]_i = (\mathbf{Q}_1 \mathbf{Q}_2 \cdots \mathbf{Q}_{i-1})^T [\,\mathbf{M}\,]_1 \mathbf{Q}_1 \mathbf{Q}_2 \cdots \mathbf{Q}_{i-1} \tag{4.6b}$$

4.3 The Kinematics of Six-Revolute Manipulators

The kinematics of serial manipulators comprises the study of the relations between *joint variables* and *Cartesian variables*. The former were defined in Section 4.2 as those determining the posture of a given manipulator, with one such variable per joint; a six-axis manipulator, like the one displayed in Fig. 4.7, thus has six joint variables, θ_1, θ_2, ..., θ_6. The Cartesian variables of a manipulator, in turn, are those variables defining the pose of the EE;

since six independent variables are needed to define the pose of a rigid body, the manipulator of Fig. 4.7 thus contains six Cartesian variables.

The study outlined above pertains to the *geometry* of the manipulator, for it involves one single pose of the EE. Besides geometry, the kinematics of manipulators comprises the study of the relations between the time-rates of change of the joint variables, referred to as the *joint rates*, and the twist of the EE. Additionally, the relations between the second time-derivatives of the joint variables, referred to as the *joint accelerations*, with the time-rate of change of the twist of the EE are also studied in this chapter.

In this section and in Section 4.4 we study the geometry of manipulators. In this regard, we distinguish two problems, commonly referred to as the *direct* and the *inverse* kinematic problems, or DKP and correspondingly, IKP, for brevity. In the DKP, the six joint variables of a given six-axis manipulator are assumed to be known, the problem consisting of finding the pose of the EE. In the IKP, on the contrary, the pose of the EE is given, while the six joint variables that produce this pose are to be found.

The DKP reduces to matrix multiplications, and as we shall show presently, poses no major problem. The IKP, however, is more challenging, for it involves intensive variable-elimination and nonlinear-equation solving. Indeed, in the most general case, the IKP amounts to eliminating five out of the six unknowns, with the aim of reducing the problem to a single monovariate polynomial of up to 16th degree. While finding the roots of a polynomial of this degree is no longer an insurmountable task, reducing the underlying system of nonlinear equations to a monovariate polynomial requires intensive computer-algebra work that must be very carefully planned to avoid the introduction of spurious roots and, with this, an increase in the degree of that polynomial. For this reason, we limit this chapter to the study of the geometric IKP of *decoupled* six-axis manipulators, to be defined presently. The IKP of the most general six-revolute serial manipulator is studied in Chapter 8.

In studying the DKP of six-axis manipulators, we need not limit ourselves to a particular architecture. We thus study here the DKP of general manipulators, such as the one sketched in Fig. 4.7. This manipulator consists of seven rigid bodies, or links, coupled by six revolute joints. Correspondingly, we have seven frames, $\mathcal{F}_1$, $\mathcal{F}_2$, ..., $\mathcal{F}_7$, the ith frame fixed to the $(i-1)$st link, $\mathcal{F}_1$ being termed the *base frame*, because it is fixed to the base of the manipulator. Manipulators with joints of the prismatic type are simpler to study and can be treated using correspondingly simpler procedures.

A line $\mathcal{L}_i$ is associated with the axis of the ith revolute joint, and a positive direction along this line is defined arbitrarily through a unit vector $\mathbf{e}_i$. For a prismatic pair, a line $\mathcal{L}_i$ can be also defined, as a line having the direction of the pair but whose location is undefined; the analyst, then, has the freedom to locate this axis conveniently. Thus, a rotation of the ith link with respect to the $(i-1)$st link or correspondingly, of $\mathcal{F}_{i+1}$ with respect to $\mathcal{F}_i$, is totally defined by the geometry of the said link, i.e., by the DH parameters a_i, b_i, and α_i, plus $\mathbf{e}_i$ and its associated joint variable θ_i. Then, the DH parameters and the joint variables define uniquely the posture of

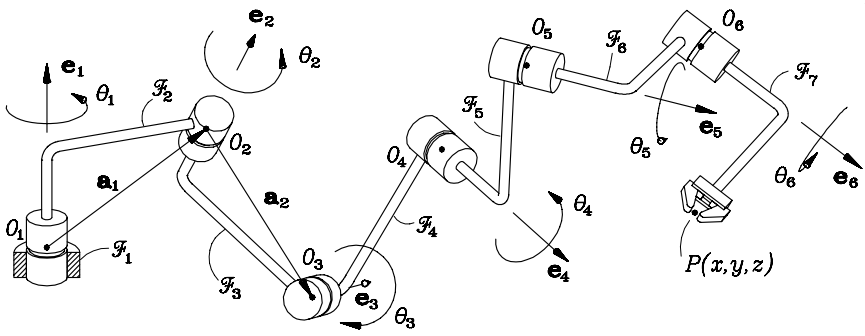

FIGURE 4.7. Serial six-axis manipulator.

the manipulator. In particular, the relative position and orientation of $\mathcal{F}_{i+1}$ with respect to $\mathcal{F}_i$ is given by matrix $\mathbf{Q}_i$ and vector $\mathbf{a}_i$, respectively, which were defined in Section 4.2 and are displayed below for quick reference:

$$\mathbf{Q}_i = \begin{bmatrix} \cos\theta_i & -\lambda_i \sin\theta_i & \mu_i \sin\theta_i \\ \sin\theta_i & \lambda_i \cos\theta_i & -\mu_i \cos\theta_i \\ 0 & \mu_i & \lambda_i \end{bmatrix}, \quad \mathbf{a}_i = \begin{bmatrix} a_i \cos\theta_i \\ a_i \sin\theta_i \\ b_i \end{bmatrix} \tag{4.7}$$

Thus, $\mathbf{Q}_i$ and $\mathbf{a}_i$ denote, respectively, the matrix rotating $\mathcal{F}_i$ into an orientation coincident with that of $\mathcal{F}_{i+1}$ and the vector joining the origin of $\mathcal{F}_i$ with that of $\mathcal{F}_{i+1}$, directed from the former to the latter. Moreover, $\mathbf{Q}_i$ and $\mathbf{a}_i$, as given in eq.(4.7), are represented in $\mathcal{F}_i$ coordinates. The equations leading to the kinematic model under study are known as the *kinematic displacement equations*. It is noteworthy that the problem under study is equivalent to the *input-output analysis problem* of a seven-revolute linkage with one degree of freedom and one single kinematic loop (Duffy, 1980). Because of this equivalence with a *closed kinematic chain*, sometimes the displacement equations are also termed *closure equations*. These equations relate the orientation of the EE, as produced by the joint coordinates, with the prescribed orientation $\mathbf{Q}$ and the position vector $\mathbf{p}$ of the *operation point* P of the EE. That is, the orientation $\mathbf{Q}$ of the EE is obtained as a result of the six individual rotations $\{\,\mathbf{Q}_i\,\}_1^6$ about each revolute axis through an angle θ_i, in a *sequential order*, from 1 to 6. If, for example, the foregoing relations are expressed in $\mathcal{F}_1$, then

$$[\,\mathbf{Q}_6\,]_1[\,\mathbf{Q}_5\,]_1[\,\mathbf{Q}_4\,]_1[\,\mathbf{Q}_3\,]_1[\,\mathbf{Q}_2\,]_1[\,\mathbf{Q}_1\,]_1 = [\,\mathbf{Q}\,]_1 \tag{4.8a}$$

$$[\,\mathbf{a}_1\,]_1 + [\,\mathbf{a}_2\,]_1 + [\,\mathbf{a}_3\,]_1 + [\,\mathbf{a}_4\,]_1 + [\,\mathbf{a}_5\,]_1 + [\,\mathbf{a}_6\,]_1 = [\,\mathbf{p}\,]_1 \tag{4.8b}$$

Notice that the above equations require that all vectors and matrices involved be expressed *in the same coordinate frame*. However, we derived in Section 4.2 general expressions for $\mathbf{Q}_i$ and $\mathbf{a}_i$ in $\mathcal{F}_i$, eqs.(4.1e) and (4.3b),

respectively. It is hence convenient to represent the foregoing relations in each individual frame, which can be readily done by means of similarity transformations. Indeed, if we apply the transformations (4.5a & b) to each of $[\,\mathbf{a}_i\,]_1$ and $[\,\mathbf{Q}_i\,]_1$, respectively, we obtain $\mathbf{a}_i$ or correspondingly, $\mathbf{Q}_i$, in $\mathcal{F}_i$. Therefore, eq.(4.8a) becomes

$$[\,\mathbf{Q}_1\,]_1[\,\mathbf{Q}_2\,]_2[\,\mathbf{Q}_3\,]_3[\,\mathbf{Q}_4\,]_4[\,\mathbf{Q}_5\,]_5[\,\mathbf{Q}_6\,]_6 = [\,\mathbf{Q}\,]_1$$

Now for compactness, let us represent $[\,\mathbf{Q}\,]_1$ simply by $\mathbf{Q}$ and let us recall the abbreviated notation introduced in eq.(4.1d), whereby $[\,\mathbf{Q}_i\,]_i$ is denoted simply by $\mathbf{Q}_i$, thereby obtaining

$$\mathbf{Q}_1\mathbf{Q}_2\mathbf{Q}_3\mathbf{Q}_4\mathbf{Q}_5\mathbf{Q}_6 = \mathbf{Q} \tag{4.9a}$$

Likewise, eq.(4.8b) becomes

$$\mathbf{a}_1 + \mathbf{Q}_1(\mathbf{a}_2 + \mathbf{Q}_2\mathbf{a}_3 + \mathbf{Q}_2\mathbf{Q}_3\mathbf{a}_4 + \mathbf{Q}_2\mathbf{Q}_3\mathbf{Q}_4\mathbf{a}_5 + \mathbf{Q}_2\mathbf{Q}_3\mathbf{Q}_4\mathbf{Q}_5\mathbf{a}_6) = \mathbf{p} \tag{4.9b}$$

in which both sides are given in base-frame coordinates. Equations (4.9a & b) above can be cast in a more compact form if homogeneous transformations, as defined in Section 2.5, are now introduced. Thus, if we let $\mathbf{T}_i \equiv \{\,\mathbf{T}_i\,\}_i$ be the 4×4 matrix transforming $\mathcal{F}_{i+1}$-coordinates into $\mathcal{F}_i$-coordinates, the foregoing equations can be written in 4×4 matrix form, namely,

$$\mathbf{T}_1\mathbf{T}_2\mathbf{T}_3\mathbf{T}_4\mathbf{T}_5\mathbf{T}_6 = \mathbf{T} \tag{4.10}$$

with $\mathbf{T}$ denoting the transformation of coordinates from the end-effector frame to the base frame. Thus, $\mathbf{T}$ contains the pose of the end-effector.

In order to ease the discussion ahead, we introduce now a few definitions. A scalar, vector, or matrix expression is said to be *multilinear* in a set of vectors $\{\,\mathbf{v}_i\}_1^N$ if those vectors appear only linearly in the same expression. This does not prevent products of components of those vectors from occurring, as long as each product contains only one component of the same vector. Alternatively, we can say that the expression of interest is multilinear in the aforementioned set of vectors if and only if the partial derivative of that expression with respect to vector $\mathbf{v}_i$ is independent of $\mathbf{v}_i$, for $i = 1, \ldots, N$. For example, every matrix $\mathbf{Q}_i$ and every vector $\mathbf{a}_i$, defined in eqs.(4.1e) and (4.3b), respectively, is linear in vector $\mathbf{x}_i$, where $\mathbf{x}_i$ is defined as

$$\mathbf{x}_i \equiv \begin{bmatrix} \cos\theta_i \\ \sin\theta_i \end{bmatrix} \tag{4.11}$$

Moreover, the product $\mathbf{Q}_1\mathbf{Q}_2\mathbf{Q}_3\mathbf{Q}_4\mathbf{Q}_5\mathbf{Q}_6$ appearing in eq.(4.9a) is *hexalinear*, or simply, *multilinear*, in vectors $\{\,\mathbf{x}_i\,\}_1^6$. Likewise, the sum appearing in eq.(4.9b) is multilinear in the same set of vectors. By the same token, a scalar, vector, or matrix expression is said to be *multiquadratic* in the same set of vectors if those vectors appear at most quadratically in the

said expression. That is, the expression of interest may contain products of the components of all those vectors, as long as those products contain, in turn, a maximum of two components of the same vector, including the same component squared. Qualifiers like *multicubic*, *multiquartic*, etc., bear similar meanings.

Further, we partition matrix $\mathbf{Q}_i$ rowwise and columnwise, namely,

$$\mathbf{Q}_i \equiv \begin{bmatrix} \mathbf{m}_i^T \\ \mathbf{n}_i^T \\ \mathbf{o}_i^T \end{bmatrix} \equiv [\, \mathbf{p}_i \quad \mathbf{q}_i \quad \mathbf{u}_i \,] \tag{4.12}$$

It is pointed out that the third row of $\mathbf{Q}_i$, $\mathbf{o}_i^T$, is independent of θ_i, a fact that will be found useful in the forthcoming derivations. Furthermore, note that according to the DH notation, the unit vector $\mathbf{e}_i$ in the direction of the ith joint axis in Fig. 4.7 has $\mathcal{F}_i$-components given by

$$[\, \mathbf{e}_i \,]_i = \begin{bmatrix} 0 \\ 0 \\ 1 \end{bmatrix} \equiv \mathbf{e} \tag{4.13}$$

Henceforth, $\mathbf{e}$ is used to represent a 3-dimensional array with its last component equal to unity, its other components vanishing. Thus, we have

$$\mathbf{Q}_i \mathbf{o}_i \equiv \mathbf{Q}_i^T \mathbf{u}_i = \mathbf{e} \tag{4.14a}$$

or

$$\mathbf{u}_i = \mathbf{Q}_i \mathbf{e}, \quad \mathbf{o}_i = \mathbf{Q}_i^T \mathbf{e} \tag{4.14b}$$

That is, if we regard $\mathbf{e}$ in the first of the foregoing relations as $[\, \mathbf{e}_{i+1} \,]_{i+1}$, and as $[\, \mathbf{e}_i \,]_i$ in the second relation, then, from the coordinate transformations of eqs.(4.4a & b),

$$\mathbf{u}_i = [\, \mathbf{e}_{i+1} \,]_i, \quad \text{and} \quad \mathbf{o}_i = [\, \mathbf{e}_i \,]_{i+1} \tag{4.15}$$

4.4 The IKP of Decoupled Manipulators

Industrial manipulators are frequently supplied with a special architecture that allows a decoupling of the positioning problem from the orientation problem. In fact, a determinant design criterion in this regard has been that the manipulator be kinematically invertible, i.e., that it lend itself to a closed-form inverse kinematics solution. Although the class of manipulators with this feature is quite broad, we will focus on a special kind, the most frequently encountered in commercial manipulators, that we will term *decoupled*. Decoupled manipulators were defined in Section 4.2 as those whose last three joints have intersecting axes. These joints, then, constitute the *wrist* of the manipulator, which is said to be *spherical*, because when the

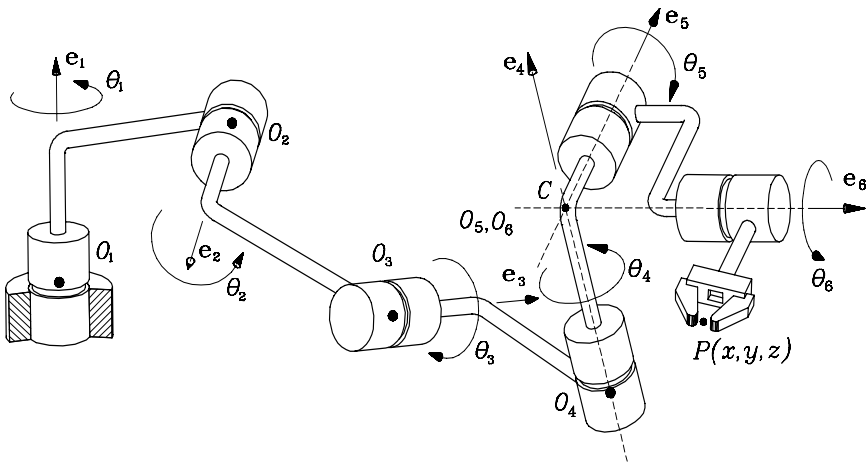

FIGURE 4.8. A general 6R manipulator with decoupled architecture.

point of intersection of the three wrist axes, C, is kept fixed, all the points of the wrist move on spheres centered at C. In terms of the DH parameters of the manipulator, in a decoupled manipulator $a_4 = a_5 = b_5 = 0$, and thus, the origins of frames 5 and 6 are coincident. All other DH parameters can assume arbitrary values. A general decoupled manipulator is shown in Fig. 4.8, where the wrist is represented as a concatenation of three revolutes with intersecting axes.

In the two subsections below, a procedure is derived for determining all the inverse kinematics solutions of decoupled manipulators. In view of the decoupled architecture of these manipulators, we study their inverse kinematics by decoupling the positioning problem from the orientation problem.

4.4.1 The Positioning Problem

The inverse kinematics of the robotic manipulators under study begins by *decoupling* the positioning and orientation problems. Moreover, we must solve first the positioning problem, which is done in this subsection.

Let C denote the intersection of axes 4, 5, and 6, i.e., the center of the spherical wrist, and let $\mathbf{c}$ denote the position vector of this point. Clearly, the position of C is independent of joint angles θ_4, θ_5, and θ_6; hence, only the first three joints are to be considered for this analysis. The arm structure depicted in Fig. 4.9 will then be analyzed. From that figure,

$$\mathbf{a}_1 + \mathbf{Q}_1\mathbf{a}_2 + \mathbf{Q}_1\mathbf{Q}_2\mathbf{a}_3 + \mathbf{Q}_1\mathbf{Q}_2\mathbf{Q}_3\mathbf{a}_4 = \mathbf{c} \tag{4.16}$$

where the two sides are expressed in $\mathcal{F}_1$-coordinates. This equation can be readily rewritten in the form

$$\mathbf{a}_2 + \mathbf{Q}_2\mathbf{a}_3 + \mathbf{Q}_2\mathbf{Q}_3\mathbf{a}_4 = \mathbf{Q}_1^T(\mathbf{c} - \mathbf{a}_1)$$

or if we recall eq.(4.3d),

$$\mathbf{Q}_2(\mathbf{b}_2 + \mathbf{Q}_3\mathbf{b}_3 + \mathbf{Q}_3\mathbf{Q}_4\mathbf{b}_4) = \mathbf{Q}_1^T\mathbf{c} - \mathbf{b}_1$$

However, since we are dealing with a decoupled manipulator, we have

$$\mathbf{a}_4 \equiv \mathbf{Q}_4\mathbf{b}_4 \equiv \begin{bmatrix} 0 \\ 0 \\ b_4 \end{bmatrix} \equiv b_4\mathbf{e}$$

which has been rewritten as the product of constant b_4 times the unit vector $\mathbf{e}$ defined in eq.(4.13).

Thus, the product $\mathbf{Q}_3\mathbf{Q}_4\mathbf{b}_4$ reduces to

$$\mathbf{Q}_3\mathbf{Q}_4\mathbf{b}_4 \equiv b_4\mathbf{Q}_3\mathbf{e} \equiv b_4\mathbf{u}_3$$

with $\mathbf{u}_i$ defined in eq.(4.14b). Hence, eq.(4.16) leads to

$$\mathbf{Q}_2(\mathbf{b}_2 + \mathbf{Q}_3\mathbf{b}_3 + b_4\mathbf{u}_3) = \mathbf{Q}_1^T\mathbf{c} - \mathbf{b}_1 \tag{4.17}$$

Further, an expression for $\mathbf{c}$ can be derived in terms of $\mathbf{p}$, the position vector of the operation point of the EE, and $\mathbf{Q}$, namely,

$$\mathbf{c} = \mathbf{p} - \mathbf{Q}_1\mathbf{Q}_2\mathbf{Q}_3\mathbf{Q}_4\mathbf{a}_5 - \mathbf{Q}_1\mathbf{Q}_2\mathbf{Q}_3\mathbf{Q}_4\mathbf{Q}_5\mathbf{a}_6 \tag{4.18a}$$

Now, since $a_5 = b_5 = 0$, we have that $\mathbf{a}_5 = \mathbf{0}$, eq.(4.18a) thus yielding

$$\mathbf{c} = \mathbf{p} - \mathbf{Q}\mathbf{Q}_6^T\mathbf{a}_6 \equiv \mathbf{p} - \mathbf{Q}\mathbf{b}_6 \tag{4.18b}$$

Moreover, the base coordinates of P and C, and hence, the $\mathcal{F}_1$-components of their position vectors $\mathbf{p}$ and $\mathbf{c}$, are defined as

$$[\,\mathbf{p}\,]_1 = \begin{bmatrix} x \\ y \\ z \end{bmatrix}, \quad [\,\mathbf{c}\,]_1 = \begin{bmatrix} x_C \\ y_C \\ z_C \end{bmatrix}$$

so that eq.(4.18b) can be expanded in the form

$$\begin{bmatrix} x_C \\ y_C \\ z_C \end{bmatrix} = \begin{bmatrix} x - (q_{11}a_6 + q_{12}b_6\mu_6 + q_{13}b_6\lambda_6) \\ y - (q_{21}a_6 + q_{22}b_6\mu_6 + q_{23}b_6\lambda_6) \\ z - (q_{31}a_6 + q_{32}b_6\mu_6 + q_{33}b_6\lambda_6) \end{bmatrix} \tag{4.18c}$$

where q_{ij} is the (i, j) entry of $[\mathbf{Q}]_1$, and the positioning problem now becomes one of finding the first three joint angles necessary to position point C at a point of base coordinates x_C, y_C, and z_C. We thus have three unknowns, but we also have three equations at our disposal, namely, the three scalar equations of eq.(4.17), and we should be able to solve the problem at hand.

In solving the foregoing system of equations, we first note that (i) the left-hand side of eq.(4.17) appears multiplied by $\mathbf{Q}_2$; and (ii) θ_2 does not appear in the right-hand side. This implies that (i) if the Euclidean norms

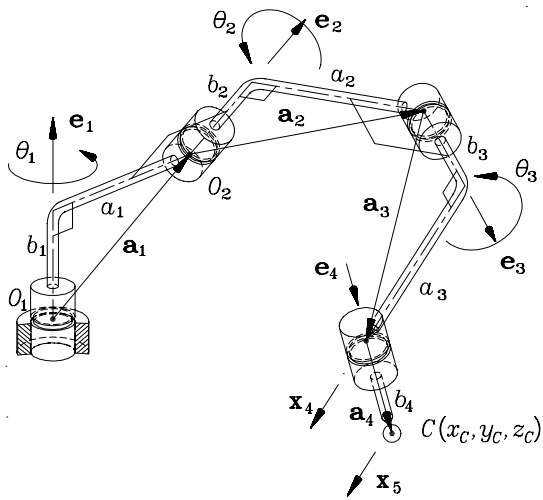

FIGURE 4.9. Three-axis, serial, positioning manipulator.

of the two sides of that equation are equated, the resulting equation will not contain θ_2; and (*ii*) the third scalar equation of the same equation is independent of θ_2, by virtue of the structure of the $\mathbf{Q}_i$ matrices displayed in eq.(4.1e). Thus, we have two equations free of θ_2, which allows us to calculate the two remaining unknowns θ_1 and θ_3.

Let the Euclidean norm of the left-hand side of eq.(4.17) be denoted by l, that of its right-hand side by r. We then have

$$l^2 \equiv a_2^2 + b_2^2 + a_3^2 + b_3^2 + b_4^2 + 2\mathbf{b}_2^T\mathbf{Q}_3\mathbf{b}_3 + 2b_4\mathbf{b}_2^T\mathbf{u}_3 + 2\lambda_3 b_3 b_4$$
$$r^2 \equiv \|\mathbf{c}\|^2 + \|\mathbf{b}_1\|^2 - 2\mathbf{b}_1^T\mathbf{Q}_1^T\mathbf{c}$$

from which it is apparent that l^2 is linear in $\mathbf{x}_3$ and r^2 is linear in $\mathbf{x}_1$, for $\mathbf{x}_i$ defined in eq.(4.11). Upon equating l^2 with r^2, then, an equation linear in $\mathbf{x}_1$ and $\mathbf{x}_3$—not bilinear in these vectors—is readily derived, namely,

$$Ac_1 + Bs_1 + Cc_3 + Ds_3 + E = 0 \tag{4.19a}$$

whose coefficients do not contain any unknown, i.e.,

$$A = 2a_1x_C \tag{4.19b}$$
$$B = 2a_1y_C \tag{4.19c}$$
$$C = 2a_2a_3 - 2b_2b_4\mu_2\mu_3 \tag{4.19d}$$
$$D = 2a_3b_2\mu_2 + 2a_2b_4\mu_3 \tag{4.19e}$$
$$E = a_2^2 + a_3^2 + b_2^2 + b_3^2 + b_4^2 - a_1^2 - x_C^2 - y_C^2 - (z_C - b_1)^2 + 2b_2b_3\lambda_2 + 2b_2b_4\lambda_2\lambda_3 + 2b_3b_4\lambda_3 \tag{4.19f}$$

Moreover, the third scalar equation of eq.(4.17) takes on the form

$$Fc_1 + Gs_1 + Hc_3 + Is_3 + J = 0 \tag{4.20a}$$

whose coefficients, again, do not contain any unknown, as shown below:

$$F = y_C\mu_1 \tag{4.20b}$$
$$G = -x_C\mu_1 \tag{4.20c}$$
$$H = -b_4\mu_2\mu_3 \tag{4.20d}$$
$$I = a_3\mu_2 \tag{4.20e}$$
$$J = b_2 + b_3\lambda_2 + b_4\lambda_2\lambda_3 - (z_C - b_1)\lambda_1 \tag{4.20f}$$

Thus, we have derived two nonlinear equations in θ_1 and θ_3 that are linear in c_1, s_1, c_3, and s_3. Each of these equations thus defines a contour in the θ_1-θ_3 plane, their intersections determining all real solutions to the problem at hand.

Note that if c_i and s_i are substituted for their equivalents in terms of $\tan(\theta_i/2)$, for $i = 1, 3$, then two biquadratic polynomial equations in $\tan(\theta_1/2)$ and $\tan(\theta_3/2)$ are derived. Thus, one can eliminate one of these variables from the foregoing equations, thereby reducing the two equations to a single quartic polynomial equation in the other variable. The quartic equation thus resulting is called the *characteristic equation* of the problem at hand. Alternatively, the two above equations, eqs.(4.19a) and (4.20a), can be solved for, say, c_1 and s_1 in terms of the data and c_3 and s_3, namely,

$$c_1 = \frac{-G(Cc_3 + Ds_3 + E) + B(Hc_3 + Is_3 + J)}{\Delta_1} \tag{4.21a}$$
$$s_1 = \frac{F(Cc_3 + Ds_3 + E) - A(Hc_3 + Is_3 + J)}{\Delta_1} \tag{4.21b}$$

with Δ_1 defined as

$$\Delta_1 = AG - FB = -2a_1\mu_1(x_C^2 + y_C^2) \tag{4.21c}$$

Note that in trajectory planning, to be studied in Chapter 5, Δ_1 can be computed *off-line*, i.e., prior to setting the manipulator into operation, for it is a function solely of the manipulator parameters and the Cartesian coordinates of a point lying on the path to be tracked. Moreover, the above calculations are possible as long as Δ_1 does not vanish. Now, Δ_1 vanishes if and only if any of the factors a_1, μ_1, and $x_C^2 + y_C^2$ does. The first two conditions are architecture-dependent, whereas the third is position-dependent. The former occur frequently in industrial manipulators, although not both at the same time. If both parameters a_1 and μ_1 vanished, then the arm would be useless to position arbitrarily a point in space. The third condition, i.e., the vanishing of $x_C^2 + y_C^2$, means that point C lies on the Z_1 axis. Now, even if neither a_1 nor μ_1 vanishes, the manipulator can be positioned

in a configuration at which point C lies on the Z_1 axis. Such a configuration is termed the *first singularity*. Note, however, that with point C being located on the Z_1 axis, any motion of the first joint, with the two other joints locked, does not change the location of C. For the moment, it will be assumed that Δ_1 does not vanish, the particular cases under which it does being studied later. Next, both sides of eqs.(4.21a & b) are squared, the squares thus obtained are then added, and the sum is equated to 1, which leads to a quadratic equation in $\mathbf{x}_3$, namely,

$$Kc_3^2 + Ls_3^2 + Mc_3s_3 + Nc_3 + Ps_3 + Q = 0 \tag{4.22}$$

whose coefficients, after simplification, are given below:

$$K = 4a_1^2H^2 + \mu_1^2C^2 \tag{4.23a}$$
$$L = 4a_1^2I^2 + \mu_1^2D^2 \tag{4.23b}$$
$$M = 2(4a_1^2HI + \mu_1^2CD) \tag{4.23c}$$
$$N = 2(4a_1^2HJ + \mu_1^2CE) \tag{4.23d}$$
$$P = 2(4a_1^2IJ + \mu_1^2DE) \tag{4.23e}$$
$$Q = 4a_1^2J^2 + \mu_1^2E^2 - 4a_1^2\mu_1^2\rho^2 \tag{4.23f}$$

with ρ^2 defined as

$$\rho^2 \equiv x_C^2 + y_C^2$$

Now, two well-known trigonometric identities are introduced, namely,

$$c_3 \equiv \frac{1-\tau_3^2}{1+\tau_3^2},\ s_3 \equiv \frac{2\tau_3}{1+\tau_3^2},\ \text{where } \tau_3 \equiv \tan(\frac{\theta_3}{2}) \tag{4.24}$$

Henceforth, the foregoing identities will be referred to as the *tan-half-angle identities*. We will be resorting to them throughout the book. Upon substitution of the foregoing identities into eq.(4.22), a quartic equation in τ_3 is obtained, i.e.,

$$R\tau_3^4 + S\tau_3^3 + T\tau_3^2 + U\tau_3 + V = 0 \tag{4.25}$$

whose coefficients are all computable from the data. After some simplifications, these coefficients take on the forms

$$R = 4a_1^2(J-H)^2 + \mu_1^2(E-C)^2 - 4\rho^2a_1^2\mu_1^2 \tag{4.26a}$$
$$S = 4[4a_1^2I(J-H) + \mu_1^2D(E-C)] \tag{4.26b}$$
$$T = 2[4a_1^2(J^2-H^2+2I^2) + \mu_1^2(E^2-C^2+2D^2) - 4\rho^2a_1^2\mu_1^2] \tag{4.26c}$$
$$U = 4[4a_1^2I(H+J) + \mu_1^2D(C+E)] \tag{4.26d}$$
$$V = 4a_1^2(J+H)^2 + \mu_1^2(E+C)^2 - 4\rho^2a_1^2\mu_1^2 \tag{4.26e}$$

Furthermore, let $\{\ (\tau_3)_i\ \}_1^4$ be the four roots of eq.(4.25). Thus, up to four possible values of θ_3 can be obtained, namely,

$$(\theta_3)_i = 2\arctan[(\tau_3)_i], \quad i = 1,2,3,4 \tag{4.27}$$

Once the four values of θ_3 are available, each of these is substituted into eqs.(4.21a & b), which thus produce four different values of θ_1. For each value of θ_1 and θ_3, then, one value of θ_2 can be computed from the first two scalar equations of eq.(4.17), which are displayed below:

$$A_{11}\cos\theta_2 + A_{12}\sin\theta_2 = x_C\cos\theta_1 + y_C\sin\theta_1 - a_1 \tag{4.28a}$$

$$-A_{12}\cos\theta_2 + A_{11}\sin\theta_2 = -x_C\lambda_1\sin\theta_1 + y_C\lambda_1\cos\theta_1 + (z_C - b_1)\mu_1 \tag{4.28b}$$

where

$$A_{11} \equiv a_2 + a_3\cos\theta_3 + b_4\mu_3\sin\theta_3 \tag{4.28c}$$

$$A_{12} \equiv -a_3\lambda_2\sin\theta_3 + b_3\mu_2 + b_4\lambda_2\mu_3\cos\theta_3 + b_4\mu_2\lambda_3 \tag{4.28d}$$

Thus, if A_{11} and A_{12} do not vanish simultaneously, angle θ_2 is readily computed in terms of θ_1 and θ_3 from eqs.(4.28a & b) as

$$\cos\theta_2 = \frac{1}{\Delta_2}\{A_{11}(x_C\cos\theta_1 + y_C\sin\theta_1 - a_1) - A_{12}[-x_C\lambda_1\sin\theta_1 + y_C\lambda_1\cos\theta_1 + (z_C - b_1)\mu_1]\} \tag{4.29a}$$

$$\sin\theta_2 = \frac{1}{\Delta_2}\{A_{12}(x_C\cos\theta_1 + y_C\sin\theta_1 - a_1) + A_{11}[-x_C\lambda_1\sin\theta_1 + y_C\lambda_1\cos\theta_1 + (z_C - b_1)\mu_1]\} \tag{4.29b}$$

where Δ_2 is defined as

$$\begin{aligned}\Delta_2 &\equiv A_{11}^2 + A_{12}^2 \\ &\equiv a_2^2 + a_3^2(\cos^2\theta_3 + \lambda_2^2\sin^2\theta_3) + b_4^2\mu_3^2(\sin^2\theta_3 + \lambda_2^2\cos^2\theta_3) \\ &\quad + 2a_2a_3\cos\theta_3 + 2a_2b_4\mu_3\sin\theta_3 \\ &\quad + 2\lambda_2\mu_2(b_3 + b_4\lambda_3)(b_4\mu_3\cos\theta_3 - a_3\sin\theta_3) \\ &\quad + 2a_3b_4(1 - \lambda_2^2)\mu_3\sin\theta_3\cos\theta_3 + (b_3 + \lambda_3b_4)^2\mu_2^2\end{aligned} \tag{4.29c}$$

the case in which $\Delta_2 = 0$, which leads to what is termed here the *second singularity*, being discussed presently.

Takano (1985) considered the solution of the positioning problem for all possible combinations of prismatic and revolute pairs in the regional structure of a manipulator, thereby finding that

1. In the case of arms containing either three revolutes, or two revolutes and one prismatic pair, with a general layout in all cases, a quartic equation in $\cos\theta_3$ was obtained;

2. in the case of one revolute and two prismatic pairs, the positioning problem was reduced to a single quadratic equation, the problem at hand thus admitting two solutions;

3. finally, for three prismatic pairs, a single linear equation was derived, the problem thus admitting a unique solution.

The Vanishing of Δ_1

In the above derivations we have assumed that neither μ_1 nor a_1 vanishes. However, if either $\mu_1 = 0$ or $a_1 = 0$, then one can readily show that eq.(4.25) reduces to a quadratic equation, and hence, this case differs essentially from the general one. Note that one of these conditions can occur, and the second occurs indeed frequently, but both together never occur, because their simultaneous occurrence would render the manipulator useless for a three-dimensional task. We thus have the two cases discussed below:

1. $\mu_1 = 0$, $a_1 \neq 0$. In this case, one has

$$A,\, B \neq 0, \quad F = G = 0$$

Under these conditions, eq.(4.20a) and the tan-half-angle identities given in eq.(4.24) yield

$$(J - H)\tau_3^2 + 2I\tau_3 + (J + H) = 0$$

which thus produces two values of τ_3, namely,

$$(\tau_3)_{1,2} = \frac{-I \pm \sqrt{I^2 - J^2 + H^2}}{J - H} \tag{4.30a}$$

Once two values of θ_3 have been determined according to the above equation, θ_1 can be found using eq.(4.19a) and the tan-half-angle identities, thereby deriving

$$(E' - A)\tau_1^2 + 2B\tau_1 + (E' + A) = 0$$

where

$$E' = Cc_3 + Ds_3 + E, \quad \tau_1 \equiv \tan\left(\frac{\theta_1}{2}\right)$$

whose roots are

$$(\tau_1)_{1,2} = \frac{-B \pm \sqrt{B^2 - E'^2 + A^2}}{E' - A} \tag{4.30b}$$

Thus, two values of θ_1 are found for each of the two values of θ_3, which results in four positioning solutions. Values of θ_2 are obtained using eqs.(4.29a & b).

2. $a_1 = 0$, $\mu_1 \neq 0$. In this case, one has an architecture similar to that of the robot of Fig. 4.3. We have now

$$A = B = 0, \quad F, G \neq 0$$

Under the present conditions, eq.(4.19a) reduces to

$$(E - C)\tau_3^2 + 2D\tau_3 + (E + C) = 0$$

which produces two values of τ_3, namely,

$$(\tau_3)_{1,2} = \frac{-D \pm \sqrt{D^2 - E^2 + C^2}}{E - C} \tag{4.31a}$$

With the two values of θ_3 obtained, θ_1 can be found using eq.(4.20a) and the tan-half-angle identities to produce

$$(J' - F)\tau_1^2 + 2G\tau_1 + (J' + F) = 0$$

where

$$J' = Hc_3 + Is_3 + J, \quad \tau_1 \equiv \tan\left(\frac{\theta_1}{2}\right)$$

whose roots are

$$(\tau_1)_{1,2} = \frac{-G \pm \sqrt{G^2 - J'^2 + F^2}}{J' - F} \tag{4.31b}$$

Once again, the solution results in a cascade of two quadratic equations, one for θ_3 and one for θ_1, which yields four positioning solutions. As above, θ_2 is then determined using eqs.(4.29a & b). Note that for the special case of the manipulator of Fig. 4.3, we have

$$a_1 = b_2 = 0, \quad \alpha_1 = \alpha_3 = 90^\circ, \quad \alpha_2 = 0^\circ$$

and hence,

$$H = I = 0, \quad E = a_2^2 + a_3^2 + b_3^2 + b_4^2 - \left[x_C^2 + y_C^2 + (z_C - b_1)^2\right],$$

$$C = 2a_2a_3, \quad D = 2a_2b_4, \quad F = y_C, \quad G = -x_C, \quad J = b_3$$

In this case, the foregoing solutions reduce to

$$(\tau_3)_{1,2} = \frac{-D \pm \sqrt{C^2 + D^2 - E^2}}{E - C}, \quad (\tau_1)_{1,2} = \frac{x_C \pm \sqrt{x_C^2 + y_C^2 - b_3^2}}{b_3 - y_C}$$

A robot with the architecture studied here is the Puma, which is displayed in Fig. 4.10 in its four distinct postures for the same location of its wrist center. Notice that the orientation of the EE is kept constant in all four postures.

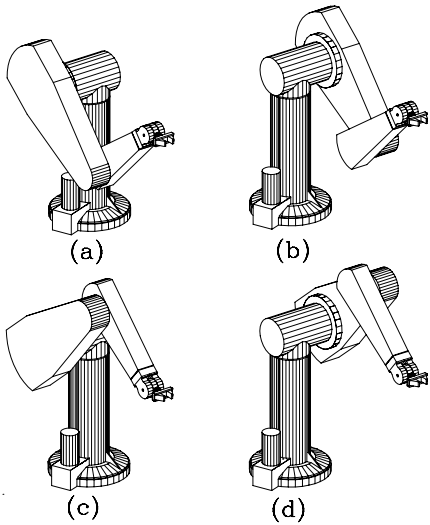

FIGURE 4.10. The four arm configurations for the positioning problem of the Puma robot: (a) and (b), elbow down; (a) and (c), shoulder fore; (c) and (d), elbow up; (b) and (d), shoulder aft.

The Vanishing of Δ_2

In some instances, Δ_2, as defined in eq.(4.29c), may vanish, thereby preventing the calculation of θ_2 from eqs.(4.29a & b). This posture, termed the second singularity, occurs if both coefficients A_{11} and A_{12} of eqs.(4.28a & b) vanish. Note that from their definitions, eqs.(4.28c & d), these coefficients are not only position- but also architecture-dependent. Thus, an arbitrary manipulator cannot take on this configuration unless its geometric dimensions allow it. This type of singularity will be termed architecture-dependent, to distinguish it from others that are common to all robots, regardless of their particular architectures.

We can now give a geometric interpretation of the singularity at hand: First, note that the right-hand side of eq.(4.17), from which eqs.(4.28a & b) were derived, is identical to $\mathbf{Q}_1^T(\mathbf{c}-\mathbf{a}_1)$, which means that this expression is nothing but the $\mathcal{F}_2$-representation of the position vector of C. That is, the components of vector $\mathbf{Q}_1^T(\mathbf{c}-\mathbf{a}_1)$ are the $\mathcal{F}_2$-components of vector $\overrightarrow{O_2C}$. Therefore, the right-hand sides of eqs.(4.28a & b) are, respectively, the X_2- and Y_2-components of vector $\overrightarrow{O_2C}$. Consequently, if $A_{11} = A_{12} = 0$, then the two foregoing components vanish and, hence, point C lies on the Z_2 axis. The first singularity thus occurs when point C lies on the axis of the first revolute, while the second occurs when the same point lies on the axis of the second revolute.

Many industrial manipulators are designed with an orthogonal architecture, which means that the angles between neighbor axes are multiples of 90°. Moreover, with the purpose of maximizing their workspace, orthogonal manipulators are designed with their second and third links of equal lengths, thereby rendering them vulnerable to this type of singularity. An architecture common to many manipulators such as the Cincinnati-Milacron, ABB, Fanuc, and others, comprises a planar two-axis layout with equal link lengths, which is capable of turning about an axis orthogonal to these two axes. This layout allows for the architecture singularity under discussion, as shown in Fig. 4.11a. The well-known Puma manipulator is similar to the aforementioned manipulators, except that it is supplied with what is called a shoulder offset b_3, as illustrated in Fig. 4.3. This offset, however, does not prevent the Puma from attaining the same singularity as depicted in Fig. 4.11b. Note that in the presence of this singularity, angle θ_2 is undetermined, but θ_1 and θ_3 are determined in the case of the Puma robot. However, in the presence of the singularity of Fig. 4.11a, neither θ_1 nor θ_2 are determined; only θ_3 of the arm structure is determined.

Example 4.4.1 *A manipulator with a common orthogonal architecture is displayed in Fig. 4.12 in an arbitrary configuration. The arm architecture of this manipulator has the DH parameters shown below:*

$$a_1 = 0, \quad b_1 = b_2 = b_3 = 0, \quad \alpha_1 = 90^\circ, \quad \alpha_2 = 0^\circ$$

Find its inverse kinematics solutions.

Solution: A common feature of this architecture is that it comprises $a_2 = b_4$. In the present discussion, however, the latter feature need not be included, and hence, the result that follows applies even in its absence. In this case,

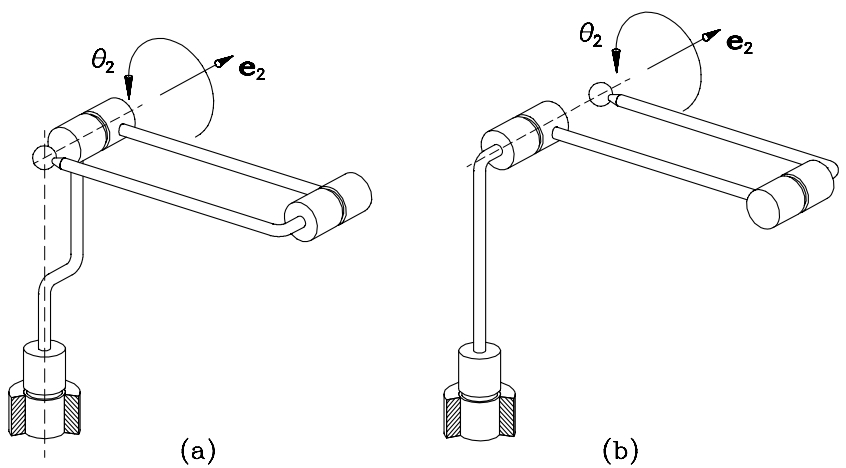

FIGURE 4.11. Architecture-dependent singularities of (a) the Cincinnati--Milacron and (b) the Puma robots.

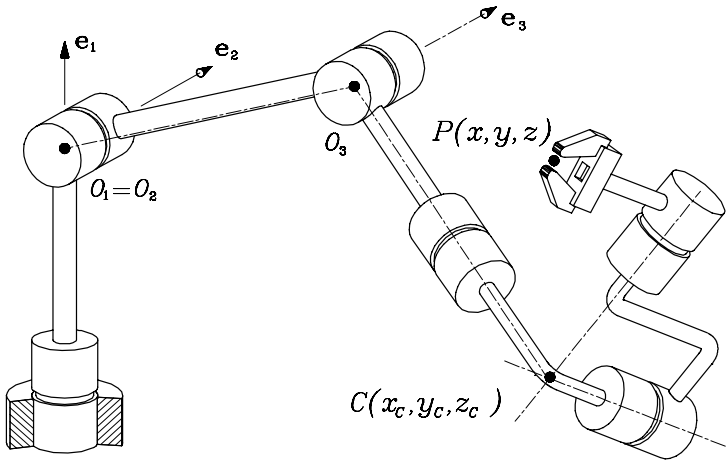

FIGURE 4.12. An orthogonal decoupled manipulator.

coefficients C, D, and E take on the forms

$$C = 2a_2a_3, \quad D = 0, \quad E = a_2^2 + a_3^2 - (x_C^2 + y_C^2 + z_C^2)$$

Hence,

$$E - C = (a_2 - a_3)^2 - (x_C^2 + y_C^2 + z_C^2), \quad E + C = (a_2 + a_3)^2 - (x_C^2 + y_C^2 + z_C^2)$$

Moreover,

$$H = I = J = 0$$

and so

$$J' = 0, \quad F = y_C, \quad G = -x_C$$

The radical of eq.(4.31b) reduces to $x_C^2 + y_C^2$. Thus,

$$\tan\left(\frac{\theta_1}{2}\right) = \frac{x_C \pm \sqrt{x_C^2 + y_C^2}}{-y_C} \equiv \frac{-1 \pm \sqrt{1 + (y_C/x_C)^2}}{y_C/x_C} \tag{4.32a}$$

Now we recall the relation between $\tan(\theta_1/2)$ and $\tan\theta_1$, namely,

$$\tan\left(\frac{\theta_1}{2}\right) \equiv \frac{-1 \pm \sqrt{1 + \tan^2\theta_1}}{\tan\theta_1} \tag{4.32b}$$

Upon comparison of eqs.(4.32a) and (4.32b), it is apparent that

$$\theta_1 = \arctan\left(\frac{y_C}{x_C}\right)$$

a result that can be derived geometrically for this simple arm architecture. Given that the arctan(·) function is double-valued, its two values differing

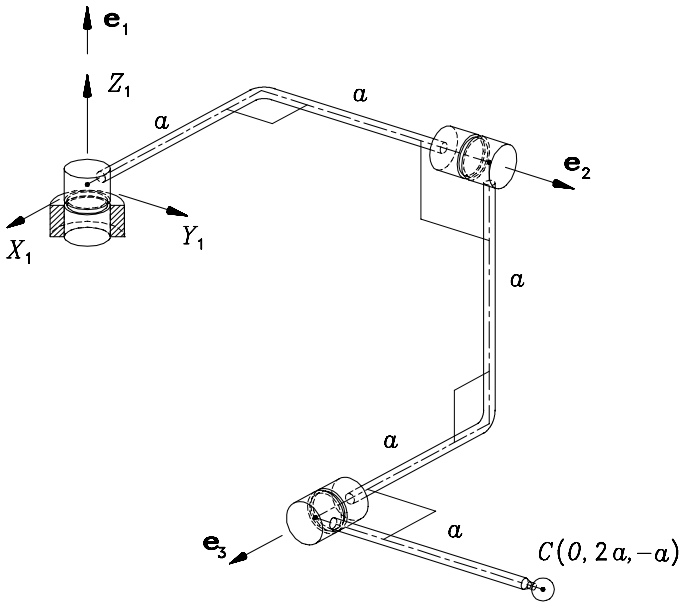

FIGURE 4.13. An orthogonal *RRR* manipulator.

in 180°, we obtain here, again, two values for θ_1. On the other hand, θ_3 is calculated from eq.(4.31a) as

$$(\tau_3)_{1,2} = \pm\frac{\sqrt{C^2 - E^2}}{E - C}$$

thereby obtaining two values of θ_3. As a consequence, the inverse positioning problem of this arm architecture admits four solutions as well. These solutions give rise to two pairs of arm postures that are usually referred to as *elbow-up* and *elbow-down*.

Example 4.4.2 *Find all real inverse kinematic solutions of the manipulator shown in Fig. 4.13, when point C of its end-effector has the base coordinates* $C(0,\ 2a,\ -a)$.

Solution: The Denavit-Hartenberg parameters of this manipulator are derived from Fig. 4.14, where the coordinate frames involved are indicated. In defining the coordinate frames of that figure, the Denavit-Hartenberg notation was followed, with Z_4 defined, arbitrarily, as parallel to Z_3. From Fig. 4.14, then, we have

$$a_1 = a_2 = a_3 = b_2 = b_3 = a, \quad b_1 = b_4 = 0, \quad \alpha_1 = \alpha_2 = 90^\circ, \quad \alpha_3 = 0^\circ$$

One inverse kinematic solution can be readily inferred from the geometry of Fig. 4.14. For illustration purposes, and in order to find all other inverse kinematic solutions, we will use the procedure derived above. To this

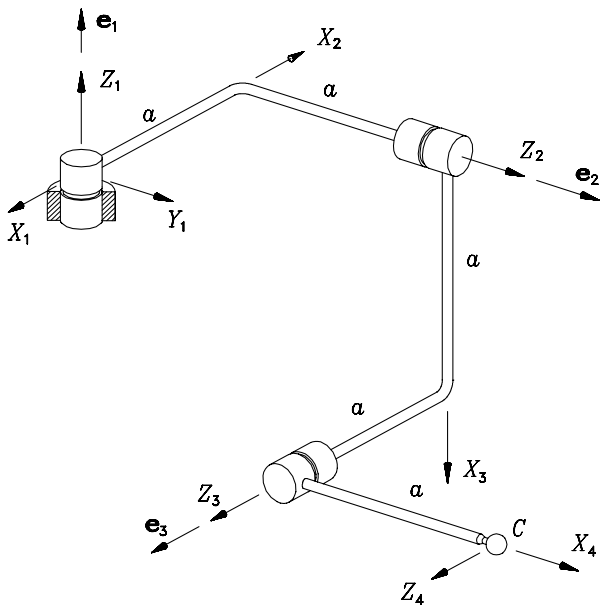

FIGURE 4.14. The coordinate frames of the orthogonal *RRR* manipulator.

end, we first proceed to calculate the coefficients of the quartic polynomial equation, eq.(4.25), which are given, nevertheless, in terms of coefficients K, ..., Q of eqs.(4.23a–f). These coefficients are given, in turn, in terms of coefficients A, ..., J of eqs.(4.19b–f) and (4.20b–f). We then proceed to calculate all the necessary coefficients in the proper order:

$$A = 0, \quad B = 4a^2, \quad C = D = -E = 2a^2$$
$$F = 2a, \quad G = H = 0, \quad I = J = a$$

Moreover,

$$K = 4a^4, \quad L = 8a^4, \quad M = 8a^4, \quad N = -8a^4, \quad P = 0, \quad Q = -8a^4,$$

The set of coefficients sought thus reduces to

$$R = K - N + Q = 4a^4$$
$$S = 2(P - M) = -16a^4$$
$$T = 2(Q + 2L - K) = 8a^4$$
$$U = 2(M + P) = 16a^4$$
$$V = K + N + Q = -12a^4$$

which leads to the quartic equation given below:

$$\tau_3^4 - 4\tau_3^3 + 2\tau_3^2 + 4\tau_3 - 3 = 0$$

with four real roots, namely,

$$(\tau_3)_1 = (\tau_3)_2 = 1, \quad (\tau_3)_3 = -1, \quad (\tau_3)_4 = 3$$

These roots yield the θ_3 values that follow:

$$(\theta_3)_1 = (\theta_3)_2 = 90^\circ, \quad (\theta_3)_3 = -90^\circ, \quad (\theta_3)_4 = 143.13^\circ$$

The quartic polynomial thus admits one double root, which means that at the configurations resulting from this root, two solutions meet, thereby producing a *singularity*, an issue that is discussed in Subsection 4.5.2. Below, we calculate the remaining angles for each solution: Angle θ_1 is computed from relations (4.21a–c), where $\Delta_1 = -8a^3$.

The first two roots, $(\theta_3)_1 = (\theta_3)_2 = 90^\circ$, yield $c_3 = 0$ and $s_3 = 1$. Hence, eqs.(4.21a & b) lead to

$$c_1 = \frac{B(I+J)}{\Delta_1} = \frac{4a^2(a+a)}{-8a^3} = -1$$
$$s_1 = \frac{F(D+E)}{\Delta_1} = \frac{2a(2a^2-2a^2)}{-8a^3} = 0$$

and hence,

$$(\theta_1)_1 = (\theta_1)_2 = 180^\circ$$

With θ_1 known, θ_2 is computed from the first two of eqs.(4.17), namely,

$$c_2 = 0, \quad s_2 = -1$$

and hence,

$$(\theta_2)_1 = (\theta_2)_2 = -90^\circ$$

The remaining roots are treated likewise. These are readily calculated as shown below:

$$(\theta_1)_3 = -90^\circ, \quad (\theta_2)_3 = 0, \quad (\theta_1)_4 = 143.13^\circ, \quad (\theta_2)_4 = 0$$

It is noteworthy that the architecture of this manipulator does not allow for the second singularity, associated with $\Delta_2 = 0$.

Example 4.4.3 *For the same manipulator of Example 4.4.2, find all real inverse kinematic solutions when point C of its end-effector has the base coordinates C(0, a, 0), as displayed in Fig. 4.15.*

Solution: In this case, one obtains, successively,

$$A = 0, \quad B = C = D = E = 2a^2,$$
$$F = a, \quad G = 0 \quad H = 0, \quad I = J = a$$
$$K = 4a^6, L = M = N = 8a^6, \quad P = 16a^6, \quad Q = 4a^6$$
$$R = 0, \quad S = 16a^6, \quad T = 32a^6, \quad U = 48a^6, \quad V = 16a^6$$

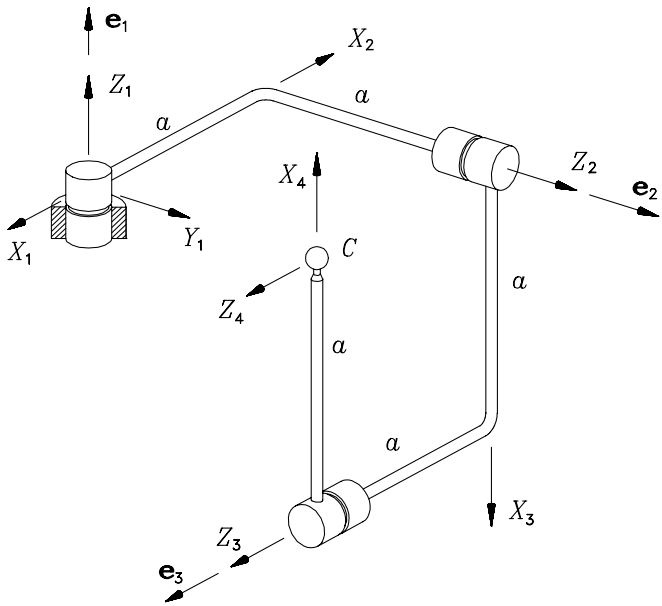

FIGURE 4.15. Manipulator configuration for $C(0,\ a,\ 0)$.

Moreover, for this case, the quartic eq.(4.22) degenerates into a cubic equation, namely,

$$\tau_3^3 + 2\tau_3^2 + 3\tau_3 + 1 = 0$$

whose roots are readily found as

$$(\tau_3)_1 = -0.43016, \quad (\tau_3)_{2,3} = -0.78492 \pm j1.30714$$

where j is the imaginary unit, i.e., $j \equiv \sqrt{-1}$. That is, only one real solution is obtained, namely, $(\theta_3)_1 = -46.551°$. However, shown in Fig. 4.15 is a quite symmetric posture of this manipulator at the given position of point C of its end-effector, which does not correspond to the real solution obtained above. In fact, the solution yielding the posture of Fig. 4.15 disappeared because of the use of the quartic polynomial equation in $\tan(\theta_3/2)$. Note that if the two contours derived from eqs.(4.19a) and (4.20a) are plotted, as in Fig. 4.16, their intersections yield the two real roots, including the one leading to the posture of Fig. 4.15.

The explanation of how the fourth root of the quartic equation disappeared is given below: Let us write the quartic polynomial in full, with a "small" leading coefficient ϵ, namely,

$$\epsilon\tau_3^4 + \tau_3^3 + 2\tau_3^2 + 3\tau_3 + 1 = 0$$

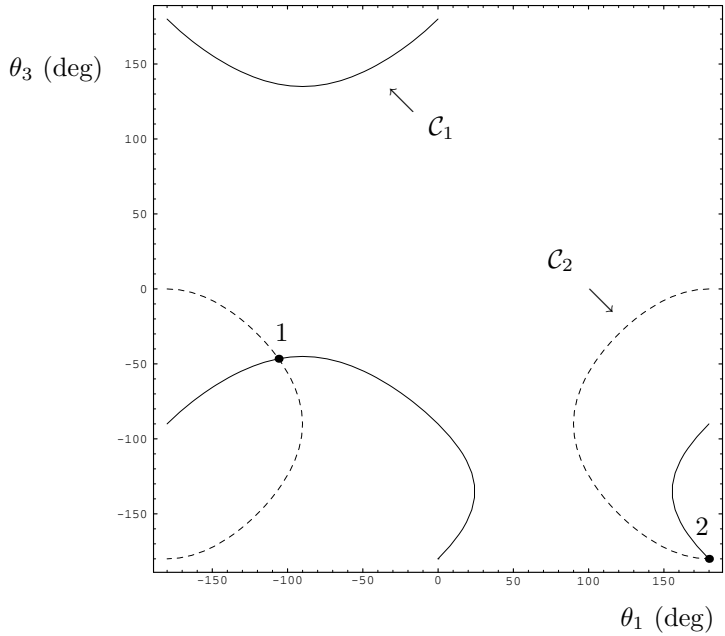

FIGURE 4.16. Contours producing the two real solutions for Example 4.4.3.

Upon dividing both sides of the foregoing equation by τ_3^4, we obtain

$$\epsilon + \frac{1}{\tau_3} + \frac{2}{\tau_3^2} + \frac{3}{\tau_3^3} + \frac{1}{\tau_3^4} = 0$$

from which it is clear that the original equation is satisfied as $\epsilon \to 0$ if and only if $\tau_3 \to \pm\infty$, i.e, if $\theta_3 = 180°$. It is then apparent that the missing root is $\theta_3 = 180°$. The remaining angles are readily calculated as

$$(\theta_1)_1 = -105.9°, \quad (\theta_2)_1 = -149.35°, \quad (\theta_1)_4 = 180°, \quad (\theta_2)_4 = 180°$$

4.4.2 The Orientation Problem

Now the orientation inverse kinematic problem is addressed. This problem consists of determining the wrist angles that will produce a prescribed orientation of the end-effector. This orientation, in turn, is given in terms of the rotation matrix $\mathbf{Q}$ taking the end-effector from its home attitude to its current one. Alternatively, the orientation can be given by the natural invariants of the rotation matrix, vector $\mathbf{e}$ and angle ϕ. Moreover, since θ_1, θ_2, and θ_3 are available, $\mathbf{Q}_1$, $\mathbf{Q}_2$, and $\mathbf{Q}_3$ become data for this problem. One now has the general layout of Fig. 4.17, where angles $\{\,\theta_i\,\}_4^6$ are to be determined from the problem data, which are in this case the orientation

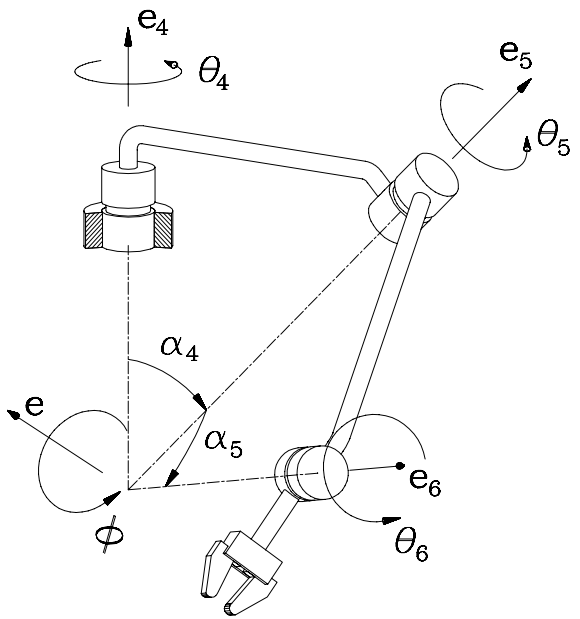

FIGURE 4.17. General architecture of a spherical wrist.

of the end-effector and the architecture of the wrist; the latter is defined by angles α_4 and α_5, neither of which can be either 0 or π.

Now, since the orientation of the end-effector is given, we know the components of vector $\mathbf{e}_6$ in any coordinate frame. In particular, let

$$[\,\mathbf{e}_6\,]_4 = \begin{bmatrix} \xi \\ \eta \\ \zeta \end{bmatrix} \tag{4.33}$$

Moreover, the components of vector $\mathbf{e}_5$ in $\mathcal{F}_4$ are nothing but the entries of the third column of matrix $\mathbf{Q}_4$, i.e.,

$$[\,\mathbf{e}_5\,]_4 = \begin{bmatrix} \mu_4 \sin\theta_4 \\ -\mu_4 \cos\theta_4 \\ \lambda_4 \end{bmatrix} \tag{4.34}$$

Furthermore, vectors $\mathbf{e}_5$ and $\mathbf{e}_6$ make an angle α_5, and hence,

$$\mathbf{e}_6^T \mathbf{e}_5 = \lambda_5 \quad \text{or} \quad [\,\mathbf{e}_6\,]_4^T [\,\mathbf{e}_5\,]_4 = \lambda_5 \tag{4.35}$$

Upon substitution of eqs.(4.33) and (4.34) into eq.(4.35), we obtain

$$\xi\mu_4 \sin\theta_4 - \eta\mu_4 \cos\theta_4 + \zeta\lambda_4 = \lambda_5 \tag{4.36}$$

which can be readily transformed, with the aid of the tan-half-angle identities, into a quadratic equation in $\tau_4 \equiv \tan(\theta_4/2)$, namely,

$$(\lambda_5 - \eta\mu_4 - \zeta\lambda_4)\tau_4^2 - 2\xi\mu_4\tau_4 + (\lambda_5 + \eta\mu_4 - \zeta\lambda_4) = 0 \tag{4.37}$$

its two roots being given by

$$\tau_4 = \frac{\xi\mu_4 \pm \sqrt{(\xi^2+\eta^2)\mu_4^2 - (\lambda_5 - \zeta\lambda_4)^2}}{\lambda_5 - \zeta\lambda_4 - \eta\mu_4} \tag{4.38}$$

Note that the two foregoing roots are real as long as the radical is positive, the two roots merging into a single one when the radical vanishes. Thus, a negative radical means an attitude of the EE that is not feasible with the wrist. It is to be pointed out here that a three-revolute spherical wrist is kinematically equivalent to a spherical joint. However, the spherical wrist differs essentially from a spherical joint in that the latter has, kinematically, an unlimited workspace—a physical spherical joint, of course, has a limited workspace by virtue of its mechanical construction—and can orient a rigid body arbitrarily. Therefore, the workspace $\mathcal{W}$ of the wrist is not unlimited, but rather defined by the set of values of ξ, η, and ζ that satisfy the two relations shown below:

$$\xi^2 + \eta^2 + \zeta^2 = 1 \tag{4.39a}$$

$$f(\xi,\eta,\zeta) \equiv (\xi^2+\eta^2)\mu_4^2 - (\lambda_5 - \zeta\lambda_4)^2 \geq 0 \tag{4.39b}$$

In view of condition (4.39a), however, relation (4.39b) simplifies to an inequality in ζ alone, namely,

$$F(\zeta) \equiv \zeta^2 - 2\lambda_4\lambda_5\zeta - (\mu_4^2 - \lambda_5^2) \leq 0 \tag{4.40}$$

As a consequence,

1. $\mathcal{W}$ is a region of the unit sphere $\mathcal{S}$ centered at the origin of the three-dimensional space;
2. $\mathcal{W}$ is bounded by the curve $F(\zeta) = 0$ on the sphere;
3. the wrist attains its singular configurations along the curve $F(\zeta) = 0$ lying on the surface of $\mathcal{S}$.

In order to gain more insight on the shape of the workspace $\mathcal{W}$, let us look at the boundary defined by $F(\zeta) = 0$. Upon setting $F(\zeta)$ to zero, we obtain a quadratic equation in ζ, whose two roots can be readily found to be

$$\zeta_{1,2} = \lambda_4\lambda_5 \pm |\mu_4\mu_5| \tag{4.41}$$

which thus defines two planes, Π_1 and Π_2, parallel to the ξ-η plane of the three-dimensional space, intersecting the ζ-axis at ζ_1 and ζ_2, respectively. Thus, the workspace $\mathcal{W}$ of the spherical wrist at hand is that region of the surface of the unit sphere $\mathcal{S}$ contained between Π_1 and Π_2. For example, a common wrist design involves an orthogonal architecture, i.e., $\alpha_4 = \alpha_5 = 90°$. For such wrists,

$$\zeta_{1,2} = \pm 1$$

and hence, orthogonal wrists become singular when $[\,\mathbf{e}_6\,]_4 = [\,0,\,0,\,\pm 1\,]^T$, i.e., when the fourth and the sixth axes are aligned. Thus, the workspace of orthogonal spherical wrists is the whole surface of the unit sphere centered at the origin, the singularity curve thus degenerating into two points, namely, the two intersections of this sphere with the ζ-axis. If one views $\zeta = 0$ as the equatorial plane, then the two singularity points of the workspace are the poles.

An alternative design is the so-called *three-roll wrist* of some Cincinnati-Milacron robots, with $\alpha_4 = \alpha_5 = 120°$, thereby leading to $\lambda_4 = \lambda_5 = -1/2$ and $\mu_4 = \mu_5 = \sqrt{3}/2$. For this wrist, the two planes Π_1 and Π_2 are found below: First, we note that with the foregoing values,

$$\zeta_{1,2} = 1,\, -\frac{1}{2}$$

and hence, the workspace of this wrist is the part of the surface of the unit sphere $\mathcal{S}$ that lies between the planes Π_1 and Π_2 parallel to the ξ-η plane, intersecting the ζ-axis at $\zeta_1 = 1$ and $\zeta_2 = -1/2$, respectively. Hence, if $\zeta = 0$ is regarded as the equatorial plane, then the points of the sphere $\mathcal{S}$ that are outside of the workspace of this wrist are those lying at a latitude of less than $-30°$. The singularity points are thus the north pole and the parallel of latitude $-30°$.

Once θ_4 is calculated from the two foregoing values of τ_4, if these are real, angle θ_5 is obtained uniquely for each value of θ_4, as explained below: First, eq.(4.9a) is rewritten in a form in which the data are collected in the right-hand side, which produces

$$\mathbf{Q}_4\mathbf{Q}_5\mathbf{Q}_6 = \mathbf{R} \tag{4.42a}$$

with $\mathbf{R}$ defined as

$$\mathbf{R} = \mathbf{Q}_3^T\mathbf{Q}_2^T\mathbf{Q}_1^T\mathbf{Q} \tag{4.42b}$$

Moreover, let the entries of $\mathbf{R}$ in the fourth coordinate frame be given as

$$[\,\mathbf{R}\,]_4 = \begin{bmatrix} r_{11} & r_{12} & r_{13} \\ r_{21} & r_{22} & r_{23} \\ r_{31} & r_{32} & r_{33} \end{bmatrix}$$

Expressions for θ_5 and θ_6 can be readily derived by solving first for $\mathbf{Q}_5$ from eq.(4.42a), namely,

$$\mathbf{Q}_5 = \mathbf{Q}_4^T\mathbf{R}\mathbf{Q}_6^T \tag{4.43}$$

Now, by virtue of the form of the $\mathbf{Q}_i$ matrices, as appearing in eq.(4.1e), it is apparent that the third row of $\mathbf{Q}_i$ does not contain θ_i. Hence, the third column of the matrix product of eq.(4.43) is independent of θ_6. Thus, two equations for θ_5 are obtained by equating the first two components of the third columns of that equation, thereby obtaining

$$\begin{aligned} \mu_5 s_5 &= (\mu_6 r_{12} + \lambda_6 r_{13})c_4 + (\mu_6 r_{22} + \lambda_6 r_{23})s_4 \\ -\mu_5 c_5 &= -\lambda_4(\mu_6 r_{12} + \lambda_6 r_{13})s_4 + \lambda_4(\mu_6 r_{22} + \lambda_6 r_{23})c_4 + \mu_4(\mu_6 r_{32} + \lambda_6 r_{33}) \end{aligned}$$

which thus yield a unique value of θ_5 for every value of θ_4. Finally, with θ_4 and θ_5 known, it is a simple matter to calculate θ_6. This is done upon solving for $\mathbf{Q}_6$ from eq.(4.42a), i.e.,

$$\mathbf{Q}_6 = \mathbf{Q}_5^T \mathbf{Q}_4^T \mathbf{R}$$

and if the partitioning (4.12) of $\mathbf{Q}_i$ is now recalled, a useful vector equation is derived, namely,

$$\mathbf{p}_6 = \mathbf{Q}_5^T \mathbf{Q}_4^T \mathbf{r}_1 \tag{4.44}$$

where $\mathbf{r}_1$ is the first column of $\mathbf{R}$. Let $\mathbf{w}$ denote the product $\mathbf{Q}_4^T \mathbf{r}_1$, i.e.,

$$\mathbf{w} \equiv \mathbf{Q}_4^T \mathbf{r}_1 \equiv \begin{bmatrix} r_{11}c_4 + r_{21}s_4 \\ -\lambda_4(r_{11}s_4 - r_{21}c_4) + \mu_4 r_{31} \\ \mu_4(r_{11}s_4 - r_{21}c_4) + \lambda_4 r_{31} \end{bmatrix}$$

Hence,

$$\mathbf{Q}_5^T \mathbf{Q}_4^T \mathbf{r}_1 \equiv \begin{bmatrix} w_1 c_5 + w_2 s_5 \\ \lambda_5(-w_1 s_5 + w_2 c_5) + w_3 \mu_5 \\ \mu_5(w_1 s_5 - w_2 c_5) + w_3 \lambda_5 \end{bmatrix}$$

in which w_i denotes the ith component of $\mathbf{w}$. Hence, c_6 and s_6 are determined from the first two scalar equations of eq.(4.44), namely,

$$\begin{aligned} c_6 &= w_1 c_5 + w_2 s_5 \\ s_6 &= -w_1 \lambda_5 s_5 + w_2 \lambda_5 c_5 + w_3 \mu_5 \end{aligned}$$

thereby deriving a unique value of θ_6 for every pair of values (θ_4, θ_5). In summary, then, two values of θ_4 have been determined, each value determining, in turn, one single corresponding set of θ_5 and θ_6 values. Therefore, there are two sets of solutions for the orientation problem under study, which lead to two corresponding wrist postures. The two distinct postures of an orthogonal three-revolute spherical wrist for a given orientation of its EE are displayed in Fig. 4.18.

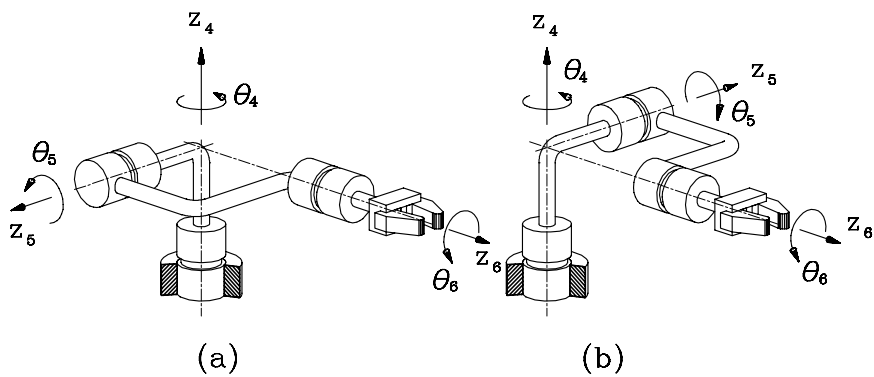

FIGURE 4.18. The two configurations of a three-axis spherical wrist.

When combined with the four postures of a decoupled manipulator leading to one and the same location of its wrist center—positioning problem—a maximum of eight possible combinations of joint angles for a single pose of the end-effector of a decoupled manipulator are found.

4.5 Velocity Analysis of Serial Manipulators

The relationships between the prescribed twist of the EE, also referred to as the *Cartesian velocity* of the manipulator, and the corresponding joint-rates are derived in this section. First, a serial n-axis manipulator containing only revolute pairs is considered. Then, relations associated with prismatic pairs are introduced, and finally, the joint rates of six-axis manipulators are calculated in terms of the EE twist. Particular attention is given to decoupled manipulators, for which simplified velocity relations are derived.

We consider here the manipulator of Fig. 4.19, in which a joint coordinate θ_i, a joint rate $\dot{\theta}_i$, and a unit vector $\mathbf{e}_i$ are associated with each revolute axis. The X_i, Y_i, Z_i coordinate frame, attached to the $(i-1)$st link, is not shown, but its origin O_i is indicated. The relations that follow are apparent from that figure.

$$\begin{aligned}
\boldsymbol{\omega}_0 &= \mathbf{0} \\
\boldsymbol{\omega}_1 &= \dot{\theta}_1 \mathbf{e}_1 \\
\boldsymbol{\omega}_2 &= \dot{\theta}_1 \mathbf{e}_1 + \dot{\theta}_2 \mathbf{e}_2 \\
&\vdots \\
\boldsymbol{\omega}_n &= \dot{\theta}_1 \mathbf{e}_1 + \dot{\theta}_2 \mathbf{e}_2 + \cdots + \dot{\theta}_n \mathbf{e}_n
\end{aligned} \tag{4.45}$$

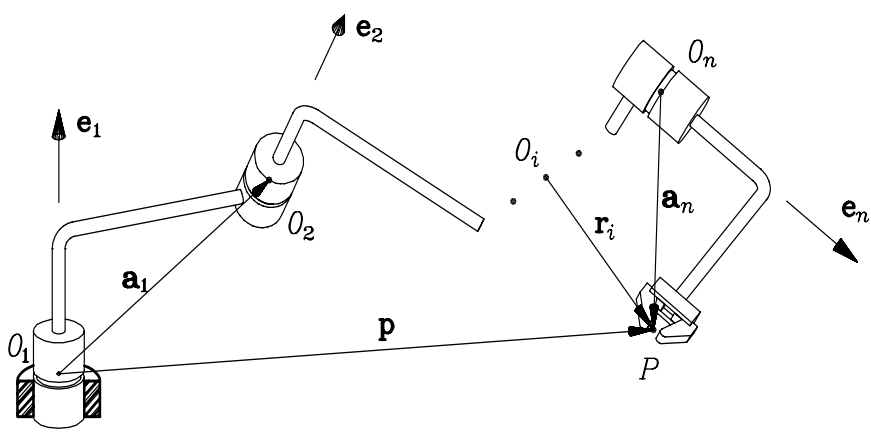

FIGURE 4.19. General n-axis manipulator.

and if the angular velocity of the EE is denoted by $\boldsymbol{\omega}$, then

$$\boldsymbol{\omega} \equiv \boldsymbol{\omega}_n = \dot{\theta}_1 \mathbf{e}_1 + \dot{\theta}_2 \mathbf{e}_2 + \cdots + \dot{\theta}_n \mathbf{e}_n = \sum_1^n \dot{\theta}_i \mathbf{e}_i$$

Likewise, from Fig. 4.19, one readily derives

$$\mathbf{p} = \mathbf{a}_1 + \mathbf{a}_2 + \cdots + \mathbf{a}_n \tag{4.46}$$

where $\mathbf{p}$ denotes the position vector of point P of the EE. Moreover, notice that all vectors of the above equation must be expressed in the same frame; otherwise, the addition would not be possible—vector $\mathbf{a}_i$ was defined as expressed in the ith frame in eq.(4.3c). Upon differentiating both sides of eq.(4.46), we have

$$\dot{\mathbf{p}} = \dot{\mathbf{a}}_1 + \dot{\mathbf{a}}_2 + \cdots + \dot{\mathbf{a}}_n \tag{4.47}$$

where

$$\dot{\mathbf{a}}_i = \boldsymbol{\omega}_i \times \mathbf{a}_i, \quad i = 1, 2, \ldots, n \tag{4.48}$$

Furthermore, substitution of eqs.(4.45) and (4.48) into eq.(4.47) yields

$$\begin{aligned} \dot{\mathbf{p}} = \dot{\theta}_1 \mathbf{e}_1 \times \mathbf{a}_1 + (\dot{\theta}_1 \mathbf{e}_1 + \dot{\theta}_2 \mathbf{e}_2) \times \mathbf{a}_2 + \\ \vdots \\ + (\dot{\theta}_1 \mathbf{e}_1 + \dot{\theta}_2 \mathbf{e}_2 + \cdots + \dot{\theta}_n \mathbf{e}_n) \times \mathbf{a}_n \end{aligned} \tag{4.49}$$

which can be readily rearranged as

$$\begin{aligned} \dot{\mathbf{p}} = \dot{\theta}_1 \mathbf{e}_1 \times (\mathbf{a}_1 + \mathbf{a}_2 + \cdots + \mathbf{a}_n) + \dot{\theta}_2 \mathbf{e}_2 \times (\mathbf{a}_2 + \mathbf{a}_3 + \cdots + \mathbf{a}_n) \\ + \cdots + \dot{\theta}_n \mathbf{e}_n \times \mathbf{a}_n \end{aligned}$$

Now vector $\mathbf{r}_i$ is defined as that joining O_i with P, directed from the former to the latter, i.e.,

$$\mathbf{r}_i \equiv \mathbf{a}_i + \mathbf{a}_{i+1} + \cdots + \mathbf{a}_n \tag{4.50}$$

and hence, $\dot{\mathbf{p}}$ can be rewritten as

$$\dot{\mathbf{p}} = \sum_1^n \dot{\theta}_i \mathbf{e}_i \times \mathbf{r}_i$$

Further, let $\mathbf{A}$ and $\mathbf{B}$ denote the $3 \times n$ matrices defined as

$$\mathbf{A} \equiv [\, \mathbf{e}_1 \quad \mathbf{e}_2 \quad \cdots \quad \mathbf{e}_n \,] \tag{4.51a}$$

$$\mathbf{B} \equiv [\, \mathbf{e}_1 \times \mathbf{r}_1 \quad \mathbf{e}_2 \times \mathbf{r}_2 \quad \cdots \quad \mathbf{e}_n \times \mathbf{r}_n \,] \tag{4.51b}$$

Furthermore, the n-dimensional *joint-rate vector* $\dot{\boldsymbol{\theta}}$ is defined as

$$\dot{\boldsymbol{\theta}} \equiv [\, \dot{\theta}_1 \quad \dot{\theta}_2 \quad \cdots \quad \dot{\theta}_n \,]^T$$

Thus, $\boldsymbol{\omega}$ and $\dot{\mathbf{p}}$ can be expressed in a more compact form as

$$\boldsymbol{\omega} = \mathbf{A}\dot{\boldsymbol{\theta}}, \quad \dot{\mathbf{p}} = \mathbf{B}\dot{\boldsymbol{\theta}}$$

the twist of the EE being defined, in turn, as

$$\mathbf{t} \equiv \begin{bmatrix} \boldsymbol{\omega} \\ \dot{\mathbf{p}} \end{bmatrix} \tag{4.52}$$

The EE twist is thus related to the joint-rate vector $\dot{\boldsymbol{\theta}}$ in the form

$$\mathbf{J}\dot{\boldsymbol{\theta}} = \mathbf{t} \tag{4.53}$$

where $\mathbf{J}$ is the *Jacobian matrix*, or *Jacobian*, for brevity, of the manipulator under study, first introduced by Whitney (1972). The Jacobian is defined as the $6 \times n$ matrix shown below:

$$\mathbf{J} = \begin{bmatrix} \mathbf{A} \\ \mathbf{B} \end{bmatrix} \tag{4.54a}$$

or

$$\mathbf{J} = \begin{bmatrix} \mathbf{e}_1 & \mathbf{e}_2 & \cdots & \mathbf{e}_n \\ \mathbf{e}_1 \times \mathbf{r}_1 & \mathbf{e}_2 \times \mathbf{r}_2 & \cdots & \mathbf{e}_n \times \mathbf{r}_n \end{bmatrix} \tag{4.54b}$$

Clearly, an alternative definition of the foregoing Jacobian matrix can be given as

$$\mathbf{J} = \frac{\partial \mathbf{t}}{\partial \dot{\boldsymbol{\theta}}}$$

Moreover, if $\mathbf{j}_i$ denotes the ith column of $\mathbf{J}$, one has

$$\mathbf{j}_i = \begin{bmatrix} \mathbf{e}_i \\ \mathbf{e}_i \times \mathbf{r}_i \end{bmatrix}$$

It is important to note that if the axis of the ith revolute is denoted by $\mathcal{R}_i$, then $\mathbf{j}_i$ is nothing but the Plücker array of that line, with the moment of $\mathcal{R}_i$ being taken with respect to the operation point P of the EE.

On the other hand, if the ith pair is not rotational, but prismatic, then the $(i-1)$st and the ith links have the same angular velocity, for a prismatic pair does not allow any relative rotation. However, vector $\mathbf{a}_i$ joining the origins of the ith and $(i+1)$st frames is no longer of constant magnitude but undergoes a change of magnitude along the axis of the prismatic pair. That is,

$$\boldsymbol{\omega}_i = \boldsymbol{\omega}_{i-1}, \quad \dot{\mathbf{a}}_i = \boldsymbol{\omega}_{i-1} \times \mathbf{a}_i + \dot{b}_i \mathbf{e}_i$$

One can readily prove, in this case, that

$$\begin{aligned} \boldsymbol{\omega} &= \dot{\theta}_1 \mathbf{e}_1 + \dot{\theta}_2 \mathbf{e}_2 + \cdots + \dot{\theta}_{i-1} \mathbf{e}_{i-1} + \dot{\theta}_{i+1} \mathbf{e}_{i+1} + \cdots + \dot{\theta}_n \mathbf{e}_n \\ \dot{\mathbf{p}} &= \dot{\theta}_1 \mathbf{e}_1 \times \mathbf{r}_1 + \dot{\theta}_2 \mathbf{e}_2 \times \mathbf{r}_2 + \cdots + \dot{\theta}_{i-1} \mathbf{e}_{i-1} \times \mathbf{r}_{i-1} + \dot{b}_i \mathbf{e}_i \\ &\quad + \dot{\theta}_{i+1} \mathbf{e}_{i+1} \times \mathbf{r}_{i+1} + \cdots + \dot{\theta}_n \mathbf{e}_n \times \mathbf{a}_n \end{aligned}$$

from which it is apparent that the relation between the twist of the EE and the joint-rate vector is formally identical to that appearing in eq.(4.53) if vector $\dot{\boldsymbol{\theta}}$ is defined as

$$\dot{\boldsymbol{\theta}} \equiv [\, \dot{\theta}_1 \quad \dot{\theta}_2 \quad \cdots \quad \dot{\theta}_{i-1} \quad \dot{b}_i \quad \dot{\theta}_{i+1} \quad \cdots \quad \dot{\theta}_n \,]^T$$

and the ith column of $\mathbf{J}$ changes to

$$\mathbf{j}_i = \begin{bmatrix} \mathbf{0} \\ \mathbf{e}_i \end{bmatrix} \tag{4.56}$$

Note that the Plücker array of the axis of the ith joint, if prismatic, is that of a line at infinity lying in a plane normal to the unit vector $\mathbf{e}_i$, as defined in eq.(3.35).

In particular, for six-axis manipulators, $\mathbf{J}$ is a 6×6 matrix. Whenever this matrix is nonsingular, eq.(4.53) can be solved for $\dot{\boldsymbol{\theta}}$, namely,

$$\dot{\boldsymbol{\theta}} = \mathbf{J}^{-1}\mathbf{t} \tag{4.57}$$

Equation (4.57) is only symbolic, for the inverse of the Jacobian matrix need not be computed explicitly. Indeed, in the general case, matrix $\mathbf{J}$ cannot be inverted symbolically, and hence, $\dot{\boldsymbol{\theta}}$ is computed using a numerical procedure, the most suitable one being the *Gauss-elimination algorithm*, also known as *LU decomposition* (Golub and Van Loan, 1989). Gaussian elimination produces the solution by recognizing that a system of linear equations is most easily solved when it is in either upper- or lower-triangular form. To exploit this fact, matrix $\mathbf{J}$ is factored into the *unique* $\mathbf{L}$ and $\mathbf{U}$ factors in the form:

$$\mathbf{J} = \mathbf{L}\mathbf{U} \tag{4.58a}$$

where $\mathbf{L}$ is lower- and $\mathbf{U}$ is upper-triangular. Moreover, they have the forms

$$\mathbf{L} = \begin{bmatrix} 1 & 0 & \cdots & 0 \\ l_{21} & 1 & \cdots & 0 \\ \vdots & \vdots & \ddots & \vdots \\ l_{n1} & l_{n2} & \cdots & 1 \end{bmatrix} \tag{4.58b}$$

$$\mathbf{U} = \begin{bmatrix} u_{11} & u_{12} & \cdots & u_{1n} \\ 0 & u_{22} & \cdots & u_{2n} \\ \vdots & \vdots & \ddots & \vdots \\ 0 & 0 & \cdots & u_{nn} \end{bmatrix} \tag{4.58c}$$

where in the particular case at hand, $n = 6$. Thus, the unknown vector of joint rates can now be computed from two triangular systems, namely,

$$\mathbf{L}\mathbf{y} = \mathbf{t}, \quad \mathbf{U}\dot{\boldsymbol{\theta}} = \mathbf{y} \tag{4.59}$$

The latter equations are then solved, first for $\mathbf{y}$ and then for $\dot{\boldsymbol{\theta}}$, by application of only forward and backward substitutions, respectively. The LU

decomposition of an $n \times n$ matrix requires M'_n multiplications and A'_n additions, whereas the forward substitution needed in solving the lower-triangular system of eq.(4.59) requires M''_n multiplications and A''_n additions. Moreover, the backward substitution needed in solving the upper-triangular system of eq.(4.59) requires M'''_n multiplications and A'''_n additions. These figures are (Dahlquist and Björck, 1974)

$$M'_n = \frac{n^3}{3} + \frac{n^2}{2} + \frac{n}{6}, \qquad A'_n = \frac{n^3}{3} - \frac{n}{3} \tag{4.60a}$$

$$M''_n = \frac{n(n-1)}{2}, \qquad A''_n = \frac{n(n-1)}{2} \tag{4.60b}$$

$$M'''_n = \frac{n(n+1)}{2}, \qquad A'''_n = \frac{n(n-1)}{2} \tag{4.60c}$$

Thus, the solution of a system of n linear equations in n unknowns, using the LU-decomposition method, can be accomplished with M_n multiplications and A_n additions, as given below (Dahlquist and Björck, 1974):

$$M_n = \frac{n}{6}(2n^2 + 9n + 1), \quad A_n = \frac{n}{3}(n^2 + 3n - 4) \tag{4.61a}$$

Hence, the velocity resolution of a six-axis manipulator of *arbitrary architecture* requires M_6 multiplications and A_6 additions, as given below:

$$M_6 = 127, \quad A_6 = 100 \tag{4.61b}$$

Decoupled manipulators allow an even simpler velocity resolution. For manipulators with this type of architecture, it is more convenient to deal with the velocity of the center C of the wrist than with that of the operation point P. Thus, one has

$$\mathbf{t}_C = \mathbf{J}\dot{\boldsymbol{\theta}}$$

where $\mathbf{t}_C$ is defined as

$$\mathbf{t}_C = \begin{bmatrix} \boldsymbol{\omega} \\ \dot{\mathbf{c}} \end{bmatrix}$$

and can be obtained from $\mathbf{t}_P \equiv [\boldsymbol{\omega}^T, \dot{\mathbf{p}}^T]^T$ using the twist-transfer formula given by eqs.(3.84) and (3.85) as

$$\mathbf{t}_C = \begin{bmatrix} \mathbf{1} & \mathbf{O} \\ \mathbf{P} - \mathbf{C} & \mathbf{1} \end{bmatrix} \mathbf{t}_P$$

with $\mathbf{C}$ and $\mathbf{P}$ defined as the cross-product matrices of the position vectors $\mathbf{c}$ and $\mathbf{p}$, respectively.

If in general, $\mathbf{J}_A$ denotes the Jacobian defined for a point A of the EE and $\mathbf{J}_B$ that defined for another point B, then the relation between $\mathbf{J}_A$ and $\mathbf{J}_B$ is

$$\mathbf{J}_B = \mathbf{U}\mathbf{J}_A \tag{4.62a}$$

where the 6×6 matrix $\mathbf{U}$ is defined as

$$\mathbf{U} \equiv \begin{bmatrix} \mathbf{1} & \mathbf{O} \\ \mathbf{A}-\mathbf{B} & \mathbf{1} \end{bmatrix} \tag{4.62b}$$

while $\mathbf{A}$ and $\mathbf{B}$ are now the cross-product matrices of the position vectors $\mathbf{a}$ and $\mathbf{b}$ of points A and B, respectively. Moreover, this matrix $\mathbf{U}$ is identical to the matrix defined under the same name in eq.(3.31), and hence, it belongs to the 6×6 unimodular group, i.e., the group of 6×6 matrices whose determinant is unity. Thus,

$$\det(\mathbf{J}_B) = \det(\mathbf{J}_A) \tag{4.63}$$

We have then proven the result below:

Theorem 4.5.1: *The determinant of the Jacobian matrix of a six-axis manipulator is not affected under a change of* operation point *of the EE.*

Note, however, that the Jacobian matrix itself changes under a change of operation point. By analogy with the twist- and the wrench-transfer formulas, eq.(4.62a) can be called the *Jacobian-transfer formula*.

Since C is on the last three joint axes, its velocity is not affected by the motion of the last three joints, and we can write

$$\dot{\mathbf{c}} = \dot{\theta}_1 \mathbf{e}_1 \times \mathbf{r}_1 + \dot{\theta}_2 \mathbf{e}_2 \times \mathbf{r}_2 + \dot{\theta}_3 \mathbf{e}_3 \times \mathbf{r}_3$$

where in the case of a decoupled manipulator, vector $\mathbf{r}_i$ is defined as that directed from O_i to C. On the other hand, we have

$$\boldsymbol{\omega} = \dot{\theta}_1 \mathbf{e}_1 + \dot{\theta}_2 \mathbf{e}_2 + \dot{\theta}_3 \mathbf{e}_3 + \dot{\theta}_4 \mathbf{e}_4 + \dot{\theta}_5 \mathbf{e}_5 + \dot{\theta}_6 \mathbf{e}_6$$

and thus, the Jacobian takes on the following simple form

$$\mathbf{J} = \begin{bmatrix} \mathbf{J}_{11} & \mathbf{J}_{12} \\ \mathbf{J}_{21} & \mathbf{O} \end{bmatrix} \tag{4.64}$$

where $\mathbf{O}$ denotes the 3×3 zero matrix, the other 3×3 blocks being given below, *for manipulators with revolute pairs only*, as

$$\mathbf{J}_{11} = [\, \mathbf{e}_1 \quad \mathbf{e}_2 \quad \mathbf{e}_3 \,] \tag{4.65a}$$

$$\mathbf{J}_{12} = [\, \mathbf{e}_4 \quad \mathbf{e}_5 \quad \mathbf{e}_6 \,] \tag{4.65b}$$

$$\mathbf{J}_{21} = [\, \mathbf{e}_1 \times \mathbf{r}_1 \quad \mathbf{e}_2 \times \mathbf{r}_2 \quad \mathbf{e}_3 \times \mathbf{r}_3 \,] \tag{4.65c}$$

Further, vector $\dot{\boldsymbol{\theta}}$ is *partitioned* accordingly:

$$\dot{\boldsymbol{\theta}} \equiv \begin{bmatrix} \dot{\boldsymbol{\theta}}_a \\ \dot{\boldsymbol{\theta}}_w \end{bmatrix}$$

where

$$\dot{\boldsymbol{\theta}}_a \equiv \begin{bmatrix} \dot{\theta}_1 \\ \dot{\theta}_2 \\ \dot{\theta}_3 \end{bmatrix}, \quad \dot{\boldsymbol{\theta}}_w \equiv \begin{bmatrix} \dot{\theta}_4 \\ \dot{\theta}_5 \\ \dot{\theta}_6 \end{bmatrix}$$

Henceforth, the three components of $\dot{\boldsymbol{\theta}}_a$ will be referred to as the *arm rates*, whereas those of $\dot{\boldsymbol{\theta}}_w$ will be called the *wrist rates*. Now eqs.(4.53) can be written, for this particular case, as

$$\mathbf{J}_{11}\dot{\boldsymbol{\theta}}_a + \mathbf{J}_{12}\dot{\boldsymbol{\theta}}_w = \boldsymbol{\omega} \tag{4.66a}$$

$$\mathbf{J}_{21}\dot{\boldsymbol{\theta}}_a = \dot{\mathbf{c}} \tag{4.66b}$$

from which the solution is derived successively from the two systems of three equations and three unknowns that follow:

$$\mathbf{J}_{21}\dot{\boldsymbol{\theta}}_a = \dot{\mathbf{c}} \tag{4.67a}$$

$$\mathbf{J}_{12}\dot{\boldsymbol{\theta}}_w = \boldsymbol{\omega} - \mathbf{J}_{11}\dot{\boldsymbol{\theta}}_a \tag{4.67b}$$

From the general expressions (4.60), then, it is apparent that each of the foregoing systems can be solved with the numbers of operations shown below:

$$M_3 = 23, \quad A_3 = 14$$

Since the computation of the right-hand side of eq.(4.67b) requires, additionally, nine multiplications and nine additions, the total numbers of operations required to perform one joint-rate resolution of a decoupled manipulator, M_v multiplications and A_v additions, are given by

$$M_v = 55, \quad A_v = 37 \tag{4.68}$$

which are fairly low figures and can be performed in a matter of microseconds using a modern processor.

It is apparent from the foregoing kinematic relations that eq.(4.67a) should be first solved for $\dot{\boldsymbol{\theta}}_a$; with this value available, eq.(4.67b) can then be solved for $\dot{\boldsymbol{\theta}}_w$. We thus have, symbolically,

$$\dot{\boldsymbol{\theta}}_a = \mathbf{J}_{21}^{-1}\dot{\mathbf{c}} \tag{4.69}$$

$$\dot{\boldsymbol{\theta}}_w = \mathbf{J}_{12}^{-1}(\boldsymbol{\omega} - \mathbf{J}_{11}\dot{\boldsymbol{\theta}}_a) \tag{4.70}$$

Now, if we recall the concept of reciprocal bases introduced in Subsection 2.7.1, the above inverses can be represented explicitly. Indeed, let

$$\Delta_{21} \equiv \det(\mathbf{J}_{21}) = (\mathbf{e}_1 \times \mathbf{r}_1) \times (\mathbf{e}_2 \times \mathbf{r}_2) \cdot (\mathbf{e}_3 \times \mathbf{r}_3) \tag{4.71}$$

$$\Delta_{12} \equiv \det(\mathbf{J}_{12}) = \mathbf{e}_4 \times \mathbf{e}_5 \cdot \mathbf{e}_6 \tag{4.72}$$

Then

$$\mathbf{J}_{21}^{-1} = \frac{1}{\Delta_{21}} \begin{bmatrix} [(\mathbf{e}_2 \times \mathbf{r}_2) \times (\mathbf{e}_3 \times \mathbf{r}_3)]^T \\ [(\mathbf{e}_3 \times \mathbf{r}_3) \times (\mathbf{e}_1 \times \mathbf{r}_1)]^T \\ [(\mathbf{e}_1 \times \mathbf{r}_1) \times (\mathbf{e}_2 \times \mathbf{r}_2)]^T \end{bmatrix} \tag{4.73}$$

$$\mathbf{J}_{12}^{-1} = \frac{1}{\Delta_{12}} \begin{bmatrix} (\mathbf{e}_5 \times \mathbf{e}_6)^T \\ (\mathbf{e}_6 \times \mathbf{e}_4)^T \\ (\mathbf{e}_4 \times \mathbf{e}_5)^T \end{bmatrix} \tag{4.74}$$

Therefore,

$$\dot{\boldsymbol{\theta}}_a = \frac{1}{\Delta_{21}} \begin{bmatrix} (\mathbf{e}_2 \times \mathbf{r}_2) \times (\mathbf{e}_3 \times \mathbf{r}_3) \cdot \mathbf{c} \\ (\mathbf{e}_3 \times \mathbf{r}_3) \times (\mathbf{e}_1 \times \mathbf{r}_1) \cdot \mathbf{c} \\ (\mathbf{e}_1 \times \mathbf{r}_1) \times (\mathbf{e}_2 \times \mathbf{r}_2) \cdot \mathbf{c} \end{bmatrix} \tag{4.75a}$$

and if we let

$$\boldsymbol{\varpi} \equiv \boldsymbol{\omega} - \mathbf{J}_{11}\dot{\theta}_a \tag{4.75b}$$

where $\boldsymbol{\varpi}$ is read *varpi*, then

$$\dot{\boldsymbol{\theta}}_w = \frac{1}{\Delta_{12}} \begin{bmatrix} \mathbf{e}_5 \times \mathbf{e}_6 \cdot \boldsymbol{\varpi} \\ \mathbf{e}_6 \times \mathbf{e}_4 \cdot \boldsymbol{\varpi} \\ \mathbf{e}_4 \times \mathbf{e}_5 \cdot \boldsymbol{\varpi} \end{bmatrix} \tag{4.75c}$$

4.5.1 Jacobian Evaluation

The evaluation of the Jacobian matrix of a manipulator with n revolutes is discussed in this subsection, the presence of a prismatic pair leading to simplifications that will be outlined. Our aim here is to devise algorithms requiring a minimum number of operations, for these calculations are needed in real-time applications. We assume at the outset that all joint variables producing the desired EE pose are available. We divide this subsection into two subsubsections, one for the evaluation of the upper part of the Jacobian matrix and one for the evaluation of its lower part.

Evaluation of Submatrix **A**

The upper part **A** of the Jacobian matrix is composed of the set $\{ \mathbf{e}_i \}_1^n$, and hence, our aim here is the calculation of these unit vectors. Note, moreover, that vector $[\mathbf{e}_i]_1$ is nothing but the last column of $\mathbf{P}_{i-1} \equiv \mathbf{Q}_1 \cdots \mathbf{Q}_{i-1}$, our task then being the calculation of these matrix products. According to the DH nomenclature,

$$[\mathbf{e}_i]_i = [0 \quad 0 \quad 1]^T$$

Hence, $[\mathbf{e}_1]_1$ is available at no cost. However, each of the remaining $[\mathbf{e}_i]_1$ vectors, for $i = 2, \ldots, n$, is obtained as the last column of matrices $\mathbf{P}_{i-1}$. The *recursive calculation* of these matrices is described below:

$$\begin{aligned} \mathbf{P}_1 &\equiv \mathbf{Q}_1 \\ \mathbf{P}_2 &\equiv \mathbf{P}_1 \mathbf{Q}_2 \\ &\vdots \\ \mathbf{P}_n &\equiv \mathbf{P}_{n-1} \mathbf{Q}_n \end{aligned}$$

and hence, a simple algorithm follows:

$$\begin{aligned}
&\mathbf{P}_1 \leftarrow \mathbf{Q}_1 \\
&\texttt{For i = 2 to n do} \\
&\quad \mathbf{P}_i \leftarrow \mathbf{P}_{i-1}\mathbf{Q}_i \\
&\texttt{enddo}
\end{aligned}$$

Now, since $\mathbf{P}_1$ is identical to $\mathbf{Q}_1$, the first product appearing in the do-loop, $\mathbf{P}_1\mathbf{Q}_2$, is identical to $\mathbf{Q}_1\mathbf{Q}_2$, whose two factors have a special structure. The computation of this product, then, requires special treatment, which warrants further discussion because of its particular features. From the structure of matrices $\mathbf{Q}_i$, as displayed in eq.(4.1e), we have

$$\mathbf{P}_2 \equiv \begin{bmatrix} \cos\theta_1 & -\lambda_1 \sin\theta_1 & \mu_1 \sin\theta_1 \\ \sin\theta_1 & \lambda_1 \cos\theta_1 & -\mu_1 \cos\theta_1 \\ 0 & \mu_1 & \lambda_1 \end{bmatrix} \begin{bmatrix} \cos\theta_2 & -\lambda_2 \sin\theta_2 & \mu_2 \sin\theta_2 \\ \sin\theta_2 & \lambda_2 \cos\theta_2 & -\mu_2 \cos\theta_2 \\ 0 & \mu_2 & \lambda_2 \end{bmatrix}$$

The foregoing product is calculated now by first computing the products $\lambda_1\lambda_2$, $\lambda_1\mu_2$, $\mu_1\mu_2$, and $\lambda_2\mu_1$, which involve only constant quantities, these terms thus being posture-independent. Thus, in tracking a prescribed Cartesian trajectory, the manipulator posture changes continuously, and hence, its joint variables also change. However, its DH parameters, those defining its architecture, remain constant. Therefore, the four above products remain constant and are computed prior to tracking a trajectory, i.e., *off-line*. In computing these products, we store them as

$$\lambda_{12} \equiv \lambda_1\lambda_2, \quad \mu_{21} \equiv \lambda_1\mu_2, \quad \mu_{12} \equiv \mu_1\mu_2, \quad \lambda_{21} \equiv \lambda_2\mu_1$$

Next, we perform the *on-line* computations. First, let[1]

$$\begin{aligned}
\sigma &\leftarrow \lambda_1 \sin\theta_2 \\
\tau &\leftarrow \sin\theta_1 \cos\theta_2 \\
\upsilon &\leftarrow \cos\theta_1 \cos\theta_2 \\
u &\leftarrow \cos\theta_1 \sin\theta_2 + \lambda_1\tau \\
v &\leftarrow \sin\theta_1 \sin\theta_2 - \lambda_1\upsilon
\end{aligned}$$

and hence,

$$\mathbf{P}_2 = \begin{bmatrix} \upsilon - \sigma \sin\theta_1 & -\lambda_2 u + \mu_{12} \sin\theta_1 & \mu_2 u + \lambda_{21} \sin\theta_1 \\ \tau + \sigma \cos\theta_1 & -\lambda_2 v - \mu_{12} \cos\theta_1 & \mu_2 v - \lambda_{21} \cos\theta_1 \\ \mu_1 \sin\theta_2 & \lambda_{21} \cos\theta_2 + \mu_{21} & -\mu_{12} \cos\theta_2 + \lambda_{12} \end{bmatrix}$$

[1] Although υ and v look similar, they should not be confused with each other, the former being the lowercase Greek letter *upsilon*. As a matter of fact, no confusion should arise, because upsilon is used only once, and does not appear further in the book.

As the reader can verify, the foregoing calculations consume 20 multiplications and 10 additions. Now, we proceed to compute the remaining products in the foregoing do-loop.

Here, notice that the product $\mathbf{P}_{i-1}\mathbf{Q}_i$, for $3 \leq i \leq n$, can be computed *recursively*, as described below: Let $\mathbf{P}_{i-1}$ and $\mathbf{P}_i$ be given as

$$\mathbf{P}_{i-1} \equiv \begin{bmatrix} p_{11} & p_{12} & p_{13} \\ p_{21} & p_{22} & p_{23} \\ p_{31} & p_{32} & p_{33} \end{bmatrix}$$

$$\mathbf{P}_i \equiv \begin{bmatrix} p'_{11} & p'_{12} & p'_{13} \\ p'_{21} & p'_{22} & p'_{23} \\ p'_{31} & p'_{32} & p'_{33} \end{bmatrix}$$

Now matrix $\mathbf{P}_i$ is computed by first defining

$$\begin{aligned} u_i &= p_{11}\sin\theta_i - p_{12}\cos\theta_i \\ v_i &= p_{21}\sin\theta_i - p_{22}\cos\theta_i \\ w_i &= p_{31}\sin\theta_i - p_{32}\cos\theta_i \end{aligned} \tag{4.76a}$$

and

$$\begin{aligned} p'_{11} &= p_{11}\cos\theta_i + p_{12}\sin\theta_i \\ p'_{12} &= -u_i\lambda_i + p_{13}\mu_i \\ p'_{13} &= u_i\mu_i + p_{13}\lambda_i \\ p'_{21} &= p_{21}\cos\theta_i + p_{22}\sin\theta_i \\ p'_{22} &= -v_i\lambda_i + p_{23}\mu_i \\ p'_{23} &= v_i\mu_i + p_{23}\lambda_i \\ p'_{31} &= p_{31}\cos\theta_i + p_{32}\sin\theta_i \\ p'_{32} &= -w_i\lambda_i + p_{33}\mu_i \\ p'_{33} &= w_i\mu_i + p_{33}\lambda_i \end{aligned} \tag{4.76b}$$

Computing u_i, v_i, and w_i requires six multiplications and three additions, whereas each of the p'_{ij} entries requires two multiplications and one addition. Hence, the computation of each $\mathbf{P}_i$ matrix requires 24 multiplications and 12 additions, the total number of operations required to compute the $n-2$ products $\{\mathbf{P}_i\}_2^{n-1}$ thus being $24(n-2)+20 = 24n-28$ multiplications and $12(n-2)+10 = 12n-14$ additions, for $n \geq 2$. Moreover, $\mathbf{P}_1$, i.e., $\mathbf{Q}_1$, requires four multiplications and no additions, the total number of multiplications M_A and additions A_A required to compute matrix $\mathbf{A}$ thus being

$$M_A = 24n - 24, \quad A_A = 12n - 14 \tag{4.77}$$

Before concluding this section, a remark is in order: The reader may realize that $\mathbf{P}_n$ is nothing but $\mathbf{Q}$, and hence, the same reader may wonder

whether we could not save some operations in the foregoing computations by stopping the above recursive algorithm at $n-1$, rather than at n. This is not a good idea, for the above equality holds if and only if the manipulator is capable of tracking *perfectly* a given trajectory. However, reality is quite different, and errors are always present when tracking. As a matter of fact, the mismatch between $\mathbf{P}_n$ and $\mathbf{Q}$ is very useful in estimating orientation errors, which are then used in a feedback-control scheme to synthesize the corrective signals that are meant to correct those errors.

Evaluation of Submatrix $\mathbf{B}$

The computation of submatrix $\mathbf{B}$ of the Jacobian is studied here. This submatrix comprises the set of vectors $\{\, \mathbf{e}_i \times \mathbf{r}_i \,\}_1^n$. We thus proceed first to the computation of vectors $\mathbf{r}_i$, for $i = 1, \ldots, n$, which is most efficiently done using a recursive scheme, similar to that of Horner for polynomial evaluation (Henrici, 1964), namely,

$$
\begin{aligned}
&[\,\mathbf{r}_6\,]_6 \leftarrow [\,\mathbf{a}_6\,]_6 \\
&\texttt{For i = 5 to 1 do} \\
&\quad [\,\mathbf{r}_i\,]_i \leftarrow [\,\mathbf{a}_i\,]_i + \mathbf{Q}_i[\,\mathbf{r}_{i+1}\,]_{i+1} \\
&\texttt{enddo}
\end{aligned}
$$

In the foregoing algorithm, a simple scheme is introduced to perform the product $\mathbf{Q}_i[\,\mathbf{r}_{i+1}\,]_{i+1}$, in order to economize operations: if we let $[\,\mathbf{r}_{i+1}\,]_{i+1} = [\,r_1,\, r_2,\, r_3\,]^T$, then

$$
\begin{aligned}
\mathbf{Q}_i[\,\mathbf{r}_{i+1}\,]_{i+1} &= \begin{bmatrix} \cos\theta_i & -\lambda_i \sin\theta_i & \mu_i \sin\theta_i \\ \sin\theta_i & \lambda_i \cos\theta_i & -\mu_i \cos\theta_i \\ 0 & \mu_i & \lambda_i \end{bmatrix} \begin{bmatrix} r_1 \\ r_2 \\ r_3 \end{bmatrix} \\
&= \begin{bmatrix} r_1 \cos\theta_i - u \sin\theta_i \\ r_1 \sin\theta_i + u \cos\theta_i \\ r_2\mu_i + r_3\lambda_i \end{bmatrix}
\end{aligned} \tag{4.78a}
$$

where

$$
u \equiv r_2\lambda_i - r_3\mu_i \tag{4.78b}
$$

Therefore, the product of matrix $\mathbf{Q}_i$ by an arbitrary vector consumes eight multiplications and four additions.

Furthermore, each vector $[\,\mathbf{a}_i\,]_i$, for $i = 1, \ldots, n$, requires two multiplications and no additions, as made apparent from their definitions in eq.(4.3b). Moreover, from the foregoing evaluation of $\mathbf{Q}_i[\,\mathbf{r}_{i+1}\,]_{i+1}$, it is apparent that each vector $\mathbf{r}_i$, in frame $\mathcal{F}_i$, is computed with 10 multiplications and seven additions—two more multiplications are needed to calculate each vector $[\,\mathbf{a}_i\,]_i$ and three more additions are required to add the latter to vector $\mathbf{Q}_i[\,\mathbf{r}_{i+1}\,]_{i+1}$—the whole set of vectors $\{\,\mathbf{r}_i\,\}_1^n$ thus being computed, in $\mathcal{F}_i$-coordinates, with $10(n-1) + 2 = 10n - 8$ multiplications and $7(n-1)$

additions, where one coordinate transformation, that of $\mathbf{r}_1$, is not counted, since this vector is computed directly in $\mathcal{F}_1$.

Now we turn to the transformation of the components of all the foregoing vectors into $\mathcal{F}_1$-coordinates. First, note that we can proceed now in two ways: in the first, we transform the individual vectors $\mathbf{e}_i$ and $\mathbf{r}_i$ from $\mathcal{F}_i$- into $\mathcal{F}_1$-coordinates and then compute their cross product; in the second, we first perform the cross products and then transform each of these products into $\mathcal{F}_1$-coordinates. It is apparent that the second approach is more efficient, which is why we choose it here.

In order to calculate the products $\mathbf{e}_i \times \mathbf{r}_i$ in $\mathcal{F}_i$-coordinates, we let $[\,\mathbf{r}_i\,]_i = [\,\rho_1,\,\rho_2,\,\rho_3\,]^T$. Moreover, $[\,\mathbf{e}_i\,]_i = [\,0,\,0,\,1\,]^T$, and hence,

$$[\,\mathbf{e}_i \times \mathbf{r}_i\,]_i = \begin{bmatrix} -\rho_2 \\ \rho_1 \\ 0 \end{bmatrix}$$

which is thus obtained at no cost. Now, the transformation from $\mathcal{F}_i$- into $\mathcal{F}_1$-coordinates is simply

$$[\,\mathbf{e}_i \times \mathbf{r}_i\,]_1 = \mathbf{P}_{i-1}[\,\mathbf{e}_i \times \mathbf{r}_i\,]_i \tag{4.79}$$

In particular, $[\,\mathbf{e}_1 \times \mathbf{r}_1\,]_1$ needs no transformation, for its two factors are given in $\mathcal{F}_1$-coordinates. The $\mathcal{F}_1$-components of the remaining cross products are computed using the general transformation of eq.(4.79). In the case at hand, this transformation requires, for each i, six multiplications and three additions, for this transformation involves the product of a full 3×3 matrix, $\mathbf{P}_{i-1}$, by a 3-dimensional vector, $\mathbf{e}_i \times \mathbf{r}_i$, whose third component vanishes. Thus, the computation of matrix $\mathbf{B}$ requires M_B multiplications and A_B additions, as given below:

$$M_B = 16n - 14, \quad A_B = 10(n-1) \tag{4.80}$$

In total, then, the evaluation of the complete Jacobian requires M_J multiplications and A_J additions, namely,

$$M_J = 40n - 38, \quad A_J = 22n - 24 \tag{4.81}$$

In particular, for a six-revolute manipulator, these figures are 202 multiplications and 108 additions.

Now, if the manipulator contains some prismatic pairs, the foregoing figures diminish correspondingly. Indeed, if the ith joint is prismatic, then the ith column of the Jacobian matrix changes as indicated in eq.(4.56). Hence, one cross-product calculation is spared, along with the associated coordinate transformation. As a matter of fact, as we saw above, the cross product is computed at no cost in local coordinates, and so each prismatic pair of the manipulator reduces the foregoing numbers of operations by only one coordinate transformation, i.e., by 10 multiplications and seven additions.

4.5.2 Singularity Analysis of Decoupled Manipulators

In performing the computation of the joint rates for a decoupled manipulator, it was assumed that neither $\mathbf{J}_{12}$ nor $\mathbf{J}_{21}$ is singular. If the latter is singular, then none of the joint rates can be evaluated, even if the former is nonsingular. However, if $\mathbf{J}_{21}$ is nonsingular, then eq.(4.66a) can be solved for the arm rates even if $\mathbf{J}_{12}$ is singular. Each of these sub-Jacobians is analyzed for singularities below.

We will start analyzing $\mathbf{J}_{21}$, whose singularity determines whether any joint-rate resolution is possible at all. First, we note from eq.(4.65c) that the columns of $\mathbf{J}_{21}$ are the three vectors $\mathbf{e}_1 \times \mathbf{r}_1$, $\mathbf{e}_2 \times \mathbf{r}_2$, and $\mathbf{e}_3 \times \mathbf{r}_3$. Hence, $\mathbf{J}_{21}$ becomes singular if either these three vectors become coplanar or at least one of them vanishes. Furthermore, neither the relative layout of these three vectors nor their magnitudes change if the manipulator undergoes a motion about the first revolute axis while keeping the second and the third revolute axes locked. This means that θ_1 does not affect the singularity of the manipulator, a result that can also be derived from invariance arguments—see Section 2.6—and by noticing that singularity is, indeed, an invariant property. Hence, whether a configuration is singular or not is independent of the viewpoint of the observer, a change in θ_1 being nothing but a change of viewpoint.

The singularity of a three-revolute arm for positioning tasks was analyzed by Burdick (1995), by recognizing that (*i*) given three arbitrary lines in space, the three revolute axes in our case, it is always possible to find a set of lines that intersects all three, and (*ii*) the moments of the three lines about any point on the intersecting line are all zero. As a matter of fact, the locus of those lines is a quadric ruled surface, namely, a one-sheet hyperboloid—see Exercise 3.4. Therefore, if the endpoint of the third moving link lies in this quadric, the manipulator is in a singular posture, and velocities of C along the intersecting line cannot be produced. This means that the manipulator has lost, to a *first order*, one degree of freedom. Here we emphasize that this loss is meaningful only at a first order because, in fact, a motion along that intersecting line may still be possible, provided that the full nonlinear relations of eq.(4.16) are considered. If such a motion is at all possible, however, then it is so only in one direction, as we shall see in Case 2 below. Motions in the opposite direction are not feasible because of the rigidity of the links.

We will illustrate the foregoing concepts as they pertain to the most common types of industrial manipulators, i.e., those of the orthogonal type. In these cases, two consecutive axes either intersect at right angles or are parallel; most of the time, the first two axes intersect at right angles and the last two are parallel. Below we study each of these cases separately.

Case 1: Two consecutive axes intersect and C lies in their plane. Here, the ruled hyperboloid containing the lines that intersect all

three axes degenerates into a plane, namely, that of the two intersecting axes. For conciseness, let us assume that the first two axes intersect, but the derivations are the same if the intersecting axes are the last two. Moreover, let O_{12} be the intersection of the first two axes, Π_{12} being the plane of these axes and $\mathbf{n}_{12}$ its normal. If we recall the notation adopted in Section 4.5, we have now that the vector directed from O_{12} to C can be regarded as both $\mathbf{r}_1$ and $\mathbf{r}_2$. Furthermore, $\mathbf{e}_1 \times \mathbf{r}_1$ and $\mathbf{e}_2 \times \mathbf{r}_2$ $(= \mathbf{e}_2 \times \mathbf{r}_1)$ are both parallel to $\mathbf{n}_{12}$. Hence, the first two axes can only produce velocities of C in the direction of $\mathbf{n}_{12}$. As a consequence, velocities of C in Π_{12} and perpendicular to $\mathbf{e}_3 \times \mathbf{r}_3$ cannot be produced in the presence of this singularity. The set of infeasible velocities, then, lies in a line normal to $\mathbf{n}_{12}$ and $\mathbf{e}_3 \times \mathbf{r}_3$, whose direction is the geometric representation of the nullspace of $\mathbf{J}_{21}^T$. Likewise, the manipulator can withstand forces applied at C in the direction of the same line purely by reaction wrenches, i.e., without any motor torques. The last issue falls into the realm of manipulator statics, upon which we will elaborate in Section 4.7.

We illustrate this singularity, termed here *shoulder singularity*, in a manipulator with the architecture of Fig. 4.3, as postured in Fig. 4.20. In this figure, the line intersecting all three arm axes is not as obvious and needs further explanation. This line is indicated by $\mathcal{L}$ in that figure, and is parallel to the second and third axes. It is apparent that this line intersects the first axis at right angles at a point I. Now, if we take into account that all parallel lines intersect at infinity, then it becomes apparent that $\mathcal{L}$ intersects the axis of the third revolute as well, and hence, $\mathcal{L}$ intersects all three axes.

Case 2: Two consecutive axes are parallel and C lies in their plane, as shown in Fig. 4.21. For conciseness, again, we assume that the parallel axes are now the last two, a rather common case in commercial manipulators, but the derivations below are the same if the parallel axes are the first two. We now let Π_{23} be the plane of the last two axes and $\mathbf{n}_{23}$ its normal. Furthermore, $\mathbf{e}_3 = \mathbf{e}_2$, $\mathbf{r}_2 = \mathbf{r}_1$, and $\mathbf{e}_2 \times \mathbf{r}_3 = \alpha(\mathbf{e}_2 \times \mathbf{r}_2)$, where

$$\alpha = \frac{\sqrt{a_3^2 + b_4^2}}{a_2 + \sqrt{a_3^2 + b_4^2}}$$

in terms of the Denavit-Hartenberg notation, thereby making apparent that the last two columns of $\mathbf{J}_{21}$ are linearly dependent. Moreover, $\mathbf{e}_2 \times \mathbf{r}_2$ and, consequently, $\mathbf{e}_3 \times \mathbf{r}_3$ are parallel to $\mathbf{n}_{23}$, the last two axes being capable of producing velocities of C only in the direction of $\mathbf{n}_{23}$. Hence, velocities of C in Π_{23} that are normal to $\mathbf{e}_1 \times \mathbf{r}_1$, i.e., along line $\mathcal{L}$, cannot be produced in this configuration, and the manipulator loses, again, to a first-order approximation, one degree of freedom. The set of infeasible velocities, then, is parallel to the line $\mathcal{L}$ of Fig. 4.21, whose direction is the geometric representation of

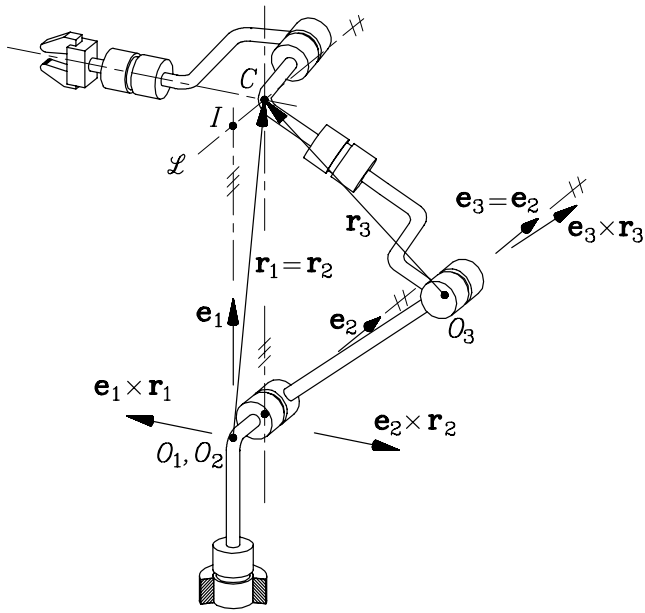

FIGURE 4.20. Shoulder singularity of the Puma robot.

the nullspace of $\mathbf{J}_{21}^T$. The singularity displayed in the foregoing figure, termed here the *elbow singularity*, pertains also to a manipulator with the architecture of Fig. 4.3. Notice that motions along $\mathcal{L}$ in the posture displayed in Fig. 4.21 are possible, but only in one direction, from C to O_2.

With regard to the wrist singularities, these were already studied when solving the orientation problem for the inverse kinematics of decoupled manipulators. Here, we study the same in light of the sub-Jacobian $\mathbf{J}_{12}$ of eq.(4.65b). This sub-Jacobian obviously vanishes when the wrist is so configured that its three revolute axes are coplanar, which thus leads to

$$\mathbf{e}_4 \times \mathbf{e}_5 \cdot \mathbf{e}_6 = 0$$

Note that when studying the orientation problem of decoupled manipulators, we found that orthogonal wrists are singular when the sixth and fourth axes are aligned, in full agreement with the foregoing condition. Indeed, if these two axes are aligned, then $\mathbf{e}_4 = -\mathbf{e}_6$, and the above equation holds.

4.5.3 Manipulator Workspace

The workspace of spherical wrists for orientation tasks was discussed in Subsection 4.4.2. Here we focus on the workspaces of three-axis positioning manipulators in light of their singularities.

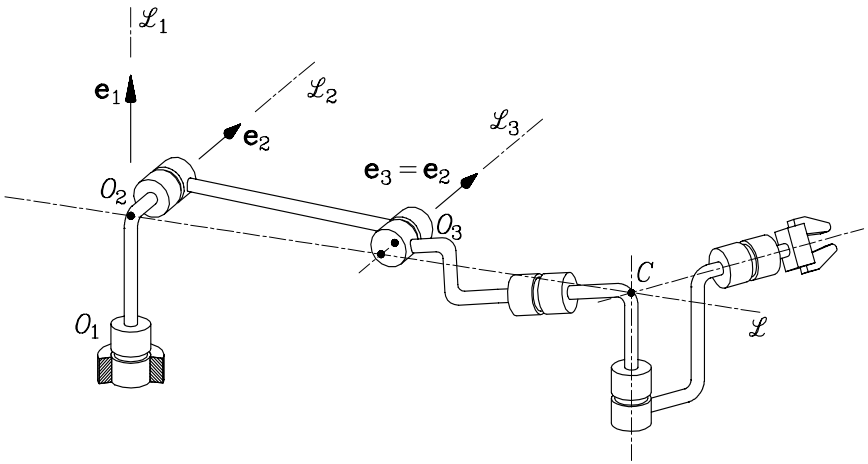

FIGURE 4.21. Elbow singularity of the Puma robot.

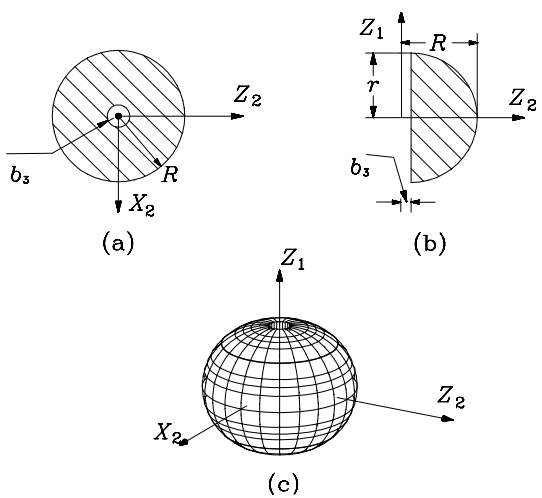

FIGURE 4.22. Workspace of a Puma manipulator (a) top view; (b) side view; (c) perspective.

In order to gain insight into the problem, we study first the workspace of manipulators with the architecture of Fig. 4.3. Figures 4.20 and 4.21 show such a manipulator with point C at the limit of its positioning capabilities in one direction, i.e., at the boundary of its workspace. Moreover, with regard to the posture of Fig. 4.20, it is apparent that the first singularity is preserved if (i) point C moves on a line parallel to the first axis and intersecting the second axis; and (ii) with the second and third joints locked, the first joint goes through a full turn. Under the second motion, the line of the first motion sweeps a circular cylinder whose axis is the first manipulator axis and with radius equal to b_3, the shoulder offset. This cylinder constitutes a part of the workspace boundary, the other part consisting of a spherical surface. Indeed, the second singularity is preserved if (i) with point C in the plane of the second and third axes, the second joint makes a full turn, thereby tracing a circle with center on $\mathcal{L}_2$, a distance b_3 from the first axis, and radius $r = a_2 + \sqrt{a_3^2 + b_4^2}$; and (ii) with point C still in the plane of the second and third joints, the first joint makes a full turn. Under the second motion, the circle generated by the first motion describes a sphere of radius $R = \sqrt{b_3^2 + r^2}$ because any point of that circle lies a distance R from the intersection of the first two axes. This point thus becomes the center of the sphere, which is the second part of the workspace, as shown in Fig. 4.22.

The determination of the workspace boundaries of more general manipulators requires, obviously, more general approaches, like that proposed by Ceccarelli (1996). By means of an alternative approach, Ranjbaran et al. (1992) found the workspace boundary with the aid of the general characteristic equation of a three-revolute manipulator. This equation is a quartic polynomial, as displayed in eq.(4.25). From the discussion of Subsection 4.4.1, it is apparent that at singularities, two distinct roots of the IKP merge into a single one. This happens at points where the plot of the characteristic polynomial of eq.(4.25) is tangent to the τ_3 axis, which occurs in turn at points where the derivative of this polynomial with respect to τ_3 vanishes. The condition for θ_3 to correspond to a point C on the boundary of the workspace is, then, that both the characteristic polynomial and its derivative with respect to τ_3 vanish concurrently. These two polynomials are displayed below:

$$P(\tau_3) \equiv R\tau_3^4 + S\tau_3^3 + T\tau_3^2 + U\tau_3 + V = 0 \tag{4.82a}$$

$$P'(\tau_3) \equiv 4R\tau_3^3 + 3S\tau_3^2 + 2T\tau_3 + U = 0 \tag{4.82b}$$

with coefficients R, S, T, U, and V defined in eqs.(4.26a–e). From these equations and eqs.(4.19d–f) and (4.20d–f), it is apparent that the foregoing coefficients are solely functions of the manipulator architecture and the Cartesian coordinates of point C. Moreover, from the same equations, it is clear that the above coefficients are all *quadratic* in $\rho^2 \equiv x_C^2 + y_C^2$ and *quartic* in z_C. Thus, since the Cartesian coordinates x_C and y_C do not

appear in the foregoing coefficients explicitly, the workspace is symmetric about the Z_1 axis, a result to be expected by virtue of the independence of singularities from angle θ_1. Hence, the workspace boundary is given by a function $f(\rho^2, z_C) = 0$ that can be derived by eliminating τ_3 from eqs.(4.82a & b). This can be readily done by resorting to any elimination procedure, the simplest one being *dialytic elimination*, as discussed below.

In order to eliminate τ_3 from the above two equations, we proceed in two steps: In the first step, six additional polynomial equations are derived from eqs.(4.82a & b) by multiplying the two sides of each of these equations by τ_3, τ_3^2, and τ_3^3, thereby obtaining a total of eight polynomial equations in τ_3, namely,

$$\begin{aligned}
R\tau_3^7 + S\tau_3^6 + T\tau_3^5 + U\tau_3^4 + V\tau_3^3 &= 0\\
4R\tau_3^6 + 3S\tau_3^5 + 2T\tau_3^4 + U\tau_3^3 &= 0\\
R\tau_3^6 + S\tau_3^5 + T\tau_3^4 + U\tau_3^3 + V\tau_3^2 &= 0\\
4R\tau_3^5 + 3S\tau_3^4 + 2T\tau_3^3 + U\tau_3^2 &= 0\\
R\tau_3^5 + S\tau_3^4 + T\tau_3^3 + U\tau_3^2 + V\tau_3 &= 0\\
4R\tau_3^4 + 3S\tau_3^3 + 2T\tau_3^2 + U\tau_3 &= 0\\
R\tau_3^4 + S\tau_3^3 + T\tau_3^2 + U\tau_3 + V &= 0\\
4R\tau_3^3 + 3S\tau_3^2 + 2T\tau_3 + U &= 0
\end{aligned}$$

In the second elimination step we write the above eight equations in *linear homogeneous form*, namely,

$$\mathbf{M}\boldsymbol{\tau}_3 = \mathbf{0} \tag{4.83a}$$

with the 8×8 matrix $\mathbf{M}$ and the 8-dimensional vector $\boldsymbol{\tau}_3$ defined as

$$\mathbf{M} \equiv \begin{bmatrix}
R & S & T & U & V & 0 & 0 & 0\\
0 & 4R & 3S & 2T & U & 0 & 0 & 0\\
0 & R & S & T & U & V & 0 & 0\\
0 & 0 & 4R & 3S & 2T & U & 0 & 0\\
0 & 0 & R & S & T & U & V & 0\\
0 & 0 & 0 & 4R & 3S & 2T & U & 0\\
0 & 0 & 0 & R & S & T & U & V\\
0 & 0 & 0 & 0 & 4R & 3S & 2T & U
\end{bmatrix}, \quad \boldsymbol{\tau}_3 = \begin{bmatrix}
\tau_3^7\\ \tau_3^6\\ \tau_3^5\\ \tau_3^4\\ \tau_3^3\\ \tau_3^2\\ \tau_3\\ 1
\end{bmatrix} \tag{4.83b}$$

It is now apparent that any feasible solution of eq.(4.83a) must be nontrivial, and hence, $\mathbf{M}$ must be singular. The desired boundary equation is then derived from the singularity condition on $\mathbf{M}$, i.e.,

$$f(\rho^2, z_C) \equiv \det(\mathbf{M}) = 0 \tag{4.84}$$

Note that all entries of matrix $\mathbf{M}$ are linear in the coefficients R, S, ..., V, which are, in turn, quadratic in ρ^2 and quartic in z_C. Therefore, the workspace boundary is a surface of 16th degree in ρ^2 and of 32nd degree in z_C.

We used the foregoing procedure, with the help of symbolic computations, to obtain a rendering of the workspace boundary of the manipulator of Figs. 4.13–4.15, the workspace thus obtained being displayed in Fig. 4.23.

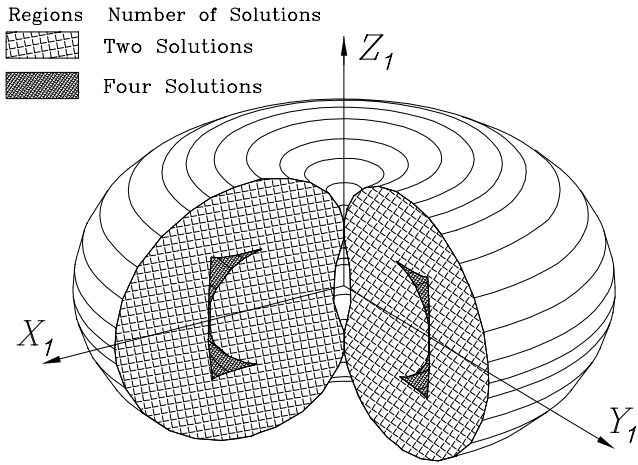

FIGURE 4.23. The workspace of the manipulator of Figs. 4. 17–19.

4.6 Acceleration Analysis of Serial Manipulators

The subject of this section is the computation of vector $\ddot{\boldsymbol{\theta}}$ of second joint-variable derivatives, also called the *joint accelerations*. This vector is computed from Cartesian position, velocity, and acceleration data. To this end, both sides of eq.(4.53) are differentiated with respect to time, thus obtaining

$$\mathbf{J}\ddot{\boldsymbol{\theta}} = \dot{\mathbf{t}} - \dot{\mathbf{J}}\dot{\boldsymbol{\theta}} \tag{4.85}$$

and hence,

$$\ddot{\boldsymbol{\theta}} = \mathbf{J}^{-1}(\dot{\mathbf{t}} - \dot{\mathbf{J}}\dot{\boldsymbol{\theta}}) \tag{4.86}$$

From eq.(4.85), it is clear that the joint-acceleration vector is computed in exactly the same way as the joint-rate vector. In fact, the LU decomposition of $\mathbf{J}$ is the same in this case and hence, need not be recomputed. All that is needed is the solution of a lower- and an upper-triangular system, namely,

$$\mathbf{Lz} = \dot{\mathbf{t}} - \dot{\mathbf{J}}\dot{\boldsymbol{\theta}}, \quad \mathbf{U}\ddot{\boldsymbol{\theta}} = \mathbf{z}$$

The two foregoing systems are solved first for $\mathbf{z}$ and then for $\ddot{\boldsymbol{\theta}}$ by forward and backward substitution, respectively. The first of the foregoing systems is solved with M_n'' multiplications and A_n'' additions; the second with M_n''' multiplications and A_n''' additions. These figures appear in eqs.(4.62b & c). Thus, the total numbers of multiplications, M_t, and additions, A_t, that the forward and backward solutions of the aforementioned systems require are

$$M_t = n^2, \quad A_t = n(n-1) \tag{4.87}$$

In eq.(4.85), the right-hand side comprises two terms, the first being the specified time-rate of change of the twist of the EE, or twist-rate, for brevity,

which is readily available. The second term is not available and must be computed. This term involves the product of the time-derivative of $\mathbf{J}$ times the previously computed joint-rate vector. Hence, in order to evaluate the right-hand side of that equation, all that is further required is $\dot{\mathbf{J}}$. From eq.(4.54a), one has

$$\dot{\mathbf{J}} = \begin{bmatrix} \dot{\mathbf{A}} \\ \dot{\mathbf{B}} \end{bmatrix}$$

where, from eqs.(4.51a & b),

$$\dot{\mathbf{A}} = [\, \dot{\mathbf{e}}_1 \quad \dot{\mathbf{e}}_2 \quad \cdots \quad \dot{\mathbf{e}}_n \,] \tag{4.88a}$$

$$\dot{\mathbf{B}} = [\, \dot{\mathbf{u}}_1 \quad \dot{\mathbf{u}}_2 \quad \cdots \quad \dot{\mathbf{u}}_n \,] \tag{4.88b}$$

and $\mathbf{u}_i$ denotes $\mathbf{e}_i \times \mathbf{r}_i$, for $i = 1, 2, \ldots, n$. Moreover,

$$\dot{\mathbf{e}}_1 = \boldsymbol{\omega}_0 \times \mathbf{e}_1 = \mathbf{0} \tag{4.89a}$$

$$\dot{\mathbf{e}}_i = \boldsymbol{\omega}_{i-1} \times \mathbf{e}_i \equiv \boldsymbol{\omega}_i \times \mathbf{e}_i, \quad i = 2, 3, \ldots, n \tag{4.89b}$$

and

$$\dot{\mathbf{u}}_i = \dot{\mathbf{e}}_i \times \mathbf{r}_i + \mathbf{e}_i \times \dot{\mathbf{r}}_i, \quad i = 1, 2, \ldots, n \tag{4.89c}$$

Next, an expression for $\dot{\mathbf{r}}_i$ is derived by time-differentiating both sides of eq.(4.50), which produces

$$\dot{\mathbf{r}}_i = \dot{\mathbf{a}}_i + \dot{\mathbf{a}}_{i+1} + \cdots + \dot{\mathbf{a}}_n, \quad i = 1, 2, \ldots n$$

Recalling eq.(4.48), the above equation reduces to

$$\dot{\mathbf{r}}_i = \boldsymbol{\omega}_i \times \mathbf{a}_i + \boldsymbol{\omega}_{i+1} \times \mathbf{a}_{i+1} + \cdots + \boldsymbol{\omega}_n \times \mathbf{a}_n \tag{4.90}$$

Substitution of eqs.(4.89) and (4.90) into eqs.(4.88a & b) leads to

$$\dot{\mathbf{A}} = [\, \mathbf{0} \quad \boldsymbol{\omega}_1 \times \mathbf{e}_2 \quad \cdots \quad \boldsymbol{\omega}_{n-1} \times \mathbf{e}_n \,]$$

$$\dot{\mathbf{B}} = [\, \mathbf{e}_1 \times \dot{\mathbf{r}}_1 \quad \boldsymbol{\omega}_{12} \times \mathbf{r}_2 + \mathbf{e}_2 \times \dot{\mathbf{r}}_2 \quad \cdots \quad \boldsymbol{\omega}_{n-1,n} \times \mathbf{r}_n + \mathbf{e}_n \times \dot{\mathbf{r}}_n \,]$$

with $\dot{\mathbf{r}}_k$ and $\boldsymbol{\omega}_{k,k+1}$ defined as

$$\dot{\mathbf{r}}_k \equiv \sum_{k}^{n} \boldsymbol{\omega}_i \times \mathbf{a}_i, \quad k = 1, \ldots, n \tag{4.91a}$$

$$\boldsymbol{\omega}_{k,k+1} \equiv \boldsymbol{\omega}_k \times \mathbf{e}_{k+1}, \quad k = 1, \ldots, n-1 \tag{4.91b}$$

The foregoing expressions are invariant and hence, valid in any coordinate frame. However, they are going to be incorporated into matrix $\dot{\mathbf{J}}$, and then the latter is to be multiplied by vector $\dot{\boldsymbol{\theta}}$, as indicated in eq.(4.85). Thus, eventually all columns of both $\dot{\mathbf{A}}$ and $\dot{\mathbf{B}}$ will have to be represented in the same coordinate frame. Hence, coordinate transformations will have to be introduced in the foregoing matrix columns in order to have all of these

represented in the same coordinate frame, say, the first one. We then have the expansion below:

$$\dot{\mathbf{J}}\dot{\boldsymbol{\theta}} = \dot{\theta}_1 \begin{bmatrix} \mathbf{0} \\ \dot{\mathbf{u}}_1 \end{bmatrix} + \dot{\theta}_2 \begin{bmatrix} \dot{\mathbf{e}}_2 \\ \dot{\mathbf{u}}_2 \end{bmatrix} + \cdots + \dot{\theta}_n \begin{bmatrix} \dot{\mathbf{e}}_n \\ \dot{\mathbf{u}}_n \end{bmatrix} \tag{4.92}$$

The right-hand side of eq.(4.92) is computed recursively as described below in five steps, the number of operations required being included at the end of each step.

1. Compute $\{\,[\,\boldsymbol{\omega}_i\,]_i\,\}_1^n$:

   $[\,\boldsymbol{\omega}_1\,]_1 \;\leftarrow\; \dot{\theta}_1[\,\mathbf{e}_1\,]_1$

   `For i = 1 to n − 1 do`

   $[\,\boldsymbol{\omega}_{i+1}\,]_{i+1} \;\leftarrow \dot{\theta}_{i+1}[\,\mathbf{e}_{i+1}\,]_{i+1} + \mathbf{Q}_i^T[\,\boldsymbol{\omega}_i\,]_i$

   `enddo` $\qquad 8(n-1)\,M \;\&\; 5(n-1)\,A$

2. Compute $\{\,[\,\dot{\mathbf{e}}_i\,]_i\,\}_1^n$:

   $[\,\dot{\mathbf{e}}_1\,]_1 \;\leftarrow\; [\,\mathbf{0}\,]_1$

   `For i = 2 to n do`

   $[\,\dot{\mathbf{e}}_i\,]_i \;\leftarrow [\,\boldsymbol{\omega}_i \times \mathbf{e}_i\,]_i$

   `enddo` $\qquad 0M \;\&\; 0A$

3. Compute $\{\,[\,\dot{\mathbf{r}}_i\,]_i\,\}_1^n$:

   $[\,\dot{\mathbf{r}}_n\,]_n \;\leftarrow [\,\boldsymbol{\omega}_n \times \mathbf{a}_n\,]_n$

   `For i = n − 1 to 1 do`

   $[\,\dot{\mathbf{r}}_i\,]_i \;\leftarrow [\,\boldsymbol{\omega}_i \times \mathbf{a}_i\,]_i + \mathbf{Q}_i[\,\dot{\mathbf{r}}_{i+1}\,]_{i+1}$

   `enddo` $\qquad (14n-8)M \;\&\; (10n-7)A$

4. Compute $\{\,[\,\dot{\mathbf{u}}_i\,]_i\,\}_1^n$ using the expression appearing in eq.(4.89c):

   $[\,\dot{\mathbf{u}}_1\,]_1 \;\leftarrow [\,\mathbf{e}_1 \times \dot{\mathbf{r}}_1\,]_1$ $\qquad$ `For i = 2 to n do`

   $[\,\dot{\mathbf{u}}_i\,]_i \;\leftarrow [\,\dot{\mathbf{e}}_i \times \mathbf{r}_i + \mathbf{e}_i \times \dot{\mathbf{r}}_i\,]_i$

   `enddo` $\qquad 4(n-1)\,M \;\&\; 3(n-1)\,A$

5. Compute $\dot{\mathbf{J}}\dot{\boldsymbol{\theta}}$:

   Let $\mathbf{v} \equiv \dot{\mathbf{J}}\dot{\boldsymbol{\theta}}$, which is a 6-dimensional vector. A coordinate transformation of its two 3-dimensional vector components will be implemented using the 6×6 matrices $\mathbf{U}_i$, which are defined as

$$\mathbf{U}_i \equiv \begin{bmatrix} \mathbf{Q}_i & \mathbf{O} \\ \mathbf{O} & \mathbf{Q}_i \end{bmatrix}$$

   where $\mathbf{O}$ stands for the 3×3 zero matrix. Thus, the foregoing 6×6 matrices are block-diagonal, their diagonal blocks being simply matrices $\mathbf{Q}_i$. One then has the algorithm below:

$$[\,\mathbf{v}\,]_n \;\leftarrow \dot{\theta}_n \begin{bmatrix} \dot{\mathbf{e}}_n \\ \dot{\mathbf{u}}_n \end{bmatrix}_n$$

   `For i = n - 1 to 1 do`

$$[\,\mathbf{v}\,]_i \;\leftarrow\; \dot{\theta}_i \begin{bmatrix} \dot{\mathbf{e}}_i \\ \dot{\mathbf{u}}_i \end{bmatrix}_i + \mathbf{U}_i [\,\mathbf{v}\,]_{i+1}$$

   `enddo`

$$\dot{\mathbf{J}}\dot{\boldsymbol{\theta}} \leftarrow [\,\mathbf{v}\,]_1 \qquad\qquad 21(n-1) + 4\,M \;\&\; 13(n-1)\,A$$

   thereby completing the computation of $\dot{\mathbf{J}}\dot{\boldsymbol{\theta}}$.

The figures given above for the floating-point operations involved were obtained based on a few facts, namely,

1. It is recalled that $[\,\mathbf{e}_i\,]_i = [\,0,\, 0,\, 1\,]^T$. Moreover, if we let $[\,\mathbf{w}\,]_i = [\,w_x,\, w_y,\, w_z\,]^T$ be an arbitrary 3-dimensional vector, then

$$[\,\mathbf{e}_i \times \mathbf{w}\,]_i = \begin{bmatrix} -w_y \\ w_x \\ 0 \end{bmatrix}$$

   this product thus requiring zero multiplications and zero additions.

2. $[\,\dot{\mathbf{e}}_i\,]_i$, computed as in eq.(4.89b), takes on the form $[\,\omega_y,\, -\omega_x,\, 0\,]^T$, where ω_x and ω_y are the X_i and Y_i components of $\boldsymbol{\omega}_i$. Moreover, let $[\,\mathbf{r}_i\,]_i = [\,x,\, y,\, z\,]^T$. Then

$$[\,\dot{\mathbf{e}}_i \times \mathbf{r}_i\,]_i = \begin{bmatrix} -z\omega_x \\ -z\omega_y \\ x\omega_x + y\omega_y \end{bmatrix}$$

   and this product is computed with four multiplications and one addition.

3. As found in Subsection 4.5.1, any coordinate transformation from $\mathcal{F}_i$ to $\mathcal{F}_{i+1}$, or vice versa, of any 3-dimensional vector is computed with eight multiplications and four additions.

Thus, the total numbers of multiplications and additions required to compute $\dot{\mathbf{J}}\dot{\boldsymbol{\theta}}$ in frame $\mathcal{F}_1$, denoted by M_J and A_J, respectively, are as shown below:

$$M_J = 47n - 37, \quad A_J = 31n - 28$$

Since the right-hand side of eq.(4.85) involves the algebraic sum of two 6-dimensional vectors, then, the total numbers of multiplications and additions needed to compute the aforementioned right-hand side, denoted by M_r and A_r, are

$$M_r = 47n - 37, \quad A_r = 31n - 22$$

These figures yield 245 multiplications and 164 additions for a six-revolute manipulator of arbitrary architecture. Finally, if the latter figures are added to those of eq.(4.87), one obtains the numbers of multiplications and additions required for an acceleration resolution of a six-revolute manipulator of arbitrary architecture as

$$M_a = 281, \quad A_a = 194$$

Furthermore, for six-axis, decoupled manipulators, the operation counts of steps 1 and 2 above do not change. However, step 3 is reduced by 42 multiplications and 30 additions, whereas step 4 by 12 multiplications and 9 additions. Moreover, step 5 is reduced by 63 multiplications and 39 additions. With regard to the solution of eq.(4.85) for $\ddot{\boldsymbol{\theta}}$, an additional reduction of *floating-point operations*, or flops, is obtained, for now we need only 18 multiplications and 12 additions to solve two systems of three equations with three unknowns, thereby saving 18 multiplications and 18 additions. Thus, the corresponding figures for such a manipulator, M'_a and A'_a, respectively, are

$$M'_a = 146, \quad A'_a = 98$$

4.7 Static Analysis of Serial Manipulators

In this section, the static analysis of a serial n-axis manipulator is undertaken, particular attention being given to six-axis, decoupled manipulators. Let τ_i be the torque acting at the ith revolute or the force acting at the ith prismatic pair. Moreover, let $\boldsymbol{\tau}$ be the n-dimensional vector of joint forces and torques, whose ith component is τ_i, whereas $\mathbf{w} = [\,\mathbf{n}^T, \mathbf{f}^T\,]^T$ denotes the wrench acting on the EE, with $\mathbf{n}$ denoting the resultant moment and $\mathbf{f}$ the resultant force applied at point P of the end-effector of the manipulator

of Fig. 4.19. Then the power exerted on the manipulator by all forces and moments acting on the end-effector is

$$\Pi_E = \mathbf{w}^T\mathbf{t} = \mathbf{n}^T\boldsymbol{\omega} + \mathbf{f}^T\dot{\mathbf{p}}$$

whereas the power exerted on the manipulator by all joint motors, Π_J, is

$$\Pi_J = \boldsymbol{\tau}^T\dot{\boldsymbol{\theta}} \tag{4.93}$$

Under static, conservative conditions, there is neither power dissipation nor change in the kinetic energy of the manipulator, and hence, the two foregoing powers are equal, which is just a restatement of the *First Law of Thermodynamics* or equivalently, the *Principle of Virtual Work*, i.e.,

$$\mathbf{w}^T\mathbf{t} = \boldsymbol{\tau}^T\dot{\boldsymbol{\theta}} \tag{4.94a}$$

Upon substitution of eq.(4.53) into eq.(4.94a), we obtain

$$\mathbf{w}^T\mathbf{J}\dot{\boldsymbol{\theta}} = \boldsymbol{\tau}^T\dot{\boldsymbol{\theta}} \tag{4.94b}$$

which is a relation valid for arbitrary $\dot{\boldsymbol{\theta}}$. Under these conditions, if $\mathbf{J}$ is not singular, eq.(4.94b) leads to

$$\mathbf{J}^T\mathbf{w} = \boldsymbol{\tau} \tag{4.95}$$

This equation relates the wrench acting on the EE with the joint forces and torques exerted by the actuators. Therefore, this equation finds applications in the *sensing* of the wrench $\mathbf{w}$ acting on the EE by means of torque sensors located at the revolute axes. These sensors measure the motor-supplied torques via the current flowing through the motor armatures, the sensor readouts being the joint torques—or forces, in the case of prismatic joints—$\{\,\tau_k\,\}_1^n$, grouped into vector $\boldsymbol{\tau}$.

For a six-axis manipulator, in the absence of singularities, the foregoing equation can be readily solved for $\mathbf{w}$ in the form

$$\mathbf{w} = \mathbf{J}^{-T}\boldsymbol{\tau}$$

where $\mathbf{J}^{-T}$ stands for the inverse of $\mathbf{J}^T$. Thus, using the figures recorded in eq.(4.61b), $\mathbf{w}$ can be computed from eq.(4.95) with 127 multiplications and 100 additions for a manipulator of arbitrary architecture. However, if the manipulator is of the decoupled type, the Jacobian takes on the form appearing in eq.(4.64), and hence, the foregoing computation can be performed in two steps, namely,

$$\begin{aligned}\mathbf{J}_{12}^T\mathbf{n}_w &= \boldsymbol{\tau}_w\\ \mathbf{J}_{21}^T\mathbf{f} &= \boldsymbol{\tau}_a - \mathbf{J}_{11}^T\mathbf{n}_w\end{aligned}$$

where $\mathbf{n}_w$ is the resultant moment acting on the end-effector when $\mathbf{f}$ is applied at the center of the wrist, while $\boldsymbol{\tau}$ has been partitioned as

$$\boldsymbol{\tau} \equiv \begin{bmatrix}\boldsymbol{\tau}_a\\ \boldsymbol{\tau}_w\end{bmatrix}$$

with $\boldsymbol{\tau}_a$ and $\boldsymbol{\tau}_w$ defined as the wrist and the arm torques, respectively. These two vectors are given, in turn, as

$$\boldsymbol{\tau}_a = \begin{bmatrix} \tau_1 \\ \tau_2 \\ \tau_3 \end{bmatrix}, \quad \boldsymbol{\tau}_w = \begin{bmatrix} \tau_4 \\ \tau_5 \\ \tau_6 \end{bmatrix}$$

Hence, the foregoing calculations, as pertaining to a six-axis, decoupled manipulator, are performed with 55 multiplications and 37 additions, which follows from a result that was derived in Section 4.5 and is summarized in eq.(4.68).

In solving for the wrench acting on the EE from the above relations, the wrist equilibrium equation is first solved for $\mathbf{n}_w$, thus obtaining

$$\mathbf{n}_w = \mathbf{J}_{12}^{-T} \boldsymbol{\tau}_w \tag{4.96}$$

where $\mathbf{J}_{12}^{-T}$ stands for the inverse of $\mathbf{J}_{12}^{T}$, and is available in eq.(4.74). Therefore,

$$\begin{aligned} \mathbf{n}_w &= \frac{1}{\Delta_{12}} [\, (\mathbf{e}_5 \times \mathbf{e}_6) \quad (\mathbf{e}_6 \times \mathbf{e}_4) \quad (\mathbf{e}_4 \times \mathbf{e}_5) \,] \, \boldsymbol{\tau}_w \\ &= \frac{1}{\Delta_{12}} [\, \tau_4 (\mathbf{e}_5 \times \mathbf{e}_6) + \tau_5 (\mathbf{e}_6 \times \mathbf{e}_4) + \tau_6 (\mathbf{e}_4 \times \mathbf{e}_5) \,] \end{aligned} \tag{4.97}$$

Now, if we let

$$\overline{\boldsymbol{\tau}}_a \equiv \boldsymbol{\tau}_a - \mathbf{J}_{11}^{T} \mathbf{n}_w \tag{4.98}$$

we have, from eq.(4.73),

$$\mathbf{f} = [\, \mathbf{u}_2 \times \mathbf{u}_3 \quad \mathbf{u}_3 \times \mathbf{u}_1 \quad \mathbf{u}_1 \times \mathbf{u}_2 \,] \, \frac{\overline{\boldsymbol{\tau}}_a}{\Delta_{21}}$$

where

$$\mathbf{u}_i \equiv \mathbf{e}_i \times \mathbf{r}_i$$

or

$$\mathbf{f} = \frac{1}{\Delta_{21}} [\, \overline{\tau}_1 (\mathbf{u}_2 \times \mathbf{u}_3) + \overline{\tau}_2 (\mathbf{u}_3 \times \mathbf{u}_1) + \overline{\tau}_3 (\mathbf{u}_1 \times \mathbf{u}_2) \,] \tag{4.99}$$

4.8 Planar Manipulators

Shown in Fig. 4.24 is a three-axis planar manipulator. Note that in this case, the DH parameters b_i and α_i vanish, for $i = 1, 2, 3$, the nonvanishing parameters a_i being indicated in the same figure. Below we proceed with the displacement, velocity, acceleration, and static analyses of this manipulator. Here, we recall a few relations of planar mechanics that will be found useful in the discussion below.

A 2×2 matrix $\mathbf{A}$ can be partitioned either columnwise or rowwise, as shown below:

$$\mathbf{A} \equiv [\,\mathbf{a} \quad \mathbf{b}\,] \equiv \begin{bmatrix} \mathbf{c}^T \\ \mathbf{d}^T \end{bmatrix}$$

where $\mathbf{a}$, $\mathbf{b}$, $\mathbf{c}$, and $\mathbf{d}$ are all 2-dimensional column vectors. Furthermore, let $\mathbf{E}$ be defined as an orthogonal matrix rotating 2-dimensional vectors through an angle of 90° counterclockwise. Hence,

$$\mathbf{E} \equiv \begin{bmatrix} 0 & -1 \\ 1 & 0 \end{bmatrix} \tag{4.100}$$

We thus have

Fact 4.8.1

$$\mathbf{E}^{-1} = \mathbf{E}^T = -\mathbf{E}$$

and hence,

Fact 4.8.2

$$\mathbf{E}^2 = -\mathbf{1}$$

where $\mathbf{1}$ *is the* 2×2 *identity matrix.*

Moreover,

Fact 4.8.3

$$\det(\mathbf{A}) = -\mathbf{a}^T\mathbf{E}\mathbf{b} = \mathbf{b}^T\mathbf{E}\mathbf{a} = -\mathbf{c}^T\mathbf{E}\mathbf{d} = \mathbf{d}^T\mathbf{E}\mathbf{c}$$

and

Fact 4.8.4

$$\mathbf{A}^{-1} = \frac{1}{\det(\mathbf{A})}\begin{bmatrix} \mathbf{b}^T \\ -\mathbf{a}^T \end{bmatrix}\mathbf{E} = \frac{1}{\det(\mathbf{A})}\mathbf{E}\,[\,-\mathbf{d} \quad \mathbf{c}\,]$$

4.8.1 Displacement Analysis

The inverse kinematics of the manipulator at hand now consists of determining the values of angles θ_i, for $i = 1, 2, 3$, that will place the end-effector so that its operation point P will be positioned at the prescribed Cartesian coordinates x, y and be oriented at a given angle ϕ with the X axis of Fig. 4.24. Note that this manipulator can be considered as decoupled, for the end-effector can be placed at the desired pose by first positioning point O_3 with the aid of the first two joints and then orienting it with the third joint only. We then solve for the joint angles in two steps, one for positioning and one for orienting.

We now have, from the geometry of Fig. 4.24,

$$a_1c_1 + a_2c_{12} = x$$
$$a_1s_1 + a_2s_{12} = y$$

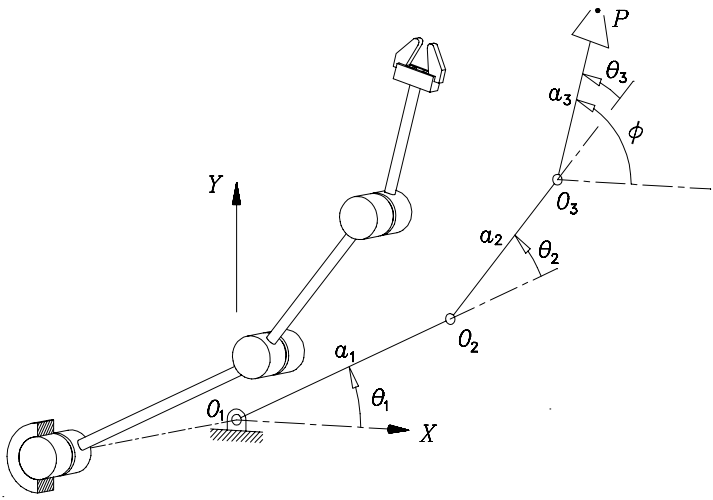

FIGURE 4.24. Three-axis planar manipulator.

where x and y denote the Cartesian coordinates of point O_3, while c_{12} and s_{12} stand for $\cos(\theta_1+\theta_2)$ and $\sin(\theta_1+\theta_2)$, respectively. We have thus derived two equations for the two unknown angles, from which we can determine these angles in various ways. For example, we can solve the problem using a semigraphical approach similar to that of Subsection 8.2.2.

Indeed, from the two foregoing equations we can eliminate both c_{12} and s_{12} by solving for the second terms of the left-hand sides of those equations, namely,

$$a_2 c_{12} = x - a_1 c_1 \tag{4.101a}$$

$$a_2 s_{12} = y - a_1 s_1 \tag{4.101b}$$

If both sides of the above two equations are now squared, then added,

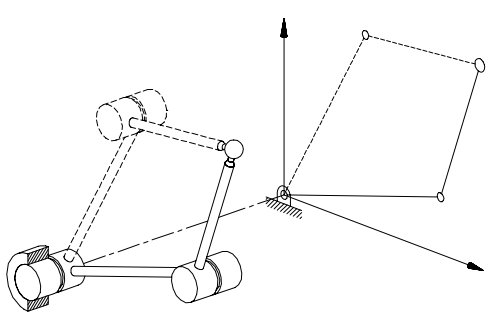

FIGURE 4.25. The two real solutions of a planar manipulator.

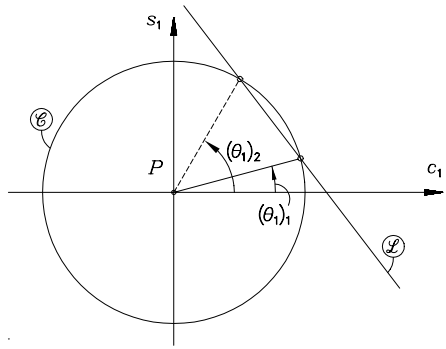

FIGURE 4.26. The two real values of θ_1 depicted in Fig. 4.25.

and the ensuing sum is equated to a_2^2, we obtain, after simplification, a linear equation in c_1 and s_1 that represents a line $\mathcal{L}$ in the c_1-s_1 plane:

$$\mathcal{L}: \qquad -a_1^2 + a_2^2 + 2a_1 x c_1 + 2a_1 y s_1 - (x^2 + y^2) = 0 \tag{4.102}$$

Clearly, the two foregoing variables are constrained by a quadratic equation defining a circle $\mathcal{C}$ in the same plane:

$$\mathcal{C}: \qquad c_1^2 + s_1^2 = 1$$

which is a circle $\mathcal{C}$ of unit radius centered at the origin of the aforementioned plane. The real roots of interest are then obtained as the intersections of $\mathcal{L}$ and $\mathcal{C}$. Thus, the problem can admit (i) two real and distinct roots, if the line and the circle intersect; (ii) one repeated root if the line is tangent to the circle; and (iii) no real root if the line does not intersect the circle.

With c_1 and s_1 known, angle θ_1 is fully determined. Note that the two real intersections of $\mathcal{L}$ with $\mathcal{C}$ provide each one value of θ_1, as depicted in Fig. 4.26.

Once θ_1 and θ_2 are available, θ_3 is readily derived from the geometry of Fig. 4.24, namely,

$$\theta_3 = \phi - (\theta_1 + \theta_2)$$

and hence, each pair of (θ_1, θ_2) values yields one single value for θ_3. Since we have two such pairs, the problem admits two real solutions.

4.8.2 Velocity Analysis

Velocity analysis is most easily accomplished if the general velocity relations derived in Section 4.5 are recalled and adapted to planar manipulators. Thus we have, as in eq.(4.53),

$$\mathbf{J}\dot{\boldsymbol{\theta}} = \mathbf{t} \tag{4.103a}$$

where now,

$$\mathbf{J} \equiv \begin{bmatrix} \mathbf{e}_1 & \mathbf{e}_2 & \mathbf{e}_3 \\ \mathbf{e}_1 \times \mathbf{r}_1 & \mathbf{e}_2 \times \mathbf{r}_2 & \mathbf{e}_3 \times \mathbf{r}_3 \end{bmatrix}, \quad \dot{\boldsymbol{\theta}} \equiv \begin{bmatrix} \dot{\theta}_1 \\ \dot{\theta}_2 \\ \dot{\theta}_3 \end{bmatrix}, \quad \mathbf{t} \equiv \begin{bmatrix} \boldsymbol{\omega} \\ \dot{\mathbf{p}} \end{bmatrix} \tag{4.103b}$$

and $\{ \mathbf{r}_i \}_1^3$ are defined as in eq.(4.50), i.e., as the vectors directed from O_i to P. As in the previous subsection, we assume here that the manipulator moves in the X-Y plane, and hence, all revolute axes are parallel to the Z axis, vectors $\mathbf{e}_i$ and $\mathbf{r}_i$, for $i = 1, 2, 3$, thus taking on the forms

$$\mathbf{e}_1 = \mathbf{e}_2 = \mathbf{e}_3 = \mathbf{e} \equiv \begin{bmatrix} 0 \\ 0 \\ 1 \end{bmatrix}, \quad \mathbf{r}_i = \begin{bmatrix} x_i \\ y_i \\ 0 \end{bmatrix}$$

with $\mathbf{t}$ reducing to

$$\mathbf{t} = [\, 0 \quad 0 \quad \dot{\phi} \quad \dot{x}_P \quad \dot{y}_P \quad 0 \,]^T \tag{4.103c}$$

in which $\dot{x}_P$ and $\dot{y}_P$ denote the components of the velocity of P. Thus,

$$\mathbf{e}_i \times \mathbf{r}_i = \begin{bmatrix} -y_i \\ x_i \\ 0 \end{bmatrix}$$

and hence, the foregoing cross product can be expressed as

$$\mathbf{e}_i \times \mathbf{r}_i = \begin{bmatrix} \mathbf{E}\mathbf{s}_i \\ 0 \end{bmatrix}$$

where $\mathbf{E}$ was defined in eq.(4.100) and $\mathbf{s}_i$ is the 2-dimensional projection of $\mathbf{r}_i$ onto the x-y plane of motion, i.e., $\mathbf{s}_i \equiv [\, x_i \quad y_i \,]^T$. Equation (4.103a) thus reduces to

$$\begin{bmatrix} \mathbf{0} & \mathbf{0} & \mathbf{0} \\ 1 & 1 & 1 \\ \mathbf{E}\mathbf{s}_1 & \mathbf{E}\mathbf{s}_2 & \mathbf{E}\mathbf{s}_3 \\ 0 & 0 & 0 \end{bmatrix} \dot{\boldsymbol{\theta}} = \begin{bmatrix} \mathbf{0} \\ \dot{\phi} \\ \dot{\mathbf{p}} \\ 0 \end{bmatrix} \tag{4.104}$$

where $\mathbf{0}$ is the 2-dimensional zero vector and $\dot{\mathbf{p}}$ is now reduced to $\dot{\mathbf{p}} \equiv [\, \dot{x}, \, \dot{y} \,]^T$. In summary, then, by working only with the three nontrivial equations of eq.(4.104), we can represent the velocity relation using a 3×3 Jacobian in eq.(4.103a). To this end, we redefine $\mathbf{J}$ and $\mathbf{t}$ as

$$\mathbf{J} \equiv \begin{bmatrix} 1 & 1 & 1 \\ \mathbf{E}\mathbf{s}_1 & \mathbf{E}\mathbf{s}_2 & \mathbf{E}\mathbf{s}_3 \end{bmatrix}, \quad \mathbf{t} \equiv \begin{bmatrix} \dot{\phi} \\ \dot{\mathbf{p}} \end{bmatrix} \tag{4.105}$$

The velocity resolution of this manipulator thus reduces to solving for the three joint rates from eq.(4.103a), with $\mathbf{J}$ and $\mathbf{t}$ defined as in eq.(4.105), which thus leads to the system below:

$$\begin{bmatrix} 1 & 1 & 1 \\ \mathbf{E}\mathbf{s}_1 & \mathbf{E}\mathbf{s}_2 & \mathbf{E}\mathbf{s}_3 \end{bmatrix} \begin{bmatrix} \dot{\theta}_1 \\ \dot{\theta}_2 \\ \dot{\theta}_3 \end{bmatrix} = \begin{bmatrix} \dot{\phi} \\ \dot{\mathbf{p}} \end{bmatrix} \tag{4.106}$$

Solving for $\{\dot{\theta}_i\}_1^3$ is readily done by first reducing the system of equations appearing in eq.(4.103a) to one of two equations in two unknowns by resorting to Gaussian elimination. Indeed, if the first scalar equation of eq.(4.106) is multiplied by $\mathbf{E}\mathbf{s}_1$ and the product is subtracted from the 2-dimensional vector equation, we obtain

$$\begin{bmatrix} 1 & 1 & 1 \\ \mathbf{0} & \mathbf{E}(\mathbf{s}_2 - \mathbf{s}_1) & \mathbf{E}(\mathbf{s}_3 - \mathbf{s}_1) \end{bmatrix} \begin{bmatrix} \dot{\theta}_1 \\ \dot{\theta}_2 \\ \dot{\theta}_3 \end{bmatrix} = \begin{bmatrix} \dot{\phi} \\ \dot{\mathbf{p}} - \dot{\phi}\mathbf{E}\mathbf{s}_1 \end{bmatrix} \tag{4.107}$$

from which a reduced system of two equations in two unknowns is readily obtained, namely,

$$[\, \mathbf{E}(\mathbf{s}_2 - \mathbf{s}_1) \quad \mathbf{E}(\mathbf{s}_3 - \mathbf{s}_1) \,] \begin{bmatrix} \dot{\theta}_2 \\ \dot{\theta}_3 \end{bmatrix} = \dot{\mathbf{p}} - \dot{\phi}\mathbf{E}\mathbf{s}_1 \tag{4.108}$$

The system of equations (4.108) can be readily solved if Fact 4.8.4 is recalled, namely,

$$\begin{aligned} \begin{bmatrix} \dot{\theta}_2 \\ \dot{\theta}_3 \end{bmatrix} &= \frac{1}{\Delta} \begin{bmatrix} -(\mathbf{s}_3 - \mathbf{s}_1)^T\mathbf{E} \\ (\mathbf{s}_2 - \mathbf{s}_1)^T\mathbf{E} \end{bmatrix} \mathbf{E}(\dot{\mathbf{p}} - \dot{\phi}\mathbf{E}\mathbf{s}_1) \\ &= \frac{1}{\Delta} \begin{bmatrix} (\mathbf{s}_3 - \mathbf{s}_1)^T(\dot{\mathbf{p}} - \dot{\phi}\mathbf{E}\mathbf{s}_1) \\ -(\mathbf{s}_2 - \mathbf{s}_1)^T(\dot{\mathbf{p}} - \dot{\phi}\mathbf{E}\mathbf{s}_1) \end{bmatrix} \end{aligned}$$

where Δ is the determinant of the 2×2 matrix involved, i.e.,

$$\Delta \equiv \det([\, \mathbf{E}(\mathbf{s}_2 - \mathbf{s}_1) \quad \mathbf{E}(\mathbf{s}_3 - \mathbf{s}_1) \,]) \equiv -(\mathbf{s}_2 - \mathbf{s}_1)^T\mathbf{E}(\mathbf{s}_3 - \mathbf{s}_1) \tag{4.109}$$

We thus have

$$\dot{\theta}_2 = -\frac{(\mathbf{s}_3 - \mathbf{s}_1)^T(\dot{\mathbf{p}} - \dot{\phi}\mathbf{E}\mathbf{s}_1)}{(\mathbf{s}_2 - \mathbf{s}_1)^T\mathbf{E}(\mathbf{s}_3 - \mathbf{s}_1)} \tag{4.110a}$$

$$\dot{\theta}_3 = \frac{(\mathbf{s}_2 - \mathbf{s}_1)^T(\dot{\mathbf{p}} - \dot{\phi}\mathbf{E}\mathbf{s}_1)}{(\mathbf{s}_2 - \mathbf{s}_1)^T\mathbf{E}(\mathbf{s}_3 - \mathbf{s}_1)} \tag{4.110b}$$

Further, $\dot{\theta}_1$ is computed from the first scalar equation of eq.(4.106), i.e.,

$$\dot{\theta}_1 = \dot{\phi} - (\dot{\theta}_2 + \dot{\theta}_3) \tag{4.110c}$$

thereby completing the velocity analysis.

The foregoing calculations are summarized below in algorithmic form, with the numbers of multiplications and additions indicated at each stage. In those numbers, we have taken into account that a multiplication of $\mathbf{E}$ by any 2-dimensional vector incurs no computational cost, but rather a simple rearrangement of the entries of this vector, with a reversal of one sign.

1. $\mathbf{d}_{21} \leftarrow \mathbf{s}_2 - \mathbf{s}_1$ $\qquad 0M + 2A$

2. $\mathbf{d}_{31} \leftarrow \mathbf{s}_3 - \mathbf{s}_1$ $\quad 0M + 2A$

3. $\Delta \leftarrow \mathbf{d}_{31}^T \mathbf{E} \mathbf{d}_{21}$ $\quad 2M + 1A$

4. $\mathbf{u} \leftarrow \dot{\mathbf{p}} - \dot{\phi} \mathbf{E} \mathbf{s}_1$ $\quad 2M + 2A$

5. $\mathbf{u} \leftarrow \mathbf{u}/\Delta$ $\quad 2M + 0A$

6. $\dot{\theta}_2 \leftarrow \mathbf{u}^T \mathbf{d}_{31}$ $\quad 2M + 1A$

7. $\dot{\theta}_3 \leftarrow -\mathbf{u}^T \mathbf{d}_{21}$ $\quad 2M + 1A$

8. $\dot{\theta}_1 \leftarrow \dot{\phi} - \dot{\theta}_2 - \dot{\theta}_3$ $\quad 0M + 2A$

The complete calculation of joint rates thus consumes only $10M$ and $11A$, which represents a savings of about 67% of the computations involved if Gaussian elimination is applied without regarding the algebraic structure of the Jacobian $\mathbf{J}$ and its kinematic and geometric significance. In fact, the solution of an arbitrary system of three equations in three unknowns requires, from eq.(4.61a), 28 additions and 23 multiplications. If the cost of calculating the right-hand side is added, namely, $4A$ and $6M$, a total of $32A$ and $29M$ is required to solve for the joint rates if straightforward Gaussian elimination is used.

4.8.3 Acceleration Analysis

The calculation of the joint accelerations needed to produce a given twist rate of the EE is readily accomplished by differentiating both sides of eq.(4.103a), with definitions (4.105), i.e.,

$$\mathbf{J}\ddot{\boldsymbol{\theta}} + \dot{\mathbf{J}}\dot{\boldsymbol{\theta}} = \dot{\mathbf{t}}$$

from which we readily derive a system of equations similar to eq.(4.103a) with $\ddot{\boldsymbol{\theta}}$ as unknown, namely,

$$\mathbf{J}\ddot{\boldsymbol{\theta}} = \dot{\mathbf{t}} - \dot{\mathbf{J}}\dot{\boldsymbol{\theta}}$$

where

$$\dot{\mathbf{J}} = \begin{bmatrix} 0 & 0 & 0 \\ \mathbf{E}\dot{\mathbf{s}}_1 & \mathbf{E}\dot{\mathbf{s}}_2 & \mathbf{E}\dot{\mathbf{s}}_3 \end{bmatrix}, \quad \ddot{\boldsymbol{\theta}} \equiv \begin{bmatrix} \ddot{\theta}_1 \\ \ddot{\theta}_2 \\ \ddot{\theta}_3 \end{bmatrix}, \quad \dot{\mathbf{t}} \equiv \begin{bmatrix} \ddot{\phi} \\ \ddot{\mathbf{p}} \end{bmatrix}$$

and

$$\begin{aligned} \dot{\mathbf{s}}_3 &= (\dot{\theta}_1 + \dot{\theta}_2 + \dot{\theta}_3)\mathbf{E}\mathbf{a}_3 \\ \dot{\mathbf{s}}_2 &= \dot{\mathbf{a}}_2 + \dot{\mathbf{s}}_3 = (\dot{\theta}_1 + \dot{\theta}_2)\mathbf{E}\mathbf{a}_2 + \dot{\mathbf{s}}_3 \\ \dot{\mathbf{s}}_1 &= \dot{\mathbf{a}}_1 + \dot{\mathbf{s}}_2 = \dot{\theta}_1 \mathbf{E}\mathbf{s}_1 + \dot{\mathbf{s}}_2 \end{aligned}$$

Now we can proceed by Gaussian elimination to solve for the joint accelerations in exactly the same manner as in Subsection 4.8.2, thereby obtaining the counterpart of eq.(4.108), namely,

$$[\,\mathbf{E}(\mathbf{s}_2 - \mathbf{s}_1) \quad \mathbf{E}(\mathbf{s}_3 - \mathbf{s}_1)\,] \begin{bmatrix} \ddot{\theta}_2 \\ \ddot{\theta}_3 \end{bmatrix} = \mathbf{w} \tag{4.111a}$$

with $\mathbf{w}$ defined as

$$\mathbf{w} \equiv \ddot{\mathbf{p}} - \mathbf{E}(\dot{\theta}_1\dot{\mathbf{s}}_1 + \dot{\theta}_2\dot{\mathbf{s}}_2 + \dot{\theta}_3\dot{\mathbf{s}}_3 + \ddot{\phi}\mathbf{s}_1) \tag{4.111b}$$

and hence, similar to eqs.(4.110a–c), one has

$$\ddot{\theta}_2 = \frac{(\mathbf{s}_3 - \mathbf{s}_1)^T\mathbf{w}}{\Delta} \tag{4.112a}$$

$$\ddot{\theta}_3 = -\frac{(\mathbf{s}_2 - \mathbf{s}_1)^T\mathbf{w}}{\Delta} \tag{4.112b}$$

$$\ddot{\theta}_1 = \ddot{\phi} - (\dot{\theta}_2 + \dot{\theta}_3) \tag{4.112c}$$

Below we summarize the foregoing calculations in algorithmic form, indicating the numbers of operations required at each stage.

1. $\dot{\mathbf{s}}_3 \leftarrow (\dot{\theta}_1 + \dot{\theta}_2 + \dot{\theta}_3)\mathbf{E}\mathbf{a}_3$ $\qquad 2M$ & $2A$
2. $\dot{\mathbf{s}}_2 \leftarrow (\dot{\theta}_1 + \dot{\theta}_2)\mathbf{E}\mathbf{a}_2 + \dot{\mathbf{s}}_3$ $\qquad 2M$ & $3A$
3. $\dot{\mathbf{s}}_1 \leftarrow \dot{\theta}_1\mathbf{E}\mathbf{s}_1 + \dot{\mathbf{s}}_2$ $\qquad 2M$ & $2A$
4. $\mathbf{w}$ $leftarrow\ddot{\mathbf{p}} - \mathbf{E}(\dot{\theta}_1\dot{\mathbf{s}}_1 + \dot{\theta}_2\dot{\mathbf{s}}_2 + \dot{\theta}_3\dot{\mathbf{s}}_3 + \ddot{\phi}\mathbf{s}_1)$ $\qquad 8M$ & $8A$
5. $\mathbf{w} \leftarrow \mathbf{w}/\Delta$ $\qquad 2M + 0A$
6. $\ddot{\theta}_2 \leftarrow \mathbf{w}^T\mathbf{d}_{31}$ $\qquad 2M + 1A$
7. $\ddot{\theta}_3 \leftarrow -\mathbf{w}^T\mathbf{d}_{21}$ $\qquad 2M + 1A$
8. $\ddot{\theta}_1 \leftarrow \ddot{\phi} - (\ddot{\theta}_2 + \ddot{\theta}_3)$ $\qquad 0M + 2A$

where $\mathbf{d}_{21}$, $\mathbf{d}_{31}$, and Δ are available from velocity calculations. The joint accelerations thus require a total of 20 multiplications and 19 additions. These figures represent substantial savings when compared with the numbers of operations required if plain Gaussian elimination were used, namely, 33 multiplications and 35 additions.

It is noteworthy that in the foregoing algorithm, we have replaced neither the sum $\dot{\theta}_1 + \dot{\theta}_2 + \dot{\theta}_3$ nor $\dot{\theta}_1\mathbf{E}(\mathbf{s}_1 + \mathbf{s}_2 + \mathbf{s}_3)$ by ω and correspondingly, by $\dot{\mathbf{p}}$, because in path tracking, there is no perfect match between joint and Cartesian variables. In fact, joint-rate and joint-acceleration calculations are needed in feedback control schemes to estimate the position, velocity, and acceleration errors by proper corrective actions.

4.8.4 Static Analysis

Here we assume that a planar wrench acts at the end-effector of the manipulator appearing in Fig. 4.24. In accordance with the definition of the planar twist in Subsection 4.8.2, eq.(4.105), the planar wrench is now defined as

$$\mathbf{w} \equiv \begin{bmatrix} n \\ \mathbf{f} \end{bmatrix} \tag{4.113}$$

where n is the scalar couple acting on the end-effector and $\mathbf{f}$ is the 2-dimensional force acting at the operation point P of the end-effector. If additionally, we denote by $\boldsymbol{\tau}$ the 3-dimensional vector of joint torques, the planar counterpart of eq.(4.95) follows, i.e.,

$$\mathbf{J}^T \mathbf{w} = \boldsymbol{\tau} \tag{4.114}$$

where

$$\mathbf{J}^T = \begin{bmatrix} 1 & (\mathbf{E}\mathbf{s}_1)^T \\ 1 & (\mathbf{E}\mathbf{s}_2)^T \\ 1 & (\mathbf{E}\mathbf{s}_3)^T \end{bmatrix}$$

Now, in order to solve for the wrench $\mathbf{w}$ acting on the end-effector, given the joint torques $\boldsymbol{\tau}$ and the posture of the manipulator, we can still apply our compact Gaussian-elimination scheme, as introduced in Subsection 4.8.2. To this end, we subtract the first scalar equation from the second and the third scalar equations of eq.(4.114), which renders the foregoing system in the form

$$\begin{bmatrix} 1 & (\mathbf{E}\mathbf{s}_1)^T \\ 0 & [\mathbf{E}(\mathbf{s}_2 - \mathbf{s}_1)]^T \\ 0 & [\mathbf{E}(\mathbf{s}_3 - \mathbf{s}_1)]^T \end{bmatrix} \begin{bmatrix} n \\ \mathbf{f} \end{bmatrix} = \begin{bmatrix} \tau_1 \\ \tau_2 - \tau_1 \\ \tau_3 - \tau_1 \end{bmatrix}$$

Thus, the last two equations have been decoupled from the first one, which allows us to solve them separately, i.e., we have reduced the system to one of two equations in two unknowns, namely,

$$\begin{bmatrix} [\mathbf{E}(\mathbf{s}_2 - \mathbf{s}_1)]^T \\ [\mathbf{E}(\mathbf{s}_3 - \mathbf{s}_1)]^T \end{bmatrix} \mathbf{f} = \begin{bmatrix} \tau_2 - \tau_1 \\ \tau_3 - \tau_1 \end{bmatrix} \tag{4.115}$$

from which we readily obtain

$$\mathbf{f} = \begin{bmatrix} [\mathbf{E}(\mathbf{s}_2 - \mathbf{s}_1)]^T \\ [\mathbf{E}(\mathbf{s}_3 - \mathbf{s}_1)]^T \end{bmatrix}^{-1} \begin{bmatrix} \tau_2 - \tau_1 \\ \tau_3 - \tau_1 \end{bmatrix} \tag{4.116}$$

and hence, upon expansion of the above inverse,

$$\mathbf{f} = \frac{1}{\Delta} \left[(\tau_2 - \tau_1)(\mathbf{s}_3 - \mathbf{s}_1) - (\tau_3 - \tau_1)(\mathbf{s}_2 - \mathbf{s}_1) \right] \tag{4.117}$$

where Δ is exactly as defined in eq.(4.109). Finally, the resultant moment n acting on the end-effector is readily calculated from the first scalar equation of eq.(4.114), namely, as

$$n = \tau_1 + \mathbf{s}_1^T \mathbf{E} \mathbf{f}$$

thereby completing the static analysis of the manipulator under study. A quick analysis of computational costs shows that the foregoing solution needs $8M$ and $6A$, or a savings of about 70% if straightforward Gaussian elimination is applied.

4.9 Kinetostatic Performance Indices

The balance of Part I of the book does not depend on this section, which can thus be skipped. We have included it here because (*i*) it is a simple matter to render the section self-contained, while introducing the concept of *condition number* and its relevance in robotics; (*ii*) kinetostatic performance can be studied with the background of the material included up to this section; and (*iii*) kinetostatic performance is becoming increasingly relevant as a design criterion and as a figure of merit in robot control.

A *kinetostatic performance index* of a robotic mechanical system is a scalar quantity that measures how well the system behaves with regard to force and motion transmission, the latter being understood in the differential sense, i.e., at the velocity level. Now, a kinetostatic performance index, or kinetostatic index for brevity, may be needed to assess the performance of a robot at the design stage, in which case we need a posture-independent index. In this case, the index becomes a function of the robot architecture only. If, on the other hand, we want to assess the performance of a *given* robot while performing a task, what we need is a posture-dependent index. In many instances, this difference is not mentioned in the robotics literature, although it is extremely important. Moreover, while performance indices can be defined for all kinds of robotic mechanical systems, we focus here on those associated with serial manipulators, which are the ones studied most intensively.

Among the various performance indices that have been proposed, one can cite the concept of *service angle*, first introduced by Vinogradov et al. (1971), and the *conditioning* of robotic manipulators, as proposed by Yang and Lai (1985). Yoshikawa (1985), in turn, introduced the concept of *manipulability*, which is defined as the square root of the determinant of the product of the manipulator Jacobian by its transpose. Paul and Stevenson (1983) used the absolute value of the determinant of the Jacobian to assess the kinematic performance of spherical wrists. Note that for square Jacobians, Yoshikawa's manipulability is identical to the absolute value of the determinant of the Jacobian, and hence, the latter coincides with Paul and Stevenson's performance index. It should be pointed out that these indices were defined for control purposes and hence, are posture-dependent. Germane to these concepts is that of *dextrous workspace*, introduced by Kumar and Waldron (1981), and used for geometric optimization by Vijaykumar et al. (1986). Although the concepts of service angle and manipulability are clearly different, they touch upon a common underlying issue, namely, the

kinematic, or alternatively, the static performance of a manipulator from an accuracy viewpoint.

What is at stake when discussing the manipulability of a robotic manipulator is a measure of the *invertibility* of the associated Jacobian matrix, since this is required for velocity and force-feedback control. One further performance index is based on the *condition number* of the Jacobian, which was first used by Salisbury and Craig (1982) to design mechanical fingers. Here, we shall call such an index the *conditioning* of the manipulator. For the sake of brevity, we devote the discussion below to only two indices, namely, manipulability and conditioning. Prior to discussing these indices, we recall a few facts from linear algebra.

Although the concepts discussed here are equally applicable to square and rectangular matrices, we shall focus on the former. First, we give a geometric interpretation of the mapping induced by an $n \times n$ matrix $\mathbf{A}$. Here, we do not assume any particular structure of $\mathbf{A}$, which can thus be totally arbitrary. However, by invoking the *polar-decomposition theorem* (Strang, 1988), we can factor $\mathbf{A}$ as

$$\mathbf{A} \equiv \mathbf{RU} \equiv \mathbf{VR} \tag{4.118}$$

where $\mathbf{R}$ is orthogonal, although not necessarily proper, while $\mathbf{U}$ and $\mathbf{V}$ are both at least positive-semidefinite. Moreover, if $\mathbf{A}$ is nonsingular, then $\mathbf{U}$ and $\mathbf{V}$ are both positive-definite, and $\mathbf{R}$ is unique. Clearly, $\mathbf{U}$ can be readily determined as the positive-semidefinite or correspondingly, positive-definite *square root* of the product $\mathbf{A}^T\mathbf{A}$, which is necessarily positive-semidefinite; it is, in fact, positive-definite if $\mathbf{A}$ is nonsingular. We recall here that the square root of arbitrary matrices was briefly discussed in Subsection 2.3.6. The square root of a positive-semidefinite matrix can be most easily understood if that matrix is assumed to be in diagonal form, which is possible because such a matrix is necessarily symmetric, and every symmetric matrix is diagonalizable. The matrix at hand being positive-semidefinite, its eigenvalues are nonnegative, and hence, their square roots are all real. The positive-semidefinite square root of interest is, then, readily obtained as the diagonal matrix whose nontrivial entries are the nonnegative square roots of the aforementioned eigenvalues. With $\mathbf{U}$ determined, $\mathbf{R}$ can be found uniquely only if $\mathbf{A}$ is nonsingular, in which case $\mathbf{U}$ is positive-definite. If this is the case, then we have

$$\mathbf{R} = \mathbf{U}^{-1}\mathbf{A} \tag{4.119a}$$

It is a simple matter to show that $\mathbf{V}$ can be found, in turn, as a similarity transformation of $\mathbf{U}$, namely, as

$$\mathbf{V} = \mathbf{RUR}^T \tag{4.119b}$$

Now, let vector $\mathbf{x}$ be mapped by $\mathbf{A}$ into $\mathbf{z}$, i.e.,

$$\mathbf{z} = \mathbf{Ax} \equiv \mathbf{RUx} \tag{4.120a}$$

Moreover, let

$$\mathbf{y} \equiv \mathbf{U}\mathbf{x} \tag{4.120b}$$

and hence, we have a concatenation of mappings, namely, $\mathbf{U}$ maps $\mathbf{x}$ into $\mathbf{y}$, while $\mathbf{R}$ maps $\mathbf{y}$ into $\mathbf{z}$. Thus, by virtue of the nature of matrices $\mathbf{R}$ and $\mathbf{U}$, the latter maps the unit n-dimensional ball into an n-axis ellipsoid whose semiaxis lengths bear the ratios of the eigenvalues of $\mathbf{U}$. Moreover, $\mathbf{R}$ maps this ellipsoid into another one with identical semiaxes, except that it is rotated about its center or reflected, depending upon whether $\mathbf{R}$ is proper or improper orthogonal. In fact, the eigenvalues of $\mathbf{U}$ or, for that matter, those of $\mathbf{V}$, are nothing but the *singular values* of $\mathbf{A}$. Yoshikawa (1985) explained the foregoing relations resorting to the *singular-value decomposition theorem*. We prefer to invoke the polar-decomposition theorem instead, because of the geometric nature of the latter, as opposed to the former, which is of an algebraic nature—it is based on a diagonalization of either $\mathbf{U}$ or $\mathbf{V}$, which is really not needed.

We illustrate the two mappings $\mathbf{U}$ and $\mathbf{R}$ in Fig. 4.27, where we orient the X, Y, and Z axes along the three eigenvectors of $\mathbf{U}$. Therefore, the semiaxes of the ellipsoid are oriented as the eigenvectors of $\mathbf{U}$ as well. If $\mathbf{A}$ is singular, then the ellipsoid degenerates into one with at least one vanishing semiaxis. On the other hand, if matrix $\mathbf{A}$ is *isotropic*, i.e., if all its singular values are identical, then it maps the unit ball into another ball, either enlarged or shrunken.

For our purposes, we can regard the Jacobian of a serial manipulator as mapping the unit ball in the space of joint rates into a rotated or reflected ellipsoid in the space of Cartesian velocities, or twists. Now, let us assume that the polar decomposition of $\mathbf{J}$ is given by $\mathbf{R}$ and $\mathbf{U}$, the manipulability μ of the robot under study thus becoming

$$\mu \equiv |\det(\mathbf{J})| \equiv |\det(\mathbf{R})||\det(\mathbf{U})| \tag{4.121a}$$

Since $\mathbf{R}$ is orthogonal, the absolute value of its determinant is unity.

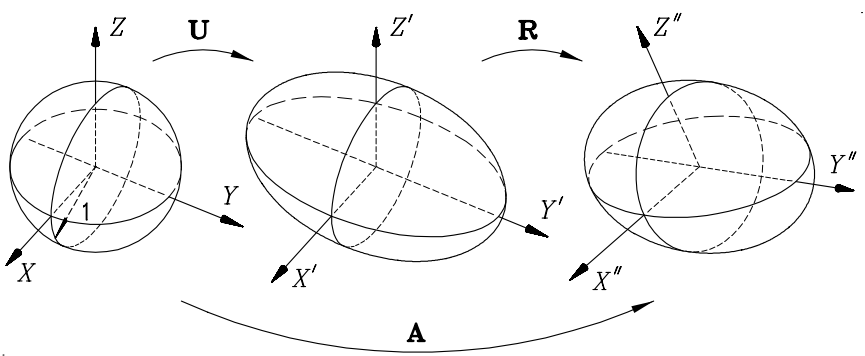

FIGURE 4.27. Geometric representation of mapping induced by matrix $\mathbf{A}$.

Additionally, the determinant of $\mathbf{U}$ is nonnegative, and hence,

$$\mu = \det(\mathbf{U}) \tag{4.121b}$$

which shows that the manipulability is the product of the eigenvalues of $\mathbf{U}$ or equivalently, of the singular values of $\mathbf{J}$. Now, the product of those singular values, in the geometric interpretation of the mapping induced by $\mathbf{J}$, is proportional to the volume of the ellipsoid at hand, and hence, μ can be interpreted as a measure of the volume of that ellipsoid. It is apparent that the manipulability defined in eq.(4.121b) is posture-dependent. For example, if $\mathbf{J}$ is singular, at least one of the semiaxes of the ellipsoid vanishes, and so does its volume. Manipulators at singular configurations thus have a manipulability of zero.

Now, if we want to use the concept of manipulability to define a posture-independent kinetostatic index, we have to define this index in a *global sense*. This can be done in the same way as the magnitude of a vector is defined, namely, as the sum of the squares of its components. In this way, the *global manipulability* can be defined as the integral of a certain power of the manipulability over the whole workspace of the manipulator, which would amount to defining the index as a *norm* of the manipulability in a space of functions. For example, we can use the maximum manipulability attained over the whole workspace, thereby ending up with what would be like a Chebyshev norm; alternatively, we can use the *root-mean square* (rms) value of the manipulability, thereby ending up with a measure similar to the Euclidean norm.

Furthermore, if we have a Jacobian $\mathbf{J}$ *whose entries all have the same units*, then we can define its condition number $\kappa(\mathbf{J})$ as the ratio of the largest singular value σ_l of $\mathbf{J}$ to the smallest one, σ_s, i.e.,

$$\kappa(\mathbf{J}) \equiv \frac{\sigma_l}{\sigma_s} \tag{4.122}$$

Note that $\kappa(\mathbf{J})$ can attain values from 1 to infinity. Clearly, the condition number attains its minimum value of unity for matrices with identical singular values; such matrices map the unit ball into another ball, although of a different size, and are, thus, called *isotropic*. By extension, *isotropic* manipulators are those whose Jacobian matrix can attain isotropic values. On the other side of the spectrum, singular matrices have a smallest singular value that vanishes, and hence, their condition number is infinity. The condition number of $\mathbf{J}$ can be thought of as indicating the *distortion* of the unit ball in the space of joint-variables. The larger this distortion, the greater the condition number, the worst-conditioned Jacobians being those that are singular. For these, one of the semiaxes of the ellipsoid vanishes and the ellipsoid degenerates into what would amount to an elliptical disk in the 3-dimensional space.

The condition number of a square matrix can also be understood as a measure of the relative roundoff-error amplification of the computed results

upon solving a linear system of equations associated with that matrix, with respect to the relative roundoff error of the data (Dahlquist and Björck, 1974; Golub and van Loan, 1989). Based on the condition number of the Jacobian, a posture-independent *kinematic conditioning index* of robotic manipulators can now be defined as a global measure of the condition number, or its reciprocal for that matter, which is better behaved because it is bounded between 0 and unity.

Now, if the entries of $\mathbf{J}$ have different units, the foregoing definition of $\kappa(\mathbf{J})$ cannot be applied, for we would face a problem of ordering singular values of different units from largest to smallest. We resolve this inconsistency by defining a *characteristic length*, by which we divide the Jacobian entries that have units of length, thereby producing a new Jacobian that is dimensionally homogeneous. We shall therefore divide our study into (*i*) manipulators for only positioning tasks, (*ii*) manipulators for only orientation tasks, and (*iii*) manipulators for both positioning and orientation tasks. The characteristic length will be introduced when studying the third category.

In the sequel, we will need an interesting property of isotropic matrices that is recalled below. First note that given the polar decomposition of a square matrix $\mathbf{A}$ of eq.(4.118), its singular values are simply the—nonnegative—eigenvalues of matrix $\mathbf{U}$, or those of $\mathbf{V}$, for both matrices have identical eigenvalues. Moreover, if $\mathbf{A}$ is isotropic, all the foregoing eigenvalues are identical, say equal to σ, and hence, matrices $\mathbf{U}$ and $\mathbf{V}$ are proportional to the $n \times n$ identity matrix, i.e.,

$$\mathbf{U} = \mathbf{V} = \sigma \mathbf{1} \tag{4.123}$$

In this case, then,

$$\mathbf{A} = \sigma \mathbf{R} \tag{4.124a}$$

which means that isotropic square matrices are proportional to rectangular matrices. As a consequence, then,

$$\mathbf{A}^T \mathbf{A} = \sigma^2 \mathbf{1} \tag{4.124b}$$

Given an arbitrary manipulator of the serial type with a Jacobian matrix whose entries all have the same units, we can calculate its condition number and use a global measure of this to define a posture-independent kinetostatic index. Let κ_m be the minimum value attained by the condition number of the dimensionally homogeneous Jacobian over the whole workspace. Note that $1/\kappa_m$ can be regarded as a Chebyshev norm of the reciprocal of $\kappa(\mathbf{J})$, because now $1/\kappa_m$ represents the maximum value of this reciprocal in the whole workspace. We then introduce a posture-independent performance index, the *kinematic conditioning index*, or KCI for brevity, defined as

$$\text{KCI} = \frac{1}{\kappa_m} \times 100 \tag{4.125}$$

Notice that since the condition number is bounded from below, the KCI is bounded from above by a value of 100%. Manipulators with a KCI of 100% are those identified above as isotropic because their Jacobians have, at the configuration of minimum condition number, all their singular values identical and different from zero.

While the condition number of $\mathbf{J}$ defined in eq.(4.122) is conceptually simple, for it derives from the polar-decomposition theorem, it is by no means computationally simple. First, it relies on the eigenvalues of $\mathbf{J}^T\mathbf{J}$, which only in special cases can be found in symbolic form; second, even if eigenvalues are available symbolically, their ordering from smallest to largest varies with the manipulator architecture and posture. An alternative definition of $\kappa(\mathbf{J})$ that is computationally simpler relies on the general definition of the concept, namely (Golub and van Loan, 1989),

$$\kappa(\mathbf{J}) = \|\mathbf{J}\|\|\mathbf{J}^{-1}\| \tag{4.126a}$$

where $\|\cdot\|$ stands for the matrix norm (Golub and van Loan, 1989). While any norm can be used in the above definition, the one that is most convenient for our purposes is the *Frobenius norm* $\|\cdot\|_F$, defined as

$$\|\mathbf{J}\|_F = \sqrt{\frac{1}{n}\mathrm{tr}(\mathbf{J}\mathbf{J}^T)} \tag{4.126b}$$

where we have assumed that $\mathbf{J}$ is of $n \times n$. Although a symbolic expression for $\mathbf{J}^{-1}$ is not always possible, this expression is more frequently available than one for the eigenvalues of $\mathbf{J}^T\mathbf{J}$. Moreover, from the polar-decomposition theorem and Theorem 2.6.3, one can readily verify that

$$\|\mathbf{J}\|_F = \sqrt{\frac{1}{n}\mathrm{tr}(\mathbf{J}^T\mathbf{J})} \tag{4.126c}$$

4.9.1 Positioning Manipulators

Here, again, we shall distinguish between planar and spatial manipulators. These are studied separately.

Planar Manipulators

If the manipulator of Fig. 4.24 is limited to positioning tasks, we can dispense with its third axis, the manipulator thus reducing to the one shown in Fig. 4.25; its Jacobian reduces correspondingly to

$$\mathbf{J} = [\,\mathbf{E}\mathbf{s}_1 \quad \mathbf{E}\mathbf{s}_2\,]$$

with s_i denoting the two-dimensional versions of vectors $\mathbf{r}_i$ of the Denavit-Hartenberg notation, as introduced in Fig. 4.19. Now, if we want to design this manipulator for maximum manipulability, we need first to determine its

manipulability as given by eq.(4.121a) or correspondingly, as $\mu = |\det(\mathbf{J})|$. Now, note that

$$\det(\mathbf{J}) = \det(\mathbf{E}\,[\,\mathbf{s}_1 \quad \mathbf{s}_2\,]) = \det(\mathbf{E})\det([\,\mathbf{s}_1 \quad \mathbf{s}_2\,])$$

and since matrix $\mathbf{E}$ is orthogonal, its determinant equals unity. Thus, the determinant of interest is now calculated using Fact 4.8.3 of Section 4.8, namely,

$$\det(\mathbf{J}) = -\mathbf{s}_1^T\mathbf{E}\mathbf{s}_2 \tag{4.127}$$

Therefore,

$$\mu = |\mathbf{s}_1^T\mathbf{E}\mathbf{s}_2| \equiv \|\mathbf{s}_1\|\|\mathbf{s}_2\|\,|\sin(\mathbf{s}_1,\,\mathbf{s}_2)|$$

where $(\mathbf{s}_1,\,\mathbf{s}_2)$ stands for the angle between the two vectors inside the parentheses. Now let us denote the manipulator reach with R, i.e., $R = a_1 + a_2$, and let $a_k = R\rho_k$, where ρ_k, for $k = 1, 2$, is a dimensionless number. As the reader can readily verify, μ turns out to be twice the area of triangle O_1O_2P, with the notation adopted at the outset. Hence,

$$\mu = R^2\rho_1\rho_2|\sin\theta_2| \tag{4.128}$$

with ρ_1 and ρ_2 subjected to

$$\rho_1 + \rho_2 = 1 \tag{4.129}$$

The design problem at hand, then, can be formulated as an optimization problem aimed at maximizing μ as given in eq.(4.128) over ρ_1 and ρ_2, subject to the constraint (4.129). This optimization problem can be readily solved using, for example, Lagrange multipliers, thereby obtaining

$$\rho_1 = \rho_2 = \frac{1}{2}, \quad \theta_2 = \pm\frac{\pi}{2}$$

the absolute value of $\sin\theta_2$ attaining its maximum value when $\theta_2 = \pm 90°$. The maximum manipulability thus becomes

$$\mu_{\max} = \frac{R^2}{4} \tag{4.130}$$

Incidentally, the equal-length condition maximizes the workspace volume as well.

On the other hand, if we want to minimize the condition number of $\mathbf{J}$, we should aim at rendering it isotropic, which means that the product $\mathbf{J}^T\mathbf{J}$ should be proportional to the identity matrix, and so,

$$\begin{bmatrix} \mathbf{s}_1^T\mathbf{s}_1 & \mathbf{s}_1^T\mathbf{s}_2 \\ \mathbf{s}_1^T\mathbf{s}_2 & \mathbf{s}_2^T\mathbf{s}_2 \end{bmatrix} = \begin{bmatrix} \sigma^2 & 0 \\ 0 & \sigma^2 \end{bmatrix}$$

where σ is the repeated singular value of $\mathbf{J}$. Hence, for $\mathbf{J}$ to be isotropic, all we need is that the two vectors $\mathbf{s}_1$ and $\mathbf{s}_2$ have the same norm and that

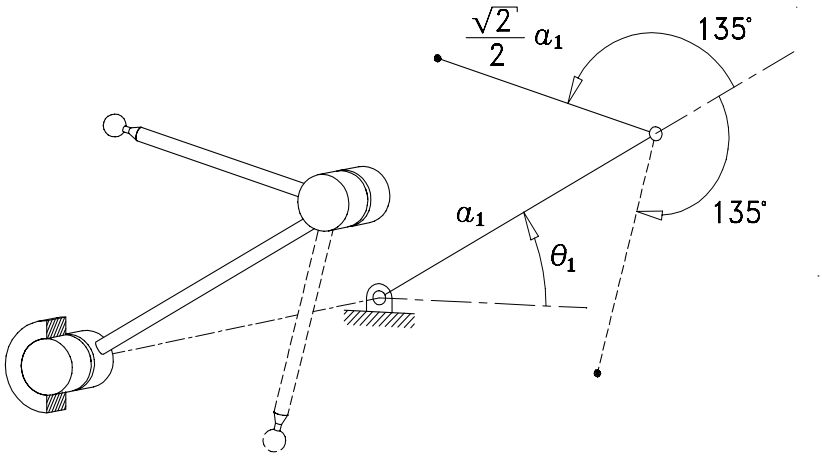

FIGURE 4.28. A two-axis isotropic manipulator.

they lie at right angles. The solution is a manipulator with link lengths observing a ratio of $\sqrt{2}/2$, i.e., with $a_1/a_2 = \sqrt{2}/2$, and the two link axes at an angle of 135°, as depicted in Fig. 4.28. Manipulators of the above type, used as mechanical fingers, were investigated by Salisburg and Craig (1982), who found that these manipulators can be rendered isotropic if given the foregoing dimensions and configured as shown in Fig. 4.28.

Spatial Manipulators

Now we have a manipulator like that depicted in Fig. 4.9, its Jacobian matrix taking on the form

$$\mathbf{J} = [\,\mathbf{e}_1 \times \mathbf{r}_1 \quad \mathbf{e}_2 \times \mathbf{r}_2 \quad \mathbf{e}_3 \times \mathbf{r}_3\,] \tag{4.131}$$

The condition for isotropy of this kind of manipulator takes on the form of eq.(4.124b), which thus leads to

$$\sum_{1}^{3} (\mathbf{e}_k \times \mathbf{r}_k)(\mathbf{e}_k \times \mathbf{r}_k)^T = \sigma^2 \mathbf{1} \tag{4.132}$$

This condition can be attained by various designs, one example being the manipulator of Fig. 4.15. Another isotropic manipulator for 3-dimensional positioning tasks is displayed in Fig. 4.29.

Note that the manipulator of Fig. 4.29 has an orthogonal architecture, the ratio of its last link length to the length of the intermediate link being, as in the 2-dimensional case, $\sqrt{2}/2$. Since the first axis does not affect singularities, neither does it affect isotropy, and hence, not only does one location of the operation point exist that renders the manipulator isotropic, but a whole locus, namely, the circle known as the *isotropy circle*, indicated in the same figure. By the same token, the manipulator of Fig. 4.28 has

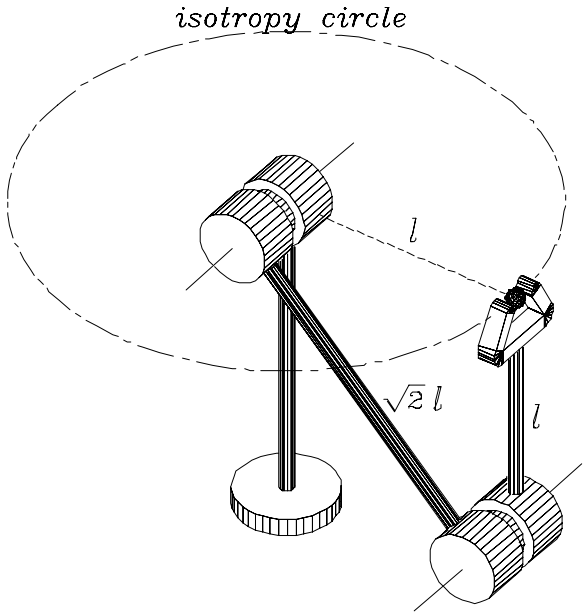

FIGURE 4.29. An isotropic manipulator for 3-dimensional positioning tasks.

an isotropy circle centered at the center of the first joint, with a radius of $(\sqrt{2}/2)a_1$.

4.9.2 Orienting Manipulators

We now have a three-revolute manipulator like that depicted in Fig. 4.17, its Jacobian taking on the simple form

$$\mathbf{J} = [\,\mathbf{e}_1 \quad \mathbf{e}_2 \quad \mathbf{e}_3\,] \tag{4.133}$$

and hence, the isotropy condition of eq. (4.124b) leads to

$$\sum_1^3 \mathbf{e}_k \mathbf{e}_k^T = \sigma^2 \mathbf{1} \tag{4.134}$$

What the foregoing condition states is that a spherical wrist for orienting tasks is isotropic if its three unit vectors $\{\mathbf{e}_k\}_1^3$ are so laid out that the three products $\mathbf{e}_k \mathbf{e}_k^T$, for $k = 1, 2, 3$, add up to a multiple of the 3×3 identity matrix. This is the case if the three foregoing unit vectors are orthonormal, which occurs in orthogonal wrists when the two planes defined by the corresponding pairs of neighboring axes are at right angles. Moreover, the value of σ in this case can be readily found if we take the trace of both

sides of the above equation, which yields

$$\sum_{1}^{3} \mathbf{e}_k \cdot \mathbf{e}_k = 3\sigma^2 \tag{4.135}$$

and hence, $\sigma = 1$, because all three vectors on the left-hand side are of unit magnitude. In summary, then, orthogonal wrists, which are rather frequent among industrial manipulators, are isotropic. Here we have an example of engineering insight leading to an optimal design, for such wrists existed long before isotropy was introduced as a design criterion for manipulators. Moreover, notice that from the results of Subsection 4.4.2, spherical manipulators with an orthogonal architecture have a maximum workspace volume. That is, isotropic manipulators of the spherical type have two optimality properties: they have both a maximum workspace volume and a maximum KCI. Apparently, the manipulability of orthogonal spherical wrists is also optimal, as the reader is invited to verify, when the wrist is postured so that its three axes are mutually orthogonal. In this posture, the manipulability of the wrist is unity.

4.9.3 Positioning and Orienting Manipulators

We saw already in Subsubsection 4.9.1 that the optimization of the two indices studied here—the condition number of the Jacobian matrix and the manipulability—leads to different manipulators. In fact, the two indices entail even deeper differences, as we shall see presently. First and foremost, as we shall prove for both planar and spatial manipulators, the manipulability μ is independent of the operation point P of the end-effector, while the condition number is not. One more fundamental difference is that while calculating the manipulability of manipulators meant for both positioning and orienting tasks poses no problem, the condition number cannot be calculated, at least directly, for this kind of manipulator. Indeed, in order to determine the condition number of the Jacobian matrix, we must order its singular values from largest to smallest. However, in the presence of positioning and orienting tasks, three of these singular values, namely, those associated with orientation, are dimensionless, while those associated with positioning have units of length, thereby making impossible such an ordering. We resolve this dimensional inhomogeneity by introducing a normalizing *characteristic length*. Upon dividing the three *positioning* rows, i.e., the bottom rows, of the Jacobian by this length, a nondimensional Jacobian is obtained whose singular values are nondimensional as well. The characteristic length is then defined as the normalizing length that renders the condition number of the Jacobian matrix a minimum. Below we shall determine the characteristic length for isotropic manipulators; determining the same for nonisotropic manipulators requires solving a minimization problem that calls for numerical techniques, as illustrated with an example.

Planar Manipulators

In the ensuing development, we will need the planar counterpart of the twist-transfer formula of Subsection 3.4.2. First, we denote the 3-dimensional twist of a rigid body undergoing planar motion, defined at a point A, by $\mathbf{t}_A$; when defined at point B, the corresponding twist is denoted by $\mathbf{t}_B$, i.e.,

$$\mathbf{t}_A \equiv \begin{bmatrix} \omega \\ \dot{\mathbf{a}} \end{bmatrix}, \quad \mathbf{t}_B \equiv \begin{bmatrix} \omega \\ \dot{\mathbf{b}} \end{bmatrix} \tag{4.136}$$

The relation between the two twists, or the *planar twist-transfer formula*, is given by a linear transformation $\mathbf{U}$ as

$$\mathbf{t}_B = \mathbf{U}\mathbf{t}_A \tag{4.137a}$$

where $\mathbf{U}$ is now defined as

$$\mathbf{U} = \begin{bmatrix} 1 & \mathbf{0}^T \\ \mathbf{E}(\mathbf{b}-\mathbf{a}) & \mathbf{1}_2 \end{bmatrix} \tag{4.137b}$$

with $\mathbf{a}$ and $\mathbf{b}$ representing the position vectors of points A and B, and $\mathbf{1}_2$ stands for the 2×2 identity matrix. Moreover, $\mathbf{U}$ is, not surprisingly, a member of the 3×3 unimodular group, i.e.,

$$\det(\mathbf{U}) = 1$$

Because of the planar twist-transfer formula, the Jacobian defined at an operation point B is related to that defined at an operation point A of the same end-effector by the same linear transformation $\mathbf{U}$, i.e., if we denote the two Jacobians by $\mathbf{J}_A$ and $\mathbf{J}_B$, then

$$\mathbf{J}_B = \mathbf{U}\mathbf{J}_A \tag{4.138}$$

and if we denote by μ_A and μ_B the manipulability calculated at points A and B, respectively, then

$$\mu_B = |\det(\mathbf{J}_B)| = |\det(\mathbf{U})||\det(\mathbf{J}_A)| = |\det(\mathbf{J}_A)| = \mu_A \tag{4.139}$$

thereby proving that the manipulability is insensitive to a change of operation point, or to a change of end-effector, for that matter. Note that a similar analysis for the condition number cannot be completed at this stage because as pointed out earlier, the condition number of these Jacobian matrices cannot even be calculated directly.

In order to resolve the foregoing dimensional inhomogeneity, we introduce the characteristic length L, which will be defined as that rendering the Jacobian dimensionally homogeneous and optimally conditioned, i.e., with a minimum condition number. We thus redefine the Jacobian matrix of interest as

$$\mathbf{J} \equiv \begin{bmatrix} 1 & 1 & 1 \\ \frac{1}{L}\mathbf{E}\mathbf{r}_1 & \frac{1}{L}\mathbf{E}\mathbf{r}_2 & \frac{1}{L}\mathbf{E}\mathbf{r}_3 \end{bmatrix} \tag{4.140}$$

Now, if we want to size the manipulator at hand by properly choosing its geometric parameters so as to render it isotropic, we must observe the isotropy condition, eq.(4.124b), which readily leads to

$$\begin{bmatrix} 3 & \frac{1}{L}\sum_1^3 \mathbf{r}_k^T\mathbf{E}^T \\ \frac{1}{L}\mathbf{E}\sum_1^3 \mathbf{r}_k & \frac{1}{L^2}\mathbf{E}[\sum_1^3(\mathbf{r}_k\mathbf{r}_k^T)]\mathbf{E}^T \end{bmatrix} = \begin{bmatrix} \sigma^2 & 0 & 0 \\ 0 & \sigma^2 & 0 \\ 0 & 0 & \sigma^2 \end{bmatrix} \tag{4.141}$$

and hence,

$$\sigma^2 = 3 \tag{4.142a}$$

$$\sum_1^3 \mathbf{r}_k = \mathbf{0} \tag{4.142b}$$

$$\frac{1}{L^2}\mathbf{E}\left(\sum_1^3(\mathbf{r}_k\mathbf{r}_k^T)\right)\mathbf{E}^T = \sigma^2\mathbf{1}_2 \tag{4.142c}$$

What eq.(4.142a) states is simply that the triple singular value of the isotropic $\mathbf{J}$ is $\sqrt{3}$; eq.(4.142b) states, in turn, that the operation point is the centroid of the centers of all manipulator joints if its Jacobian matrix is isotropic. Now, in order to gain more insight into eq.(4.142c), we note that since $\mathbf{E}$ is orthogonal and $\sigma^2 = 3$, this equation can be rewritten in a simpler form, namely,

$$\frac{1}{L^2}\left(\sum_1^3(\mathbf{r}_k\mathbf{r}_k^T)\right) = (3)\mathbf{1}_2 \tag{4.143}$$

Further, if we recall the definition of the moment of inertia of a rigid body, we can immediately realize that the moment of inertia $\mathbf{I}_P$ of a set of particles of unit mass located at the centers of the manipulator joints, with respect to the operation point P, is given by

$$\mathbf{I}_P \equiv \sum_1^3 \left(\|\mathbf{r}_k\|^2\mathbf{1}_2 - \mathbf{r}_k\mathbf{r}_k^T\right) \tag{4.144}$$

from which it is apparent that the moment of inertia of the set comprises two parts, the first being isotropic—it is a multiple of the 2×2 identity matrix—the second not necessarily so. However, the second part has the form of the left-hand side of eq.(4.143). Hence, eq.(4.143) states that if the manipulator under study is isotropic, then its joint centers are located, at the isotropic configuration, at the corners of a triangle that has *circular inertial symmetry*. What we mean by this is that the 2×2 moment of inertia of the set of particles, with entries I_{xx}, I_{xy}, and I_{yy}, is similar to that of a circle, i.e., with $I_{xx} = I_{yy}$ and $I_{xy} = 0$. An obvious candidate for such a triangle is, obviously, an equilateral triangle, the operation point

thus coinciding with the center of the triangle. Since the corners of an equilateral triangle are at equal distances d from the center, and these distances are nothing but $\|\mathbf{r}_k\|$, then the condition below is readily derived for isotropy:

$$\|\mathbf{r}_k\|^2 = d^2 \tag{4.145}$$

In order to compute the characteristic length of the manipulator under study, let us take the trace of both sides of eq.(4.143), thereby obtaining

$$\frac{1}{L^2}\sum_{1}^{3}\|\mathbf{r}_k\|^2 = 6$$

and hence, upon substituting eq.(4.145) into the foregoing relation, an expression for the characteristic length, *as pertaining to planar isotropic manipulators*, is readily derived, namely,

$$L = \frac{\sqrt{2}}{2}d \tag{4.146}$$

It is now a simple matter to show that the three link lengths of this isotropic manipulator are $a_1 = a_2 = \sqrt{3}d$ and $a_3 = d$. Such a manipulator is sketched in an isotropic configuration in Fig. 4.30.

Spatial Manipulators

The entries of the Jacobian of a six-axis manipulator meant for both positioning and orienting tasks are dimensionally inhomogeneous as well. Indeed, as discussed in Section 4.5, the ith column of $\mathbf{J}$ is composed of the

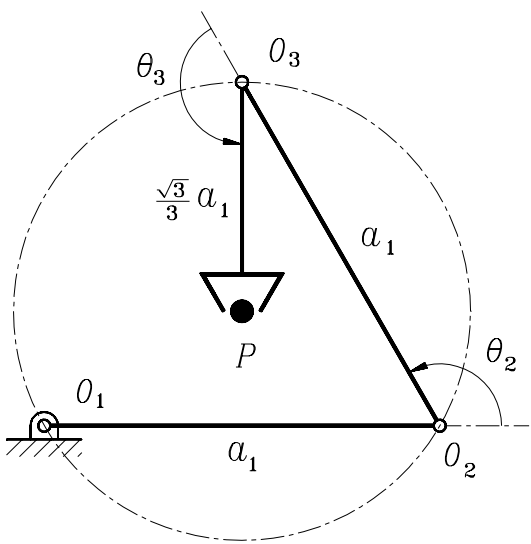

FIGURE 4.30. The planar 3-R isotropic manipulator.

Plücker coordinates of the ith axis of the manipulator, namely,

$$\mathbf{J} = \begin{bmatrix} \mathbf{e}_1 & \mathbf{e}_2 & \mathbf{e}_3 & \mathbf{e}_4 & \mathbf{e}_5 & \mathbf{e}_6 \\ \mathbf{e}_1 \times \mathbf{r}_1 & \mathbf{e}_2 \times \mathbf{r}_2 & \mathbf{e}_3 \times \mathbf{r}_3 & \mathbf{e}_4 \times \mathbf{r}_4 & \mathbf{e}_5 \times \mathbf{r}_5 & \mathbf{e}_6 \times \mathbf{r}_6 \end{bmatrix} \tag{4.147}$$

Now it is apparent that the first three rows of $\mathbf{J}$ are dimensionless, whereas the remaining three, corresponding to the *moments* of the axes with respect to the operation point of the end-effector, have units of length. This dimensional inhomogeneity is resolved in the same way as in the case of planar manipulators for both positioning and orienting tasks, i.e., by means of a characteristic length. This length is defined as the one that minimizes the condition number of the dimensionless Jacobian thus obtained. We then redefine the Jacobian as

$$\mathbf{J} \equiv \begin{bmatrix} \mathbf{e}_1 & \mathbf{e}_2 & \mathbf{e}_3 & \mathbf{e}_4 & \mathbf{e}_5 & \mathbf{e}_6 \\ \frac{1}{L}\mathbf{e}_1 \times \mathbf{r}_1 & \frac{1}{L}\mathbf{e}_2 \times \mathbf{r}_2 & \frac{1}{L}\mathbf{e}_3 \times \mathbf{r}_3 & \frac{1}{L}\mathbf{e}_4 \times \mathbf{r}_4 & \frac{1}{L}\mathbf{e}_5 \times \mathbf{r}_5 & \frac{1}{L}\mathbf{e}_6 \times \mathbf{r}_6 \end{bmatrix} \tag{4.148}$$

and hence, the isotropy condition of eq.(4.124b) leads to

$$\sum_1^6 \mathbf{e}_k \mathbf{e}_k^T = \sigma^2 \mathbf{1} \tag{4.149a}$$

$$\sum_1^6 \mathbf{e}_k (\mathbf{e}_k \times \mathbf{r}_k)^T = \mathbf{O} \tag{4.149b}$$

$$\frac{1}{L^2} \sum_1^6 (\mathbf{e}_k \times \mathbf{r}_k)(\mathbf{e}_k \times \mathbf{r}_k)^T = \sigma^2 \mathbf{1} \tag{4.149c}$$

where $\mathbf{1}$ is the 3×3 identity matrix, and $\mathbf{O}$ is the 3×3 zero matrix. Now, if we take the trace of both sides of eq.(4.149a), we obtain

$$\sigma^2 = 2 \quad \text{or} \quad \sigma = \sqrt{2}$$

Furthermore, we take the trace of both sides of eq.(4.149c), which yields

$$\frac{1}{L^2} \sum_1^6 \|\mathbf{e}_k \times \mathbf{r}_k\|^2 = 3\sigma^2$$

But $\|\mathbf{e}_k \times \mathbf{r}_k\|^2$ is nothing but the square of the distance d_k of the kth revolute axis to the operation point, the foregoing equation thus yielding

$$L = \sqrt{\frac{1}{6} \sum_1^6 d_k^2}$$

i.e., *the characteristic length of a spatial six-revolute isotropic manipulator is the root-mean square of the distances of the revolute axes to the operation point when the robot finds itself at the posture of minimum condition number.*

Furthermore, eq.(4.149a) states that if $\{ \mathbf{e}_k \}_1^6$ is regarded as the set of position vectors of points $\{ P_k \}_1^6$ on the surface of the unit sphere, then the moment-of-inertia matrix of the set of equal masses located at these points has *spherical symmetry*. What the latter means is that any direction of the 3-dimensional space is a principal axis of inertia of the foregoing set. Likewise, eq.(4.149c) states that if $\{ \mathbf{e}_k \times \mathbf{r}_k \}_1^6$ is regarded as the set of position vectors of points $\{ Q_k \}$ in the 3-dimensional Euclidean space, then the moment-of-inertia matrix of the set of equal masses located at these points has spherical symmetry.

Now, in order to gain insight into eq.(4.149b), let us take the axial vector of both sides of that equation, thus obtaining

$$\sum_1^6 \mathbf{e}_k \times (\mathbf{e}_k \times \mathbf{r}_k) = \mathbf{0} \tag{4.150}$$

with $\mathbf{0}$ denoting the 3-dimensional zero vector. Furthermore, let us denote by $\mathbf{E}_k$ the cross-product matrix of $\mathbf{e}_k$, the foregoing equation thus taking on the form

$$\sum_1^6 \mathbf{E}_k^2 \mathbf{r}_k = \mathbf{0}$$

However,

$$\mathbf{E}_k^2 = -\mathbf{1} + \mathbf{e}_k \mathbf{e}_k^T$$

for every k, and hence, eq.(4.150) leads to

$$\sum_1^6 (\mathbf{1} - \mathbf{e}_k \mathbf{e}_k^T) \mathbf{r}_k = \mathbf{0}$$

Moreover, $(\mathbf{1} - \mathbf{e}_k \mathbf{e}_k^T) \mathbf{r}_k$ is nothing but the normal component of $\mathbf{r}_k$ with respect to $\mathbf{e}_k$, as defined in Section 2.2. Let us denote this component by $\mathbf{r}_k^\perp$, thereby obtaining an alternative expression for the foregoing equation, namely,

$$\sum_1^6 \mathbf{r}_k^\perp = \mathbf{0} \tag{4.151}$$

The geometric interpretation of the foregoing equation is readily derived: To this end, let O'_k be the foot of the perpendicular to the kth revolute axis from the operation point P; then, $\mathbf{r}_k$ is the vector directed from O'_k to P. Therefore, *the operation point of an isotropic manipulator, configured at the isotropic posture is the centroid of the set* $\{ O'_k \}_1^6$ *of perpendicular feet from the operation point.*

A six-axis manipulator designed with an isotropic architecture, DIESTRO, is displayed in Fig. 4.31. The Denavit-Hartenberg parameters of this manipulator are given in Table 4.1. DIESTRO is characterized by identical link lengths a and offsets identical with this common link length, besides

TABLE 4.1. DH Parameters of DIESTRO

i	a_i (mm)	b_i (mm)	α_i	θ_i
1	50	50	90°	θ_1
2	50	50	-90°	θ_2
3	50	50	90°	θ_3
4	50	50	-90°	θ_4
5	50	50	90°	θ_5
6	50	50	-90°	θ_6

FIGURE 4.31. DIESTRO, a six-axis isotropic manipulator.

twist angles of 90° between all pairs of neighboring axes. Not surprisingly, the characteristic length of this manipulator is a.

Example 4.9.1 *Find the KCI and the characteristic length of the Fanuc Arc Mate robot whose DH parameters are given in Table 4.2.*

Solution: Apparently, what we need is the minimum value $\kappa_{\min}$ that the condition number of the manipulator Jacobian can attain, in order to calculate its KCI as indicated in eq.(4.125). Now, the Fanuc Arc Mate robot is a six-revolute manipulator for positioning and orienting tasks. Hence, its Jacobian matrix has to be first recast in nondimensional form, as in eq.(4.148). Next, we find L, along with the joint variables that determine the posture of minimum condition number via an optimization procedure. Prior to the formulation of the underlying optimization problem, however, we must realize that the first joint, accounting for motions of the manipulator as a single rigid body, does not affect its Jacobian condition number.

We thus define the *design vector* $\mathbf{x}$ of the optimization problem at hand as

$$\mathbf{x} \equiv [\,\theta_2 \quad \theta_3 \quad \theta_4 \quad \theta_5 \quad \theta_6 \quad L\,]$$

and set up the optimization problem as

$$\min_{\mathbf{x}} \kappa(\mathbf{J})$$

The condition number having been defined as the ratio of the largest to the smallest singular values of the Jacobian matrix at hand, the gradient of the above objective function, $\partial\kappa/\partial\mathbf{x}$, is apparently elusive to calculate. Thus, we use a direct-search method, i.e., a method not requiring any partial derivatives, but rather, only objective-function evaluations, to solve the above optimization problem. There are various methods of this kind at our disposal; the one we chose is the *simplex method*, as implemented in Matlab. The results reported are displayed below:

$$\mathbf{x}_{\text{opt}} = [\,26.82^\circ \quad -56.06^\circ \quad 15.79^\circ \quad -73.59^\circ \quad -17.83^\circ \quad 0.3573\,]$$

where the last entry, the characteristic length of the robot, is in meters, i.e.,

$$L = 357.3 \text{ mm}$$

Furthermore, the minimum condition number attained at the foregoing posture, with the characteristic length found above, is

$$\kappa_m = 2.589$$

Therefore, the KCI of the Fanuc Arc Mate is

$$\text{KCI} = 38.625\%$$

and so this robot is apparently far from being kinematically isotropic. To be sure, the KCI of this manipulator can still be improved dramatically by noting that the condition number is highly dependent on the location of the operation point of the end-effector. As reported by Tandirci et al. (1992), an optimum selection of the operation point for the robot at hand yields a

TABLE 4.2. DH Parameters of the Fanuc Arc Mate Manipulator

i	a_i (mm)	b_i (mm)	α_i	θ_i
1	200	810	90°	θ_1
2	600	0	0°	θ_2
3	130	30	90°	θ_3
4	0	550	90°	θ_4
5	0	100	90°	θ_5
6	0	100	0°	θ_6

minimum condition number of 1.591, which thus leads to a KCI of 62.85%. The point of the EE that yields the foregoing minimum is thus termed the *characteristic point* of the manipulator in the foregoing reference. Its location in the EE is given by the DH parameters a_6 and b_6, namely,

$$a_6 = 223.6 \text{ mm}, \quad b_6 = 274.2 \text{ mm}$$

5

Trajectory Planning: Pick-and-Place Operations

5.1 Introduction

The motions undergone by robotic mechanical systems should be, as a rule, as smooth as possible; i.e., abrupt changes in position, velocity, and acceleration should be avoided. Indeed, abrupt motions require unlimited amounts of power to be implemented, which the motors cannot supply because of their physical limitations. On the other hand, abrupt motion changes arise when the robot collides with an object, a situation that should also be avoided. While smooth motions can be planned with simple techniques, as described below, these are no guarantees that no abrupt motion changes will occur. In fact, if the work environment is cluttered with objects, whether stationary or mobile, collisions may occur. Under ideal conditions, a flexible manufacturing cell is a work environment in which all objects, machines and workpieces alike, move with preprogrammed motions that by their nature, can be predicted at any instant. Actual situations, however, are far from being ideal, and system failures are unavoidable. Unpredictable situations should thus be accounted for when designing a robotic system, which can be done by supplying the system with sensors for the automatic detection of unexpected events or by providing for human monitoring. Nevertheless, robotic systems find applications not only in the well-structured environments of flexible manufacturing cells, but also in unstructured environments such as exploration of unknown terrains and systems in which humans are present. The planning of robot motions in the latter case is

obviously much more challenging than in the former. Robot motion planning in unstructured environments calls for techniques beyond the scope of those studied in this book, involving such areas as pattern recognition and artificial intelligence. For this reason, we have devoted this book to the planning of robot motions in structured environments only.

Two typical tasks call for trajectory planning techniques, namely,

- pick-and-place operations (PPO), and
- continuous paths (CP).

We will study PPO in this chapter, with Chapter 9 devoted to CP. Moreover, we will focus on simple robotic manipulators of the serial type, although these techniques can be directly applied to other, more advanced, robotic mechanical systems.

5.2 Background on PPO

In PPO, a robotic manipulator is meant to take a workpiece from a given *initial pose*, specified by the position of one of its points and its orientation with respect to a certain coordinate frame, to a *final pose*, specified likewise. However, how the object moves from its initial to its final pose is immaterial, as long as the motion is smooth and no collisions occur. Pick-and-place operations are executed in elementary manufacturing operations such as loading and unloading of belt conveyors, tool changes in machine tools, and simple assembly operations such as putting roller bearings on a shaft. The common denominator of these tasks is *material handling*, which usually requires the presence of conventional machines whose motion is very simple and is usually characterized by a uniform velocity. In some instances, such as in *packing operations*, a set of workpieces, e.g., in a magazine, is to be relocated in a prescribed pattern in a container, which constitutes an operation known as *palletizing*. Although palletizing is a more elaborate operation than simple pick-and-place, it can be readily decomposed into a sequence of the latter operations.

It should be noted that although the initial and the final poses in a PPO are prescribed in the Cartesian space, robot motions are implemented in the joint space. Hence, the planning of PPO will be conducted in the latter space, which brings about the need of mapping the motion thus planned into the Cartesian space, in order to ensure that the robot will not collide with other objects in its surroundings. The latter task is far from being that simple, since it involves the rendering of the motion of all the moving links of the robot, each of which has a particular geometry. An approach to path planning first proposed by Lozano-Pérez (1981) consists of mapping the obstacles in the joint space, thus producing obstacles in the joint space in the form of regions that the joint-space trajectory should avoid. The

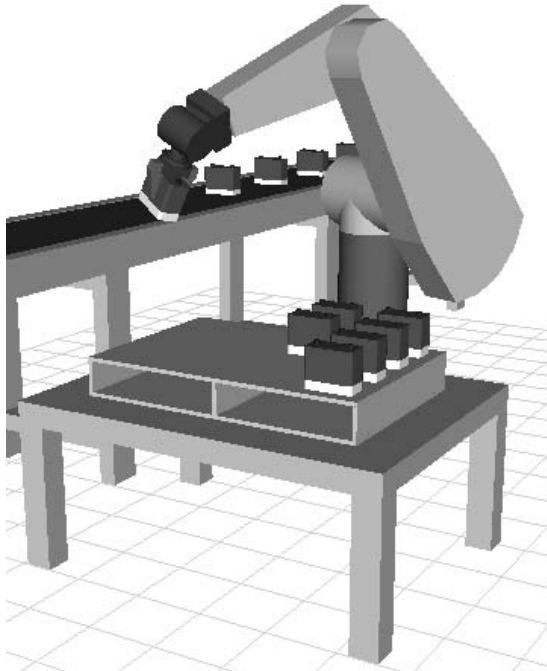

FIGURE 5.1. Still image of the animation of a palletizing operation.

idea can be readily implemented for simple planar motions and simple geometries of the obstacles. However, for general 3-D motions and arbitrary geometries, the computational requirements make the procedure impractical. A more pragmatic approach would consist of two steps, namely, (*i*) planning a preliminary trajectory in the joint space, disregarding the obstacles, and (*ii*) visually verifying if collisions occur with the aid of a graphics system rendering the animation of the robot motion in the presence of obstacles. The availability of powerful graphics hardware enables the fast animation of robot motions within a highly realistic environment. Shown in Fig. 5.1 is a still image of the animation produced by RVS, the McGill University *Robot-Visualization System*, of the motion of a robot performing a palletizing operation. Commercial software for robot-motion rendering is available.

By inspection of the kinematic closure equations of robotic manipulators—see eqs.(4.5a & b)—it is apparent that in the absence of singularities, the mapping of joint to Cartesian variables, and vice versa, is continuous. Hence, a smooth trajectory planned in the joint space is guaranteed to be smooth in the Cartesian space, and the other way around, as long as the trajectory does not encounter a singularity.

In order to proceed to synthesize the joint trajectory, we must then start by mapping the initial and final poses of the workpiece, which is assumed to be rigidly attached to the EE of the manipulator, into manipulator configurations described in the joint space. This is readily done with the

methods described in Chapter 4. Let the vector of joint variables at the initial and final robot configurations be denoted by $\boldsymbol{\theta}_I$ and $\boldsymbol{\theta}_F$, respectively. Moreover, the initial pose in the Cartesian space is defined by the position vector $\mathbf{p}_I$ of the operation point P of the EE and a rotation matrix $\mathbf{Q}_I$. Likewise, the final pose in the Cartesian space is defined by the position vector $\mathbf{p}_F$ of P and the rotation matrix $\mathbf{Q}_F$. Moreover, let $\dot{\mathbf{p}}_I$ and $\ddot{\mathbf{p}}_I$ denote the velocity and acceleration of P, while $\boldsymbol{\omega}_I$ and $\dot{\boldsymbol{\omega}}_I$ denote the angular velocity and angular acceleration of the workpiece, all of these at the initial pose. These variables at the final pose are denoted likewise, with the subscript I changed to F. Furthermore, we assume that time is counted from the initial pose, i.e., at this pose, $t = 0$. If the operation takes place in time T, then at the final pose, $t = T$. We have thus the set of conditions that define a smooth motion between the initial and the final poses, namely,

$$\mathbf{p}(0) = \mathbf{p}_I \qquad \dot{\mathbf{p}}(0) = \mathbf{0} \qquad \ddot{\mathbf{p}}(0) = \mathbf{0} \tag{5.1a}$$
$$\mathbf{Q}(0) = \mathbf{Q}_I \qquad \boldsymbol{\omega}(0) = \mathbf{0} \qquad \dot{\boldsymbol{\omega}}(0) = \mathbf{0} \tag{5.1b}$$
$$\mathbf{p}(T) = \mathbf{p}_F \qquad \dot{\mathbf{p}}(T) = \mathbf{0} \qquad \ddot{\mathbf{p}}(T) = \mathbf{0} \tag{5.1c}$$
$$\mathbf{Q}(T) = \mathbf{Q}_F \qquad \boldsymbol{\omega}(T) = \mathbf{0} \qquad \dot{\boldsymbol{\omega}}(T) = \mathbf{0} \tag{5.1d}$$

In the absence of singularities, then, the conditions of zero velocity and acceleration imply zero joint velocity and acceleration, and hence,

$$\boldsymbol{\theta}(0) = \boldsymbol{\theta}_I \qquad \dot{\boldsymbol{\theta}}(0) = \mathbf{0} \qquad \ddot{\boldsymbol{\theta}}(0) = \mathbf{0} \tag{5.2a}$$
$$\boldsymbol{\theta}(T) = \boldsymbol{\theta}_F \qquad \dot{\boldsymbol{\theta}}(T) = \mathbf{0} \qquad \ddot{\boldsymbol{\theta}}(T) = \mathbf{0} \tag{5.2b}$$

5.3 Polynomial Interpolation

A simple inspection of conditions (5.2a) and (5.2b) reveals that a linear interpolation between initial and final configurations will not work here, and neither will a quadratic interpolation, for its slope vanishes only at a single point. Hence, a higher-order interpolation is needed. On the other hand, these conditions imply, in turn, six conditions for every joint trajectory, which means that if a polynomial is to be employed to represent the motion of every joint, then this polynomial should be at least of the fifth degree. We thus start by studying trajectory planning with the aid of a 5th-degree polynomial.

5.3.1 A 3-4-5 Interpolating Polynomial

In order to represent each joint motion, we use here a fifth-order polynomial $s(\tau)$, namely,

$$s(\tau) = a\tau^5 + b\tau^4 + c\tau^3 + d\tau^2 + e\tau + f \tag{5.3}$$

such that

$$0 \leq s \leq 1, \qquad 0 \leq \tau \leq 1 \tag{5.4}$$

and

$$\tau = \frac{t}{T} \tag{5.5}$$

We will thus aim at a *normal polynomial* that, upon scaling both its argument and the polynomial itself, will allow us to represent each of the joint variables θ_j throughout its range of motion, so that

$$\theta_j(t) = \theta_j^I + (\theta_j^F - \theta_j^I)s(\tau) \tag{5.6a}$$

where θ_j^I and θ_j^F are the given initial and final values of the jth joint variable. In vector form, eq.(5.6a) becomes

$$\boldsymbol{\theta}(t) = \boldsymbol{\theta}_I + (\boldsymbol{\theta}_F - \boldsymbol{\theta}_I)s(\tau) \tag{5.6b}$$

and hence,

$$\dot{\boldsymbol{\theta}}(t) = (\boldsymbol{\theta}_F - \boldsymbol{\theta}_I)s'(\tau)\dot{\tau}(t) = (\boldsymbol{\theta}_F - \boldsymbol{\theta}_I)\frac{1}{T}s'(\tau) \tag{5.6c}$$

Likewise,

$$\ddot{\boldsymbol{\theta}}(t) = \frac{1}{T^2}(\boldsymbol{\theta}_F - \boldsymbol{\theta}_I)s''(\tau) \tag{5.6d}$$

and

$$\dddot{\boldsymbol{\theta}}(t) = \frac{1}{T^3}(\boldsymbol{\theta}_F - \boldsymbol{\theta}_I)s'''(\tau) \tag{5.6e}$$

What we now need are the values of the coefficients of $s(\tau)$ that appear in eq.(5.3). These are readily found by recalling conditions (5.2a & b), upon consideration of eqs.(5.6b–d). We thus obtain the end conditions for $s(\tau)$, namely,

$$s(0) = 0, \quad s'(0) = 0, \quad s''(0) = 0, \quad s(1) = 1, \quad s'(1) = 0, \quad s''(1) = 0 \tag{5.7}$$

The derivatives of $s(\tau)$ appearing above are readily derived from eq.(5.3), i.e.,

$$s'(\tau) = 5a\tau^4 + 4b\tau^3 + 3c\tau^2 + 2d\tau + e \tag{5.8}$$

and

$$s''(\tau) = 20a\tau^3 + 12b\tau^2 + 6c\tau + 2d \tag{5.9}$$

Thus, the first three conditions of eq.(5.7) lead to

$$f = e = d = 0 \tag{5.10}$$

while the last three conditions yield three linear equations in a, b, and c, namely,

$$a + b + c = 1 \tag{5.11a}$$

$$5a + 4b + 3c = 0 \tag{5.11b}$$

$$20a + 12b + 6c = 0 \tag{5.11c}$$

Upon solving the three foregoing equations for the three aforementioned unknowns, we obtain

$$a = 6, \qquad b = -15, \qquad c = 10 \tag{5.12}$$

and hence, the normal polynomial sought is

$$s(\tau) = 6\tau^5 - 15\tau^4 + 10\tau^3 \tag{5.13}$$

which is called a *3-4-5 polynomial.*

This polynomial and its first three derivatives, all normalized to fall within the $(-1, 1)$ range, are shown in Fig. 5.2. Note that the smoothness conditions imposed at the outset are respected and that the curve thus obtained is a monotonically growing function of τ, a rather convenient property for the problem at hand.

It is thus possible to determine the evolution of each joint variable if we know both its end values and the time T required to complete the motion. If no extra conditions are imposed, we then have the freedom to perform

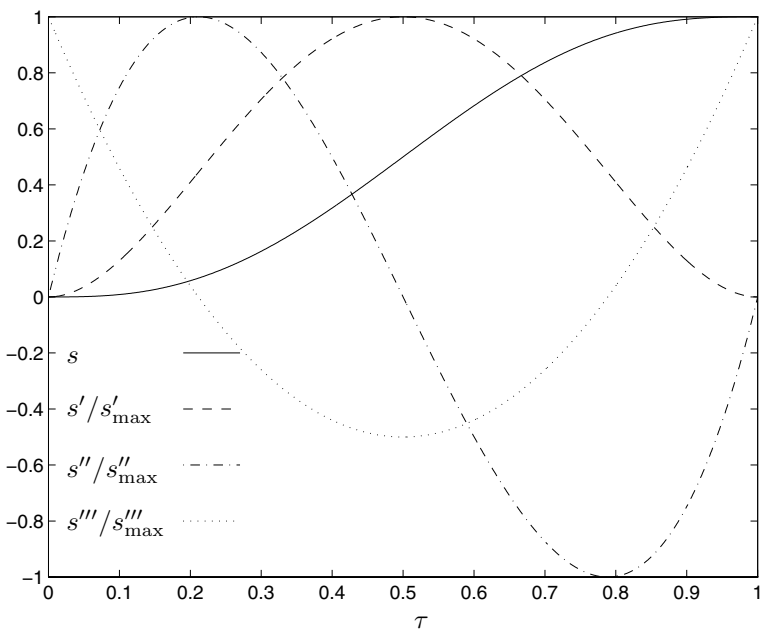

FIGURE 5.2. 3-4-5 interpolation polynomial and its derivatives.

the desired motion in as short a time T as possible. Note, however, that this time cannot be given an arbitrarily small value, for we must respect the motor specifications on maximum velocity and maximum torque, the latter being the subject of Chapter 6. In order to ease the discussion, we limit ourselves to specifications of maximum joint velocity and acceleration rather than maximum torque. From the form of function $\theta_j(t)$ of eq.(5.6a), it is apparent that this function takes on extreme values at points corresponding to those at which the normal polynomial attains its extrema. In order to find the values of τ at which the first and second derivatives of $s(\tau)$ attain maximum values, we need to zero its second and third derivatives. These derivatives are displayed below:

$$s'(\tau) = 30\tau^4 - 60\tau^3 + 30\tau^2 \tag{5.14a}$$

$$s''(\tau) = 120\tau^3 - 180\tau^2 + 60\tau \tag{5.14b}$$

$$s'''(\tau) = 360\tau^2 - 360\tau + 60 \tag{5.14c}$$

from which it is apparent that the second derivative vanishes at the two ends of the interval $0 \leq \tau \leq 1$. Additionally, the same derivative vanishes at the midpoint of the same interval, i.e., at $\tau = 1/2$. Hence, the maximum value of $s'(\tau)$, $s'_{\max}$, is readily found as

$$s'_{\max} = s'\left(\frac{1}{2}\right) = \frac{15}{8} \tag{5.15}$$

and hence, the maximum value of the jth joint rate takes on the value

$$(\dot{\theta_j})_{\max} = \frac{15(\theta_j^F - \theta_j^I)}{8T} \tag{5.16}$$

which becomes negative, and hence, a local minimum, if the difference in the numerator is negative. The values of τ at which the second derivative attains its extreme values are likewise determined. The third derivative vanishes at two intermediate points τ_1 and τ_2 of the interval $0 \leq \tau \leq 1$, namely, at

$$\tau_{1,2} = \frac{1}{2} \pm \frac{\sqrt{3}}{6} \tag{5.17}$$

and hence, the maximum value of $s''(\tau)$ is readily found as

$$s''_{\max} = s''\left(\frac{1}{2} - \frac{\sqrt{3}}{6}\right) = \frac{10\sqrt{3}}{3} \tag{5.18}$$

while the minimum is given as

$$s''_{\min} = s''\left(\frac{1}{2} + \frac{\sqrt{3}}{6}\right) = -\frac{10\sqrt{3}}{3} \tag{5.19}$$

Therefore, the maximum value of the joint acceleration is as shown below:

$$(\ddot{\theta}_j)_{\max} = \frac{10\sqrt{3}}{3}\frac{(\theta_j^F - \theta_j^I)}{T^2} \tag{5.20}$$

Likewise,

$$s'''_{\max} = s'''(0) = s'''(1) = 60$$

and hence,

$$(\dddot{\theta}_j)_{\max} = 60\frac{\theta_j^F - \theta_j^I}{T^3} \tag{5.21}$$

Thus, eqs.(5.16) and (5.20) allow us to determine T for each joint so that the joint rates and accelerations lie within the allowed limits. Obviously, since the motors of different joints are different, the minimum values of T allowed by the joints will be, in general, different. Of those various values of T, we will, of course, choose the largest one.

5.3.2 A 4-5-6-7 Interpolating Polynomial

Now, from eq.(5.14c), it is apparent that the third derivative of the normal polynomial does not vanish at the end points of the interval of interest. This implies that the third time derivative of $\theta_j(t)$, also known as the joint *jerk*, does not vanish at those ends either. It is desirable to have this derivative as smooth as the first two, but this requires us to increase the order of the normal polynomial. In order to attain the desired smoothness, we will then impose two more conditions, namely,

$$s'''(0) = 0, \qquad s'''(1) = 0 \tag{5.22}$$

We now have eight conditions on the normal polynomial, which means that the polynomial degree should be increased to seven, namely,

$$s(\tau) = a\tau^7 + b\tau^6 + c\tau^5 + d\tau^4 + e\tau^3 + f\tau^2 + g\tau + h \tag{5.23a}$$

whose derivatives are readily determined as shown below:

$$s'(\tau) = 7a\tau^6 + 6b\tau^5 + 5c\tau^4 + 4d\tau^3 + 3e\tau^2 + 2f\tau + g \tag{5.23b}$$
$$s''(\tau) = 42a\tau^5 + 30b\tau^4 + 20c\tau^3 + 12d\tau^2 + 6e\tau + 2f \tag{5.23c}$$
$$s'''(\tau) = 210a\tau^4 + 120b\tau^3 + 60c\tau^2 + 24d\tau + 6e \tag{5.23d}$$

The first three conditions of eq.(5.7) and the first condition of eq.(5.22) readily lead to

$$e = f = g = h = 0 \tag{5.24}$$

Furthermore, the last three conditions of eq.(5.7) and the second condition of eq.(5.22) lead to four linear equations in four unknowns, namely,

$$a + b + c + d = 1 \tag{5.25a}$$
$$7a + 6b + 5c + 4d = 0 \tag{5.25b}$$
$$42a + 30b + 20c + 12d = 0 \tag{5.25c}$$
$$210a + 120b + 60c + 24d = 0 \tag{5.25d}$$

and hence, we obtain the solution

$$a = -20, \qquad b = 70, \qquad c = -84, \qquad d = 35 \tag{5.26}$$

the desired polynomial thus being

$$s(\tau) = -20\tau^7 + 70\tau^6 - 84\tau^5 + 35\tau^4 \tag{5.27}$$

which is a *4-5-6-7 polynomial.* This polynomial and its first three derivatives, normalized to fall within the range $(-1, 1)$, are plotted in Fig. 5.3. Note that the 4-5-6-7 polynomial is similar to that of Fig. 5.2, except that the third derivative of the former vanishes at the extremes of the interval of interest. As we will presently show, this smoothness has been obtained at the expense of higher maximum values of the first and second derivatives.

We now determine the maximum values of the velocity and acceleration produced with this motion. To this end, we display below the first three

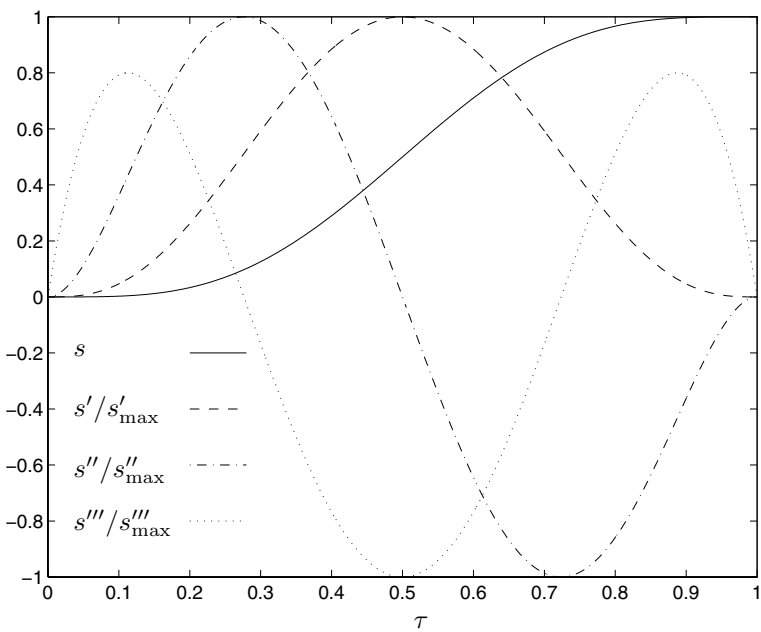

FIGURE 5.3. 4-5-6-7 interpolating polynomial and its derivatives.

derivatives, namely,

$$s'(\tau) = -140\tau^6 + 420\tau^5 - 420\tau^4 + 140\tau_3 \tag{5.28a}$$
$$s''(\tau) = -840\tau^5 + 2100\tau^4 - 1680\tau^3 + 420\tau^2 \tag{5.28b}$$
$$s'''(\tau) = -4200\tau^4 + 8400\tau^3 - 5040\tau^2 + 840\tau \tag{5.28c}$$

The first derivative attains its extreme values at points where the second derivative vanishes. Upon zeroing the latter, we obtain

$$\tau^2(-2\tau^3 + 5\tau^2 - 4\tau + 1) = 0 \tag{5.29}$$

which clearly contains a double root at $\tau = 0$. Moreover, the cubic polynomial in the parentheses above admits one real root, namely, $\tau = 1/2$, which yields the maximum value of $s'(\tau)$, i.e.,

$$s'_{\max} = s'\left(\frac{1}{2}\right) = \frac{35}{16} \tag{5.30}$$

whence the maximum value of the jth joint rate is found as

$$(\dot{\theta}_j)_{\max} = \frac{35(\theta_j^F - \theta_j^I)}{16T} \tag{5.31}$$

Likewise, the points of maximum joint acceleration are found upon zeroing the third derivative of $s(\tau)$, namely,

$$s'''(\tau) = -4200\tau^4 + 8400\tau^3 - 5040\tau^2 + 840\tau = 0 \tag{5.32}$$

or

$$\tau(\tau - 1)(5\tau^2 - 5\tau + 1) = 0 \tag{5.33}$$

which yields, in addition to the two end points, two intermediate extreme points, namely,

$$\tau_{1,2} = \frac{1}{2} \pm \frac{\sqrt{5}}{10} \tag{5.34}$$

and hence, the maximum value of acceleration is found to be

$$s''_{\max} = s''(\tau_1) = \frac{84\sqrt{5}}{25} \tag{5.35}$$

the minimum occurring at $\tau = \tau_2$, with $s''_{\min} = -s''_{\max}$. The maximum value of the jth joint acceleration is thus

$$(\ddot{\theta}_j)_{\max} = \frac{84\sqrt{5}}{25}\left(\frac{\theta_j^F - \theta_j^I}{T^2}\right) \tag{5.36}$$

which becomes a minimum if the difference in the numerator is negative. Likewise, the zeroing of the fourth derivative leads to

$$-20\tau^3 + 30\tau^2 - 12\tau + 1 = 0$$

whose three roots are

$$\tau_1 = \frac{1 - \sqrt{3/5}}{2}, \quad \tau_2 = \frac{1}{2}, \quad \tau_1 = \frac{1 + \sqrt{3/5}}{2}$$

and hence,

$$s'''_{\max} = s'''\left(\frac{1 \pm \sqrt{3/5}}{2}\right) = 42, \quad s'''_{\min} = s'''(0.5) = -\frac{105}{2}$$

i.e.,

$$\max_{\tau}\{|s'''(\tau)|\} = \frac{105}{2} \equiv s'''_M \tag{5.37}$$

As in the case of the fifth-order polynomial, it is possible to use the foregoing relations to determine the minimum time T during which it is possible to perform a given PPO while observing the physical limitations of the motors.

5.4 Cycloidal Motion

An alternative motion that produces zero velocity and acceleration at the ends of a finite interval is the *cycloidal motion*. In normal form, this motion is given by

$$s(\tau) = \tau - \frac{1}{2\pi}\sin 2\pi\tau \tag{5.38a}$$

its derivatives being readily derived as

$$s'(\tau) = 1 - \cos 2\pi\tau \tag{5.38b}$$

$$s''(\tau) = 2\pi \sin 2\pi\tau \tag{5.38c}$$

$$s'''(\tau) = 4\pi^2 \cos 2\pi\tau \tag{5.38d}$$

The cycloidal motion and its first three time-derivatives, normalized to fall within the range $(-1, 1)$, are shown in Fig. 5.4. Note that while this motion, indeed, has zero velocity and acceleration at the ends of the interval $0 \le \tau \le 1$, its jerk is nonzero at these points and hence, exhibits jump discontinuities at the ends of that interval.

When implementing the cycloidal motion in PPO, we have, for the jth joint,

$$\theta_j(t) = \theta_j^I + (\theta_j^F - \theta_j^I)s(\tau) \tag{5.39a}$$

$$\dot{\theta}_j(t) = \frac{\theta_j^F - \theta_j^I}{T}s'(\tau) \tag{5.39b}$$

$$\ddot{\theta}_j(t) = \frac{\theta_j^F - \theta_j^I}{T^2}s''(\tau) \tag{5.39c}$$

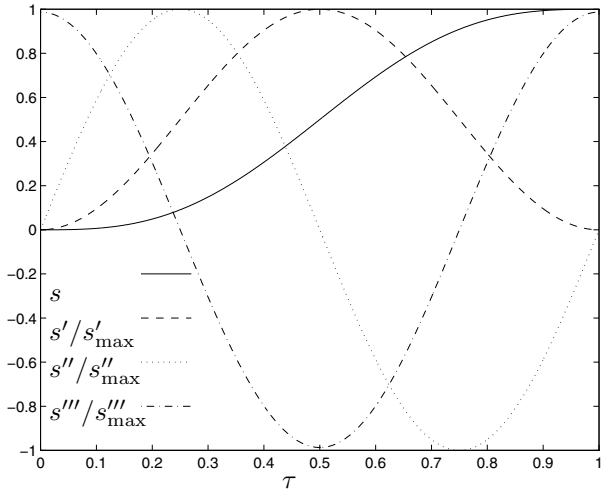

FIGURE 5.4. The normal cycloidal motion and its time derivatives.

Moreover, as the reader can readily verify, under the assumption that $\theta_j^F > \theta_j^I$, this motion attains its maximum velocity at the center of the interval, i.e., at $\tau = 0.5$, the maximum being

$$s'_{\max} = s'(0.5) = 2$$

and hence,

$$(\dot{\theta}_j)_{\max} = \frac{2}{T}(\theta_j^F - \theta_j^I) \tag{5.40a}$$

Likewise, the jth joint acceleration attains its maximum and minimum values at $\tau = 0.25$ and $\tau = 0.75$, respectively, i.e.,

$$s''_{\max} = s''(0.25) = s''(0.75) = 2\pi \tag{5.40b}$$

and hence,

$$(\ddot{\theta}_j)_{\max} = \frac{2\pi}{T^2}(\theta_j^F - \theta_j^I), \quad (\ddot{\theta}_j)_{\min} = -\frac{2\pi}{T^2}(\theta_j^F - \theta_j^I) \tag{5.40c}$$

Moreover, $s'''(\tau)$ attains its extrema at the ends of the interval, i.e.,

$$s'''_{\max} = s'''(0) = s'''(1) = 4\pi^2 \tag{5.41}$$

and hence,

$$(\dddot{\theta}_j)_{\max} = \frac{4\pi^2}{T^3}(\theta_j^F - \theta_j^I) \tag{5.42}$$

Thus, if motion is constrained by the maximum speed delivered by the motors, the minimum time T_j for the jth joint to produce the given PPO can be readily determined from eq.(5.40a) as

$$T_j = \frac{2(\theta_j^F - \theta_j^I)}{(\dot{\theta}_j)_{\max}} \tag{5.43}$$

and hence, the minimum time in which the operation can take place can be readily found as

$$T_{\min} = 2 \max_j \left\{ \frac{\theta_j^F - \theta_j^I}{(\dot{\theta}_j)_{\max}} \right\} \tag{5.44}$$

If joint-acceleration constraints are imposed, then a similar procedure can be followed to find the minimum time in which the operation can be realized. As a matter of fact, rather than maximum joint accelerations, maximum joint torques are to be respected. How to determine these torques is studied in detail in Chapter 6.

5.5 Trajectories with Via Poses

The polynomial trajectories discussed above do not allow the specification of intermediate Cartesian poses of the EE. All they guarantee is that the Cartesian trajectories prescribed at the initial and final instants are met. One way of verifying the feasibility of the Cartesian trajectories thus synthesized was outlined above and consists of using a graphics system, preferably with animation capabilities, to produce an animated rendering of the robot motion, thereby allowing for verification of collisions. If the latter occur, we can either try alternative branches of the inverse kinematics solutions computed at the end poses or modify the trajectory so as to eliminate collisions. We discuss below the second approach. This is done with what are called *via poses*, i.e., poses of the EE in the Cartesian space that lie between the initial and the final poses, and are determined so as to avoid collisions. For example, if upon approaching the final pose of the PPO, the manipulator is detected to interfere with the surface on which the workpiece is to be placed, a via pose is selected close to the final point so that at this pose, the workpiece is far enough from the surface. From inverse kinematics, values of the joint variables can be determined that correspond to the aforementioned via poses. These values can now be regarded as points on the joint-space trajectory and are hence called *via points*. Obviously, upon plotting each joint variable vs. time, via points appear as points on those plots as well.

The introduction of via points in the joint-space trajectories amounts to an increase in the number of conditions to be satisfied by the desired trajectory. For example, in the case of the polynomial trajectory synthesized for continuity up to second derivatives, we can introduce two via points by requiring that

$$s(\tau_1) = s_1, \qquad s(\tau_2) = s_2 \tag{5.45}$$

where τ_1, τ_2, s_1, and s_2 depend on the via poses prescribed and the instants at which these poses are desired to occur. Hence, s_1 and s_2 differ from joint

to joint, although the occurrence instants τ_1 and τ_2 are the same for all joints. Thus, we will have to determine one normal polynomial for each joint. Furthermore, the ordinate values s_1 and s_2 of the normal polynomial at via points are determined from the corresponding values of the joint variable determined, in turn, from given via poses through inverse kinematics. Once the via values of the joint variables are known, the ordinate values of the via points of the normal polynomial are found from eq.(5.6a). Since we have now eight conditions to satisfy, namely, the six conditions (5.7) plus the two conditions (5.45), we need a seventh-order polynomial, i.e.,

$$s(\tau) = a\tau^7 + b\tau^6 + c\tau^5 + d\tau^4 + e\tau^3 + f\tau^2 + g\tau + h \tag{5.46}$$

Again, the first three conditions of eq.(5.7) lead to the vanishing of the last three coefficients, i.e.,

$$f = g = h = 0 \tag{5.47}$$

Further, the five remaining conditions are now introduced, which leads to a system of five linear equations in five unknowns, namely,

$$a + b + c + d + e = 1 \tag{5.48a}$$
$$7a + 6b + 5c + 4d + 3e = 0 \tag{5.48b}$$
$$42a + 30b + 20c + 12d + 6e = 0 \tag{5.48c}$$
$$\tau_1^7 a + \tau_1^6 b + \tau_1^5 c + \tau_1^4 d + \tau_1^3 e = s_1 \tag{5.48d}$$
$$\tau_2^7 a + \tau_2^6 b + \tau_2^5 c + \tau_2^4 d + \tau_2^3 e = s_2 \tag{5.48e}$$

where τ_1, τ_2, s_1, and s_2 are all data. For example, if the via poses occur at 10% and 90% of T, we have

$$\tau_1 = 1/10, \qquad \tau_2 = 9/10 \tag{5.48f}$$

the polynomial coefficients being found as

$$a = 100(12286 + 12500s_1 - 12500s_2)/729 \tag{5.49a}$$
$$b = 100(-38001 - 48750s_1 + 38750s_2)/729 \tag{5.49b}$$
$$c = (1344358 + 2375000s_1 - 1375000s_2)/243 \tag{5.49c}$$
$$d = (-1582435 - 4625000s_1 + 1625000s_2)/729 \tag{5.49d}$$
$$e = 10(12159 + 112500s_1 - 12500s_2)/729 \tag{5.49e}$$

The shape of each joint trajectory thus depends on the values of s_1 and s_2 found from eq.(5.6a) for that trajectory.

5.6 Synthesis of PPO Using Cubic Splines

When the number of via poses increases, the foregoing approach may become impractical, or even unreliable. Indeed, forcing a trajectory to pass

through a number of via points and meet endpoint conditions is equivalent to interpolation. We have seen that an increase in the number of conditions to be met by the normal polynomial amounts to an increase in the degree of this polynomial. Now, finding the coefficients of the interpolating polynomial requires solving a system of linear equations. As we saw in Section 4.9, the computed solution, when solving a system of linear equations, is corrupted with a relative roundoff error that is roughly equal to the relative roundoff error of the data multiplied by an amplification factor that is known as the *condition number* of the system matrix. As we increase the order of the interpolating polynomial, the associated condition number rapidly increases, a fact that numerical analysts discovered some time ago (Kahaner et al., 1989). In order to cope with this problem, *orthogonal polynomials*, such as those bearing the names of *Chebyshev, Laguerre, Legendre*, and so on, have been proposed. While orthogonal polynomials alleviate the problem of a large condition number, they do this only up to a certain extent. As an alternative to higher-order polynomials, *spline functions* have been found to offer more robust interpolation schemes (Dierckx, 1993). Spline functions, or *splines*, for brevity, are piecewise polynomials with continuity properties imposed at the *supporting points*. The latter are those points at which two neighboring polynomials join.

The attractive feature of splines is that they are defined as a set of rather lower-degree polynomials joined at a number of supporting points. Moreover, the matrices that arise from an interpolation problem associated with a spline function are such that their condition number is only slightly dependent on the number of supporting points, and hence, splines offer the possibility of interpolating over a virtually unlimited number of points without producing serious numerical conditioning problems.

Below we expand on periodic cubic splines, for these will be shown to be specially suited for path planning in robotics.

A cubic spline function $s(x)$ connecting N points P_k $(x_k, \quad y_k)$, for $k = 1, 2, \ldots, N$, is a *function* defined *piecewise* by $N - 1$ cubic polynomials joined at the points P_k, such that $s(x_k) = y_k$. Furthermore, the spline function thus defined is twice differentiable everywhere in $x_1 \leq x \leq x_N$. Hence, cubic splines are said to be C^2 functions, i.e., to have continuous derivatives up to the second order.

Cubic splines are optimal in the sense that they minimize a *functional*, i.e., an integral defined as

$$F = \int_0^T s''^2(x)\, dx$$

subject to the constraints

$$s(x_k) = y_k, \qquad k = 1, \ldots, N$$

where x_k and y_k are given. The aforementioned optimality property has a simple kinematic interpretation: Among all functions defining a motion

so that the plot of this function passes through a set of points $P_1(x_1,\, s_1)$, $P_2(x_2,\, s_2)$, $\ldots$, $P_N(x_N,\, s_N)$ in the x-s plane, the cubic spline is the one containing the minimum *acceleration magnitude*. In fact, F, as given above, is the square of the *Euclidean norm* (Halmos, 1974) of $s''(x)$, i.e., F turns out to be a measure of the *magnitude* of the acceleration of a displacement program given by $s(x)$, if we interpret s as displacement and x as time.

Let $P_k(x_k,\ y_k)$ and $P_{k+1}(x_{k+1},\ y_{k+1})$ be two consecutive supporting points. The kth cubic polynomial $s_k(x)$ between those points is assumed to be given by

$$s_k(x) = A_k\,(x - x_k)^3 + B_k\,(x - x_k)^2 + C_k\,(x - x_k) + D_k \quad (5.50a)$$

for $x_k \le x \le x_{k+1}$. Thus, for the spline $s(x)$, $4(N-1)$ coefficients A_k, B_k, C_k, D_k, for $k = 1, \ldots, N-1$, are to be determined. These coefficients will be computed presently in terms of the given function values $\{s_k\}_1^N$ and the second derivatives of the spline at the supporting points, $\{s_k''(x_k)\}_1^N$, as explained below:

We will need the first and second derivatives of $s_k(x)$ as given above, namely,

$$s_k'(x) = 3A_k(x - x_k)^2 + 2B_k(x - x_k) + C_k \quad (5.50b)$$

$$s_k''(x) = 6A_k(x - x_k) + 2B_k \quad (5.50c)$$

whence the relations below follow immediately:

$$B_k = \frac{1}{2}s_k'' \quad (5.51a)$$

$$C_k = s_k' \quad (5.51b)$$

$$D_k = s_k \quad (5.51c)$$

where we have used the abbreviations

$$s_k \equiv s(x_k), \quad s_k' \equiv s'(x_k), \quad s_k'' \equiv s''(x_k) \quad (5.52)$$

Furthermore, let

$$\Delta x_k \equiv x_{k+1} - x_k \quad (5.53)$$

From the above relations, we have expressions for coefficients B_k and D_k in terms of s_k'' and s_k, respectively, but the expression for C_k is given in terms of s_k'. What we would like to have are similar expressions for A_k and C_k, i.e., in terms of s_k and s_k''. The relations sought will be found by imposing the continuity conditions on the spline function and its first and second derivatives with respect to x at the supporting points. These conditions are, then, for $k = 1, 2, \ldots, N-1$,

$$s_k(x_{k+1}) = s_{k+1} \quad (5.54a)$$

$$s_k'(x_{k+1}) = s_{k+1}' \quad (5.54b)$$

$$s_k''(x_{k+1}) = s_{k+1}'' \quad (5.54c)$$

Upon substituting $s''_k(x_{k+1})$, as given by eq.(5.50c), into eq.(5.54c), we obtain

$$6A_k\Delta x_k + 2B_k = 2B_{k+1}$$

but from eq.(5.51a), we have already an expression for B_k, and hence, one for B_{k+1} as well. Substituting these two expressions in the above equation, we obtain an expression for A_k, namely,

$$A_k = \frac{1}{6\,\Delta x_k}\,(s''_{k+1} - s''_k) \tag{5.54d}$$

Furthermore, if we substitute $s_k(x_{k+1})$, as given by eq.(5.50a), into eq.(5.54a), we obtain

$$A_k(\Delta x_k)^3 + B_k(\Delta x_k)^2 + C_k\Delta x_k + D_k = s_{k+1}$$

But we already have values for A_k and B_k from eqs.(5.54d) and (5.51a), respectively. Upon substituting these values in the foregoing equation, we obtain the desired expression for C_k in terms of function and second-derivative values, i.e.,

$$C_k = \frac{\Delta s_k}{\Delta x_k} - \frac{1}{6}\,\Delta x_k\,(s''_{k+1} + 2s''_k) \tag{5.54e}$$

In summary, then, we now have expressions for all four coefficients of the kth polynomial in terms of function and second-derivative values at the supporting points, namely,

$$A_k = \frac{1}{6\,\Delta x_k}\,(s''_{k+1} - s''_k) \tag{5.55a}$$

$$B_k = \frac{1}{2}\,s''_k \tag{5.55b}$$

$$C_k = \frac{\Delta s_k}{\Delta x_k} - \frac{1}{6}\,\Delta x_k\,(s''_{k+1} + 2s''_k) \tag{5.55c}$$

$$D_k = s_k \tag{5.55d}$$

with

$$\Delta s_k \equiv s_{k+1} - s_k \tag{5.55e}$$

Furthermore, from the requirement of continuity in the first derivative, eq.(5.54b), after substitution of eq.(5.50b), one obtains

$$3A_k(\Delta x_k)^2 + 2B_k\Delta x_k + C_k = C_{k+1}$$

or if we shift to the previous polynomials,

$$3A_{k-1}(\Delta x_{k-1})^2 + 2B_{k-1}\Delta x_{k-1} + C_{k-1} = C_k$$

Now, if we substitute expressions (5.55a–c) in the above equation, a linear system of $N-2$ simultaneous equations for the N unknowns $\{s''_k\}_1^N$ is obtained, namely,

$$\begin{aligned}&(\Delta x_k)s''_{k+1} + 2(\Delta x_{k-1} + \Delta x_k)s''_k + (\Delta x_{k-1})s''_{k-1} \\ &= 6\left(\frac{\Delta s_k}{\Delta x_k} - \frac{\Delta s_{k-1}}{\Delta x_{k-1}}\right), \quad \text{for} \quad k = 2, \ldots, N-1\ . \end{aligned} \tag{5.56}$$

Further, let $\mathbf{s}$ be the N-dimensional vector whose kth component is s_k, with vector $\mathbf{s}''$ being defined likewise, i.e.,

$$\mathbf{s} = [\, s_1, \cdots, s_N \,]^T, \qquad \mathbf{s}'' = [\, s''_1, \cdots, s''_N \,]^T \tag{5.57}$$

The relationship between $\mathbf{s}$ and $\mathbf{s}''$ of eq.(5.56) can then be written in vector form as

$$\mathbf{A}\,\mathbf{s}'' = 6\,\mathbf{C}\,\mathbf{s} \tag{5.58a}$$

where $\mathbf{A}$ and $\mathbf{C}$ are $(N-2)\times N$ matrices defined as:

$$\mathbf{A} = \begin{bmatrix} \alpha_1 & 2\alpha_{1,2} & \alpha_2 & 0 & \cdots & 0 & 0 \\ 0 & \alpha_2 & 2\alpha_{2,3} & \alpha_3 & \cdots & 0 & 0 \\ \vdots & \vdots & \ddots & \ddots & \ddots & \vdots & \vdots \\ 0 & 0 & \ldots & \alpha_{N'''} & 2\alpha_{N''',N''} & \alpha_{N''} & 0 \\ 0 & 0 & 0 & \cdots & \alpha_{N''} & 2\alpha_{N'',N'} & \alpha_{N'} \end{bmatrix} \tag{5.58b}$$

and

$$\mathbf{C} = \begin{bmatrix} \beta_1 & -\beta_{1,2} & \beta_2 & 0 & \cdots & 0 & 0 \\ 0 & \beta_2 & -\beta_{2,3} & \beta_3 & \cdots & 0 & 0 \\ \vdots & \vdots & \ddots & \ddots & \ddots & \vdots & \vdots \\ 0 & 0 & \cdots & \beta_{N'''} & -\beta_{N''',N''} & \beta_{N''} & 0 \\ 0 & 0 & 0 & \cdots & \beta_{N''} & -\beta_{N'',N'} & \beta_{N'} \end{bmatrix} \tag{5.58c}$$

while for $i, j, k = 1, \ldots, N-1$,

$$\alpha_k \equiv \Delta x_k, \quad \alpha_{i,j} \equiv \alpha_i + \alpha_j, \tag{5.58d}$$

$$\beta_k \equiv 1/\alpha_k, \quad \beta_{i,j} \equiv \beta_i + \beta_j \tag{5.58e}$$

and

$$N' \equiv N-1, \qquad N'' \equiv N-2, \qquad N''' \equiv N-3 \tag{5.58f}$$

Thus, two additional equations are needed to render eq.(5.58a) a determined system. The additional equations are derived, in turn, depending upon the class of functions one is dealing with, which thus gives rise to various types of splines. For example, if s''_1 and s''_N are defined as zero,

then one obtains *natural cubic splines*, the name arising by an analogy with beam analysis. Indeed, in beam theory, the boundary conditions of a simply-supported beam establish the vanishing of the bending moments at the ends. From beam theory, moreover, the bending moment is proportional to the second derivative of the *elastica*, or *neutral axis*, of the beam with respect to the abscissa along the beam axis in the undeformed configuration. In this case, vector $\mathbf{s}''$ becomes of dimension $N-2$, and hence, matrix $\mathbf{A}$ becomes, correspondingly, of $(N-2)\times(N-2)$, namely,

$$\mathbf{A}=\begin{bmatrix} 2\alpha_{1,2} & \alpha_2 & 0 & \cdots & 0 \\ \alpha_2 & 2\alpha_{2,3} & \alpha_3 & \cdots & 0 \\ \vdots & \ddots & \ddots & \ddots & \vdots \\ 0 & \dots & \alpha_{N'''} & 2\alpha_{N''',N''} & \alpha_{N''} \\ 0 & 0 & \cdots & \alpha_{N''} & 2\alpha_{N'',N'} \end{bmatrix} \tag{5.59}$$

On the other hand, if one is interested in periodic functions, which is often the case when synthesizing pick-and-place motions, then the conditions $s_1=s_N$, $s_1'=s_N'$, $s_1''=s_N''$ are imposed, thereby producing *periodic cubic splines*. The last of these conditions is used to eliminate one unknown in eq.(5.58a), while the second condition, namely the continuity of the first derivative, is used to add an equation. We have, then,

$$s_1'=s_N' \tag{5.60}$$

which can be written, using eq.(5.54b), as

$$s_1'=s_{N-1}'(x_N) \tag{5.61}$$

Upon substituting $s_{N-1}'(x_N)$, as given by eq.(5.50b), into the above equation, we obtain

$$s_1'=3A_{N-1}\Delta x_{N-1}^2+2B_{N-1}\Delta x_{N-1}+C_{N-1} \tag{5.62}$$

Now we use eqs.(5.55a–c) and simplify the expression thus resulting, which leads to

$$2(\Delta x_1+\Delta x_{N-1})s_1''+\Delta x_1 s_2''+\Delta x_{N-1}s_{N-1}''=6\left(\frac{\Delta s_1}{\Delta x_1}-\frac{\Delta s_{N-1}}{\Delta x_{N-1}}\right) \tag{5.63}$$

thereby obtaining the last equation required to solve the system of equations given by eqs.(5.58a–c). We thus have $(N-1)$ independent equations to solve for $(N-1)$ unknowns, namely, s_k'', for $k=1,\dots,N-1$, s_N'' being equal to s_1''. Expressions for matrices $\mathbf{A}$ and $\mathbf{C}$, as applicable to periodic cubic splines, are given in eqs.(9.59a & b).

While we focused in the above discussion on cubic splines, other types of splines could have been used. For example, Thompson and Patel (1987) used B-splines in robotics trajectory planning.

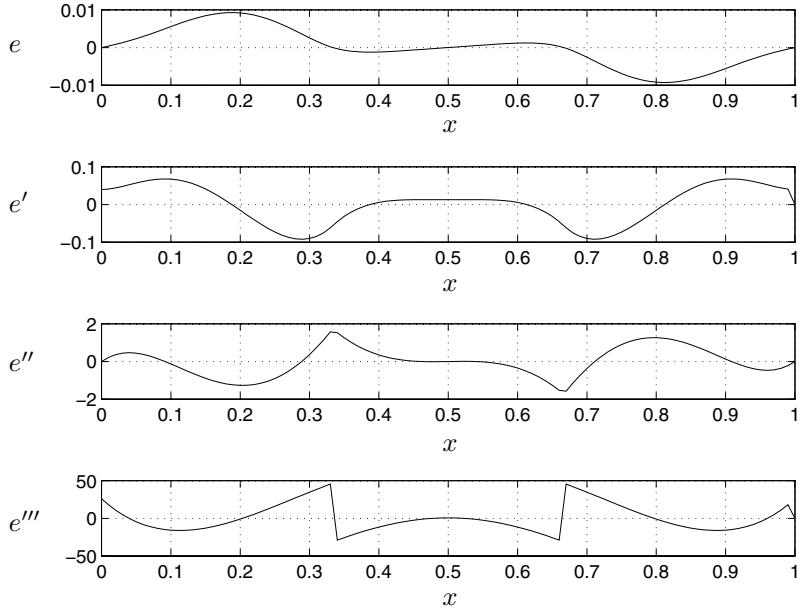

FIGURE 5.5. Errors in the approximation of a 4-5-6-7 polynomial with a natural cubic spline, using four supporting points.

Example 5.6.1 (Approximation of a 4-5-6-7 polynomial with a cubic spline) *Find the cubic spline that interpolates the 4-5-6-7 polynomial of Fig. 5.3 with $N+1$ equally-spaced supporting points and plot the interpolation error for $N = 3$ and $N = 10$.*

Solution: Let us use a natural spline, in which case the second derivative at the end points vanishes, with vector $\mathbf{s}''$ thus losing two components. That is, we now have only $N-1$ unknowns $\{ s''_k \}_1^{N-1}$ to determine. Correspondingly, matrix $\mathbf{A}$ then loses its first and last columns and hence, becomes a square $(N-1) \times (N-1)$ matrix. Moreover,

$$\Delta x_k = \frac{1}{N}, \quad k = 1, \ldots, N$$

and matrices $\mathbf{A}$ and $\mathbf{C}$ become, correspondingly,

$$\mathbf{A} = \frac{1}{N} \begin{bmatrix} 4 & 1 & 0 & \cdots & 0 \\ 1 & 4 & 1 & \cdots & 0 \\ \vdots & \ddots & \ddots & \ddots & \vdots \\ 0 & \ldots & 1 & 4 & 1 \\ 0 & 0 & \cdots & 1 & 4 \end{bmatrix}$$

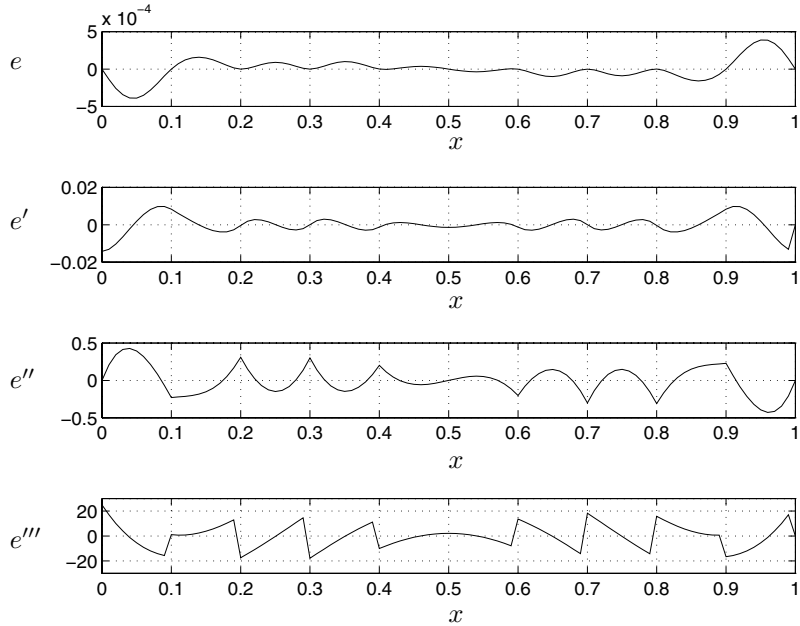

FIGURE 5.6. Errors in the approximation of a 4-5-6-7 polynomial with a natural cubic spline, using eleven supporting points.

and

$$\mathbf{C} = N \begin{bmatrix} 1 & -2 & 1 & 0 & \cdots & 0 & 0 \\ 0 & 1 & -2 & 1 & \cdots & 0 & 0 \\ \vdots & \vdots & \ddots & \ddots & \ddots & \vdots & \vdots \\ 0 & 0 & \cdots & 1 & -2 & 1 & 0 \\ 0 & 0 & 0 & \cdots & 1 & -2 & 1 \end{bmatrix}$$

the vector of second derivatives at the supporting points, $\mathbf{s}''$, then being readily obtained as

$$\mathbf{s}'' = 6\mathbf{A}^{-1}\mathbf{C}\mathbf{s}$$

With the values of the second derivatives at the supporting points known, the calculation of the spline coefficients A_k, B_k, C_k, and D_k, for $k = 1, \ldots, N$, is now straightforward. Let the interpolation error, $e(x)$, be defined as $e(x) \equiv s(x) - p(x)$, where $s(x)$ is the interpolating spline and $p(x)$ is the given polynomial. This error and its derivatives $e'(x)$, $e''(x)$, and $e'''(x)$ are plotted in Figs. 5.5 and 5.6 for $N = 3$ and $N = 10$, respectively. What we observe is an increase of more than one order of magnitude in the error as we increase the order of the derivative by one. Thus, the order of magnitude of acceleration errors is usually higher than two orders of magnitude above the displacement errors, a fact that should not be overlooked in applications.

This page intentionally left blank

6

Dynamics of Serial Robotic Manipulators

6.1 Introduction

The main objectives of this chapter are (i) to devise an algorithm for the real-time *computed torque control* and (ii) to derive the system of second-order ordinary differential equations (ODE) governing the motion of an n-axis manipulator. We will focus on serial manipulators, the dynamics of a much broader class of robotic mechanical systems, namely, parallel manipulators and mobile robots, being the subject of Chapter 10. Moreover, we will study mechanical systems with rigid links and rigid joints and will put aside systems with flexible elements, which pertain to a more specialized realm.

6.2 Inverse vs. Forward Dynamics

The two basic problems associated with the dynamics of robotic mechanical systems, namely, the *inverse* and the *forward* problems, are thoroughly discussed in this chapter. The relevance of these problems cannot be overstated: the former is essential for the computed-torque control of robotic manipulators, while the latter is required for the simulation and the real-time feedback control of the same systems. Because the inverse problem is purely algebraic, it is conceptually simpler to grasp than the forward problem, and hence, the inverse problem will be discussed first. Moreover,

the inverse problem is also computationally simpler than the forward problem. In the inverse problem, a time-history of either the Cartesian or the joint coordinates is given, and from knowledge of these histories and the architecture and inertial parameters of the system at hand, the torque or force requirements at the different actuated joints are determined as time-histories as well. In the forward problem, current values of the joint coordinates and their first time-derivatives are known at a given instant, the time-histories of the applied torques or forces being also known, along with the architecture and the inertial parameters of the manipulator at hand. With these data, the values of the joint coordinates and their time-derivatives are computed at a later sampling instant by integration of the underlying system of nonlinear ordinary differential equations.

The study of the dynamics of systems of multiple rigid bodies is classical, but up until the advent of the computer, it was limited only to theoretical results and a reduced number of bodies. First Uicker (1965) and then Kahn (1969) produced a method based on the Euler-Lagrange equations of mechanical systems of rigid bodies that they used to simulate the dynamical behavior of such systems. A breakthrough in the development of algorithms for dynamics computations was reported by Luh et al. (1980), who proposed a recursive formulation of multibody dynamics that is applicable to systems with serial kinematic chains. This formulation, based on the Newton-Euler equations of rigid bodies, allowed the calculation of the joint torques of a six-revolute manipulator with only 800 multiplications and 595 additions, a tremendous gain if we consider that the straightforward calculation of the Euler-Lagrange equations for the same type of manipulator involves 66,271 multiplications and 51,548 additions, as pointed out by Hollerbach (1980). In the foregoing reference, a recursive derivation of the Euler-Lagrange equations was proposed, whereby the computational complexity was reduced to only 2,195 multiplications and 1,719 additions.

The foregoing results provoked a discussion on the merits and demerits of each of the Euler-Lagrange and the Newton-Euler formulations. Silver (1982) pointed out that since both formulations are equivalent, they should lead to the same computational complexity. In fact, Silver showed how to derive the Euler-Lagrange equations from the Newton-Euler formulation by following an approach first introduced by Kane (1961) in connection with nonholonomic systems. Kane and Levinson (1983) then showed how Kane's equations can be applied to particular robotic manipulators and arrived at lower computational complexities. They applied the said equations to the Stanford Arm (Paul, 1981) and computed its inverse dynamics with 646 multiplications and 394 additions. Thereafter, Khalil et al. (1986) proposed a condensed recursive Newton-Euler method that reduced the computational complexity to 538 multiplications and 478 additions, for *arbitrary architectures*. Further developments in this area were reported by Balafoutis and Patel (1991), who showed that the underlying computational complexity can be reduced to 489 multiplications and 420 additions

for the most general case of a six-revolute manipulator, i.e., without exploiting particular features of the manipulator geometry. Balafoutis and Patel based their algorithm on tensor analysis, whereby tensor identities are exploited to their fullest extent in order to reduce the number of operations involved. Li and Sankar (1992), in turn, reported further savings that allowed them to bring down those numbers to 459 multiplications and 390 additions.

In this chapter, the inverse dynamics problem is solved with the well-known recursive Newton-Euler algorithm, while the forward dynamics problem is handled with a novel approach, based on the reciprocity relations between the *constraint wrenches* and the *feasible twists* of a manipulator. This technique is developed with the aid of a modeling tool known as the *natural orthogonal complement*, thoroughly discussed in Section 6.5.

Throughout the chapter, we will follow a multibody system approach, which requires a review of the underlying fundamentals.

6.3 Fundamentals of Multibody System Dynamics

6.3.1 On Nomenclature and Basic Definitions

We consider here a mechanical system composed of r rigid bodies and denote by $\mathbf{M}_i$ the 6×6 *inertia dyad*—see Section 3.8—of the ith body. Moreover, we let $\mathbf{W}_i$, already introduced in eq.(3.145), be the 6×6 *angular-velocity dyad* of the same body. As pertaining to the case at hand, the said matrices are displayed below:

$$\mathbf{M}_i \equiv \begin{bmatrix} \mathbf{I}_i & \mathbf{O} \\ \mathbf{O} & m_i\mathbf{1} \end{bmatrix}, \quad \mathbf{W}_i \equiv \begin{bmatrix} \boldsymbol{\Omega}_i & \mathbf{O} \\ \mathbf{O} & \mathbf{O} \end{bmatrix}, \quad i = 1, \ldots, r \tag{6.1}$$

where $\mathbf{1}$ and $\mathbf{O}$ denote the 3×3 identity and zero matrices, respectively, while $\boldsymbol{\Omega}_i$ and $\mathbf{I}_i$ are the angular-velocity and the inertia matrices of the ith body, this last being defined with respect to the mass center C_i of this body. Moreover, the mass of this body is denoted by m_i, whereas $\mathbf{c}_i$ and $\dot{\mathbf{c}}_i$ denote the position and the velocity vectors of C_i. Furthermore, let $\mathbf{t}_i$ denote the twist of the same body, the latter being defined in terms of the angular velocity vector $\boldsymbol{\omega}_i$, the vector of $\boldsymbol{\Omega}_i$, and the velocity of C_i. The 6-dimensional *momentum screw* $\boldsymbol{\mu}_i$ is defined likewise. Furthermore, $\mathbf{w}_i^W$ and $\mathbf{w}_i^C$ are defined as the *working wrench* and the *nonworking constraint wrench* exerted on the ith body by its neighbors, in which forces are assumed to be applied at C_i. We thus have, for $i = 1, \ldots, r$,

$$\mathbf{t}_i = \begin{bmatrix} \boldsymbol{\omega}_i \\ \dot{\mathbf{c}}_i \end{bmatrix}, \quad \boldsymbol{\mu}_i = \begin{bmatrix} \mathbf{I}_i\boldsymbol{\omega}_i \\ m_i\dot{\mathbf{c}}_i \end{bmatrix}, \quad \mathbf{w}_i^W = \begin{bmatrix} \mathbf{n}_i^W \\ \mathbf{f}_i^W \end{bmatrix}, \quad \mathbf{w}_i^C = \begin{bmatrix} \mathbf{n}_i^C \\ \mathbf{f}_i^C \end{bmatrix} \tag{6.2}$$

where superscripted $\mathbf{n}_i$ and $\mathbf{f}_i$ stand, respectively, for the moment and the force acting on the ith body, the force being applied at the mass center C_i.

Thus, whereas $\mathbf{w}_i^W$ accounts for forces and moments exerted by both the environment and the actuators, including driving forces as well as dissipative effects, $\mathbf{w}_i^C$, whose sole function is to keep the links together, accounts for those forces and moments exerted by the neighboring links, which do not produce any mechanical work. Therefore, friction wrenches applied by the $(i-1)$st and the $(i+1)$st links onto the ith link are not included in $\mathbf{w}_i^C$; rather, they are included in $\mathbf{w}_i^W$.

Clearly, from the definitions of $\mathbf{M}_i$, $\boldsymbol{\mu}_i$, and $\mathbf{t}_i$, we have

$$\boldsymbol{\mu}_i = \mathbf{M}_i \mathbf{t}_i \tag{6.3}$$

Moreover, from eq.(3.148),

$$\dot{\boldsymbol{\mu}}_i = \mathbf{M}_i \dot{\mathbf{t}}_i + \mathbf{W}_i \boldsymbol{\mu}_i = \mathbf{M}_i \dot{\mathbf{t}}_i + \mathbf{W}_i \mathbf{M}_i \mathbf{t}_i \tag{6.4}$$

We now recall the Newton-Euler equations for a rigid body, namely,

$$\mathbf{I}_i \dot{\boldsymbol{\omega}}_i = -\boldsymbol{\omega}_i \times \mathbf{I}_i \boldsymbol{\omega}_i + \mathbf{n}_i^W + \mathbf{n}_i^C \tag{6.5a}$$

$$m_i \ddot{\mathbf{c}}_i = \mathbf{f}_i^W + \mathbf{f}_i^C \tag{6.5b}$$

which can be written in compact form using the foregoing 6-dimensional twist and wrench arrays as well as the 6×6 inertia and angular-velocity dyads. We thus obtain the Newton-Euler equations of the ith body in the form

$$\mathbf{M}_i \dot{\mathbf{t}}_i = -\mathbf{W}_i \mathbf{M}_i \mathbf{t}_i + \mathbf{w}_i^W + \mathbf{w}_i^C \tag{6.5c}$$

6.3.2 The Euler-Lagrange Equations of Serial Manipulators

The Euler-Lagrange dynamical equations of a mechanical system are now recalled, as pertaining to serial manipulators. Thus, the mechanical system at hand has n degrees of freedom, its n independent generalized coordinates being the n joint variables, which are stored in the n-dimensional vector $\boldsymbol{\theta}$. We thus have

$$\frac{d}{dt}\left(\frac{\partial T}{\partial \dot{\boldsymbol{\theta}}}\right) - \frac{\partial T}{\partial \boldsymbol{\theta}} = \boldsymbol{\phi} \tag{6.6}$$

where T is a scalar function denoting the *kinetic energy* of the system and $\boldsymbol{\phi}$ is the n-dimensional vector of *generalized force*. If some forces on the right-hand side stem from a potential V, we can, then decompose $\boldsymbol{\phi}$ into two parts, $\boldsymbol{\phi}_p$ and $\boldsymbol{\phi}_n$, the former arising from V and termed the *conservative force* of the system; the latter is the *nonconservative force* $\boldsymbol{\phi}_n$. That is,

$$\boldsymbol{\phi}_p \equiv -\frac{\partial V}{\partial \boldsymbol{\theta}} \tag{6.7}$$

the above Euler-Lagrange equations thus becoming

$$\frac{d}{dt}\left(\frac{\partial L}{\partial \dot{\boldsymbol{\theta}}}\right) - \frac{\partial L}{\partial \boldsymbol{\theta}} = \boldsymbol{\phi}_n \tag{6.8}$$

where L is the *Lagrangian* of the system, defined as

$$L \equiv T - V \tag{6.9}$$

Moreover, the kinetic energy of the system is simply the sum of the kinetic energies of all the r links. Recalling eq.(3.150), which gives the kinetic energy of a rigid body in terms of 6-dimensional arrays, one has

$$T = \sum_{1}^{r} T_i = \sum_{1}^{r} \frac{1}{2} \mathbf{t}_i^T \mathbf{M}_i \mathbf{t}_i \tag{6.10}$$

whereas the vector of nonconservative generalized forces is given by

$$\boldsymbol{\phi}_n \equiv \frac{\partial \Pi^A}{\partial \dot{\boldsymbol{\theta}}} - \frac{\partial \Delta}{\partial \dot{\boldsymbol{\theta}}} \tag{6.11}$$

in which Π^A and Δ denote the power supplied to the system and the *Rayleigh dissipation function*, or for brevity, the *dissipation function* of the system.

The first of these items is discussed below; the latter is only outlined in this section but is discussed extensively in Section 6.8. First, the wrench $\mathbf{w}_i^W$ is decomposed into two parts, $\mathbf{w}_i^A$ and $\mathbf{w}_i^D$, the former being the wrench supplied by the actuators and the latter being the wrench that arises from viscous and Coulomb friction, the gravity wrench being not needed here because gravity effects are considered in the potential $V(\boldsymbol{\theta})$. We thus call $\mathbf{w}_i^A$ the *active wrench* and $\mathbf{w}_i^D$ the dissipative wrench. Here, the wrenches supplied by the actuators are assumed to be prescribed functions of time. Moreover, these wrenches are supplied by single-dof actuators in the form of forces along a line of action or moments in a given direction, both line and direction being fixed to the two bodies that are coupled by an active joint. Hence, the actuator-supplied wrenches are dependent on the posture of the manipulator as well, but not on its twist. That is, the actuator wrenches are functions of both the vector of generalized coordinates, or joint variables, and time, but not of the generalized speeds, or joint-rates. Forces dependent on the latter to be considered here are assumed to be all *dissipative*. As a consequence, they can be readily incorporated into the mathematical model at hand via the dissipation function, to be discussed in Section 6.8. Note that feedback control schemes require actuator forces that are functions not only of the generalized coordinates, but also of the generalized speeds. These forces or moments are most easily incorporated into the underlying mathematical model, once this model is derived in the state-variable space, i.e., in the space of generalized coordinates and generalized speeds.

Thus, the power supplied to the ith link, Π_i^A, is readily computed as

$$\Pi_i^A = (\mathbf{w}_i^A)^T \mathbf{t}_i \tag{6.12a}$$

Similar to the kinetic energy, then, the power supplied to the overall system is simply the sum of the individual powers supplied to each link,

and expressed as in eq.(6.12a), i.e.,

$$\Pi^A \equiv \sum_1^r \Pi_i^A \tag{6.12b}$$

Further definitions are now introduced. These are the $6n$-dimensional vectors of *manipulator twist*, $\mathbf{t}$; *manipulator momentum*, $\boldsymbol{\mu}$; *manipulator constraint wrench*, $\mathbf{w}^C$; *manipulator active wrench*, $\mathbf{w}^A$; and *manipulator dissipative wrench*, $\mathbf{w}^D$. Additionally, the $6n \times 6n$ matrices of *manipulator mass*, $\mathbf{M}$, and *manipulator angular velocity*, $\mathbf{W}$, are also introduced below:

$$\mathbf{t} = \begin{bmatrix} \mathbf{t}_1 \\ \vdots \\ \mathbf{t}_n \end{bmatrix}, \qquad \mu = \begin{bmatrix} \mu_1 \\ \vdots \\ \mu_n \end{bmatrix}, \tag{6.13a}$$

$$\mathbf{w}^C = \begin{bmatrix} \mathbf{w}_1^C \\ \vdots \\ \mathbf{w}_n^C \end{bmatrix}, \ \mathbf{w}^A = \begin{bmatrix} \mathbf{w}_1^A \\ \vdots \\ \mathbf{w}_n^A \end{bmatrix}, \ \mathbf{w}^D = \begin{bmatrix} \mathbf{w}_1^D \\ \vdots \\ \mathbf{w}_n^D \end{bmatrix} \tag{6.13b}$$

$$\mathbf{M} = \mathrm{diag}\,(\,\mathbf{M}_1,\,\ldots,\,\mathbf{M}_n\,), \qquad \mathbf{W} = \mathrm{diag}\,(\,\mathbf{W}_1,\,\ldots,\,\mathbf{W}_n\,) \tag{6.13c}$$

It is now apparent that, from definitions (6.13b & 6.13c) and relation (6.3), we have

$$\boldsymbol{\mu} = \mathbf{M}\mathbf{t} \tag{6.14}$$

Moreover, from definitions (6.1) and (6.2),

$$\dot{\boldsymbol{\mu}} = \mathbf{M}\dot{\mathbf{t}} + \mathbf{W}\mathbf{M}\mathbf{t} \tag{6.15}$$

With the foregoing definitions, then, the kinetic energy of the manipulator takes on a simple form, namely,

$$T = \frac{1}{2}\mathbf{t}^T\mathbf{M}\mathbf{t} \equiv \frac{1}{2}\mathbf{t}^T\boldsymbol{\mu} \tag{6.16}$$

which is a quadratic form in the system twist. Since the twist, on the other hand, is a linear function of the vector $\dot{\boldsymbol{\theta}}$ of joint rates, the kinetic energy turns out to be a quadratic form in the vector of joint rates. Moreover, we will assume that this form is *homogeneous* in $\dot{\boldsymbol{\theta}}$, i.e.,

$$T = \frac{1}{2}\dot{\boldsymbol{\theta}}^T\mathbf{I}(\boldsymbol{\theta})\dot{\boldsymbol{\theta}} \tag{6.17}$$

Notice that the above assumption implies that the base of the robot is fixed to an inertial base, and hence, when all joints are locked, the kinetic energy of the robot vanishes, which would not be the case if, for example, the robot were mounted on the International Space Station. If this were the

case, then the kinetic energy would not vanish even if all robot joints were locked, which means that the foregoing kinetic-energy expression would include a linear term in $\dot{\boldsymbol{\theta}}$ and a term independent of the joint-rates. In any event, it is apparent that

$$\mathbf{I}(\boldsymbol{\theta}) = \frac{\partial^2}{\partial \dot{\boldsymbol{\theta}}^2}(T) \tag{6.18}$$

which means that the $n \times n$ generalized inertia matrix is the *Hessian* matrix of the kinetic energy with respect to the vector of generalized speed.

Furthermore, the Euler-Lagrange equations can be written in the form

$$\frac{d}{dt}\left(\frac{\partial T}{\partial \dot{\boldsymbol{\theta}}}\right) - \frac{\partial T}{\partial \boldsymbol{\theta}} + \frac{\partial V}{\partial \boldsymbol{\theta}} = \boldsymbol{\phi}_n \tag{6.19a}$$

Now, from the form of T given in eq.(6.17), the partial derivatives appearing in the foregoing equation take the forms derived below:

$$\frac{\partial T}{\partial \dot{\boldsymbol{\theta}}} = \mathbf{I}(\boldsymbol{\theta})\dot{\boldsymbol{\theta}}$$

and hence,

$$\frac{d}{dt}\left(\frac{\partial T}{\partial \dot{\boldsymbol{\theta}}}\right) = \mathbf{I}(\boldsymbol{\theta})\ddot{\boldsymbol{\theta}} + \dot{\mathbf{I}}(\boldsymbol{\theta}, \dot{\boldsymbol{\theta}})\dot{\boldsymbol{\theta}} \tag{6.19b}$$

Moreover, in order to calculate the second term of the left-hand side of eq.(6.19a), we express the kinetic energy in the form

$$T = \frac{1}{2}\mathbf{p}(\boldsymbol{\theta}, \dot{\boldsymbol{\theta}})^T \dot{\boldsymbol{\theta}} \tag{6.19c}$$

where $\mathbf{p}(\boldsymbol{\theta}, \dot{\boldsymbol{\theta}})$ is the *generalized momentum* of the manipulator, defined as

$$\mathbf{p}(\boldsymbol{\theta}, \dot{\boldsymbol{\theta}}) \equiv \mathbf{I}(\boldsymbol{\theta})\dot{\boldsymbol{\theta}} \tag{6.19d}$$

Hence,

$$\frac{\partial T}{\partial \boldsymbol{\theta}} = \frac{1}{2}\left(\frac{\partial \mathbf{p}}{\partial \boldsymbol{\theta}}\right)^T \dot{\boldsymbol{\theta}} \tag{6.19e}$$

or

$$\frac{\partial T}{\partial \boldsymbol{\theta}} = \frac{1}{2}\left[\frac{\partial (\mathbf{I}\dot{\boldsymbol{\theta}})}{\partial \boldsymbol{\theta}}\right]^T \dot{\boldsymbol{\theta}} \tag{6.19f}$$

the Euler-Lagrange equations thus taking on the alternative form

$$\mathbf{I}(\boldsymbol{\theta})\ddot{\boldsymbol{\theta}} + \dot{\mathbf{I}}(\boldsymbol{\theta}, \dot{\boldsymbol{\theta}})\dot{\boldsymbol{\theta}} - \frac{1}{2}\left[\frac{\partial (\mathbf{I}\dot{\boldsymbol{\theta}})}{\partial \boldsymbol{\theta}}\right]^T \dot{\boldsymbol{\theta}} + \frac{\partial V}{\partial \boldsymbol{\theta}} = \boldsymbol{\phi}_n \tag{6.20}$$

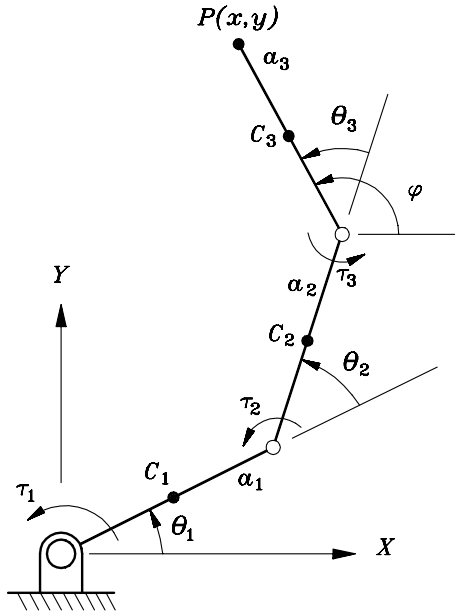

FIGURE 6.1. A planar manipulator.

Example 6.3.1 (Euler-Lagrange equations of a planar manipulator) *Consider the manipulator of Fig. 6.1, with links designed so that their mass centers, C_1, C_2, and C_3, are located at the midpoints of segments O_1O_2, O_2O_3, and O_3P, respectively. Moreover, the ith link has a mass m_i and a centroidal moment of inertia in a direction normal to the plane of motion I_i, while the joints are actuated by motors delivering torques τ_1, τ_2, and τ_3, the lubricant of the joints producing dissipative torques that we will neglect in this model. Under the assumption that gravity acts in the direction of $-Y$, find the associated Euler-Lagrange equations.*

Solution: Here we recall the kinematic analysis of Section 4.8 and the definitions introduced therein for the analysis of planar motion. In this light, all vectors introduced below are 2-dimensional, the scalar angular velocities of the links, ω_i, for $i = 1, 2, 3$, being

$$\omega_1 = \dot{\theta}_1, \quad \omega_2 = \dot{\theta}_1 + \dot{\theta}_2, \quad \omega_3 = \dot{\theta}_1 + \dot{\theta}_2 + \dot{\theta}_3$$

Moreover, the velocities of the mass centers are

$$\dot{\mathbf{c}}_1 = \frac{1}{2}\dot{\theta}_1 \mathbf{E}\mathbf{a}_1$$

$$\dot{\mathbf{c}}_2 = \dot{\theta}_1 \mathbf{E}\mathbf{a}_1 + \frac{1}{2}(\dot{\theta}_1 + \dot{\theta}_2)\mathbf{E}\mathbf{a}_2$$

$$\dot{\mathbf{c}}_3 = \dot{\theta}_1 \mathbf{E}\mathbf{a}_1 + (\dot{\theta}_1 + \dot{\theta}_2)\mathbf{E}\mathbf{a}_2 + \frac{1}{2}(\dot{\theta}_1 + \dot{\theta}_2 + \dot{\theta}_3)\mathbf{E}\mathbf{a}_3$$

the kinetic energy then becoming

$$T = \frac{1}{2}\sum_{1}^{3}(m_i\|\dot{\mathbf{c}}_i\|^2 + I_i\omega_i^2)$$

The squared magnitudes of the mass-center velocities are now computed using the expressions derived above. After simplifications, these yield

$$\begin{aligned}
\|\dot{\mathbf{c}}_1\|^2 &= \frac{1}{4}a_1^2\dot{\theta}_1^2 \\
\|\dot{\mathbf{c}}_2\|^2 &= a_1^2\dot{\theta}_1^2 + \frac{1}{4}a_2^2(\dot{\theta}_1^2 + 2\dot{\theta}_1\dot{\theta}_2 + \dot{\theta}_2^2) + a_1a_2\cos\theta_2(\dot{\theta}_1^2 + \dot{\theta}_1\dot{\theta}_2) \\
\|\dot{\mathbf{c}}_3\|^2 &= a_1^2\dot{\theta}_1^2 + a_2^2(\dot{\theta}_1^2 + 2\dot{\theta}_1\dot{\theta}_2 + \dot{\theta}_2^2) \\
&\quad + \frac{1}{4}a_3^2(\dot{\theta}_1^2 + \dot{\theta}_2^2 + \dot{\theta}_3^2 + 2\dot{\theta}_1\dot{\theta}_2 + 2\dot{\theta}_1\dot{\theta}_3 + 2\dot{\theta}_2\dot{\theta}_3) \\
&\quad + 2a_1a_2\cos\theta_2(\dot{\theta}_1^2 + \dot{\theta}_1\dot{\theta}_2) + a_1a_3\cos(\theta_2+\theta_3)(\dot{\theta}_1^2 + \dot{\theta}_1\dot{\theta}_2 + \dot{\theta}_1\dot{\theta}_3) \\
&\quad + a_2a_3\cos\theta_3(\dot{\theta}_1^2 + \dot{\theta}_2^2 + 2\dot{\theta}_1\dot{\theta}_2 + \dot{\theta}_1\dot{\theta}_3 + \dot{\theta}_2\dot{\theta}_3)
\end{aligned}$$

The kinetic energy of the whole manipulator thus becomes

$$T = \frac{1}{2}(I_{11}\dot{\theta}_1^2 + 2I_{12}\dot{\theta}_1\dot{\theta}_2 + 2I_{23}\dot{\theta}_2\dot{\theta}_3 + I_{22}\dot{\theta}_2^2 + 2I_{13}\dot{\theta}_1\dot{\theta}_3 + I_{33}\dot{\theta}_3^2)$$

with coefficients I_{ij}, for $i = 1, 2, 3$, and $j = i$ to 3 being the distinct entries of the 3×3 matrix of generalized inertia of the system. These entries are given below:

$$\begin{aligned}
I_{11} &\equiv I_1 + I_2 + I_3 + \frac{1}{4}m_1a_1^2 + m_2\left(a_1^2 + \frac{1}{4}a_2^2 + a_1a_2c_2\right) \\
&\quad + m_3\left(a_1^2 + a_2^2 + \frac{1}{4}a_3^2 + 2a_1a_2c_2 + a_1a_3c_{23} + a_2a_3c_3\right) \\
I_{12} &\equiv I_2 + I_3 + \frac{1}{2}\left[m_2\left(\frac{1}{2}a_2^2 + a_1a_2c_2\right)\right. \\
&\quad \left. + m_3\left(2a_2^2 + \frac{1}{2}a_3^2 + 2a_1a_2c_2 + a_1a_3c_{23} + 2a_2a_3c_3\right)\right] \\
I_{13} &\equiv I_3 + \frac{1}{2}m_3\left(\frac{1}{2}a_3^2 + a_1a_3c_{23} + a_2a_3c_3\right) \\
I_{22} &\equiv I_2 + I_3 + \frac{1}{4}m_2a_2^2 + m_3\left(a_2^2 + \frac{1}{4}a_3^2 + a_2a_3c_3\right) \\
I_{23} &\equiv I_3 + \frac{1}{2}m_3\left(\frac{1}{2}a_3^2 + a_2a_3c_3\right) \\
I_{33} &\equiv I_3 + \frac{1}{4}m_3a_3^2
\end{aligned}$$

where c_i and c_{ij} stand for $\cos\theta_i$ and $\cos(\theta_i + \theta_j)$, respectively. From the foregoing expressions, it is apparent that the generalized inertia matrix is

not a function of θ_1, which is only natural, for if the second and third joints are locked while leaving the first one free, the whole manipulator becomes a single rigid body pivoting about point O_1. Now, the polar moment of inertia of a rigid body in planar motion about a fixed point is constant, and hence, the first joint variable should not affect the generalized inertia matrix.

Furthermore, the potential energy of the manipulator is computed as the sum of the individual link potential energies, i.e.,

$$V = \frac{1}{2}m_1 g a_1 \sin\theta_1 + m_2 g\left[a_1 \sin\theta_1 + \frac{1}{2}a_2 \sin(\theta_1+\theta_2)\right] + m_3 g\left[a_1 \sin\theta_1 + a_2 \sin(\theta_1+\theta_2) + \frac{1}{2}a_3 \sin(\theta_1+\theta_2+\theta_3)\right]$$

while the total power delivered to the manipulator takes the form

$$\Pi = \tau_1\dot{\theta}_1 + \tau_2\dot{\theta}_2 + \tau_3\dot{\theta}_3$$

We now proceed to compute the various terms in eq.(6.20). We already have $\mathbf{I}(\boldsymbol{\theta})$, but we do not have, as yet, its time-derivative. However, the entries of $\dot{\mathbf{I}}$ are merely the time-derivatives of the entries of $\mathbf{I}$. From the above expressions for these entries, their time-rates of change are readily calculated, namely,

$$\begin{aligned}
\dot{I}_{11} &= -m_2 a_1 a_2 s_2 \dot{\theta}_2 - m_3[2a_1 a_2 s_2 \dot{\theta}_2 + a_1 a_3 s_{23}(\dot{\theta}_2+\dot{\theta}_3) + a_2 a_3 s_3 \dot{\theta}_3] \\
\dot{I}_{12} &= \frac{1}{2}\{-m_2 a_1 a_2 s_2 \dot{\theta}_2 - m_3[2a_1 a_2 s_2 \dot{\theta}_2 + a_1 a_3 s_{23}(\dot{\theta}_2+\dot{\theta}_3) + 2a_2 a_3 s_3 \dot{\theta}_3]\} \\
\dot{I}_{13} &= -\frac{1}{2}m_3[a_1 a_3 s_{23}(\dot{\theta}_2+\dot{\theta}_3) + a_2 a_3 s_3 \dot{\theta}_3] \\
\dot{I}_{22} &= -m_3 a_2 a_3 s_3 \dot{\theta}_3 \\
\dot{I}_{23} &= -\frac{1}{2}m_3 a_2 a_3 s_3 \dot{\theta}_3 \\
\dot{I}_{33} &= 0
\end{aligned}$$

with s_{ij} defined as $\sin(\theta_i+\theta_j)$. It should now be apparent that the time-rate of change of the generalized inertia matrix is independent of $\dot{\theta}_1$, as one should have expected, for this matrix is independent of θ_1. That is, if all joints but the first one are frozen, no matter how fast the first joint rotates, the manipulator moves as a single rigid body whose polar moment of inertia about O_1, the center of the first joint, is constant. As a matter of fact, I_{33} is constant for the same reason and $\dot{I}_{33}$ hence vanishes. We have,

then,[1]

$$\dot{\mathbf{I}}\dot{\boldsymbol{\theta}} \equiv \boldsymbol{\iota} = \begin{bmatrix} \dot{I}_{11}\dot{\theta}_1 + \dot{I}_{12}\dot{\theta}_2 + \dot{I}_{13}\dot{\theta}_3 \\ \dot{I}_{12}\dot{\theta}_1 + \dot{I}_{22}\dot{\theta}_2 + \dot{I}_{23}\dot{\theta}_3 \\ \dot{I}_{13}\dot{\theta}_1 + \dot{I}_{23}\dot{\theta}_2 + \dot{I}_{33}\dot{\theta}_3 \end{bmatrix}$$

whose components, ι_i, for $i = 1, 2, 3$, are readily calculated as

$$\begin{aligned}
\iota_1 = &-[m_2a_1a_2s_2 + m_3a_1(2a_2s_2 + a_3s_{23})]\dot{\theta}_1\dot{\theta}_2 - m_3a_3(a_1s_{23} + a_2s_3)\dot{\theta}_1\dot{\theta}_3 \\
&-\frac{1}{2}[m_2a_1a_2s_2 + m_3a_1(2a_2s_2 + a_3s_{23})]\dot{\theta}_2^2 - m_3a_3(a_1s_{23} + a_2s_3)\dot{\theta}_2\dot{\theta}_3 \\
&-\frac{1}{2}m_3a_3(a_1s_{23} + a_2s_3)\dot{\theta}_3^2 \\
\iota_2 = &-\frac{1}{2}[m_2a_1a_2s_2 + m_3a_1(2a_2s_2 + a_3s_{23})]\dot{\theta}_1\dot{\theta}_2 \\
&-\frac{1}{2}m_3a_3(a_1s_{23} + a_2s_3)\dot{\theta}_1\dot{\theta}_3 - m_3a_2a_3s_3\dot{\theta}_2\dot{\theta}_3 - \frac{1}{2}m_3a_2a_3s_3\dot{\theta}_3^2 \\
\iota_3 = &-\frac{1}{2}m_3a_1a_3s_{23}\dot{\theta}_1\dot{\theta}_3 - \frac{1}{2}m_3a_3(a_1s_{23} + a_2s_3)\dot{\theta}_1\dot{\theta}_3 - \frac{1}{2}m_3a_2a_3s_3\dot{\theta}_2\dot{\theta}_3
\end{aligned}$$

The next term in the right-hand side of eq.(6.20) now requires the calculation of the partial derivatives of vector $\mathbf{I}\dot{\boldsymbol{\theta}}$ with respect to the joint variables, which are computed below. Let

$$\frac{\partial(\mathbf{I}\dot{\boldsymbol{\theta}})}{\partial\boldsymbol{\theta}} \equiv \mathbf{I}'$$

its entries being denoted by I'_{ij}. This matrix, in component form, is given by

$$\mathbf{I}' = \begin{bmatrix} 0 & I_{11,2}\dot{\theta}_1 + I_{12,2}\dot{\theta}_2 + I_{13,2}\dot{\theta}_3 & I_{11,3}\dot{\theta}_1 + I_{12,3}\dot{\theta}_2 + I_{13,3}\dot{\theta}_3 \\ 0 & I_{12,2}\dot{\theta}_1 + I_{22,2}\dot{\theta}_2 + I_{23,2}\dot{\theta}_3 & I_{12,3}\dot{\theta}_1 + I_{22,3}\dot{\theta}_2 + I_{23,3}\dot{\theta}_3 \\ 0 & I_{13,2}\dot{\theta}_1 + I_{23,2}\dot{\theta}_2 + I_{33,2}\dot{\theta}_3 & I_{13,3}\dot{\theta}_1 + I_{23,3}\dot{\theta}_2 + I_{33,3}\dot{\theta}_3 \end{bmatrix}$$

with the shorthand notation $I_{ij,k}$ indicating the partial derivative of I_{ij} with respect to θ_k. As the reader can verify, these entries are given as

$$\begin{aligned}
I'_{11} &= 0 \\
I'_{12} &= -[m_2a_1a_2s_2 + m_3(2a_1a_2s_2 + a_1a_3s_{23})]\dot{\theta}_1 \\
&\quad -\frac{1}{2}[m_2a_1a_2s_2 + m_3(2a_1a_2s_2 + a_1a_3s_{23})]\dot{\theta}_2 - \frac{1}{2}m_3a_1a_3s_{23}\dot{\theta}_3 \\
I'_{13} &= -m_3(a_1a_3s_{23} + a_2a_3s_3)\dot{\theta}_1 - \frac{1}{2}m_3(a_1a_3s_{23} + 2a_2a_3s_3)\dot{\theta}_2 \\
&\quad -\frac{1}{2}m_3(a_1a_3s_{23} + a_2a_3s_3)\dot{\theta}_3
\end{aligned}$$

[1] $\boldsymbol{\iota}$ is the Greek letter *iota* and denotes a vector; according to our notation, its components are ι_1, ι_2, and ι_3.

$$
\begin{aligned}
I'_{21} &= 0 \\
I'_{22} &= -\frac{1}{2}[m_2 a_1 a_2 s_2 + m_3(2a_1 a_2 s_2 + a_1 a_3 s_{23})]\dot{\theta}_1 \\
I'_{23} &= -\frac{1}{2}m_3(a_1 a_3 s_{23} + 2a_2 a_3 s_3)\dot{\theta}_1 - m_3 a_2 a_3 s_3 \dot{\theta}_2 - \frac{1}{2}m_3 a_2 a_3 s_3 \dot{\theta}_3 \\
I'_{31} &= 0 \\
I'_{32} &= -\frac{1}{2}m_3 a_1 a_3 s_{23}\dot{\theta}_1 \\
I'_{33} &= -\frac{1}{2}m_3(a_1 a_3 s_{23} + a_2 a_3 s_3)\dot{\theta}_1 - \frac{1}{2}m_3 a_2 a_3 s_3 \dot{\theta}_2
\end{aligned}
$$

Now, we define the 3-dimensional vector $\boldsymbol{\gamma}$ below:

$$
\boldsymbol{\gamma} \equiv \left[\frac{\partial(\mathbf{I}\dot{\boldsymbol{\theta}})}{\partial \boldsymbol{\theta}}\right]^T \dot{\boldsymbol{\theta}}
$$

its three components, γ_i, for $i = 1, 2, 3$, being

$$
\begin{aligned}
\gamma_1 &= 0 \\
\gamma_2 &= -[m_2 a_1 a_2 s_2 + m_3(2a_1 a_2 s_2 + a_1 a_3 s_{23})]\dot{\theta}_1^2 \\
&\quad -[m_2 a_1 a_2 s_2 + m_3(2a_1 a_2 s_2 + a_1 a_3 s_{23})]\dot{\theta}_1 \dot{\theta}_2 \\
&\quad -m_3 a_1 a_3 s_{23}\dot{\theta}_1 \dot{\theta}_3 \\
\gamma_3 &= -m_3(a_1 a_3 s_{23} + a_2 a_3 s_3)\dot{\theta}_1^2 - m_3(a_1 a_3 s_{23} + 2a_2 a_3 s_3)\dot{\theta}_1 \dot{\theta}_2 \\
&\quad -m_3(a_1 a_3 s_{23} + a_2 a_3 s_3)\dot{\theta}_1 \dot{\theta}_3 - m_3 a_2 a_3 s_3 \dot{\theta}_3^2 - m_3 a_2 a_3 s_3 \dot{\theta}_2 \dot{\theta}_3
\end{aligned}
$$

We now turn to the computation of the partial derivatives of the potential energy:

$$
\begin{aligned}
\frac{\partial V}{\partial \theta_1} &= \frac{1}{2}m_1 g a_1 c_1 + m_2 g\left(a_1 c_1 + \frac{1}{2}a_2 c_{12}\right) + m_3 g\left(a_1 c_1 + a_2 c_{12} + \frac{1}{2}a_3 c_{123}\right) \\
\frac{\partial V}{\partial \theta_2} &= \frac{1}{2}m_2 g a_2 + m_3 g\left(a_2 c_{12} + \frac{1}{2}a_3 c_{123}\right) \\
\frac{\partial V}{\partial \theta_3} &= \frac{1}{2}m_3 g a_3 c_{123}
\end{aligned}
$$

The Euler-Lagrange equations thus reduce to

$$
\begin{aligned}
I_{11}\ddot{\theta}_1 + I_{12}\ddot{\theta}_2 + I_{13}\ddot{\theta}_3 + \iota_1 - \frac{1}{2}\gamma_1 + \frac{1}{2}m_1 g a_1 c_1 \\
+ m_2 g(a_1 c_1 + \frac{1}{2}a_2 c_{12}) + m_3 g(a_1 c_1 + a_2 c_{12} + \frac{1}{2}a_3 c_{123}) = \tau_1 \\
I_{12}\ddot{\theta}_1 + I_{22}\ddot{\theta}_2 + I_{23}\ddot{\theta}_3 + \iota_2 - \frac{1}{2}\gamma_2 + \frac{1}{2}m_2 g a_2 c_{12} \\
+ m_3 g(a_2 c_{12} + \frac{1}{2}a_3 c_{123}) = \tau_2 \\
I_{13}\ddot{\theta}_1 + I_{23}\ddot{\theta}_2 + I_{33}\ddot{\theta}_3 + \iota_3 - \frac{1}{2}\gamma_3 + \frac{1}{2}m_3 g a_3 c_{123} = \tau_3
\end{aligned}
$$

With this example, it becomes apparent that a straightforward differentiation procedure to derive the Euler-Lagrange equations of a robotic manipulator, or for that matter, of a mechanical system at large, is not practical. For example, these equations do not seem to lend themselves to symbolic manipulations for a six-axis manipulator of arbitrary architecture, given that they become quite cumbersome even for a three-axis planar manipulator with an architecture that is not so general. For this reason, procedures have been devised that lend themselves to an algorithmic treatment. We will study a procedure based on the *natural orthogonal complement* whereby the underlying equations are derived using matrix-times-vector multiplications.

6.3.3 Kane's Equations

Kane's equations (Kane and Levinson, 1983), sometimes referred to as *D'Alambert's equations in Lagrangian form* are also useful in robot dynamics (Angeles et al., 1989). A feature of Kane's equations is that they are derived from the free-body diagrams of the various rigid bodies constituting the multibody system at hand. Upon introducing generalized coordinates à la Lagrange, the mathematical model of the system is derived, which is equivalent to the underlying Euler-Lagrange equations. Kane's equations take a rather simple form, for an n-dof mechanical system, namely,

$$\boldsymbol{\phi} + \boldsymbol{\phi}^* = \mathbf{0}$$

where $\boldsymbol{\phi}$ and $\boldsymbol{\phi}^*$ are the n-dimensional vectors of generalized *active force* and *inertia force*, respectively. With the notation introduced above, these vectors are given by

$$\boldsymbol{\phi} = \sum_{i=1}^{r} \left[\left(\frac{\partial \dot{\mathbf{c}}_i}{\partial \dot{\mathbf{q}}} \right)^T \mathbf{f}_i + \left(\frac{\partial \boldsymbol{\omega}_i}{\partial \dot{\mathbf{q}}} \right)^T \mathbf{n}_i \right] \tag{6.21a}$$

and

$$\boldsymbol{\phi}^* = -\sum_{i=1}^{r} \left[\left(\frac{\partial \dot{\mathbf{c}}_i}{\partial \dot{\mathbf{q}}} \right)^T m_i \ddot{\mathbf{c}}_i + \left(\frac{\partial \boldsymbol{\omega}_i}{\partial \dot{\mathbf{q}}} \right)^T (\mathbf{I}_i \dot{\boldsymbol{\omega}}_i + \boldsymbol{\omega}_i \times \mathbf{I}_i \boldsymbol{\omega}_i) \right] . \tag{6.21b}$$

In the above expressions, $\dot{\mathbf{q}} = d\mathbf{q}/dt$ is the n-dimensional vector of *generalized speeds* in Kane's terminology, while the $n \times 3$ matrices $\partial \dot{\mathbf{c}}_i / \partial \dot{\mathbf{q}}$ and $\partial \boldsymbol{\omega}_i / \partial \dot{\mathbf{q}}$ are the *partial rates of change* of mass-center velocity and angular velocity of the ith rigid body.

6.4 Recursive Inverse Dynamics

The inverse dynamics problem associated with serial manipulators is studied here. We assume at the outset that the manipulator under study is of

the serial type with $n+1$ links including the base link and n joints of either the revolute or the prismatic type.

The underlying algorithm consists of two steps: (*i*) *kinematic computations*, required to determine the twists of all the links and their time derivatives in terms of $\boldsymbol{\theta}$, $\dot{\boldsymbol{\theta}}$, and $\ddot{\boldsymbol{\theta}}$; and (*ii*) *dynamic computations*, required to determine both the constraint and the external wrenches. Each of these steps is described below, the aim here being to calculate the desired variables with as few computations as possible, for one purpose of inverse dynamics is to permit the real-time model-based control of the manipulator. Real-time performance requires, obviously, a low number of computations. For the sake of simplicity, we decided against discussing the algorithms with the lowest computational cost, mainly because these algorithms, fully discussed by Balafoutis and Patel (1991), rely heavily on tensor calculus, which we have not studied here. Henceforth, revolute joints are referred to as R, prismatic joints as P.

6.4.1 Kinematics Computations: Outward Recursions

We will use the Denavit-Hartenberg (DH) notation introduced in Section 4.2 and hence will refer to Fig. 4.7 for the basic notation required for the kinematic analysis to be described first. Note that the calculation of each $\mathbf{Q}_i$ matrix, as given by eq.(4.1e), requires four multiplications and zero additions.

Moreover, *every 3-dimensional vector-component transfer from the $\mathcal{F}_i$ frame to the $\mathcal{F}_{i+1}$ frame requires a multiplication by $\mathbf{Q}_i^T$. Likewise, every component transfer from the $\mathcal{F}_{i+1}$ frame to the $\mathcal{F}_i$ frame requires a multiplication by $\mathbf{Q}_i$.* Therefore, we will need to account for the aforementioned component transfers, which we will generically term *coordinate transformations* between successive coordinate frames. We derive below the number of operations required for such transformations. If we have $[\,\mathbf{r}\,]_i \equiv [\,r_1,\, r_2,\, r_3\,]^T$ and we need $[\,\mathbf{r}\,]_{i+1}$, then we proceed as follows:

$$[\,\mathbf{r}\,]_{i+1} = \mathbf{Q}_i^T [\,\mathbf{r}\,]_i \tag{6.22}$$

and if we recall the form of $\mathbf{Q}_i$ from eq.(4.1e), we then have

$$[\,\mathbf{r}\,]_{i+1} = \begin{bmatrix} \cos\theta_i & \sin\theta_i & 0 \\ -\lambda_i \sin\theta_i & \lambda_i \cos\theta_i & \mu_i \\ \mu_i \sin\theta_i & -\mu_i \cos\theta_i & \lambda_i \end{bmatrix} \begin{bmatrix} r_1 \\ r_2 \\ r_3 \end{bmatrix} = \begin{bmatrix} r_1 \cos\theta_i + r_2 \sin\theta_i \\ -\lambda_i r + \mu_i r_3 \\ \mu_i r + \lambda_i r_3 \end{bmatrix} \tag{6.23a}$$

where $\lambda_i \equiv \cos\alpha_i$ and $\mu_i \equiv \sin\alpha_i$, while

$$r \equiv r_1 \sin\theta_i - r_2 \cos\theta_i \tag{6.23b}$$

Likewise, if we have $[\,\mathbf{v}\,]_{i+1} \equiv [\,v_1,\, v_2,\, v_3\,]^T$ and we need $[\,\mathbf{v}\,]_i$, we use the

component transformation given below:

$$[\,\mathbf{v}\,]_i = \begin{bmatrix} \cos\theta_i & -\lambda_i \sin\theta_i & \mu_i \sin\theta_i \\ \sin\theta_i & \lambda_i \cos\theta_i & -\mu_i \cos\theta_i \\ 0 & \mu_i & \lambda_i \end{bmatrix} \begin{bmatrix} v_1 \\ v_2 \\ v_3 \end{bmatrix} = \begin{bmatrix} v_1 \cos\theta_i - v \sin\theta_i \\ v_1 \sin\theta_i + v \cos\theta_i \\ v_2\mu_i + v_3\lambda_i \end{bmatrix} \tag{6.24a}$$

where

$$v \equiv v_2\lambda_i - v_3\mu_i \tag{6.24b}$$

It is now apparent that *every coordinate transformation between successive frames, whether forward or backward, requires eight multiplications and four additions.* Here, as in Chapter 4, we indicate the units of multiplications and additions with M and A, respectively.

The angular velocity and acceleration of the ith link are computed recursively as follows:

$$\boldsymbol{\omega}_i = \begin{cases} \boldsymbol{\omega}_{i-1} + \dot{\theta}_i \mathbf{e}_i, & \text{if the } i\text{th joint is } R \\ \boldsymbol{\omega}_{i-1}, & \text{if the } i\text{th joint is } P \end{cases} \tag{6.25a}$$

$$\dot{\boldsymbol{\omega}}_i = \begin{cases} \dot{\boldsymbol{\omega}}_{i-1} + \boldsymbol{\omega}_{i-1} \times \dot{\theta}_i \mathbf{e}_i + \ddot{\theta}_i \mathbf{e}_i, & \text{if the } i\text{th joint is } R \\ \dot{\boldsymbol{\omega}}_{i-1}, & \text{if the } i\text{th joint is } P \end{cases} \tag{6.25b}$$

for $i = 1, 2, \ldots, n$, where $\boldsymbol{\omega}_0$ and $\dot{\boldsymbol{\omega}}_0$ are the angular velocity and angular acceleration of the base link. Note that eqs.(6.25a & b) are frame-invariant; i.e., they are valid in *any* coordinate frame, as long as the same frame is used to represent all quantities involved. Below we derive the equivalent relations applicable when taking into account that quantities with a subscript i are available in $\mathcal{F}_{i+1}$-coordinates. Hence, operations involving quantities with different subscripts require a change of coordinates, which is taken care of by the corresponding rotation matrices.

In order to reduce the numerical complexity of the algorithm developed here, all vector and matrix quantities of the ith link will be expressed in $\mathcal{F}_{i+1}$. Note, however, that the two vectors $\mathbf{e}_i$ and $\mathbf{e}_{i+1}$ are fixed to the ith link, which is a potential source of confusion. Now, since $\mathbf{e}_i$ has very simple components in $\mathcal{F}_i$, namely, $[\,0,\,0,\,1\,]^T$, this will be regarded as a vector of the $(i-1)$st link. Therefore, this vector, or multiples of it, will be added to vectors bearing the $(i-1)$st subscript without any coordinate transformation. Moreover, subscripted brackets, as introduced in Section 2.2, can be avoided if all vector and matrix quantities subscripted with i, except for vector $\mathbf{e}_i$, are assumed to be expressed in $\mathcal{F}_{i+1}$. Furthermore, in view of the serial type of the underlying kinematic chain, only additions of quantities with two successive subscripts will appear in the relations below.

Quantities given in two successive frames can be added if both are expressed in the same frame, the obvious frame of choice being the frame of one of the two quantities. Hence, all we need to add two quantities with

successive subscripts is to multiply one of these by a suitable orthogonal matrix. Additionally, in view of the *outwards* recursive nature of the kinematic relations above, it is apparent that a transfer from $\mathcal{F}_i$- to $\mathcal{F}_{i+1}$-coordinates is needed, which can be accomplished by multiplying either $\mathbf{e}_i$ or any other vector with the $(i-1)$ subscript by matrix $\mathbf{Q}_i^T$. Hence, the angular velocities and accelerations are computed recursively, as indicated below:

$$\boldsymbol{\omega}_i = \begin{cases} \mathbf{Q}_i^T(\boldsymbol{\omega}_{i-1} + \dot{\theta}_i \mathbf{e}_i), & \text{if the } i\text{th joint is } R \\ \mathbf{Q}_i^T \boldsymbol{\omega}_{i-1}, & \text{if the } i\text{th joint is } P \end{cases} \tag{6.26a}$$

$$\dot{\boldsymbol{\omega}}_i = \begin{cases} \mathbf{Q}_i^T(\dot{\boldsymbol{\omega}}_{i-1} + \boldsymbol{\omega}_{i-1} \times \dot{\theta}_i \mathbf{e}_i + \ddot{\theta}_i \mathbf{e}_i), & \text{if the } i\text{th joint is } R \\ \mathbf{Q}_i^T \dot{\boldsymbol{\omega}}_{i-1}, & \text{if the } i\text{th joint is } P \end{cases} \tag{6.26b}$$

If the base link is an inertial frame, then

$$\boldsymbol{\omega}_0 = \mathbf{0}, \qquad \dot{\boldsymbol{\omega}}_0 = \mathbf{0} \tag{6.27}$$

Thus, calculating each $\boldsymbol{\omega}_i$ vector in $\mathcal{F}_{i+1}$ when $\boldsymbol{\omega}_{i-1}$ is given in $\mathcal{F}_i$ requires $8M$ and $5A$ if the ith joint is R; if it is P, the said calculation reduces to $8M$ and $4A$. Here, note that $\dot{\theta}_i \mathbf{e}_i = [\,0,\, 0,\, \dot{\theta}_i\,]^T$ in $\mathcal{F}_i$-coordinates, and hence, the vector addition of the upper right-hand side of eq.(6.26a) requires only $1A$. Furthermore, in order to determine the number of operations required to calculate $\dot{\boldsymbol{\omega}}_i$ in $\mathcal{F}_{i+1}$ when $\dot{\boldsymbol{\omega}}_{i-1}$ is available in $\mathcal{F}_i$, we note that

$$[\,\mathbf{e}_i\,]_i = \begin{bmatrix} 0 \\ 0 \\ 1 \end{bmatrix} \tag{6.28}$$

Moreover, we let

$$[\,\boldsymbol{\omega}_{i-1}\,]_i = \begin{bmatrix} \omega_x \\ \omega_y \\ \omega_z \end{bmatrix} \tag{6.29}$$

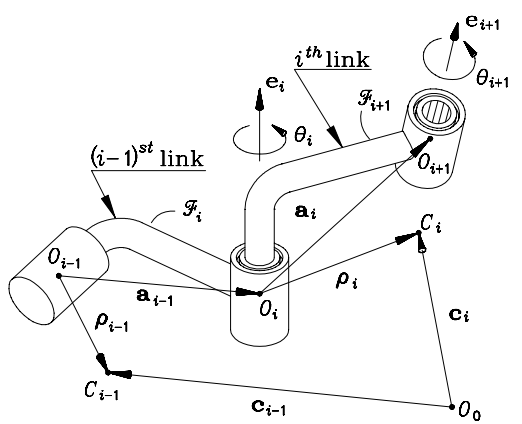

FIGURE 6.2. A revolute joint.

Hence,

$$[\,\boldsymbol{\omega}_{i-1} \times \dot{\theta}_i \mathbf{e}_i\,]_i = \begin{bmatrix} \dot{\theta}_i\,\omega_y \\ -\dot{\theta}_i\,\omega_x \\ 0 \end{bmatrix} \tag{6.30}$$

Furthermore, we note that

$$[\,\ddot{\theta}_i \mathbf{e}_i\,]_i = \begin{bmatrix} 0 \\ 0 \\ \ddot{\theta}_i \end{bmatrix} \tag{6.31}$$

and hence, the calculation of $\dot{\boldsymbol{\omega}}_i$ in $\mathcal{F}_{i+1}$ when $\dot{\boldsymbol{\omega}}_{i-1}$ is given in $\mathcal{F}_i$ requires $10M$ and $7A$ if the ith joint is R; if it is P, the same calculation requires $8M$ and $4A$.

Furthermore, let $\mathbf{c}_i$ be the position vector of C_i, the mass center of the ith link, $\boldsymbol{\rho}_i$ being the vector directed from O_i to C_i, as shown in Figs. 6.2 and 6.3. The position vectors of two successive mass centers thus observe the relationships

(i) if the ith joint is R,

$$\boldsymbol{\delta}_{i-1} \equiv \mathbf{a}_{i-1} - \boldsymbol{\rho}_{i-1} \tag{6.32a}$$

$$\mathbf{c}_i = \mathbf{c}_{i-1} + \boldsymbol{\delta}_{i-1} + \boldsymbol{\rho}_i \tag{6.32b}$$

(ii) if the ith joint is P,

$$\boldsymbol{\delta}_{i-1} \equiv \mathbf{d}_{i-1} - \boldsymbol{\rho}_{i-1} \tag{6.32c}$$

$$\mathbf{c}_i = \mathbf{c}_{i-1} + \boldsymbol{\delta}_{i-1} + b_i \mathbf{e}_i + \boldsymbol{\rho}_i \tag{6.32d}$$

where point O_i, in this case, is a point of the $(i-1)$st link conveniently defined, as dictated by the particular geometry of the manipulator at hand. The foregoing freedom in the choice of O_i is a consequence of prismatic pairs having only a defined direction but no axis, properly speaking.

Notice that in the presence of a revolute pair at the ith joint, the difference $\mathbf{a}_{i-1} - \boldsymbol{\rho}_{i-1}$ is constant in $\mathcal{F}_i$. Likewise, in the presence of a prismatic pair at the same joint, the difference $\mathbf{d}_{i-1} - \boldsymbol{\rho}_{i-1}$ is constant in $\mathcal{F}_i$. Therefore, these differences are computed off-line, their evaluation not counting toward the computational complexity of the algorithm.

Upon differentiation of both sides of eqs.(6.32b & d) with respect to time, we derive the corresponding relations between the velocities and accelerations of the mass centers of links $i-1$ and i, namely,

(i) if the ith joint is R,

$$\dot{\mathbf{c}}_i = \dot{\mathbf{c}}_{i-1} + \boldsymbol{\omega}_{i-1} \times \boldsymbol{\delta}_{i-1} + \boldsymbol{\omega}_i \times \boldsymbol{\rho}_i \tag{6.33a}$$

$$\ddot{\mathbf{c}}_i = \ddot{\mathbf{c}}_{i-1} + \dot{\boldsymbol{\omega}}_{i-1} \times \boldsymbol{\delta}_{i-1} + \boldsymbol{\omega}_{i-1} \times (\boldsymbol{\omega}_{i-1} \times \boldsymbol{\delta}_{i-1}) + \dot{\boldsymbol{\omega}}_i \times \boldsymbol{\rho}_i + \boldsymbol{\omega}_i \times (\boldsymbol{\omega}_i \times \boldsymbol{\rho}_i) \tag{6.33b}$$

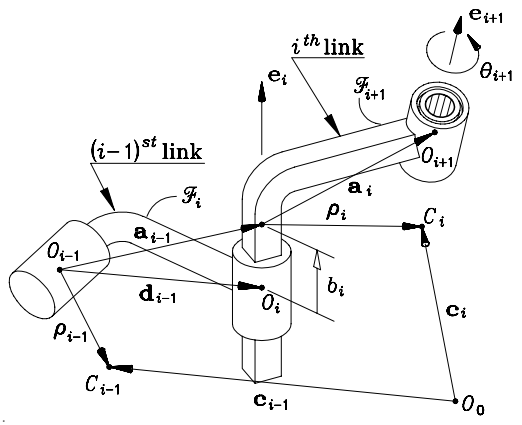

FIGURE 6.3. A prismatic joint.

(*ii*) if the ith joint is P,

$$\boldsymbol{\omega}_i = \boldsymbol{\omega}_{i-1} \tag{6.34a}$$

$$\dot{\boldsymbol{\omega}}_i = \dot{\boldsymbol{\omega}}_{i-1} \tag{6.34b}$$

$$\mathbf{u}_i \equiv \boldsymbol{\delta}_{i-1} + \boldsymbol{\rho}_i + b_i \mathbf{e}_i \tag{6.34c}$$

$$\mathbf{v}_i \equiv \boldsymbol{\omega}_i \times \mathbf{u}_i \tag{6.34d}$$

$$\dot{\mathbf{c}}_i = \dot{\mathbf{c}}_{i-1} + \mathbf{v}_i + \dot{b}_i \mathbf{e}_i \tag{6.34e}$$

$$\ddot{\mathbf{c}}_i = \ddot{\mathbf{c}}_{i-1} + \dot{\boldsymbol{\omega}}_i \times \mathbf{u}_i + \boldsymbol{\omega}_i \times (\mathbf{v}_i + 2\dot{b}_i \mathbf{e}_i) + \ddot{b}_i \mathbf{e}_i \tag{6.34f}$$

for $i = 1, 2, \ldots, n$, where $\dot{\mathbf{c}}_0$ and $\ddot{\mathbf{c}}_0$ are the velocity and acceleration of the mass center of the base link. If the latter is an inertial frame, then

$$\boldsymbol{\omega}_0 = \mathbf{0}, \quad \dot{\boldsymbol{\omega}}_0 = \mathbf{0}, \quad \dot{\mathbf{c}}_0 = \mathbf{0}, \quad \ddot{\mathbf{c}}_0 = \mathbf{0} \tag{6.35}$$

Expressions (6.32b) to (6.34f) are *invariant*, i.e., they hold in *any* coordinate frame, as long as all vectors involved are expressed in that frame. However, we have vectors that are naturally expressed in the $\mathcal{F}_i$ frame added to vectors expressed in the $\mathcal{F}_{i+1}$ frame, and hence, a coordinate transformation is needed. This coordinate transformation is taken into account in Algorithm 6.4.1, whereby the logical variable `R` is `true` if the ith joint is R; otherwise it is `false`.

In performing the foregoing calculations, we need the cross product of a vector $\mathbf{w}$ times $\mathbf{e}_i$ in $\mathcal{F}_i$ coordinates, the latter being simply $[\,\mathbf{e}_i\,]_i = [\,0,\, 0,\, 1\,]^T$, and hence, this cross product reduces to $[\,w_2,\, -w_1,\, 0\,]^T$, whereby w_k, for $k = 1, 2, 3$, are the x, y, and z $\mathcal{F}_i$-components of $\mathbf{w}$. This cross product, then, requires no multiplications and no additions. Likewise, vectors

$b_i\mathbf{e}_i$, $\dot{b}_i\mathbf{e}_i$, and $\ddot{b}_i\mathbf{e}_i$ take on the simple forms $[\,0,\,0,\,b_i\,]^T$, $[\,0,\,0,\,\dot{b}_i\,]^T$, and $[\,0,\,0,\,\ddot{b}_i\,]^T$ in $\mathcal{F}_i$. Adding any of these vectors to any other vector in $\mathcal{F}_i$ then requires one single addition.

Algorithm 6.4.1 (Outward Recursions):

read $\{\,\mathbf{Q}_i\,\}_0^{n-1}$, $\mathbf{c}_0$, $\boldsymbol{\omega}_0$, $\dot{\mathbf{c}}_0$, $\dot{\boldsymbol{\omega}}_0$, $\ddot{\mathbf{c}}_0$, $\{\boldsymbol{\rho}_i\}_1^n$, $\{\boldsymbol{\delta}_i\}_0^{n-1}$
For i = 1 to n step 1 do
update $\mathbf{Q}_i$
if R then

$$
\begin{aligned}
\mathbf{c}_i &\leftarrow \mathbf{Q}_i^T(\mathbf{c}_{i-1} + \boldsymbol{\delta}_{i-1}) + \boldsymbol{\rho}_i \\
\boldsymbol{\omega}_i &\leftarrow \mathbf{Q}_i^T(\boldsymbol{\omega}_{i-1} + \dot{\theta}_i\mathbf{e}_i) \\
\mathbf{u}_{i-1} &\leftarrow \boldsymbol{\omega}_{i-1} \times \boldsymbol{\delta}_{i-1} \\
\mathbf{v}_i &\leftarrow \boldsymbol{\omega}_i \times \boldsymbol{\rho}_i \\
\dot{\mathbf{c}}_i &\leftarrow \mathbf{Q}_i^T(\dot{\mathbf{c}}_{i-1} + \mathbf{u}_{i-1}) + \mathbf{v}_i \\
\dot{\boldsymbol{\omega}}_i &\leftarrow \mathbf{Q}_i^T(\dot{\boldsymbol{\omega}}_{i-1} + \boldsymbol{\omega}_{i-1} \times \dot{\theta}_i\mathbf{e}_i + \ddot{\theta}_i\mathbf{e}_i) \\
\ddot{\mathbf{c}}_i &\leftarrow \mathbf{Q}_i^T(\ddot{\mathbf{c}}_{i-1} + \dot{\boldsymbol{\omega}}_{i-1} \times \boldsymbol{\delta}_{i-1} + \boldsymbol{\omega}_{i-1} \times \mathbf{u}_{i-1}) \\
&\quad + \dot{\boldsymbol{\omega}}_i \times \boldsymbol{\rho}_i + \boldsymbol{\omega}_i \times \mathbf{v}_i
\end{aligned}
$$

else

$$
\begin{aligned}
\mathbf{u}_i &\leftarrow \mathbf{Q}_i^T\boldsymbol{\delta}_{i-1} + \boldsymbol{\rho}_i + b_i\mathbf{e}_i \\
\mathbf{c}_i &\leftarrow \mathbf{Q}_i^T\mathbf{c}_{i-1} + \mathbf{u}_i \\
\boldsymbol{\omega}_i &\leftarrow \mathbf{Q}_i^T\boldsymbol{\omega}_{i-1} \\
\mathbf{v}_i &\leftarrow \boldsymbol{\omega}_i \times \mathbf{u}_i \\
\mathbf{w}_i &\leftarrow \dot{b}_i\mathbf{e}_i \\
\dot{\mathbf{c}}_i &\leftarrow \mathbf{Q}_i^T\dot{\mathbf{c}}_{i-1} + \mathbf{v}_i + \mathbf{w}_i \\
\dot{\boldsymbol{\omega}}_i &\leftarrow \mathbf{Q}_i^T\dot{\boldsymbol{\omega}}_{i-1} \\
\ddot{\mathbf{c}}_i &\leftarrow \mathbf{Q}_i^T\ddot{\mathbf{c}}_{i-1} + \dot{\boldsymbol{\omega}}_i \times \mathbf{u}_i + \boldsymbol{\omega}_i \times (\mathbf{v}_i + \mathbf{w}_i + \mathbf{w}_i) + \ddot{b}_i\mathbf{e}_i
\end{aligned}
$$

endif
enddo

If, moreover, we take into account that the cross product of two arbitrary vectors requires $6M$ and $3A$, we then have the operation counts given below:

(i) If the ith joint is R,
$\mathbf{Q}_i$ requires $4M$ and $0A$
$\mathbf{c}_i$ requires $8M$ and $10A$
$\boldsymbol{\omega}_i$ requires $8M$ and $5A$
$\dot{\mathbf{c}}_i$ requires $20M$ and $16A$
$\dot{\boldsymbol{\omega}}_i$ requires $10M$ and $7A$
$\ddot{\mathbf{c}}_i$ requires $32M$ and $28A$

(ii) If the ith joint is P,
$\mathbf{Q}_i$ requires $4M$ and $0A$
$\mathbf{c}_i$ requires $16M$ and $15A$
$\boldsymbol{\omega}_i$ requires $8M$ and $4A$

TABLE 6.1. Complexity of the Kinematics Computations

Item	M	A
$\{\mathbf{Q}_i\}_1^n$	$4n$	0
$\{\boldsymbol{\omega}_i\}_1^n$	$8n$	$5n$
$\{\dot{\mathbf{c}}_i\}_1^n$	$20n$	$16n$
$\{\dot{\boldsymbol{\omega}}_i\}_1^n$	$10n$	$7n$
$\{\ddot{\mathbf{c}}_i\}_1^n$	$32n$	$28n$
Total	$82n$	$66n$

$\dot{\mathbf{c}}_i$ requires $14M$ and $11A$
$\dot{\boldsymbol{\omega}}_i$ requires $8M$ and $4A$
$\ddot{\mathbf{c}}_i$ requires $20M$ and $19A$

The computational complexity for the forward recursions of the kinematics calculations for an n-revolute manipulator, as pertaining to various algorithms, are summarized in Table 6.1. Note that if some joints are P, then these figures become lower.

6.4.2 Dynamics Computations: Inward Recursions

Moreover, a free-body diagram of the end-effector, or nth link, appears in Fig. 6.5. Note that this link is acted upon by a nonworking constraint wrench, exerted through the nth pair, and a working wrench; the latter involves both active and dissipative forces and moments. Although dissipative forces and moments are difficult to model because of dry friction and striction, they can be readily incorporated into the dynamics model, once a suitable constitutive model for these items is available. Since these forces and moments depend only on joint variables and joint rates, they can be calculated once the kinematic variables are known. For the sake of simplicity, dissipative wrenches are not included here, their discussion being the subject of Section 6.8. Hence, the force and the moment that the $(i-1)$st link exerts on the ith link through the ith joint only produce nonworking constraint and active wrenches. That is, for a revolute pair, one has

$$\mathbf{n}_i^P = \begin{bmatrix} n_i^x \\ n_i^y \\ \tau_i \end{bmatrix}, \quad \mathbf{f}_i^P = \begin{bmatrix} f_i^x \\ f_i^y \\ f_i^z \end{bmatrix} \tag{6.36}$$

in which n_i^x and n_i^y are the nonzero $\mathcal{F}_i$-components of the nonworking constraint moment exerted by the $(i-1)$st link on the ith link; obviously, this moment lies in a plane perpendicular to Z_i, whereas τ_i is the active torque applied by the motor at the said joint. Vector $\mathbf{f}_i^P$ contains only

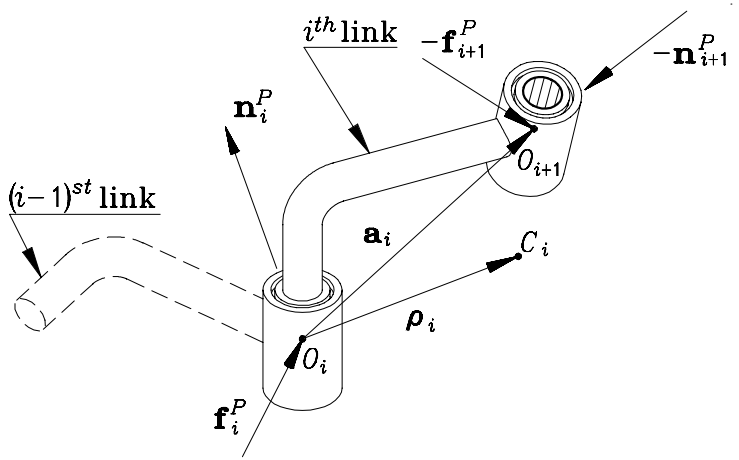

FIGURE 6.4. Free-body diagram of the ith link.

nonworking constraint forces.

For a prismatic pair, one has

$$\mathbf{n}^P = \begin{bmatrix} n_i^x \\ n_i^y \\ n_i^z \end{bmatrix}, \quad \mathbf{f}^P = \begin{bmatrix} f_i^x \\ f_i^y \\ \tau_i \end{bmatrix} \tag{6.37}$$

where vector $\mathbf{n}_i^P$ contains only nonworking constraint torques, while τ_i is now the active force exerted by the ith motor in the Z_i direction, f_i^x and f_i^y being the nonzero $\mathcal{F}_i$-components of the nonworking constraint force exerted by the ith joint on the ith link, which is perpendicular to the Z_i axis.

In the algorithm below, the driving torques or forces $\{\tau_i\}_1^n$, are computed via vectors $\mathbf{n}_i^P$ and $\mathbf{f}_i^P$. In fact, in the case of a revolute pair, τ_i is simply the third component of $\mathbf{n}_i^P$; in the case of a prismatic pair, τ_i is, accordingly, the third component of $\mathbf{f}_i^P$. From Fig. 6.5, the Newton-Euler equations of the end-effector are

$$\mathbf{f}_n^P = m_n \ddot{\mathbf{c}}_n - \mathbf{f} \tag{6.38a}$$

$$\mathbf{n}_n^P = \mathbf{I}_n \dot{\boldsymbol{\omega}}_n + \boldsymbol{\omega}_n \times \mathbf{I}_n \boldsymbol{\omega}_n - \mathbf{n} + \boldsymbol{\rho}_n \times \mathbf{f}_n^P \tag{6.38b}$$

where $\mathbf{f}$ and $\mathbf{n}$ are the external force and moment, the former being applied at the mass center of the end-effector. The Newton-Euler equations for the remaining links are derived based on the free-body diagram of Fig. 6.4, namely,

$$\mathbf{f}_i^P = m_i \ddot{\mathbf{c}}_i + \mathbf{f}_{i+1}^P \tag{6.38c}$$

$$\mathbf{n}_i^P = \mathbf{I}_i \dot{\boldsymbol{\omega}}_i + \boldsymbol{\omega}_i \times \mathbf{I}_i \boldsymbol{\omega}_i + \mathbf{n}_{i+1}^P + \boldsymbol{\delta}_i \times \mathbf{f}_{i+1}^P + \boldsymbol{\rho}_i \times \mathbf{f}_i^P \tag{6.38d}$$

with $\boldsymbol{\delta}_i$ defined as the difference $\mathbf{a}_i - \boldsymbol{\rho}_i$ in eqs.(6.32a & c).

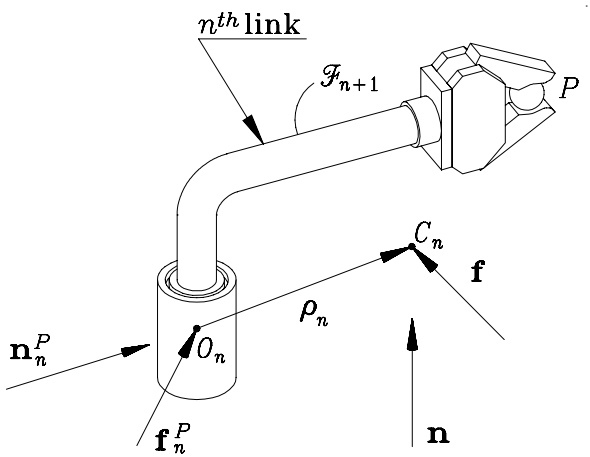

FIGURE 6.5. Free-body diagram of the end-effector.

Once the $\mathbf{n}_i^P$ and $\mathbf{f}_i^P$ vectors are available, the actuator torques and forces, denoted by τ_i, are readily computed. In fact, if the ith joint is a revolute, then

$$\tau_i = \mathbf{e}_i^T \mathbf{n}_i^P \tag{6.39}$$

which does not require any further operations, for τ_i reduces, in this case, to the Z_i component of vector $\mathbf{n}_i^P$. Similarly, if the ith joint is prismatic, then the corresponding actuator force reduces to

$$\tau_i = \mathbf{e}_i^T \mathbf{f}_i^P \tag{6.40}$$

Again, the foregoing relations are written in invariant form. In order to perform the computations involved, transformations that transfer coordinates between two successive frames are required. Here, we have to keep in mind that the components of a vector expressed in the $(i+1)$st frame can be transferred to the ith frame by multiplying the vector array in $(i+1)$st coordinates by matrix $\mathbf{Q}_i$. In taking these coordinate transformations into account, we derive the Newton-Euler algorithm from the above equations, namely,

Algorithm 6.4.2 (Inward Recursions):

$\mathbf{f}_n^P \leftarrow m_n\ddot{\mathbf{c}}_n - \mathbf{f}$
$\mathbf{n}_n^P \leftarrow \mathbf{I}_n\dot{\boldsymbol{\omega}}_n + \boldsymbol{\omega}_n \times \mathbf{I}_n\boldsymbol{\omega}_n - \mathbf{n} + \boldsymbol{\rho}_n \times \mathbf{f}_n^P$
`If R then`
$\tau_n \leftarrow (\mathbf{n}_n^P)_z$
`else`
$\tau_n \leftarrow (\mathbf{f}_n^P)_z$
`For i = n − 1 to 1 step −1 do`
$\boldsymbol{\phi}_{i+1} \leftarrow \mathbf{Q}_i\mathbf{f}_{i+1}^P$
$\mathbf{f}_i^P \leftarrow m_i\ddot{\mathbf{c}}_i + \boldsymbol{\phi}_{i+1}$
$\mathbf{n}_i^P \leftarrow \mathbf{I}_i\dot{\boldsymbol{\omega}}_i + \boldsymbol{\omega}_i \times \mathbf{I}_i\boldsymbol{\omega}_i + \boldsymbol{\rho}_i \times \mathbf{f}_i^P + \mathbf{Q}_i\mathbf{n}_{i+1}^P + \boldsymbol{\delta}_i \times \boldsymbol{\phi}_{i+1}$
`If R then`
$\tau_i \leftarrow (\mathbf{n}_i^P)_z$
`else`
$\tau_i \leftarrow (\mathbf{f}_i^P)_z$ `enddo`

Note that, within the do-loop of the foregoing algorithm, the vectors to the left of the arrow are expressed in the ith frame, while $\mathbf{f}_{i+1}^P$ and $\mathbf{n}_{i+1}^P$, to the right of the arrow, are expressed in the $(i+1)$st frame.

In calculating the computational complexity of this algorithm, note that the $\mathbf{a}_i - \boldsymbol{\rho}_i$ term is constant in the $(i+1)$st frame, and hence, it is computed *off-line*. Thus, its computation need not be accounted for. A summary of computational costs is given in Table 6.2 for an n-revolute manipulator, with the row number indicating the step in Algorithm 6.4.2.

The total numbers of multiplications M_d and additions A_d required by the foregoing algorithm are readily obtained, with the result shown below:

$$M_d = 55n - 22, \quad A_d = 44n - 14 \tag{6.41}$$

In particular, for a six-revolute manipulator, one has

$$n = 6, \quad M_d = 308, \quad A_d = 250 \tag{6.42}$$

If the kinematics computations are accounted for, then the Newton-Euler algorithm given above for the inverse dynamics of n-revolute manipulators

TABLE 6.2. Complexity of Dynamics Computations

Row #	M	A
1	3	3
2	30	27
5	$8(n-1)$	$4(n-1)$
6	$3(n-1)$	$3(n-1)$
7	$44(n-1)$	$37(n-1)$
Total	$55n-22$	$44n-14$

requires M multiplications and A additions, as given below:

$$M = 137n - 22, \quad A = 110n - 14 \tag{6.43}$$

The foregoing number of multiplications is identical to that reported by Walker and Orin (1982); however, the number of additions is slightly higher than Walker and Orin's figure, namely, $101n - 11$.

Thus, the inverse dynamics of a six-revolute manipulator requires 800 multiplications and 646 additions. These computations can be performed in a few microseconds using a modern processor. Clearly, if the aforementioned algorithms are tailored to suit particular architectures, then they can be further simplified. Note that, in the presence of a prismatic pair in the jth joint, the foregoing complexity is reduced. In fact, if this is the case, the Newton-Euler equations for the jth link remain as in eqs.(6.38c & d) for the ith link, the only difference appearing in the implementing algorithm, which is simplified, in light of the results derived in discussing the kinematics calculations.

The incorporation of gravity in the Newton-Euler algorithm is done most economically by following the idea proposed by Luh et al. (1980), namely, by declaring that the inertial base undergoes an acceleration $-\mathbf{g}$, where $\mathbf{g}$ denotes the acceleration of gravity. That is

$$\ddot{\mathbf{c}}_0 = -\mathbf{g} \tag{6.44}$$

the gravitational accelerations thus propagating forward to the EE. A comparison of various algorithms with regard to their computational complexity is displayed in Table 6.3 for an n-revolute manipulator. For $n = 6$, the corresponding figures appear in Table 6.4.

6.5 The Natural Orthogonal Complement in Robot Dynamics

In simulation studies, we need to integrate the system of ordinary differential equations (ODE) describing the dynamics of a robotic mechanical

TABLE 6.3. Complexity of Different Algorithms for Inverse Dynamics

Author(s)	Methods	Multiplications	Additions
Hollerbach (1980)	E-L	$412n - 277$	$320n - 201$
Luh et al. (1980)	N-E	$150n - 48$	$131n - 48$
Walker & Orin (1982)	N-E	$137n - 22$	$101n - 11$
Khalil et al. (1986)	N-E	$105n - 92$	$94n - 86$
Angeles et al. (1989)	Kane	$105n - 109$	$90n - 105$
Balafoutis & Patel (1991)	tensor	$93n - 69$	$81n - 65$
Li & Sankar (1992)	E-L	$88n - 69$	$76n - 66$

TABLE 6.4. Complexity of Different Algorithms for Inverse Dynamics, for $n = 6$

Author(s)	Methods	Multiplications ($n = 6$)	Additions ($n = 6$)
Hollerbach (1980)	E-L	2195	1719
Luh et al. (1980)	N-E	852	738
Walker & Orin (1982)	N-E	800	595
Hollerbach and Sahar (1983)	N-E	688	558
Kane & Levinson (1983)	Kane	646	394
Khalil et al. (1986)	N-E	538	478
Angeles et al. (1989)	Kane	521	435
Balafoutis & Patel (1991)	tensor	489	420
Li & Sankar (1992)	E-L	459	390

system. This system is known as the *mathematical model* of the system at hand. Note that the Newton-Euler equations derived above for a serial manipulator do not constitute the mathematical model because we cannot use the recursive relations derived therein to set up the underlying ODE *directly*. What we need is a model relating the *state* of the system with its external generalized forces of the form

$$\dot{\mathbf{x}} = \mathbf{f}(\mathbf{x}, \mathbf{u}), \quad \mathbf{x}(t_0) = \mathbf{x}_0 \tag{6.45}$$

where $\mathbf{x}$ is the *state vector*, $\mathbf{u}$ is the *input* or *control vector*, $\mathbf{x}_0$ is the state vector at a certain time t_0, and $\mathbf{f}(\mathbf{x}, \mathbf{u})$ is a nonlinear function of $\mathbf{x}$ and $\mathbf{u}$, derived from the dynamics of the system. The state of a dynamical system is defined, in turn, as *the set of variables that separate the past from the future of the system* (Bryson and Ho, 1975). Thus, if we take t_0 as the present time, we can predict from eqs.(6.45) the future states of the system upon integration of the initial-value problem at hand, even if we do not know the complete past history of the system in full detail. Now, if we regard the vector $\boldsymbol{\theta}$ of independent joint variables and its time-rate of change, $\dot{\boldsymbol{\theta}}$, as the vectors of generalized coordinates and generalized speeds, then an obvious definition of $\mathbf{x}$ is

$$\mathbf{x} \equiv \begin{bmatrix} \boldsymbol{\theta}^T & \dot{\boldsymbol{\theta}}^T \end{bmatrix}^T \tag{6.46}$$

The n generalized coordinates, then, define the configuration of the system, while their time-derivatives determine its generalized momentum, an item defined in eq.(6.19d). Hence, knowing $\boldsymbol{\theta}$ and $\dot{\boldsymbol{\theta}}$, we can predict the future values of these variables with the aid of eqs.(6.45).

Below we will derive the mathematical model, eq.(6.45), explicitly, as pertaining to serial manipulators, in terms of the kinematic structure of the system and its inertial properties, i.e., the mass, mass-center coordinates, and inertia matrix of each of its bodies. To this end, we first write the

underlying system of uncoupled Newton-Euler equations for each link. We have $n+1$ links numbered from 0 to n, which are coupled by n kinematic pairs. Moreover, the base link 0 need not be an inertial frame; if it is noninertial, then the force and moment exerted by the environment upon it must be known. For ease of presentation, we will assume in this section that the base frame is inertial, the modifications needed to handle a noninertial base frame to be introduced in Subsection 6.5.2.

We now recall the Newton-Euler equations of the ith body in 6-dimensional form, eqs.(6.5c), which we reproduce below for quick reference:

$$\mathbf{M}_i\dot{\mathbf{t}}_i = -\mathbf{W}_i\mathbf{M}_i\mathbf{t}_i + \mathbf{w}_i^W + \mathbf{w}_i^C, \quad i = 1, \ldots, n \tag{6.47}$$

Furthermore, the definitions of eqs.(6.13b & b) are recalled. Apparently, $\mathbf{M}$ and $\mathbf{W}$ are now $6n \times 6n$ matrices, while $\mathbf{t}$, $\mathbf{w}^C$, $\mathbf{w}^A$, and $\mathbf{w}^D$ are all $6n$-dimensional vectors. Then the foregoing $6n$ scalar equations for the n moving links take on the simple form

$$\mathbf{M}\dot{\mathbf{t}} = -\mathbf{W}\mathbf{M}\mathbf{t} + \mathbf{w}^A + \mathbf{w}^G + \mathbf{w}^D + \mathbf{w}^C \tag{6.48}$$

in which $\mathbf{w}^W$ has been decomposed into its active, gravitational, and dissipative parts $\mathbf{w}^A$, $\mathbf{w}^G$, and $\mathbf{w}^D$, respectively. Now, since gravity acts at the mass center of a body, the gravity wrench $\mathbf{w}_i^G$ acting on the ith link takes the form

$$\mathbf{w}_i^G = \begin{bmatrix} \mathbf{0} \\ m_i\mathbf{g} \end{bmatrix} \tag{6.49}$$

The mathematical model displayed in eq.(6.48) represents the *uncoupled* Newton-Euler equations of the overall manipulator. The following step of this derivation consists in representing the coupling between every two consecutive links as a *linear homogeneous system* of algebraic equations on the link twists. Moreover, we note that all kinematic pairs allow a relative one-degree-of-freedom motion between the coupled bodies. We can then express the kinematic constraints of the system in *linear homogeneous form* in the $6n$-dimensional vector of manipulator twist, namely,

$$\mathbf{K}\mathbf{t} = \mathbf{0} \tag{6.50}$$

with $\mathbf{K}$ being a $6n \times 6n$ matrix, to be derived in Subsection 6.5.1. What is important to note at the moment is that the *kinematic constraint equations*, or *constraint equations*, for brevity, eqs.(6.50), consist of a system of $6n$ scalar equations, i.e., six scalar equations for each joint, for the manipulator at hand has n joints. Moreover, when the system is in motion, $\mathbf{t}$ is different from zero, and hence, matrix $\mathbf{K}$ is singular. In fact, the dimension of the nullspace of $\mathbf{K}$, termed its *nullity*, is exactly equal to n, the degree of freedom of the manipulator. Furthermore, since the nonworking constraint wrench $\mathbf{w}^C$ produces no work on the manipulator, its sole function being

to keep the links together, the power developed by this wrench on $\mathbf{t}$, for any possible motion of the manipulator, is zero, i.e.,

$$\mathbf{t}^T \mathbf{w}^C = 0 \tag{6.51}$$

On the other hand, if the two sides of eq.(6.50) are transposed and then multiplied by a $6n$-dimensional vector $\boldsymbol{\lambda}$, one has

$$\mathbf{t}^T \mathbf{K}^T \boldsymbol{\lambda} = 0 \tag{6.52}$$

Upon comparing eqs.(6.51) and (6.52), it is apparent that $\mathbf{w}^C$ is of the form

$$\mathbf{w}^C = \mathbf{K}^T \boldsymbol{\lambda} \tag{6.53}$$

More formally, the inner product of $\mathbf{w}^C$ and $\mathbf{t}$, as stated by eq.(6.51), vanishes, and hence, $\mathbf{t}$ lies in the nullspace of $\mathbf{K}$, as stated by eq.(6.50). This means that $\mathbf{w}^C$ lies in the range of $\mathbf{K}^T$, as stated in eq.(6.53). The following step will be to represent $\mathbf{t}$ as a linear transformation of the independent generalized speeds, i.e., as

$$\mathbf{t} = \mathbf{T}\dot{\boldsymbol{\theta}} \tag{6.54}$$

with $\mathbf{T}$ defined as a $6n \times n$ matrix that can be fairly termed the *twist-shaping matrix*. Moreover, the above mapping will be referred to as the *twist-shape relations*. The derivation of expressions for matrices $\mathbf{K}$ and $\mathbf{T}$ will be described in detail in Subsection 6.5.1 below. Now, upon substitution of eq.(6.54) into eq.(6.50), we obtain

$$\mathbf{K}\mathbf{T}\dot{\boldsymbol{\theta}} = \mathbf{0} \tag{6.55a}$$

Furthermore, since the degree of freedom of the manipulator is n, the n generalized speeds $\{\dot{\theta}_i\}_1^n$ can be assigned arbitrarily. However, while doing this, eq.(6.55a) has to hold. Thus, the only possibility for this to happen is that the product $\mathbf{KT}$ vanish, i.e.,

$$\mathbf{K}\mathbf{T} = \mathbf{O} \tag{6.55b}$$

where $\mathbf{O}$ denotes the $6n \times n$ zero matrix. The above equation states that $\mathbf{T}$ is an *orthogonal complement* of $\mathbf{K}$. Because of the particular form of choosing this complement—see eq.(6.54)—we refer to $\mathbf{T}$ as the *natural orthogonal complement* of $\mathbf{K}$ (Angeles and Lee, 1988).

In the final step of this method, $\dot{\mathbf{t}}$ of eq.(6.48) is obtained from eq.(6.54), namely,

$$\dot{\mathbf{t}} = \mathbf{T}\ddot{\boldsymbol{\theta}} + \dot{\mathbf{T}}\dot{\boldsymbol{\theta}} \tag{6.56}$$

Furthermore, the uncoupled equations, eqs.(6.48), are multiplied from the left by $\mathbf{T}^T$, thereby eliminating $\mathbf{w}^C$ from those equations and reducing these to a system of only n independent equations, free of nonworking

constraint wrenches. These are nothing but the Euler-Lagrange equations of the manipulator, namely,

$$\mathbf{I}\ddot{\boldsymbol{\theta}} = -\mathbf{T}^T(\mathbf{M}\dot{\mathbf{T}} + \mathbf{W}\mathbf{M}\mathbf{T})\dot{\boldsymbol{\theta}} + \mathbf{T}^T(\mathbf{w}^A + \mathbf{w}^D + \mathbf{w}^G) \tag{6.57}$$

where $\mathbf{I}$ is the positive definite $n \times n$ *generalized inertia matrix* of the manipulator and is defined as

$$\mathbf{I} \equiv \mathbf{T}^T\mathbf{M}\mathbf{T} \tag{6.58}$$

which is identical to the inertia matrix derived using the Euler-Lagrange equations, with $\boldsymbol{\theta}$ as the vector of generalized coordinates. Now, we let $\boldsymbol{\tau}$ and $\boldsymbol{\delta}$ denote the n-dimensional vectors of active and dissipative generalized force. Moreover, we let $\mathbf{C}(\boldsymbol{\theta}, \dot{\boldsymbol{\theta}})\dot{\boldsymbol{\theta}}$ be the n-dimensional vector of *quadratic* terms of inertia force. These items are defined as

$$\begin{aligned} \boldsymbol{\tau} \equiv \mathbf{T}^T\mathbf{w}^A, \quad \boldsymbol{\delta} \equiv \mathbf{T}^T\mathbf{w}^D, \quad \boldsymbol{\gamma} = \mathbf{T}^T\mathbf{w}^G, \\ \mathbf{C}(\boldsymbol{\theta}, \dot{\boldsymbol{\theta}}) \equiv \mathbf{T}^T\mathbf{M}\dot{\mathbf{T}} + \mathbf{T}^T\mathbf{W}\mathbf{M}\mathbf{T} \end{aligned} \tag{6.59}$$

Clearly, the sum $\boldsymbol{\tau} + \boldsymbol{\delta}$ produces $\boldsymbol{\phi}$, the generalized force defined in eq.(6.11). Thus, the Euler-Lagrange equations of the system take on the form

$$\mathbf{I}\ddot{\boldsymbol{\theta}} = -\mathbf{C}\dot{\boldsymbol{\theta}} + \boldsymbol{\tau} + \boldsymbol{\delta} + \boldsymbol{\gamma} \tag{6.60}$$

If, moreover, a static wrench $\mathbf{w}^W$ acts onto the end-effector, with the force applied at the operation point, then its effect onto the above model is taken into account as indicated in eq.(4.95). Thus, a term $\mathbf{J}^T\mathbf{w}^W$ is added to the right-hand side of the above model:

$$\mathbf{I}\ddot{\boldsymbol{\theta}} = -\mathbf{C}\dot{\boldsymbol{\theta}} + \boldsymbol{\tau} + \boldsymbol{\delta} + \boldsymbol{\gamma} + \mathbf{J}^T\mathbf{w}^W \tag{6.61}$$

As a matter of fact, $\boldsymbol{\delta}$ is defined in eq.(6.59) only for conceptual reasons. In practice, this term is most easily calculated once a dissipation function in terms of the generalized coordinates and generalized speeds is available, as described in Section 6.8. Thus, $\boldsymbol{\delta}$ is computed as

$$\boldsymbol{\delta} = -\frac{\partial \Delta}{\partial \dot{\boldsymbol{\theta}}} \tag{6.62}$$

It is pointed out that the first term of the right-hand side of eq.(6.60) is *quadratic* in $\dot{\boldsymbol{\theta}}$ because matrix $\mathbf{C}$, defined in eq.(6.59), is linear in $\dot{\boldsymbol{\theta}}$. In fact, the first term of that expression is linear in a factor $\dot{\mathbf{T}}$ that is, in turn, linear in $\dot{\boldsymbol{\theta}}$. Moreover, the second term of the same expression is linear in $\mathbf{W}$, which is linear in $\dot{\boldsymbol{\theta}}$ as well. However, $\mathbf{C}$ is *nonlinear* in $\boldsymbol{\theta}$. Because of the quadratic nature of that term, it is popularly known as the vector of *Coriolis and centrifugal forces*, whereas the left-hand side of that equation is given the name of vector of *inertia forces*. Properly speaking, both the left-hand side and the first term of the right-hand side of eq.(6.60) arise from inertia forces.

Example 6.5.1 (A minimum-time trajectory) *A pick-and-place operation is to be performed with an n-axis manipulator in the shortest possible time. Moreover, the maneuver is defined so that the n-dimensional vector of joint variables is given by a common shape function $s(x)$, with $0 \leq x \leq 1$ and $0 \leq s \leq 1$, which is prescribed. Thus, for a fixed n-dimensional vector $\boldsymbol{\theta}_0$, the time-history of the joint-variable vector, $\boldsymbol{\theta}(t)$, is given by*

$$\boldsymbol{\theta}(t) = \boldsymbol{\theta}_0 + s\left(\frac{t}{T}\right)\Delta\boldsymbol{\theta}, \quad 0 \leq t \leq T$$

with T defined as the time taken by the maneuver, while $\boldsymbol{\theta}_0$ and $\boldsymbol{\theta}_0 + \Delta\boldsymbol{\theta}$ are the values of the joint-variable vector at the pick- and the place-postures of the manipulator, respectively. These vectors are computed from inverse kinematics, as explained in Chapter 4. Furthermore, the load-carrying capacity of the manipulator is specified in terms of the maximum torques delivered by the motors, namely,

$$|\tau_i| \leq \overline{\tau}_i, \quad \text{for} \quad i = 1, \ldots, n$$

where the constant values $\overline{\tau}_i$ are supplied by the manufacturer. In order to keep the analysis simple, we neglect power loses in this example. Find the minimum time in which the maneuver can take place.

Solution: Let us first calculate the vector of joint-rates and its time-derivative:

$$\dot{\boldsymbol{\theta}}(t) = \frac{1}{T}s'(x)\Delta\boldsymbol{\theta}, \quad \ddot{\boldsymbol{\theta}}(t) = \frac{1}{T^2}s''(x)\Delta\boldsymbol{\theta}, \quad x \equiv \frac{t}{T}$$

Now we substitute the above values into the mathematical model of eq.(6.60), with $\boldsymbol{\delta}(t) = \mathbf{0}$, thereby obtaining

$$\boldsymbol{\tau} = \mathbf{I}(\boldsymbol{\theta})\ddot{\boldsymbol{\theta}} + \mathbf{C}(\boldsymbol{\theta}, \dot{\boldsymbol{\theta}})\dot{\boldsymbol{\theta}}\frac{1}{T^2}s''(x)\mathbf{I}(x)\Delta\boldsymbol{\theta} + \frac{1}{T^2}s'^2(x)\mathbf{C}(x)\Delta\boldsymbol{\theta} \equiv \frac{1}{T^2}\mathbf{f}(x)$$

with $\mathbf{f}(x)$ defined, of course, as

$$\mathbf{f}(x) \equiv [\mathbf{I}(x)s''(x) + \mathbf{C}(x)s'^2(x)]\Delta\boldsymbol{\theta}$$

the $1/T^2$ factor in the term of Coriolis and centrifugal forces stemming from the quadratic nature of the $\mathbf{C}(\boldsymbol{\theta}, \dot{\boldsymbol{\theta}})\dot{\boldsymbol{\theta}}$ term. What we now have is the vector of motor torques, $\boldsymbol{\tau}$, expressed as a function of the scalar argument x. Now, let $f_i(x)$ be the ith component of vector $\mathbf{f}(x)$, and

$$F_i \equiv \max_x\{|f_i(x)|\}, \quad \text{for} \quad i = 1, \ldots, n$$

We would then like to have each value F_i produce the maximum available torque $\overline{\tau}_i$, namely,

$$\overline{\tau}_i = \frac{F_i}{T^2}, \quad i = 1, \ldots n$$

and hence, for each joint we have a value T_i of T given by

$$T_i^2 \equiv \frac{F_i}{\tau_i}, \quad i = 1, \ldots n$$

Obviously, the minimum value sought, $T_{\min}$, is nothing but the maximum of the foregoing values, i.e.,

$$T_{\min} = \max_i \{T_i\}_1^n$$

thereby completing the solution.

6.5.1 Derivation of Constraint Equations and Twist-Shape Relations

In order to illustrate the general ideas behind the method of the natural orthogonal complement, we derive below the underlying kinematic constraint equations and the twist-shape relations. We first note, from eq.(6.25a), that the relative angular velocity of the ith link with respect to the $(i-1)$st link, $\boldsymbol{\omega}_i - \boldsymbol{\omega}_{i-1}$, is $\dot{\theta}_i \mathbf{e}_i$. Thus, if matrix $\mathbf{E}_i$ is defined as the cross-product matrix of vector $\mathbf{e}_i$, then, the angular velocities of two successive links obey a simple relation, namely,

$$\mathbf{E}_i(\boldsymbol{\omega}_i - \boldsymbol{\omega}_{i-1}) = \mathbf{0} \tag{6.63}$$

Furthermore, we rewrite now eq.(6.33a) in the form

$$\dot{\mathbf{c}}_i - \dot{\mathbf{c}}_{i-1} + \mathbf{R}_i \boldsymbol{\omega}_i + \mathbf{D}_{i-1} \boldsymbol{\omega}_{i-1} = \mathbf{0} \tag{6.64}$$

where $\mathbf{D}_i$ and $\mathbf{R}_i$ are defined as the cross-product matrices of vectors $\boldsymbol{\delta}_i$, defined in Subsection 6.4.1 as $\mathbf{a}_i - \boldsymbol{\rho}_i$, and $\boldsymbol{\rho}_i$, respectively. In particular, when the first link is inertial, eqs.(6.63 & b), as pertaining to the first link, reduce to

$$\mathbf{E}_1 \boldsymbol{\omega}_1 = \mathbf{0} \tag{6.65a}$$

$$\dot{\mathbf{c}}_1 + \mathbf{R}_1 \boldsymbol{\omega}_1 = \mathbf{0} \tag{6.65b}$$

Now, eqs.(6.63) and (6.64), as well as their counterparts for $i = 1$, eqs.(6.65a & b), are further expressed in terms of the link twists, thereby producing the constraints below:

$$\mathbf{K}_{11} \mathbf{t}_1 = \mathbf{0} \tag{6.66a}$$

$$\mathbf{K}_{i,i-1} \mathbf{t}_{i-1} + \mathbf{K}_{ii} \mathbf{t}_i = \mathbf{0}, \quad i = 1, \ldots, n \tag{6.66b}$$

with $\mathbf{K}_{11}$ and $\mathbf{K}_{ij}$, for $i = 2, \ldots, n$ and $j = i-1, i$, defined as

$$\mathbf{K}_{11} \equiv \begin{bmatrix} \mathbf{E}_1 & \mathbf{O} \\ \mathbf{R}_1 & \mathbf{1} \end{bmatrix} \tag{6.67a}$$

$$\mathbf{K}_{i,i-1} \equiv \begin{bmatrix} -\mathbf{E}_i & \mathbf{O} \\ \mathbf{D}_{i-1} & -\mathbf{1} \end{bmatrix} \tag{6.67b}$$

$$\mathbf{K}_{ii} \equiv \begin{bmatrix} \mathbf{E}_i & \mathbf{O} \\ \mathbf{R}_i & \mathbf{1} \end{bmatrix} \tag{6.67c}$$

where $\mathbf{1}$ and $\mathbf{O}$ denote the 3×3 identity and zero matrices, respectively. Furthermore, from eqs.(6.66a & b) and (6.67a–c), it is apparent that matrix $\mathbf{K}$ appearing in eq.(6.55b) takes on the form

$$\mathbf{K} = \begin{bmatrix} \mathbf{K}_{11} & \mathbf{O}_6 & \mathbf{O}_6 & \cdots & \mathbf{O}_6 & \mathbf{O}_6 \\ \mathbf{K}_{21} & \mathbf{K}_{22} & \mathbf{O}_6 & \cdots & \mathbf{O}_6 & \mathbf{O}_6 \\ \vdots & \vdots & \vdots & \ddots & \vdots & \vdots \\ \mathbf{O}_6 & \mathbf{O}_6 & \mathbf{O}_6 & \cdots & \mathbf{K}_{n-1,n-1} & \mathbf{O}_6 \\ \mathbf{O}_6 & \mathbf{O}_6 & \mathbf{O}_6 & \cdots & \mathbf{K}_{n,n-1} & \mathbf{K}_{nn} \end{bmatrix} \tag{6.68}$$

with $\mathbf{O}_6$ denoting the 6×6 zero matrix.

Further, the link-twists are expressed as linear combinations of the joint-rate vector $\dot{\boldsymbol{\theta}}$. To this end, we define the $6 \times n$ *partial Jacobian* $\mathbf{J}_i$ as the matrix mapping the joint-rate vector $\dot{\boldsymbol{\theta}}$ into the twist $\mathbf{t}_i$ of that link, i.e.,

$$\mathbf{J}_i \dot{\boldsymbol{\theta}} = \mathbf{t}_i \tag{6.69}$$

whose jth column, $\mathbf{t}_{ij}$, is given, for $i, j = 1, 2, \ldots, n$, by

$$\mathbf{t}_{ij} = \begin{cases} \begin{bmatrix} \mathbf{e}_j \\ \mathbf{e}_j \times \mathbf{r}_{ij} \end{bmatrix}, & \text{if } j \leq i; \\ \begin{bmatrix} \mathbf{0} \\ \mathbf{0} \end{bmatrix}, & \text{otherwise.} \end{cases} \tag{6.70}$$

with $\mathbf{r}_{ij}$ illustrated in Fig. 6.6 and defined, for $i, j = 1, \ldots, n$, as

$$\mathbf{r}_{ij} \equiv \begin{cases} \mathbf{a}_j + \mathbf{a}_{j+1} + \cdots + \mathbf{a}_{i-1} + \boldsymbol{\rho}_i, & \text{if } j < i; \\ \boldsymbol{\rho}_i, & \text{if } j = i; \\ \mathbf{0}, & \text{otherwise.} \end{cases} \tag{6.71}$$

We can thus readily express the twist $\mathbf{t}_i$ of the ith link as a linear combination of the first i joint rates, namely,

$$\mathbf{t}_i = \dot{\theta}_1 \mathbf{t}_{i1} + \dot{\theta}_2 \mathbf{t}_{i2} + \cdots + \dot{\theta}_i \mathbf{t}_{ii}, \quad i = 1, \ldots, n \tag{6.72}$$

and hence, matrix $\mathbf{T}$ of eq.(6.54) takes the form

$$\mathbf{T} \equiv \begin{bmatrix} \mathbf{t}_{11} & \mathbf{0} & \cdots & \mathbf{0} \\ \mathbf{t}_{21} & \mathbf{t}_{22} & \cdots & \mathbf{0} \\ \vdots & \vdots & \ddots & \vdots \\ \mathbf{t}_{n1} & \mathbf{t}_{n2} & \cdots & \mathbf{t}_{nn} \end{bmatrix} \tag{6.73}$$

As a matter of verification, one can readily prove that the product of matrix $\mathbf{T}$, as given by eq.(6.73), by matrix $\mathbf{K}$, as given by eq.(6.68), vanishes, and hence, relation (6.55b) holds.

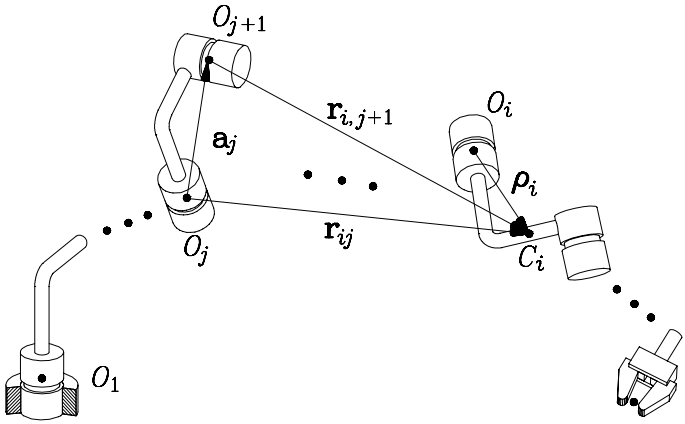

FIGURE 6.6. Kinematic subchain comprising links j, $j+1\ldots,$ i.

The kinematic constraint equations on the twists, for the case in which the ith joint is prismatic, are derived likewise. In this case, we use eqs.(6.34a & e), with the latter rewritten more conveniently for our purposes, namely,

$$\boldsymbol{\omega}_i = \boldsymbol{\omega}_{i-1} \tag{6.74a}$$

$$\dot{\mathbf{c}}_i = \dot{\mathbf{c}}_{i-1} + \boldsymbol{\omega}_{i-1} \times (\boldsymbol{\delta}_{i-1} + \boldsymbol{\rho}_i + b_i \mathbf{e}_i) + \dot{b}_i \mathbf{e}_i \tag{6.74b}$$

We now introduce one further definition:

$$\mathbf{R}'_i \equiv \mathbf{D}'_{i-1} + \mathbf{R}_i \tag{6.75}$$

where $\mathbf{D}'_{i-1}$ is the cross-product matrix of vector $\boldsymbol{\delta}_{i-1}$, defined in Subsection 6.4.1 as $\mathbf{d}_{i-1} - \boldsymbol{\rho}_{i-1}$, while $\mathbf{R}_i$ is the cross-product matrix of $\boldsymbol{\rho}_i + b_i \mathbf{e}_i$. Hence, eq.(6.74b) can be rewritten as

$$\dot{\mathbf{c}}_i - \dot{\mathbf{c}}_{i-1} + \mathbf{R}'_i \boldsymbol{\omega}_i - \dot{b}_i \mathbf{e}_i = \mathbf{0} \tag{6.76}$$

Upon multiplication of both sides of eq.(6.76) by $\mathbf{E}_i$, the term in $\dot{b}_i$ cancels, and we obtain

$$\mathbf{E}_i(\dot{\mathbf{c}}_i - \dot{\mathbf{c}}_{i-1} + \mathbf{R}'_i \boldsymbol{\omega}_i) = \mathbf{0} \tag{6.77}$$

Hence, eqs.(6.74a) and (6.77) can now be regrouped in a single 6-dimensional linear homogeneous equation in the twists, namely,

$$\mathbf{K}'_{i,i-1} \mathbf{t}_{i-1} + \mathbf{K}'_{ii} \mathbf{t}_i = \mathbf{0} \tag{6.78}$$

the associated matrices being defined below:

$$\mathbf{K}'_{i,i-1} \equiv \begin{bmatrix} -\mathbf{1} & \mathbf{O} \\ \mathbf{O} & -\mathbf{E}_i \end{bmatrix} \tag{6.79a}$$

$$\mathbf{K}'_{ii} \equiv \begin{bmatrix} \mathbf{1} & \mathbf{O} \\ \mathbf{E}_i \mathbf{R}'_i & \mathbf{E}_i \end{bmatrix} \tag{6.79b}$$

with $\mathbf{1}$ and $\mathbf{O}$ defined already as the 3×3 identity and zero matrices, respectively. If the first joint is prismatic, then the corresponding constraint equation takes on the form

$$\mathbf{K}'_{11}\mathbf{t}_1 = \mathbf{0} \tag{6.80}$$

with $\mathbf{K}'_{11}$ defined as

$$\mathbf{K}'_{11} \equiv \begin{bmatrix} \mathbf{1} & \mathbf{O} \\ \mathbf{O} & \mathbf{E}_1 \end{bmatrix} \tag{6.81}$$

Furthermore, if the kth pair is prismatic and $1 \leq k \leq i$, then the twist $\mathbf{t}_i$ of the ith link changes to

$$\mathbf{t}_i = \dot{\theta}_1\mathbf{t}_{i1} + \cdots + \dot{b}_k\mathbf{t}'_{ik} + \cdots + \dot{\theta}_i\mathbf{t}_{ii}, \quad i = 1, \ldots, n \tag{6.82}$$

where $\mathbf{t}'_{ik}$ is defined as

$$\mathbf{t}'_{ik} \equiv \begin{bmatrix} \mathbf{0} \\ \mathbf{e}_k \end{bmatrix} \tag{6.83}$$

In order to set up eq.(6.60), then all we now need is $\dot{\mathbf{T}}$, which is computed below. Two cases will be distinguished again, namely, whether the joint at hand is a revolute or a prismatic pair. In the first case, from eq.(6.70) one readily derives, for $i, j = 1, 2, \ldots, n$,

$$\dot{\mathbf{t}}_{ij} = \begin{cases} \begin{bmatrix} \boldsymbol{\omega}_j \times \mathbf{e}_j \\ (\boldsymbol{\omega}_j \times \mathbf{e}_j) \times \mathbf{r}_{ij} + \mathbf{e}_j \times \dot{\mathbf{r}}_{ij} \end{bmatrix}, & \text{if } j \leq i; \\ \begin{bmatrix} \mathbf{0} \\ \mathbf{0} \end{bmatrix}, & \text{otherwise} \end{cases} \tag{6.84}$$

where, from eq.(6.71),

$$\dot{\mathbf{r}}_{ij} = \boldsymbol{\omega}_j \times \mathbf{a}_j + \cdots + \boldsymbol{\omega}_{i-1} \times \mathbf{a}_{i-1} + \boldsymbol{\omega}_i \times \boldsymbol{\rho}_i \tag{6.85}$$

On the other hand, if the kth pair is prismatic and $1 \leq k \leq i$, then from eq.(6.83), the time-rate of change of $\mathbf{t}'_{ik}$ becomes

$$\dot{\mathbf{t}}'_{ik} = \begin{bmatrix} \mathbf{0} \\ \boldsymbol{\omega}_k \times \mathbf{e}_k \end{bmatrix} \tag{6.86}$$

thereby completing the desired derivations.

Note that the natural orthogonal complement can also be used for the inverse dynamics calculations. In this case, if the manipulator is subjected to a gravity field, then the twist-rate of the first link will have to be modified by adding a nonhomogeneous term to it, thereby accounting for the gravity-acceleration terms. This issue is discussed in Section 6.7.

6.5.2 Noninertial Base Link

Noninertial bases occur in space applications, e.g., in the case of a manipulator mounted on a space platform or on the space shuttle. A noninertial base can be readily handled with the use of the natural orthogonal complement, as discussed in this subsection. Since the base is free of attachments to an inertial frame, we have to add its six degrees of freedom (dof) to the n dof of the rest of the manipulator. Correspondingly, $\mathbf{t}$, $\mathbf{w}^C$, $\mathbf{w}^A$, and $\mathbf{w}^D$ now become $6(n+1)$-dimensional vectors. In particular, $\mathbf{t}$ takes the form

$$\mathbf{t} = [\, \mathbf{t}_0^T \quad \mathbf{t}_1^T \quad \dots \quad \mathbf{t}_n^T \,]^T \tag{6.87}$$

with $\mathbf{t}_0$ defined as the twist of the base. Furthermore, the vector of independent generalized speeds, $\dot{\boldsymbol{\theta}}$, is now of dimension $n+6$, its first six components being those of $\mathbf{t}_0$, the other n remaining as in the previous case. Thus, $\dot{\boldsymbol{\theta}}$ has the components shown below:

$$\dot{\boldsymbol{\theta}} \equiv [\, \mathbf{t}_0^T \quad \dot{\theta}_1 \quad \dots \quad \dot{\theta}_n \,]^T \tag{6.88}$$

Correspondingly, $\mathbf{T}$ becomes a $6(n+1) \times (n+6)$ matrix, namely,

$$\mathbf{T} \equiv \begin{bmatrix} \mathbf{1} & \mathbf{O} \\ \mathbf{O}' & \mathbf{T}' \end{bmatrix} \tag{6.89}$$

where $\mathbf{1}$ is the 6×6 identity matrix, $\mathbf{O}$ denotes the $6 \times n$ zero matrix, $\mathbf{O}'$ represents the $6n \times 6$ zero matrix, and $\mathbf{T}'$ is the $6n \times n$ matrix defined in eq.(6.73) as $\mathbf{T}$. Otherwise, the model remains as in the case of an inertial base.

A word of caution is in order here. Because of the presence of the twist vector $\mathbf{t}_0$ in the definition of the vector of generalized speeds above, the latter cannot, properly speaking, be regarded as a time-derivative. Indeed, as studied in Chapter 3, the angular velocity appearing in the twist vector is not a time-derivative. Hence, the vector of independent generalized speeds defined in eq.(6.88) is represented instead by $\mathbf{v}$, which does not imply a time-derivative, namely,

$$\mathbf{v} = [\, \mathbf{t}_0^T \quad \dot{\theta}_1 \quad \cdots \quad \dot{\theta}_n \,]^T \tag{6.90}$$

6.6 Manipulator Forward Dynamics

Forward dynamics is needed either for purposes of simulation or for the model-based control of manipulators (Craig, 1989), and hence, a fast calculation of the joint-variable time-histories $\boldsymbol{\theta}(t)$ is needed. These time-histories are calculated from the model displayed in eq.(6.61), reproduced below for quick reference, in terms of vector $\boldsymbol{\theta}(t)$, i.e.,

$$\mathbf{I}\ddot{\boldsymbol{\theta}} = -\mathbf{C}(\boldsymbol{\theta}, \dot{\boldsymbol{\theta}})\dot{\boldsymbol{\theta}} + \boldsymbol{\tau}(t) + \boldsymbol{\delta}(\boldsymbol{\theta}, \dot{\boldsymbol{\theta}}) + \boldsymbol{\gamma}(\boldsymbol{\theta}) + \mathbf{J}^T \mathbf{w}^W \tag{6.91}$$

Clearly, what is at stake here is the calculation of $\ddot{\boldsymbol{\theta}}$ from the foregoing model. Indeed, the right-hand side of eq.(6.91) can be calculated with the aid of the Newton-Euler recursive algorithm, as we will describe below, and needs no further discussion for the time being. Now, the calculation of $\ddot{\boldsymbol{\theta}}$ from eq.(6.91) is similar to the calculation of $\dot{\boldsymbol{\theta}}$ from the relation between the joint-rates and the twist, derived in Section 4.5. From the discussion in that section, such calculations take a number of floating-point operations, or *flops*, that is proportional to n^3, and is thus said to have a complexity of $O(n^3)$—read "order n^3." In real-time calculations, we would like to have a computational scheme of $O(n)$. In attempting to derive such schemes, Walker and Orin (1982) proposed a procedure that they called the *composite rigid-body method*, whereby the number of flops is minimized by cleverly calculating $\mathbf{I}(\boldsymbol{\theta})$ and the right-hand side of eq.(6.91) by means of the recursive Newton-Euler algorithm. In their effort, they produced an $O(n^2)$ algorithm to calculate $\ddot{\boldsymbol{\theta}}$. Thereafter, Featherstone (1983) proposed an $O(n)$ algorithm that is based, however, on the assumption that Coriolis and centrifugal forces are negligible. The same author reported an improvement to the aforementioned algorithm, namely, the *articulated-body method*, that takes into account Coriolis and centrifugal forces (Featherstone, 1987.) The outcome, for an n-revolute manipulator, is an algorithm requiring $300n - 267$ multiplications and $279n - 259$ additions. For $n = 6$, these figures yield 1,533 multiplications and 1,415 additions. Li (1989) reported an $O(n^2)$ algorithm leading to 783 multiplications and 670 additions.

In this subsection, we illustrate the application of the method of the natural orthogonal complement to the modeling of an n-axis serial manipulator for purposes of simulation. While this algorithm gives an $O(n^3)$ complexity, its derivation is straightforward and gives, for a six-axis manipulator, a computational cost similar to that of Featherstone's, namely, 1,596 multiplications and 1,263 additions. Moreover, a clever definition of coordinate frames leads to even lower figures, i.e., 1,353 multiplications and 1,165 additions, as reported by Angeles and Ma (1988). Further developments on robot dynamics using the natural orthogonal complement have been reported by Saha (1997, 1999), who proposed the *decoupled* natural orthogonal complement as a means to enable the real-time inversion of the mass matrix.

The manipulator at hand is assumed to be constituted by n moving links coupled by n kinematic pairs of the revolute or prismatic types. Again, for brevity, the base link is assumed to be inertial, noninertial bases being readily incorporated as described in Subsection 6.5.2. For the sake of conciseness, we will henceforth consider only manipulators mounted on an inertial base. Moreover, we assume that the generalized coordinates $\boldsymbol{\theta}$ and the generalized speeds $\dot{\boldsymbol{\theta}}$ are known at an instant t_k, along with the driving torque $\boldsymbol{\tau}(t)$, for $t \geq t_k$, and of course, the DH and the inertial parameters of the manipulator are assumed to be known as well. Based on the foregoing information, then, $\ddot{\boldsymbol{\theta}}$ is evaluated at t_k and, with a suitable integration

scheme, the values of $\boldsymbol{\theta}$ and $\dot{\boldsymbol{\theta}}$ are determined at instant t_{k+1}. Obviously, the governing equation (6.60) enables us to solve for $\ddot{\boldsymbol{\theta}}(t_k)$. This requires, of course, the *inversion* of the $n \times n$ matrix of generalized inertia $\mathbf{I}$. Since the said matrix is positive-definite, solving for $\ddot{\boldsymbol{\theta}}$ from eq.(6.60) can be done economically using the *Cholesky-decomposition* algorithm (Dahlquist and Björck, 1974). The sole remaining task is, then, the computation of $\mathbf{I}$, the quadratic inertia term $\mathbf{C}\dot{\boldsymbol{\theta}}$, and the dissipative torque $\boldsymbol{\delta}$. The last of these is dependent on the manipulator and the constitutive model adopted for the representation of viscous and Coulomb friction forces and will not be considered at this stage. Models for dissipative forces will be studied in Section 6.8. Thus, the discussion below will focus on the computation of $\mathbf{I}$ and $\mathbf{C}\dot{\boldsymbol{\theta}}$ appearing in the mathematical model of eq.(6.91).

Next, the $6n \times 6n$ matrix $\mathbf{M}$ is factored as

$$\mathbf{M} = \mathbf{H}^T\mathbf{H} \tag{6.92}$$

which is possible because $\mathbf{M}$ is at least positive-semidefinite. In particular, for manipulators of the type at hand, $\mathbf{M}$ is positive-definite if no link-mass is neglected. Moreover, due to the diagonal-block structure of this matrix, its factoring is straightforward. In fact, $\mathbf{H}$ is given simply by

$$\mathbf{H} = \text{diag}(\mathbf{H}_1, \ldots, \mathbf{H}_n) \tag{6.93}$$

each 6×6 block $\mathbf{H}_i$ of eq.(6.93) being given, in turn, as

$$\mathbf{H}_i = \begin{bmatrix} \mathbf{N}_i & \mathbf{O} \\ \mathbf{O} & n_i\mathbf{1} \end{bmatrix} \tag{6.94}$$

with $\mathbf{1}$ and $\mathbf{O}$ defined as the 3×3 identity and zero matrices, respectively. We thus have

$$\mathbf{M}_i = \mathbf{H}_i^T\mathbf{H}_i \tag{6.95}$$

Furthermore, $\mathbf{N}_i$ can be obtained from the Cholesky decomposition of $\mathbf{I}_i$, while n_i is the *positive* square root of m_i, i.e.,

$$\mathbf{I}_i = \mathbf{N}_i^T\mathbf{N}_i, \quad m_i = n_i^2 \tag{6.96}$$

Now, since each 6×6 $\mathbf{M}_i$ block is constant in body-fixed coordinates, the above factoring can be done off-line. From the foregoing definitions, then, the $n \times n$ matrix of generalized inertia $\mathbf{I}$ can now be expressed as

$$\mathbf{I} = \mathbf{P}^T\mathbf{P} \tag{6.97}$$

where $\mathbf{P}$ is defined, in turn, as the $6n \times n$ matrix given below:

$$\mathbf{P} \equiv \mathbf{HT} \tag{6.98}$$

The computation of $\mathbf{P}$ is now discussed. If we recall the structure of $\mathbf{T}$ from eq.(6.73) and that of $\mathbf{H}$ from eq.(6.93), along with the definition of $\mathbf{P}$, eq.(6.98), we readily obtain

$$\mathbf{P} = \begin{bmatrix} \mathbf{H}_1\mathbf{t}_{11} & \mathbf{0} & \cdots & \mathbf{0} \\ \mathbf{H}_2\mathbf{t}_{21} & \mathbf{H}_2\mathbf{t}_{22} & \cdots & \mathbf{0} \\ \vdots & \vdots & \ddots & \vdots \\ \mathbf{H}_n\mathbf{t}_{n1} & \mathbf{H}_n\mathbf{t}_{n2} & \cdots & \mathbf{H}_n\mathbf{t}_{nn} \end{bmatrix} \equiv \begin{bmatrix} \mathbf{p}_{11} & \mathbf{0} & \cdots & \mathbf{0} \\ \mathbf{p}_{21} & \mathbf{p}_{22} & \cdots & \mathbf{0} \\ \vdots & \vdots & \ddots & \vdots \\ \mathbf{p}_{n1} & \mathbf{p}_{n2} & \cdots & \mathbf{p}_{nn} \end{bmatrix} \tag{6.99}$$

with $\mathbf{0}$ denoting the 6-dimensional zero vector. Moreover, each of the above nontrivial 6-dimensional arrays $\mathbf{p}_{ij}$ is given as

$$\mathbf{p}_{ij} \equiv \mathbf{H}_i\mathbf{t}_{ij} = \begin{cases} \begin{bmatrix} \mathbf{N}_i\mathbf{e}_j \\ n_i\mathbf{e}_j \times \mathbf{r}_{ij} \end{bmatrix} & \text{if the } j\text{th joint is } R; \\ \\ \begin{bmatrix} \mathbf{0} \\ n_i\mathbf{e}_j \end{bmatrix} & \text{if the } j\text{th joint is } P \end{cases} \tag{6.100}$$

Thus, the (i, j) entry of $\mathbf{I}$ is computed as the sum of the inner products of the (k, i) and the (k, j) blocks of $\mathbf{P}$, for $k = j, \ldots, n$, i.e.,

$$I_{ij} = I_{ji} = \sum_{k=j}^{n} \mathbf{p}_{ki}^T \mathbf{p}_{kj} \tag{6.101}$$

with both $\mathbf{p}_{ki}$ and $\mathbf{p}_{kj}$ expressed in $\mathcal{F}_{k+1}$-coordinates, i.e., in kth-link coordinates. Now, the Cholesky decomposition of $\mathbf{I}$ can be expressed as

$$\mathbf{I} = \mathbf{L}^T\mathbf{L} \tag{6.102}$$

where $\mathbf{L}$ is an $n \times n$ lower-triangular matrix with positive diagonal entries. Moreover, eq.(6.91) is now rewritten as

$$\mathbf{L}^T\mathbf{L}\ddot{\boldsymbol{\theta}} = -(\mathbf{C}\dot{\boldsymbol{\theta}} - \mathbf{J}^T\mathbf{w}^W - \boldsymbol{\gamma}) + \boldsymbol{\delta} + \boldsymbol{\tau} \tag{6.103}$$

If we now recall eq.(6.91), it is apparent that the term inside the parentheses in the right-hand side of the above equation is nothing but the torque required to produce the motion prescribed by the current values of $\boldsymbol{\theta}$ and $\dot{\boldsymbol{\theta}}$, in the absence of dissipative wrenches and with zero joint accelerations, when the manipulator is acted upon by a static wrench $\mathbf{w}^W$. That is, if we call $\overline{\boldsymbol{\tau}}$ the torque $\boldsymbol{\tau}$ of eq.(6.91) under the foregoing conditions, then

$$\mathbf{C}\dot{\boldsymbol{\theta}} - \mathbf{J}^T\mathbf{w}^W - \boldsymbol{\gamma} = \boldsymbol{\tau}\big|_{\mathbf{w}^D=\mathbf{0}, \ddot{\boldsymbol{\theta}}=\mathbf{0}} \equiv \overline{\boldsymbol{\tau}} \tag{6.104}$$

which is most efficiently computed from inverse dynamics, using the recursive Newton-Euler algorithm, as described in Section 6.4 . Now eq.(6.102) is solved for $\ddot{\boldsymbol{\theta}}$ in two steps, namely,

$$\mathbf{L}^T\mathbf{x} = -\overline{\boldsymbol{\tau}} + \boldsymbol{\tau} + \boldsymbol{\delta} \tag{6.105a}$$

$$\mathbf{L}\ddot{\boldsymbol{\theta}} = \mathbf{x} \tag{6.105b}$$